TO FEEL AND TO ACT: EXPLORING MOTOR AND AFFECTIVE PROCESSES IN HUMAN AND HUMAN-ROBOT INTERACTION

RESSENTIR ET AGIR : EXPLORATION DES PROCESSUS MOTEURS ET AFFECTIFS DANS LES INTERACTIONS HUMAINES ET INTERACTIONS HUMAIN-ROBOT.

A thesis submitted
by

MARIA-ISABEL CASSO ECHALAR

for the degree
of
Philosophiæ Doctor in Psychology

to the
École Doctorale Science de l'Homme et de la Société
SCALab UMR CNRS 9193
University of Lille

November 19, 2025

Jury members:
Prof. Benoît Bardy, Université Montpellier (rapporteur)
Prof. Yvonne N. Delevoye-Turrell, Université de Lille (supervisor)
Prof. Patrick Hénaff, Bretagne INP/ENIB (president)
Dr. Juliane Honisch, University of Reading (examiner)
Dr. Dominique Knutsen, Université de Lille (examiner)
Prof. Catherine Pelachaud, Sorbonne Université (rapporteur)
Prof. Michael Richardson, Macquarie University (examiner)

To think is an act. To *feel* is a fact.

— Clarice Lispector (1986). A Hora da Estrela, p.11

ABSTRACT

Humans experience emotions continuously, and these emotions shape perception, decision-making, and the ways we interact with both our environment and with others. Despite extensive advances in affective neuroscience, relatively little is known about how affect manifests in observable motor behavior. The overall aim of this thesis was to examine how affect modulates spontaneous movement, particularly in the context of Human interaction and Human–Robot Interaction (HRI). Study 1 introduces a methodological contribution by applying motion data analysis to define kinematic parameters that identify mobility and stability challenges in early-stage Parkinson's disease, offering advantages over traditional chronometry-based assessments. In Study 2, we developed a spectral analysis technique to characterize spontaneous human oscillations (i.e., sway). This method facilitated the assessment of movement emergence and inhibition, reflecting affective changes and engagement during HRI. An experimental study (Study 2) compared human sway in interactions with a small humanoid, a tall humanoid, and a small non-humanoid robot. The results indicated that the small non-humanoid robot elicited more spontaneous movement, suggesting that robot morphology influences human motor behavior. In Study 3, we explored the role of emotional context in HRI. Findings revealed that positive contexts increased the power of spontaneous oscillations, whereas negative contexts suppressed movement. In Study 4, we investigated whether interpersonal motor synchronization is related to affective compatibility between two individuals. Results demonstrated that dyads with congruent affective states (i.e., both experiencing either positive or negative states) maintained synchronization longer than incongruent pairs. Taken together, these findings provide empirical evidence that emotions influence motor control. Across both human interaction and HRI, affective changes modulated not only the intensity of spontaneous movement but also the time spent on interpersonal synchronization. Based on this work, we propose a theoretical model of affective motor behavior that describes the influence of affect on motor processes. More broadly, this thesis proposes a theoretical framework in which affective states and movement patterns continuously shape each other through dynamic feedback loops across diverse interactive contexts.

Keywords: affective motor control; behavior; emotional context; affective compatibility; social interaction, human-robot interaction; motion data analysis

RÉSUMÉ

Les êtres humains éprouvent des émotions en continu, et ces émotions façonnent la perception, la prise de décision ainsi que les manières d'interagir avec l'environnement et avec autrui. Malgré les avancées considérables en neurosciences affectives, on sait relativement peu de choses sur la façon dont l'affect se manifeste dans le comportement moteur observable. L'objectif général de cette thèse était d'examiner comment l'affect module le mouvement spontané, en particulier dans le contexte de l'interaction humaine et de l'interaction Humain–Robot (IHR). L'Étude 1 propose une contribution méthodologique. L'analyse des données de mouvement y est utilisée pour définir des paramètres cinématiques permettant d'identifier des difficultés de mobilité et de stabilité dans le débout de maladie de Parkinson. Cette approche présente des avantages par rapport aux évaluations chronométriques classiques. L'Étude 2 développe une méthode d'analyse spectrale destinée à caractériser les oscillations humaines spontanées (balancement postural). Cette méthode permet d'évaluer l'émergence et l'inhibition du mouvement en fonction des variations affectives et de l'engagement en contexte d'IHR. L'expérimentation compare les oscillations spontanées lors d'interactions avec un petit humanoïde, un grand humanoïde et un petit robot non humanoïde. Les résultats indiquent que le petit robot non humanoïde suscite davantage de mouvement spontané. La morphologie du robot apparaît ainsi comme un facteur influençant le comportement moteur humain. L'Étude 3 examine le rôle du contexte émotionnel dans l'IHR. Les résultats montrent que les contextes positifs augmentent la puissance des oscillations spontanées, tandis que les contextes négatifs réduisent le mouvement. L'Étude 4 analyse la synchronisation motrice interpersonnelle. Les résultats révèlent que des dyades partageant un état affectif congruent (i.e., tous deux dans un état positif ou négatif) maintiennent leur synchronisation plus longtemps que des dyades incongruentes. Ces travaux démontrent empiriquement que les émotions influencent le contrôle moteur. Dans l'interaction humaine comme dans l'IHR, l'affect module à la fois l'intensité du mouvement spontané et la durée de la synchronisation interpersonnelle. Un modèle théorique du comportement moteur affectif est proposé, décrivant l'impact de l'affect sur les processus moteurs. Plus largement, cette thèse avance un cadre où états affectifs et dynamiques motrices se modifient mutuellement au sein de boucles de rétroaction dynamiques, dans divers contextes interactifs.

Mots clés : contrôle moteur-affectif; comportement; interaction sociale ; interaction humain-robot; contexte émotionnel; compatibilité affective; analyse des données de mouvement

RÉSUMÉ SUBSTANTIEL

Les êtres humains éprouvent des émotions en continu, et ces émotions façonnent la perception, la prise de décision ainsi que les manières d'interagir avec l'environnement et avec autrui. Malgré les avancées considérables en neurosciences affectives, on sait relativement peu de choses sur la façon dont l'affect se manifeste dans le comportement moteur observable. L'objectif général de cette thèse était d'examiner comment l'affect module le mouvement spontané, en particulier dans le contexte de l'interaction humaine et de l'interaction Humain–Robot (IHR). Pour ce faire, les quatre études menées adoptent des approches complémentaires, qui vont de la méthodologie clinique appliquée au mouvement, à l'analyse spectrale du balancement spontané, jusqu'à l'étude du rôle de l'affect dans la coordination interpersonnelle.

L'Étude 1 propose une contribution méthodologique essentielle. Les évaluations cliniques existantes de la maladie de Parkinson (MP) se concentrent principalement sur la stratification de la sévérité des symptômes ou du taux de progression, ce qui limite leur capacité à capturer les changements de mobilité fonctionnelle, un facteur important dans l'évaluation des résultats de la rééducation. Pour combler cette lacune, nous avons développé une méthodologie novatrice, le Functional Mobility Assessment for Parkinson's (FMA-P), qui intègre la capture de mouvement et l'analyse de la marche via une plateforme sensible à la pression afin d'explorer des aspects clés de la mobilité fonctionnelle. Pour développer le protocole FMA-P, nous avons mené une étude pilote incluant 12 personnes atteintes de MP et 12 témoins sains appariés en âge, qui ont chacun complété la séquence FMA-P trois fois. La séquence comprenait les tâches suivantes : se lever d'une chaise, marcher à travers une porte, tourner, se pencher pour ramasser et déposer un objet, puis revenir en position assise. Les résultats de l'étude 1 ont démontré que le FMA-P est un outil sensible pour identifier les déficiences fonctionnelles dans la MP. En particulier, des différences significatives entre les personnes atteintes de Parkinson (PwP) et les témoins ont été observées lors du lever de chaise (inclinaison maximale du tronc plus élevée, jerk moyen du tronc plus faible) et lors de la tâche de rotation (durée de la tâche plus longue et angle du contact du talon plus faible), fournissant des informations essentielles sur la stabilité posturale. Pour évaluer les changements de mobilité fonctionnelle au fil du temps, nous avons mené une étude d'intervention à mesures répétées sur 12 semaines avec 12 participants atteints de MP. Les résultats de l'étude 2 ont indiqué des améliorations notables de la stabilité et de l'équilibre lors des rotations. Les participants ont montré une réduction du temps de rotation et une augmentation de la rotation en lacet (yaw) de la tête, du tronc et du bassin.

En revanche, aucun changement significatif n'a été observé dans les mesures cliniques standard (c.-à-d., le Timed Up and Go et la durée des tâches). Le FMA-P offre des informations fines sur la qualité du mouvement, en faisant un outil précieux pour le diagnostic précoce, le suivi de l'efficacité des interventions, et l'orientation de stratégies de rééducation chez les personnes atteintes de MP.

L'Étude 2 étend cette approche méthodologique au champ de l'IHR et s'attache à développer une méthode d'analyse spectrale destinée à caractériser les oscillations humaines spontanées (balancement postural). Les développements dans le domaine de la robotique sociale ouvrent des opportunités intéressantes pour des applications en santé, en éducation et dans les services. Pour cela, l'étude de l'engagement dans l'interaction homme-robot (HRI) est cruciale pour améliorer la qualité des expériences interactives. Les questionnaires sont puissants pour décrire les comportements volontaires ; cependant, l'engagement est souvent un comportement implicite non volontaire qui n'atteint la conscience qu'une fois initié. Inspirés par la recherche en psychologie cognitive, nous proposons une caractéristique comportementale permettant de quantifier l'engagement dans l'HRI à travers la mesure du mouvement spontané et l'analyse spectrale par ondelettes. Pour cela, nous avons mené une expérience au cours de laquelle des participants ont écouté des histoires tristes racontées par un robot social mobile. Tout au long de l'expérience, nous avons enregistré les mouvements spontanés et non volontaires de balancement des participants grâce à un système de capture de mouvement. Les expériences ont été menées avec trois plateformes robotiques (Buddy, Pepper et Nao). Les résultats ont montré que le balancement corporel spontané peut être modulé par des robots sociaux dans une interaction dépourvue de but. Les résultats de cette étude ont été présentés à la conférence ROMAN tenue en 2024 à Pasadena, USA, et au Rhythm Production and Perception Workshop (RPPW) tenu en 2023 à Nottingham, Royaume-Uni. Les résultats avec le robot Buddy ont été présentés sous format poster à la conférence de la European Society for Cognitive Psychology (ESCOP) tenue en 2022 à Lille, France. Cette étude a été rendue possible grâce à la collaboration avec le Prof. Patrick Hénaff (École Nationale d'Ingenierus de Brest, ENIB) et le Prof. Hendry F. Chame (Laboratoire Lorrain de recherche en informatique et ses applications, Loria). Leur soutien incluait l'accès aux plateformes robotiques ainsi qu'une expertise technique et un accompagnement théorique précieux tant sur le contrôle de la plateforme robotique que sur la conception expérimentale. Le laboratoire Loria nous a fourni l'accès aux robots sociaux Nao et Pepper. Les deux pouvaient être contrôlés via Naoqi (Python-based programs) ce qui a permis une plus grande efficacité pour l'implémentation et la cohérence expérimentale. La collecte de données avec le robot Pepper a dû être effectuée sur site à Nancy, comme transporter la plateforme n'était pas possible. Enfin, ces résultats ont été obtenus dans un contexte d'HRI négatif caractérisé par un environnement sombre, où le robot racontait des histoires tristes. Ayant établi une méthode pour quantifier le mouvement spontané humain, la question qui en découle est de savoir si le contexte affectif de l'HRI peut influencer ces variations motrices. Cette interrogation ouvre la voie à l'étude suivante.

L'Étude 3 approfondit en effet le rôle du contexte affectif dans l'IHR. Cette étude examine comment le contexte affectif de l'interaction homme-robot (HRI), manipulé via des indices environnementaux et des signaux non verbaux d'un robot social, influence les états affectifs humains et leurs réponses motrices incarnées. Alors que les travaux précédents se sont concentrés sur les mesures auto-rapportées, cette étude explore les oscillations corporelles spontanées comme indicateur quantifiable de l'engagement affectif. Dans une expérience à plan mixte, quarante participants ont interagi avec le robot social Nao dans un contexte multimodal positif ou négatif. Le robot affichait des signaux corporels émotionnels congruents (i.e., joyeux et tristes) à différentes fréquences d'oscillation, tandis que les participants se trouvaient dans un environnement correspondant positif ou négatif. Nous avons recueilli des mesures auto-rapportées de l'affect et quantifié les mouvements corporels spontanés à l'aide d'un système de capture de mouvement et d'une analyse spectrale. Les résultats ont montré que le contexte négatif diminuait significativement les niveaux de valence et d'activation des participants et inhibait leurs oscillations corporelles. À l'inverse, le contexte positif n'a pas altéré l'affect auto-rapporté ; cependant, il a augmenté le mouvement spontané, particulièrement à haute fréquence d'oscillation du robot. Cela suggère que les oscillations spontanées pourraient être un indicateur plus sensible de l'engagement affectif que les mesures auto-rapportées. Cette étude a été présentée au Timing Research Forum 3 (TRF) en octobre 2023 à Lisbonne, Portugal, ainsi qu'au colloque Drôles d'Objets en avril à Nancy, France. Elle a été rendue possible grâce aux installations et à la plateforme robotique du laboratoire Loria, ainsi qu'à la collaboration avec le Prof. Patrick Hénaff (ENIB) et le Prof. Hendry F. Chame (Loria). Cette étude marque un tournant dans mon programme de recherche, car elle suggère que comprendre comment les humains adaptent leur comportement et ressentent des états affectifs en présence de robots nécessite une compréhension plus fondamentale des mêmes phénomènes dans les interactions humaines.

C'est précisément cette transition qui motive l'Étude 4, consacrée à la synchronisation motrice interpersonnelle et à son éventuelle modulation par l'affect. La synchronisation motrice interpersonnelle peut émerger intentionnellement ou spontanément dans divers contextes sociaux et a été positivement associée à des comportements affiliatifs et prosociaux. Cependant, le rôle de l'affect dans cette coordination reste encore peu exploré. Dans la présente étude, nous avons examiné si l'émergence spontanée de la synchronisation est influencée par la compatibilité des états affectifs des deux partenaires. Nous avons invité vingt-huit paires d'amis à pédaler sur des vélos statiques à leur rythme préféré tout en se faisant face. L'affect a été manipulé à l'aide de scénarios émotionnels autobiographiques et d'extraits musicaux validés, induisant soit un état positif et fortement activé, soit un état négatif faiblement activé. Les paires étaient exposées à des conditions congruentes (même état affectif) ou incongruentes (états affectifs différents). À l'aide d'un système de capture de mouvement, nous avons quantifié la synchronisation spontanée du pédalage de chaque dyade, évaluée avec les indices Time-In-Synchrony (TIS). Nos résultats montrent que le TIS diminuait sous induction affective comparé au contrôle (absence d'induction). Nous observons également une tendance non significative, mais directionnelle, vers une synchronisation plus élevée dans les conditions affectivement compatibles. En dehors de l'interaction, la manipulation affective modulait la fréquence de pédalage individuelle : l'induction positive menant à la cadence la plus élevée, soutenant l'idée que l'affect influence également le mouvement global du corps. Les résultats de cette étude ont été présentés au Workshop TMD en juin 2025 à Montpellier.

En réunissant ces études, cette thèse démontre empiriquement que les émotions influencent le contrôle moteur à plusieurs niveaux. Dans l'interaction humaine comme dans l'IHR, l'affect module l'intensité du mouvement spontané, la stabilité fonctionnelle, la réactivité au contexte émotionnel et la durée de la synchronisation interpersonnelle. Un modèle théorique du comportement moteur affectif est finalement proposé, décrivant l'impact de l'affect sur les processus moteurs et situant les dynamiques affectivo-motrices dans des boucles de rétroaction où états affectifs et comportements se modulent mutuellement, dans divers contextes interactifs.

PUBLICATIONS

ARTICLES IN CONFERENCE PROCEEDINGS

Casso, I., Chame, H. F., Hénaff, P., & Delevoye-Turell, Y. (2024b). Exploring Engagement in Human-Robot Interaction through the Quantification of Human Spontaneous Movement. *2024 33rd IEEE International Conference on Robot and Human Interactive Communication (ROMAN)*, 1768–1773. https://doi.org/10.1109/RO-MAN60168.2024.10731439

Casso, I., Rouillard, J., Si-Mohammed, H., Betrouni, N., Cabestaing, F., & Basirat, A. (2022). Preliminary study for intonation classification of imagined speech for brain-computer interface applications. *2022 30th European Signal Processing Conference (EUSIPCO)*, 1238–1242. https://doi.org/10.23919/EUSIPCO55093.2022.9909933

ARTICLES IN REFEREED JOURNALS

Köchli, S., Casso, I., Delevoye-Turrell, Y. N., Schmid, S., Rose, D. C., & Whyatt, C. (2025). A new methodological approach integrating motion capture and pressure-sensitive gait data to assess functional mobility in parkinson's disease: A two-phase study. https://doi.org/10.3390/s25195999

CONFERENCE AND POSTER SESSION PROCEEDINGS

Casso, I., Chame, H. F., Hénaff, P., & Delevoye-Turell, Y. (2023a). *L'effet de l'oscillation dans l'interaction humain-robot* [Conference session] [Drôles D'objets – Un Nouvel Art De Faire, Nancy, FR].

Casso, I., Chame, H. F., Hénaff, P., & Delevoye-Turell, Y. (2023b). *Robot oscillation frequency impacts human engagement during human-robot interaction (hri)* [Conference session] [Rhythm Perception and Production Workshop (RPPW), Nottingham, UK].

Casso, I., Chame, H. F., Hénaff, P., & Delevoye-Turell, Y. (2024a, August). *Exploring engagement in human-robot interaction through the quantification of human spontaneous movement* [Conference session] [In *2024 33rd IEEE International Conference on Robot and Human Interactive Communication (ROMAN)* (pp. 1768–1773). IEEE].

Casso, I., Chame, H. F., Henaff, P., & Delevoye-Turell, Y. N. (2023, October). *Effects of robot oscillation frequency on human motor resonance* [Poster presentation] [3rd International Conference Timing Research Forum (TRF3), Oct 2023, Lisbon, Portugal. https://hal.science/hal-04533517].

Casso, I., Chame, H. F., Hénaff, P., & Delevoye-Turrell, Y. N. (2024, May). *Sorry i overreacted: The role of affect in the modulation of motor resonance during face-to-face interaction* [Poster presentation] [The European Society for Cognitive and Affective Neuroscience, May 2024, Ghent (BE), Belgium. https://hal.science/hal-04606872].

Casso, I., Li, B., Nazir, T., & Delevoye-Turrell, Y. (2022, August). *The effect of oscillation in human-robot interaction* [Poster presentation] [22nd Conference of the European Society for Cognitive Psychology (ESCoP), Aug 2022, Lille, France. https://hal.science/hal-04428775].

Casso, I., Violet, E., & Delevoye-Turrell, Y. (2025, July). *Exploring the role of affective compatibility on the spontaneous interpersonal coordination of dyads during static pedaling* [Conference session] [Team and Multi-agent Dynamics in Digital and Physical Realities International Workshop (TMD), July 2025, Montpellier, FR].

Köchli, S., Casso, I., Whyatt, C., Schmid, S., Ungerer, M., Delevoye-Turrell, Y., & Rose, D. (2024, February). *Functional mobility assessment in parkinson's: A pilot feasibility study and a new methodological approach* [Conference session] [Current Issues in Sport Science (CISS), 9(2), 055. https://doi.org/10.36950/2024.2ciss055].

CONTENTS

LIST OF FIGURES

LIST OF TABLES

ACRONYMS

ANCOVA	Analysis of Covariance
AP	Anteroposterior
ASA	Arm Asymmetry Angle
ASIS	Anterior Superior Iliac Spine
CNS	Central Nervous System
COP	Center of Pressure
CPG	Central Pattern Generators
DOF	Degrees of Freedom
ECG	Electrocardiogram
FMA-P	Functional Mobility Assessment for Parkinson's
FLE	Freeze-like Events
FOG	Freezing of Gait
HCI	Human-Computer Interaction
HHI	Human-Human Interaction
HRI	Human-Robot Interaction
HS	Heel-Strike
IRI	Interpersonal Reactivity Index
MANCOVA	Multivariate Analysis of Covariance
MDS-UPDRS	Movement Disorder Society-sponsored revision of the Unified PD Rating Scale
mFC	Minimum Foot Clearance
ML	Mediolateral
OMC	Optical Motion Capture
PD	Parkinson's Disease
PS	Power Spectrum
PwP	People with Parkinson's
QTM	Qualysis Track Manager
RM-ANOVA	Repeated-measures analysis of variance
RoSAS	Robotic Social Attribute Scales
SME	Spontaneous Movement Engagement

TIS	Time In Synchrony
TO	Toe-Off
TUG	Timed Up and Go

Part I

INTRODUCTION

1 MOTOR CONTROL

Human movement may appear deceptively simple at first glance. Non-disabled individuals can reach for a mug of coffee, wave hello to a friend, navigate through a crowded room, or dance to their favorite song. On the other hand, individuals with disability can adopt compensatory motor strategies to grasp objects or navigate, using unique movement patterns or assistive technologies. We are capable of a near-infinite variety of actions. How is that possible? This question has been in humans' minds since ancient Greece. Plato, with his Chariot allegory, depicted that the soul could control the body like a charioteer commanding horses.

Thousands of years later, the philosophical concept of the soul transitioned to the psychological idea of the mind. In the mid-20th century, Motor control was established as a dedicated scientific field to address the mechanics of this question.

The early years of the field often focused on the brain as the primary source of control; however, it later became clear that movement could not be understood without considering the body and the physical world in which it acts.

This has led to the contemporary definition of motor control as the study of the principles that govern the interactions between the Central Nervous System (CNS), the body, and the environment (Delevoye-Turrell & Wing, 2005; Juras & Latash, 2021).

To understand how we arrived at this integrated view, this chapter provides the reader with an overview of the early years and contemporary theories that have shaped the field of motor control.

1.1 THE FUNDAMENTAL CHALLENGE

During the 1960s, neurophysiologist and mathematician Nikolai Bernstein started the discussion with the formulation of the degrees of freedom problem.

Bernstein started studying the movement of blacksmiths, observing how they struck a chisel with a hammer. Using early motion capture techniques that he developed (kymocyclography), [1] he noticed something interesting: the path of the hammer was consistent from one strike to the next, but the joint angles

1 The kymocyclographer was a high-speed shutter camera with film that moved at a consistent speed. The movement frequency of the film could be adjusted using a rotating disk with holes, which allowed light to reach the film. This technique enabled the motion to be segmented, and since the speed of the rotating disk could be varied, the frequency at which light passed

of the shoulder, elbow, and wrist were never the same. On every repetition, the same outcome was achieved with different biomechanical strategies (Bernstein, 1967; Bongaardt & Meijer, 2000). This phenomenon led Bernstein to affirm that any whole-body motor task can be performed with an unlimited number of possible solutions as a function of the degrees of freedom (Prilutsky & Zatsiorsky, 2020).

In biomechanics, the degrees of freedom DOF are "the number of independent ways a body or system can move in space" (Z.-M. Li, 2006). Going back to the observation of blacksmiths' arm movement, joints like the shoulder have 3 DOF, for movement in three dimensions (flexion-extension, abduction-adduction, and rotation). The elbow and wrist have 2 DOF each [2]. Hence, to strike a chisel with a hammer, the total amount of possible DOF of the arm increments between 6 and 7 DOF. The task can be performed with an unlimited number of muscle activations and force patterns.

The DOF problem stated that if the CNS had to consciously specify and control every single one of these variables for every moment, the "computational load" would be astronomically high, making the simplest movement an overwhelming task (Turvey, 1990).

This concept shifted the scientific perspective. Motor control's main question became a complex challenge of coordination and organization (Bongaardt & Meijer, 2000). The degrees of freedom remain a central question that every major theory of motor control has sought to answer. The early cognitive models, the dynamical systems approaches, and the optimal control frameworks that we will briefly review in this chapter possess at their core possible solutions to the puzzle that Bernstein defined nearly a century ago.

1.2 THE EMBODIED AND SELF-ORGANIZING SYSTEM

The notion of Dynamical Systems emerged through strong influences coming from natural observations in physics and biology. The central question here was: How does coordinated action emerge from the complex interactions within the system itself?

The Dynamical Systems approach focused on the bottom-up perspective, arguing that movement properties do not need to be explicitly embedded in a central motor control program. It proposed instead that actions are a natural consequence of the physical body interacting with the environment (Costa, 2000; Friston, 1995; Kelso, 1995).

This theoretical framework was influenced by the concept of ecological psychologist J.J. Gibson (2014). Ecological psychology rejected the separation

---

through the disk served as a sampling frequency. This sampling frequency could range from 60 Hz to 500 Hz, providing the system with high spatiotemporal resolution.

2 Flexion-extension and pronation-supination for the elbow, flexion-extension and radial-ulnar deviation for the wrist

of mind and body, as well as perception and action. Instead, he proposed that the organism (i.e., body and brain) and the environment are a fundamental unit of analysis (Lobo et al., 2018). For Gibson, an organism would collect information about the world (i.e., affordances) without cognitive mediation, thereby reducing the computational burden on the brain to determine its actions. Thus, behavior would emerge from the organism's capacities and the constraints imposed by the environment.

Kelso applied this notion to coordination, demonstrating that movement patterns and transitions emerge naturally from system dynamics. A classic example is the spontaneous transition between coordination patterns. Participants moved their index fingers rhythmically from side to side, typically starting with an anti-phase (i.e., alternating) pattern. When asked to increase the frequency (i.e., speed) of movement, a critical point was reached where the participant's fingers spontaneously shifted into a less complex, in-phase pattern, moving both fingers in the same direction. This shift emerged without conscious instruction; it was an emergent property of the system (i.e., the participant) settling into a more stable state that was efficient in terms of energy. This demonstrated that complex motor behavior, like the flocking of birds, could self-organize (Haken et al., 1985; Kelso, 1981, 1984).

1.3 THE COMPUTATIONAL BRAIN: FROM MOTOR PROGRAMS TO OPTIMAL CONTROL

In response to the complexity of the DOF problem, a major theoretical solution emerged from the intersection of cognitive psychology and computer sciences: perhaps the brain's control of the body was achieved through the execution of a previously defined algorithm. This was the main idea proposed by the motor program theory, a stored set of commands that could be recovered to produce a specific movement and would be "uninfluenced by peripheral feedback" (Keele, 1968) (p. 387). For example, when an individual decides to reach for their cup of coffee, their brain would execute the "pick coffee" motor program.

Richard Schmidt refined the motor program concept in 1975, proposing the Generalized Motor Program (GMP) or Motor Schema theory (R. A. Schmidt, 1975). Schmidt recognized that storing a separate program for every possible variation of an action would create a critical storage problem. The GMP considers that the brain stores a general template for a class of movements. Constant parameters of the general template would be muscle activations and their relative activation timing. The template would then be modified as a function of the specific target or goal of the movement, such as the arm force or speed required to grab the coffee cup. The GMP was a simplified solution to Keele's theory, where the main task for the brain was to determine the specific parameters that would adapt the existing stored motor program to specific physical goals.

However, the top-down concept of the brain as an executive unit faced criticism. In the motor program framework, the CNS does not consider real-time feedback from the body or the environment, accounting only for discrete movements (e.g., flipping a light switch, pressing a key on a piano) and leaving continuous, long-duration actions that need "response-produced feedback" (e.g., riding a bicycle, juggling) outside the scope of the theory, which Schmidt himself acknowledged in his 2003 paper (R. A. Schmidt, 2003).

Emmanuel Todorov proposed an alternative approach, Optimal Control Theory, to address the DOF problem from the perspective of engineering and mathematics. This framework proposed that the CNS, instead of retrieving a stored program, actively computes the best possible motor solution to achieve a goal, through the selection of motor commands that optimize (minimize) a cost function (Todorov, 2004). The cost function quantitatively assesses the performance of the musculoskeletal system. At any given time point, this cost is represented as a single scalar value that depends on the current state of the system (e.g., joint angles and velocities) and the control signals being applied (e.g., muscle activations). The total cost for an entire movement is calculated by integrating over time the instantaneous costs from the start to the end of the movement. An optimization model can be defined and named by the specific cost function to be minimized. Common examples include minimizing energy expenditure, movement duration, variance, or jerk [3](Berret et al., 2011).

This approach was illustrated by the minimum-jerk model decades before by T. Flash and N. Hogan (Flash & Hogan, 1985). The authors focused on arm movement due to its complexity. A multi-joint movement, such as reaching with the arm, demands the CNS to select one specific trajectory from a nearly infinite number of possibilities. They hypothesized that the CNS organized and coordinated the arm movement to produce the smoothest possible trajectory. This was formalized through an optimization problem to determine the unique trajectory that would minimize a specific cost function, the integral of the squared magnitude of jerk across the entire arm path. The optimization concerned only the hand kinematics on a 2D horizontal plane. During the experiments, participants were asked to move a handle from one target to another as soon as the second target was illuminated (Abend et al., 1982). The minimum-jerk model accurately predicted the hand trajectories and tangential velocities regardless of the joints involved. These studies provided evidence that trajectory planning occurs at a kinematic level, with the CNS specifying the desired energy cost of a hand trajectory rather than predefining a series of individual joint angles.

3 Jerk is the rate of change of acceleration and serves as a mathematical measure of movement smoothness

Figure 1.1
The Basic Internal Model

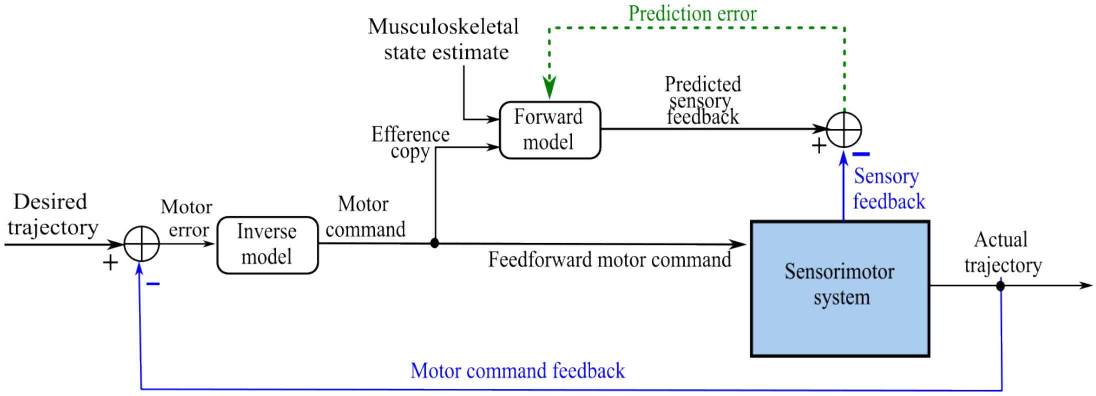

Note. Schematic of the internal model for motor control, adapted from Wolpert et al. (1998) The inverse model (i.e., controller) generates a motor command, while the forward model (i.e., predictor) anticipates the sensory outcome of that command.

The choice of minimal functions can be arbitrary, and the outcomes can be highly dependent on the choices made, which may not always correspond directly to biological reality. Moreover, traditional optimal control approaches (i.e., open-loop formulations) often overlook the role of sensory feedback. Indeed, real-time adjustments are common during movement control (Wolpert & Landy, 2012).

The work of Daniel Wolpert and colleagues integrated the dynamical system framework with neuroscientific methods. They postulated that the brain, specifically the cerebellum, performs two distinct related computational functions or internal models to control movement: the inverse and the forward models (Wolpert & Flanagan, 2001; Wolpert & Landy, 2012; Wolpert et al., 1998).

The inverse model has a controller function, providing the motor command that achieves the desired goal to the sensorimotor system. This model is crucial for fast, coordinated movements due to the time delays between sensory input and motor output. This is considered a feedforward command for accurate movement execution. The inverse model receives a feedback signal from movement execution to learn which motor commands accurately reach the desired state or trajectory (see Figure 1.1).

The forward model has a predictor function; given the current state of the musculoskeletal system and the outgoing motor command (also called efference copy, see Figure 1.1). It predicts the next state and the resulting sensory feedback that should be received by the CNS in time.

This sensory prediction is then compared to the actual sensory feedback received by the CNS. Any difference between the two creates a sensory prediction error. This error signal drives motor learning, allowing the system to constantly update and refine the forward model to become more accurate. By

Figure 1.2

The Multiple Paired Forward-Inverse Model Architecture

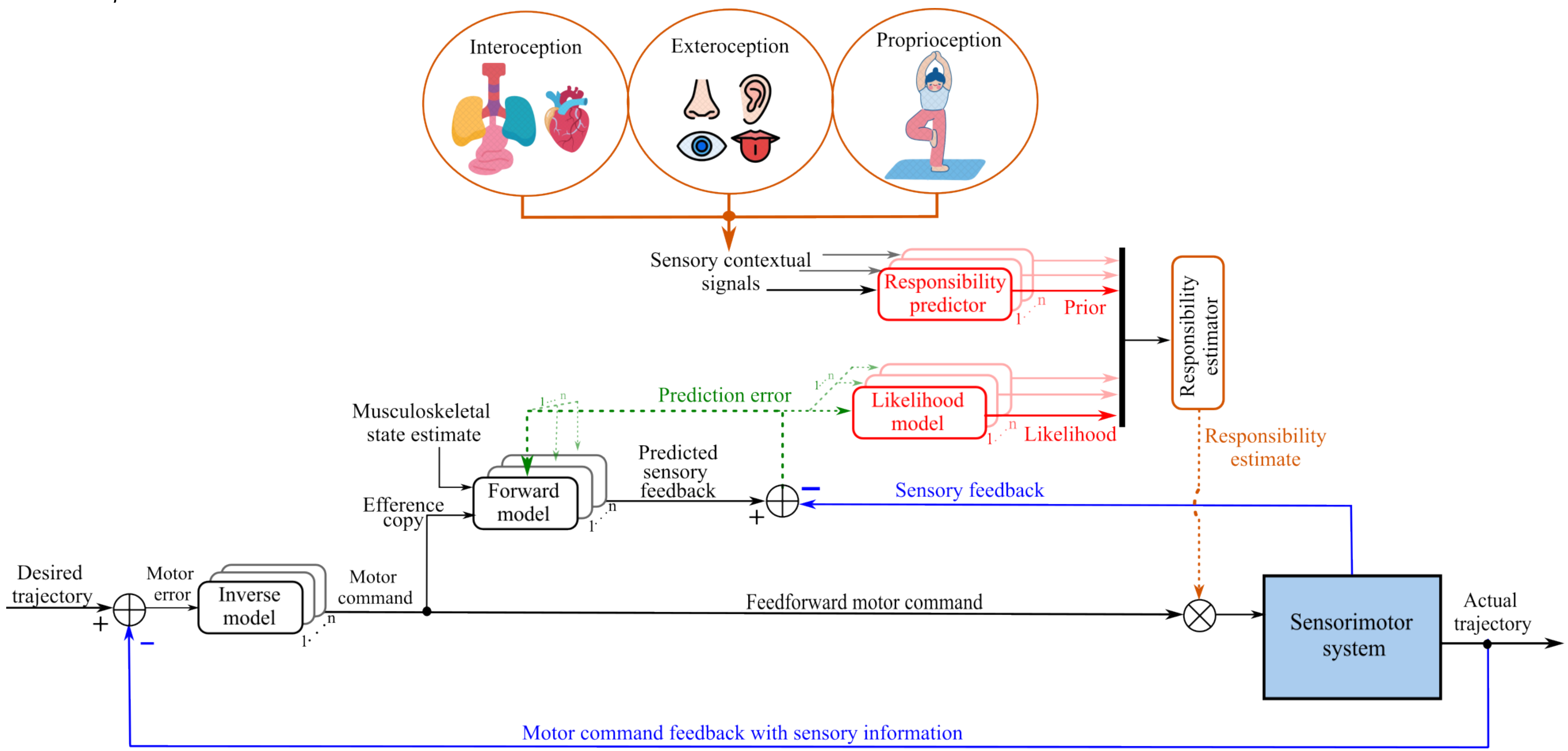

Note. Schematic adapted from Wolpert et al. (1998). This modular system consists of several inverse models, each coupled with a forward model to control movement in different contexts. The selection of the appropriate controller is governed by a *responsibility estimate*, which is calculated for each module. This estimate combines a *prior*, generated from contextual cues before movement execution, with a *likelihood*, calculated from the forward model's prediction error during movement. The final feedforward motor command is a weighted sum of the outputs from each inverse model, where the weight assigned to each module corresponds to its responsibility estimate.
(Icons: Abhiromsawat (2025), Glyphinder (2025), and Studio (2025))

predicting the outcome of a movement faster than the actual feedback arrives, the cerebellum may produce rapid corrections and may provide the means to maintain smooth, precise control, especially during fast movements.

Theoretically, a single pair of a forward and inverse control model can adapt to a single task. However, humans are capable to adapt motor actions not only to different and uncertain environmental conditions but also to changes in the body's own state. To account for this adaptability, Wolpert et al. (1998) proposed a modular approach stating that the cerebellum contains multiple modules of paired inverse and forward models (see Figure 1.2). Thus, depending on the environmental and bodily context, only the appropriate modules intervene in the motor command generation.

The modular architecture consists in several inverse models to control the system each coupled to a forward model that determines which (inverse) controller should be responsible for the current movement (Wolpert et al., 1998). This selection process relies on two processes to calculate a final responsibility estimate for each module: the responsibility prediction and the likelihood calculation.

RESPONSIBILITY PREDICTION During this process a prior is generated before the movement begins, which relies on *sensory contextual signals* to predict which module is most appropriate for the upcoming task (see Responsibility predictor in Figure 1.2). The sensory contextual signals come from multiple sensory processes that can be grouped into three broad categories: interoceptive, exteroceptive, and proprioceptive signals (Ceunen et al., 2016; Chen et al., 2021).

- Interoceptive signals are information of physiological states, gathered from internal organs such as the heart, lungs, and viscera (e.g., heart rate variability, breathing rate, bladder fullness).
- Exteroceptive signals are information coming from "outside of the body" such as vision, audition, olfaction, and touch. They provide information of the environment (e.g., appearance of an object, loud alarm, unpleasant odor).
- Proprioceptive signals are feedback information of the body's position in space and balance, gathered from muscles, joints, and skin.

LIKELIHOOD CALCULATION During this process, a likelihood is calculated for each module, which relies on the prediction error of it's corresponding forward model (see Likelihood model in Figure 1.2). A smaller error will indicate a higher likelihood that an individual module accurately represents the current context.

Finally, the Responsibility estimator combines the prior and likelihood signals to estimate the module's responsibility. The final feedforward motor command is a weighted sum of the motor commands produced by each inverse model. The weight of each module is determined by its responsibility estimate.

To illustrate the modular architecture of the predictive processing framework, let us consider the following example. Imagine an individual embarking on a hiking trip in the mountains. For simplicity, let us suppose this individual possesses three internal modules for motor control: "High-energy walking," "Tired walking," and "Slippery path walking", each with their corresponding pair of inverse and forward models.

SCENARIO 1 : HEALTHY AND RESTED HIKER The hiker has arrived to the initial point of their trip, they are full of energy ready to start.

- **Sensory context and priors:** The sensory contextual signals receive interoceptive information reporting no fatigue or pain. Proprioceptive signals report a normal posture. The responsibility predictor uses these signals to generate a high prior probability for the "High energy walking" module and low priors for the other two modules (Tired, Slippery).

- **Sensory predictions and likelihood:** To start walking, the "High energy" inverse model generates the motor command, that is also sent to the corresponding forward model (efference copy). Using the efference copy and the musculoskeletal state estimate, the forward model predicts sensory consequences that have been learned from previous walking steps healthy, high energy conditions (e.g., certain level of muscle activation, hear rate increase).

  Since the hiker is healthy and well rested the sensory feedback coming from the sensorimotor system is accurately matched by the prediction. This results in a negligible prediction error and the likelihood model assigns a high likelihood probability to the "High energy" module.

  Concurrently the "Tired" and "Slippery path" inverse models have also sent out their efference copies to their respective forward models for them to produce their own sensory predictions. However, the sensory feedback is far from the Tired and Slippery path predictions, resulting on a high prediction error. Given the individual is not Tired nor sensing a Slippery path both modules will have low likelihood probabilities.

- **Responsibility estimation:** The responsibility estimator combines the prior and likelihood probabilities from all modules, resulting in a high responsibility estimate for the "High energy" module and low probabilities for the other two modules.

- **Control and learning:** Since the "High energy" module has the highest responsibility estimate among all modules, the motor command coming from its respective inverse module will determine the final action. Conversely, the motor commands from the "Tired" and "Slippery" modules will have a low responsibility making their influence on the final motor command negligible.

The small sensory prediction error confirms the accuracy of the (musculoskeletal) state estimate and efference copy. Thus, the prediction error functions only as a fine tuning signal of the "High energy" forward model.

Since the state estimate is accurate, the actual trajectory will be nearly as exact as the desired trajectory. Consequently, the motor error resulting of the comparison of both actual and desired trajectories will be negligible. The motor error will act only as a fine tuning signal of the "High energy" inverse model.

The other modules remain unchanged, since the learning signals are specific to the relevant module and do not apply to them.

SCENARIO 2: TIRED HIKER After a few hours hiking, the physiological state of the individual has changed. They are experiencing fatigue, but must continue walking the hiking path.

- **Sensory context and priors:** The contextual cue is now receiving an interoceptive information reporting muscle fatigue and low energy. The responsibility predictor sues this signal to accord a high prior probability to the "Tired walking" module. Thus, the priors of "High energy" and "Slippery path" modules are now low, as the brain is anticipating the need to adopt a energy-saving gait.

- **Sensory predictions and likelihood:** The "Tired" inverse model generates a motor command for a slower pace (learned from previous low-energy walking steps). The efference copy sent to the corresponding forward model predicts the sensory consequences from walking while energy is low (e.g., muscle strain). Since the hiker is indeed tired, the sensory feedback will match this prediction. The result will be a small prediction error and a high likelihood probability for the "Tired" module.

  Conversely, the other two forward models receive their efference copies and own predictions. The "Healthy" and "Slippery path" predictions are highly inaccurate as the hiker has a feedback of high muscle strain and a stable ground.

- **Responsibility estimation:** The responsibility estimator combines all received priors and likelihoods and determines a high responsibility estimate for the "Tired" module, while the other two modules receive negligible estimates.

- **Control and learning:** Since the "Tired" module has the highest responsibility estimate, the motor command from its inverse model (e.g., slower energy-saving pace) will determine the final action. The influence of the other two modules is negligible.

  The small sensory prediction error of the "Tired" module serves to fine-tune its forward model. Since the sensory context was correctly predicted the actual trajectory will be as close as the desired (slower) trajectory, resulting in a minimal motor error. This error will fine-tune the "Tired" inverse model.

SCENARIO 3: SLIPPERY PATH The hiker, already experiencing fatigue, encounters slippery mud on their path. This situation presents two simultaneous contexts, an internal state of fatigue and an external environmental perturbation.

- **Sensory context and priors:** The context is not composed of interoceptive signals reporting fatigue, and exteroceptive visual signals reporting an unstable ground. Based on these cues the responsibility predictor generates a high prior probability for both "Tired" and "Slippery path" modules. Whereas the "High energy" prior is low.

- **Sensory predictions and likelihood:** As the hiker plans to step onto the mud, the "Tired" and "Slippery path" forward modules have generated their sensory predictions (e.g., high muscle strain, instability). The sensory feedback of the first step in the mud confirms these predictions. The likelihood model will accord high probabilities to these two modules.

- **Responsibility estimation:** Considering the high probabilities (prior and likelihoods) of both "Tired" and "Slippery path" modules responsibility estimator will distribute the weight of estimate between these two. For example, it might assign more weight to the "Slippery path" since there is potential fall risk.

- **Control and learning:** The final motor command will be the weighted sum of "Tired" and "Slippery path" modules, that is focused on motor stability and energy preservation. The potential motor errors are distributed to both modules, allowing them to learn a context where fatigue and ground instability are combined.

The internal model framework provides a mechanistic account of motor control and learning. On this approach, motor control is driven by the sensory input obtained from environment and the internal state of the body. The concepts of predictive processing were primarily examined in a neutral context, but we are emotional beings. This raises an important question. How do our affective states, such as fear or joy, influence our motor behaviors?

2 CORE AFFECT AS A MODULATOR OF ACTION

Emotion was already a research topic in the 19th century, with Darwin in 1872, arguing that emotional expressions are innate and evolved, common among humans and shared with other animals.

However, the role of emotions and affective phenomena has been largely overlooked in the early years of cognitive and behavioral sciences during the 20th century.

The Cognitivism approach emerged around the 1950s from the integration of cognitive processes into models of behavior, brain function, and the mind. These models seek to explain how cognitive processes shape both behavior and cognitive phenomena.

During this period, affective processes were considered as unmeasurable phenomena void of information for research questions, leading to their exclusion to minimize noise in data (Dukes et al., 2021; Mandler, 2002). This "cold" approach led cognitivist researchers to design experimental tasks that were simplified to reduce the side effects of participants' feelings to form homogeneous sample groups (Jones et al., 2015; LeDoux & Brown, 2017).

Around the 1960s, the study of affective phenomena began to gain momentum and has continued to grow in recent years. In their article "The rise of affectivism", Dukes et al. (2021) argue that the inclusion of affective processes in models of behavior, brain, and mind would actually complement Cognitivism, enhancing its explanatory and predictive power.

Although there is ongoing debate on the definitions of affective phenomena, their definition and distinction, the development of affective science has enhanced our understanding of how the brain interprets the environment and how it shapes our interactions with the world.

My thesis adopts an affectivist perspective, arguing that motor control cannot be fully comprehended without considering the continuous, modulatory influence of affective states on movement components. To develop this argument, this chapter will first establish a clear differentiation between the terms affect, emotion, and mood that are often used interchangeably. The second section will detail the theory of core affect, grounded in the neurobiological principle of allostasis and interoception. In this framework affect acts as a barometer for the body's internal state. The third section will connect this neurobiological account to motor control. Finally, I present empirical evidence demonstrating how these internal states may modulate behavior.

2.1 AFFECT, EMOTION, AND MOOD, THE GORDIAN KNOT

At present, there is no clear consensus over the definition of affect, emotion, and mood, described as a "terminological Gordian knot" by Ekkekakis (2013). These three concepts are often used interchangeably and inconsistently across several branches of psychology, resulting in even less agreement on how to assess and measure them effectively (Batson et al., 1992; Fox, 2018). Studies have drawn inconsistent results due to unclear distinctions between these constructs. For example, the term 'mood' is sometimes used, but the measurement focuses on emotional reactions (Beedie et al., 2005).

To "untangle the knot", this section presents a summary of the definitions given in the comprehensive guidebook by Ekkekakis (2013). The main features of each concept are condensed in Table 2.1.

Table 2.1
Distinctive features of Affect, Emotion, and Mood

FEATURE	CORE AFFECT	EMOTION	MOOD
Intentionality	"Free-floating", not necessarily directed at something	Oriented at something specific	Often objectless or general in nature
Duration	Continuous, always present	Short-term*	Long-term*
Intensity	Variable	Typically high	Typically low
Components	Valence (pleasure, displeasure) and arousal (energy, lethargy)	Core affect, appraisal, physiology, behavior, etc.	Core affect with mild physiology, behavior features
Causation	Always present	Triggered by a specific perceived event/object	Often diffuse, remote, or unidentifiable

Note. Adapted from Ekkekakis (2013, p. 47). * Emotions are defined to have short durations (from seconds to minutes), while moods are defined as lasting from hours to days. However, both phenomena have exhibited high variability in empirical studies. This distinction is therefore more conceptual than empirical (Brans & Verduyn, 2014).

2.1.1 *Core Affect*

Core affect is a neurophysiological state that can be consciously accessible as a simple affective feeling that does not need to be directed at anything (Russell, 2009). For instance, one might feel good or bad, or experience sensations of lethargy or energy. Core affect is experienced constantly, with its nature and intensity varying over time. It is related to changes in the autonomic system, motor and vocal behaviors, cognitive processes, and reflexes (Russell, 2003; Russell & Barrett, 1999). Affect can occur as an isolated phenomenon. However, core affect is a component of emotion and mood, impacting both independently. It can change rapidly in emotion or remain constant in mood (Sander & Scherer, 2009, p. 104).

2.1.2 *Emotion*

Emotion is also a phenomenon that unfolds over time. However, it is directed at a particular object, person, or event through a process of cognitive appraisal [1] (Frijda & Scherer, 2009; Russell, 2009). Concerning its duration, emotion is a discrete phenomenon with a defined beginning and end (Russell, 2003). According to component process models, a prototypical emotional episode is a set of synchronized psychological events (Scherer, 2005, p. 697):

- A rapid change in core affect
- The involvement of cognitive processes, including appraisal of the object's relevance and attributions about its cause
- The emergence of physiological changes in the autonomic, neural, and endocrine systems
- Congruent behavioral responses (e.g., fight, flight, or facial expressions)
- Explicit categorization of the event as a specific emotion that can be encoded into memory

According to the theory of constructed emotion, the emotional concepts are not innate but are constructed through our culture and life experiences. Our brain uses the prototypical patterns and constructed concepts to interpret incoming sensory information from our body and the environment, allowing us to make sense of our emotional state like anger or joy (Barrett, 2016).

An example extracted from Russell (2003), uses the word "pride:

"Pride can be thought as a feeling good about oneself. The 'feeling good' is core affect and the 'about oneself' is an additional cognitive component"(p. 148), making of pride an emotion (Ekkekakis, 2013, p. 39).

1 Appraisal is a process by which individuals perceive and evaluate the significance of the environment in relation to their personal concerns that includes needs, values, goals, and beliefs (Moors et al., 2013; Scherer, 2005)

2.1.3 *Mood*

The main characteristic of mood is its duration and intensity. Considered as a prolonged core affect (Russell & Barrett, 1999), mood is generally lower in intensity compared to emotional episodes (Oatley et al., 2006, p. 30). Mood is not directed at anything (e.g., being irritable about everything). Its cause can be temporally remote and not easily identifiable (Ekman, 1992; Frijda & Scherer, 2009; Russell, 2003). The primary function of mood is to modulate cognition over longer timescales (Davidson, 1994; Ekkekakis, 2013).

To further elucidate the differences between the terms presented so far, let us consider the word "sad". If we receive bad news from someone, we may feel sad, cry, and hug the person who gave us the news. This is a prototypical emotional episode. Now if at a random point of the day, we feel sad for no specific reason, this is a mood change. Both phenomena involve core affect, which is at the root of the observable changes.

In the previous sections, we focused on clearly distinguishing between affective phenomena. Based on these definitions, the following section will explore the theoretical framework that may be used to examine affective motor behavior.

2.2 THE THEORY OF CORE AFFECT

To understand core affect, we first need to grasp the concept of allostasis. Allostasis is a predictive control process by which the brain regulates the body's internal states (i.e., performs physiological or behavioral adjustments). This mechanism is essential to anticipate needs and prepare the body before they arise, ensuring efficient energy expenditure (Sterling, 2012)[2].

For the brain to effectively perform allostasis, it must maintain and update an internal model of the body's physiological state. This internal model is referred to as core affect, a neurophysiological state continuously updated with interoceptive and exteroceptive signals. A large-scale intrinsic brain network, also called the limbic system[3] is responsible for integrating the interoceptive signals to implement allostatic regulation (Terasawa et al., 2013). This network serves as a bridge between bodily regulation (physiological changes) and conscious feeling(Barrett, 2016).

An affective state is consciously accessible over two fundamental dimensions: valence, a continuum between pleasant and unpleasant feelings, and arousal, a continuum between activation and deactivation. (Russell, 1980).

2 Through allostasis, the body adjusts physiological or behavioral parameters to achieve a homeostatic balance, which is the stable state of internal conditions essential for survival.

3 Studies have identified the anterior insula and anterior cingulate cortex (ACC) as part of the interoceptive/allostatic system (Kleckner et al., 2017)

Figure 2.1
Affective Predictive Model

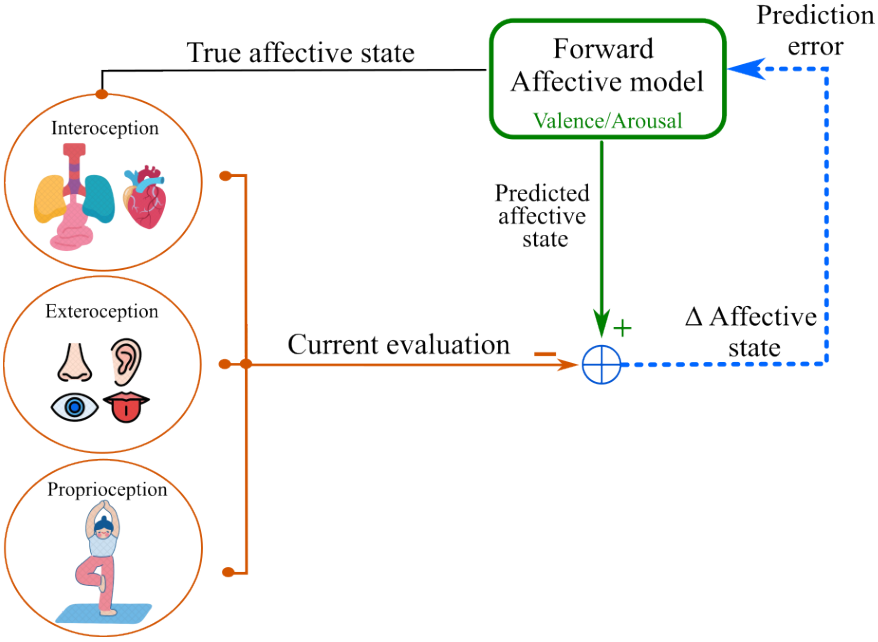

Valence serves as a measure of physiological well-being. A feeling of pleasure encodes a state a state of equilibrium in the body's resources (i.e., metabolic efficiency). A feeling of displeasure signals an allostatic imbalance that is either present or anticipated (e.g., deficit, injury, or threat) that requires correction. Arousal reflects the brain's prediction of the energy that will be required for the upcoming state. High arousal corresponds to a state of mobilization that prepares the body for possible energy expenditure (e.g., to fight or to flee). Low arousal corresponds to a state for which minimal energy expenditure will be possible (Barrett, 2016).

Core affect can be conceptualized as a continuous predictive loop (see Figure 2.1). The brain's forward affective model integrates interoceptive signals (*True affective state*) and generates an affective state prediction (Barrett & Simmons, 2015; Feldman et al., 2024; Satpute et al., 2015). The incoming interoceptive and exteroceptive signals are compared against this prediction (Seth, 2013). The resulting prediction error is used to update the brain's affective model and maintain efficient allostasis. This updating process is experienced as a change in affective state (Barrett, 2016; Lee et al., 2021).

2.2.1 *Measuring affect*

The circumplex model of core affect proposed by James Russell (1980) suggests that the two dimensions of affect can be represented following a two-dimensional space, where valence is plotted on the x-axis (horizontal) and arousal is plotted on the y-axis (vertical). Within this framework, any affective state can be located in one of four quadrants, as presented in Figure 2.2:

- High arousal, positive valence
- Low arousal, negative valence
- High arousal, negative valence
- Low arousal, positive valence

In 1989, J. Russell developed the affective grid based on the circumplex model, a tool that has gathered consensus for affect assessment. This two-dimensional grid allows researchers to gather self-reported affect in terms of valence and arousal (Russell et al., 1989). Figure 2.2 presents examples of the use of this tool.

Figure 2.2
Affect grid

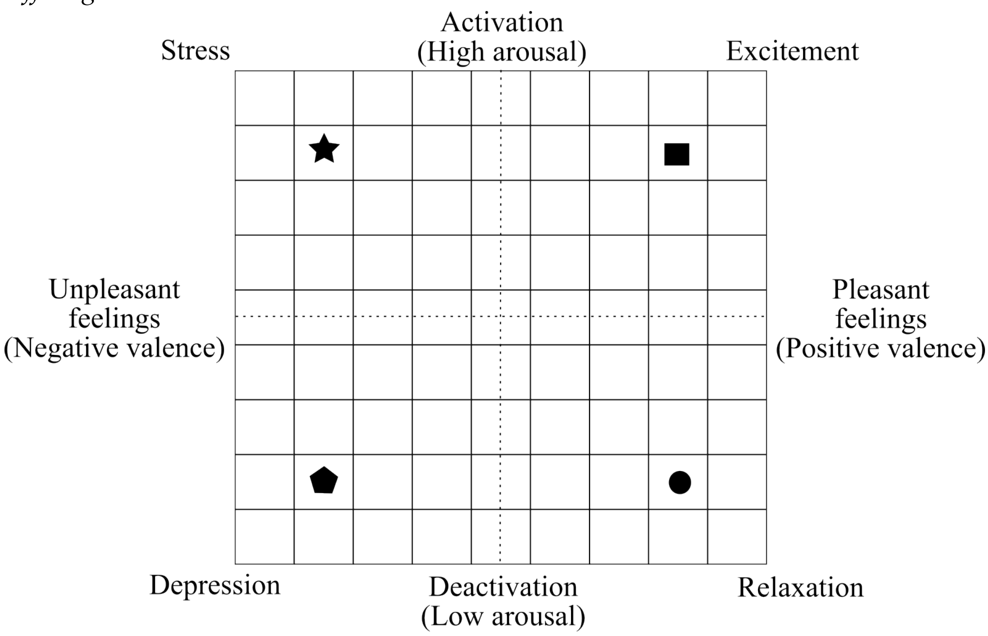

Note. The affect grid, with examples illustrating different core affect responses placed in the two-dimensional model. If we find ourselves in a busy and loud metro station at 8 a.m., then we would be in a negative state of high arousal, marked with a star. If we were at the beach listening to the waves, we would be in a positive state of low arousal, marked with a circle. If we were at a concert of our favorite artist, we could be in a positive state of high arousal, marked with a square. Finally, if we were to lose a pet, we would be in a negative state of low arousal, marked with a pentagon. Figure adapted from Brossard (2022, p. 9).

In our research team, we have developed a variation of the affect grid with numbers in order to be able to use it with either a single or a group of participants, which will be presented in the following Chapter.

2.3 AFFECT AND ACTION

Chapter 1 concluded with the examination of the work of Wolpert and colleagues, which established that the brain applies predictive models to control movement and learn from sensory errors (Wolpert & Flanagan, 2001; Wolpert et al., 1998). This section builds upon that foundation to argue that affect is a key element in the initiation and modulation of the predictive sensorimotor control loop.

Frijda and Mesquita (1994) introduced the concept of "action readiness", suggesting that emotion prepares an individual for action after being triggered by an event appraised as relevant. Ridderinkhof (2017) later integrated this perspective with the predictive coding theory, proposing that core affect is the driver for action regulation as it summarizes the internal state of the body and its relationship with the environment.

In affective science research, the notion of affect as a modulator of motor control has mostly been investigated through avoidance and approach behaviors. To illustrate the point, let's consider a few examples.

When confronted with a threatening situation, core affect transitions to a state characterized by negative valence and high arousal. This change triggers a defensive responses, preparing the body for fight-or-flight or to freeze, but it may also induce freezing which is a response characterized by inhibited movement.

This phenomenon was experimentally demonstrated by Roelofs et al. (2010) and Noordewier et al. (2020). The experiment consisted on exposing participants to emotional facial expressions while standing on a force plate to measure their body sway. Their results showed that the exposure of participants to angry faces led their body sway to be significantly reduced compared to happy or neutral ones.

Departing from traditional paradigms of approach and avoidance behavior, studies have also focused on the kinematic and body posture characteristics associated with affective states.

Studies on gait and locomotion have shown that participants who reported being in negative states of low arousal (e.g., sadness) exhibited lower walking speed, shorter step lengths, and reduced coordination between upper and lower limbs, accompanied by a slumped or stooped posture, that is, a forward flexion of the neck and trunk (Gross et al., 2012; Homagain & Martens, 2023). Conversely, participants in positive states of high arousal (e.g., joy) exhibited increased walking speed and a stable cadence while adopting an upright head and trunk postures (Brossard, 2022; Halovic & Kroos, 2018). Moreover, participants who experienced negative states of high arousal (e.g., anger) exhibited increased arm-foot coordination and feet jerk while also adopting upright postures (Brossard, 2022; Roether et al., 2009).

Similar effects of negative states of low arousal have been observed beyond gait. For instance, Wamain and Delevoye-Turrell (2015), in a static cycling experiment, reported that the head tilt was significantly lower while listening to sad music extracts.

The influence of affect had also been observed in discrete movements like knocking and drinking from a glass. Studies from Gross et al. (2010) and Pollick et al. (2001), found that high arousal emotions (e.g., anger) are associated with faster, high jerk (i.e., less smooth) movements. In contrast, low arousal emotions (e.g., sadness, calmness) are associated with slower and smoother movements.

In addition to the influence of affect on movement execution within individuals, there is empirical evidence that the emotional context of interaction can modulate action at the interpersonal level. For example, in their study on non-verbal cues of deception Zee et al. (2019), a group of participants was instructed to tell the truth or to lie during interviews while their whole-body movements were quantified. Self-reported emotion results show participants who lied felt more anxious, fearful, and guilty than those who told the truth (in the affective grid, these could be negative valenced states of moderate to high arousal), and exhibited increased movement of limbs, head, and torso. Extending this interpersonal perspective, Chang et al. (2021) carried out a speed dating experiment to evaluate romantic interest through body sway. Results show that the coupling of body sway signals of dyads can predict interest in a romantic relationship. This study also highlights that behavioral synchronization may reflect affective attunement between partners during interaction.

The evidence reviewed so far suggests a one-directional relationship where affect modulates movement; however, a complementary line of research suggests that the relationship may be bidirectional. Empirical evidence indicates the possible existence of a sensorimotor control loop in which the execution of movements and postures can provide sensory feedback that influences affective states. Shafir et al. (2016), for instance, instructed participants to perform movements that denoted happiness (e.g., jumping), and found an increase of positive valence among participants. Concurrently, Wilkes et al. (2017) instructed a cohort with mild-to-moderate depression to adopt an upright posture. Participants who adopted an upright posture reported greater positive valence states of high arousal, compared to a control group. This may explain the therapeutic effects of practices like dance therapy, which show that the execution of specific motor patterns (e.g., jumping, raising the arms) increases feelings of positively valenced affect, while decreasing the occurrence frequency of negative affective states. Together, these findings suggest that the sensory consequences of posture and movement can regulate affective states.

2.4 THE PRESENT RESEARCH PROGRAMME

With this chapter we established the theoretical basis of predictive motor control and core affect. My thesis integrates these frameworks to propose that core affect is a modulator of the motor control loop.

Specifically, my work aimed to investigate how affective state changes influenced actions during social and human-robot interaction contexts. We tested the hypothesis that induced affective states the dynamics of spontaneous human movement and tempo. Motion time-series data were used to test the hypothesis that induced affective states can change spontaneous human movement and tempo. In Chapter 3, the general methodological considerations of the present research programme are presented. Chapters 4-7 contain the experimental contributions. Specifically, in Chapter 4, a specialized methodology for kinematic analysis was established, using the motion capture data to provide a functional mobility assessment in Parkinson's Disease. In Chapter 5, wavelet analysis of 3D motion data was used to quantify human spontaneous oscillations during Human-Robot Interaction (HRI). In Chapter 6, the developed technique for spontaneous movement quantification was used to assess how the affective context of HRI modulated human behavior. In Chapter 7, analysis of pedaling motion was used to evaluate how the affective compatibility between two humans influences their time spent in synchrony. Finally, Chapter 8 provides a general discussion of the experimental findings and theoretical contributions of the research conducted throughout this programme.

Part II

GENERAL METHODOLOGY

3 METHODOLOGICAL CONSIDERATIONS

The main research question of my thesis was to understand the link between human motion and affective states. In human-robot interaction, we aimed to understand fright or flight reactions or engagement in humans based on their spontaneous movement and whether these reactions depend on emotional context or affective states. Finally, we aimed to understand how affective compatibility between dyads can influence interpersonal coordination in human interaction. In all these cases, the questions required analyzing and quantifying human movement.

The methodological approach involved acquiring kinematic data and applying preprocessing and analytical tools tailored to answer the specific queries. In this chapter, I will first present the practices for code management that allowed me to develop analysis programs. I will discuss code version control with online repositories like GitHub, as well as proper structure and annotations for public repositories.

Section 3.2 is dedicated to the selected technology for human movement analysis, as well as methodological practices to ensure quality data acquisition. In Section 3.3, I explain how to initiate the manipulation of motion data, practical preprocessing methods, and detecting acquisition noise and participant-originated artifacts. The following sections explore the use of motion data in biomechanical analyses to assess functional mobility, particularly in the context of motor impairment detection for People with Parkinson's disease (3.4.1). Next, I present a method for spontaneous body oscillations quantification using spectral analysis of motion data (3.4.2). In the following section (3.4.3), I describe a method for the quantification of interpersonal motor synchronization. Finally, in Section 3.5, I specify how affective states were assessed across the different studies.

3.1 CODE MANAGEMENT

When handling dozens of data files, complex scripts, and evolving analyses, things can get messy. One of the most valuable habits I developed during my thesis was treating my code and data as if someone else would need to use them tomorrow (often, that someone was future me). This section shares how I used version control, structured my codebase, and prepared for open sharing to make my workflow as reproducible and accessible as possible.

Version control with Git and GitHub was important to manage my analysis code. Git is a version control system that allows you to keep track of file changes over time, similar to a detailed project timeline. GitHub is a cloud-based platform where version control repositories can be stored, shared, and collaboratively edited. This setup was advantageous when I needed to change analysis strategies, test preprocessing steps, or withdraw changes that didn't work as expected. Using Git, I saved my changes incrementally and annotated each update. Hosting these repositories on GitHub also made documenting the code easier, receiving feedback from colleagues, sharing with students working on my projects, and preparing materials for open access sharing.

Concerning open access and the creation of public repositories, the Open Science MOOC provided me with valuable guidelines for making research software more accessible and reusable (Tennant et al., 2019). Following its recommendations, I implemented several best practices in my repositories, including a README file and a license file. I provided dedicated documents that outline contribution guidelines and a code of conduct. For the code of conduct, I adopted the Contributor Covenant, a widely recognized template that promotes inclusive and respectful collaboration ("Contributor Covenant: A Code of Conduct for Open Source and Other Digital Commons Communities," n.d.). These elements helped my public repositories apply open science principles of transparency and reproducibility.

3.2 MOTION CAPTURE TECHNOLOGY

Optical motion capture (OMC) is an optical technology used to record the movements of objects or humans and translate them into digital 3D data. This technique is utilized in entertainment, sports science, biomechanics, and healthcare since it enables precise analysis and replication of motion. For practical purposes, I will refer to OMC as motion capture. It is important to note that other motion capture systems are available, such as the XSENS system, which employs inertial sensors. Why choose motion capture over other devices?
Motion capture was selected as my primary data acquisition method due to its high spatial and temporal precision, which is essential for analyzing motor impairments and spontaneous movements. Unlike inertial devices or accelerometers, which often limit measurements to acceleration or angular velocity at a single point per limb, motion capture systems enable the tracking of the entire body in three dimensions over time. This capability detects subtle movement variations such as head tilt, body sway, or shoulder orientation.

3.2.1 *Equipment and Setup*

All motion capture systems include motion tracking cameras, a calibration system, and acquisition software. Qualysis cameras and the Qualysis Track Manager software (QTM) were the primary systems utilized during my thesis.

Still, I was also able to work with data collected with Vicon systems, thanks to the compatibility of motion files. There are two main categories of motion tracking cameras: marker-based and marker-less. Marker-based cameras emit infrared light that reflects off reflective (or passive) markers and returns to their source. The infrared light lets the cameras track the markers in three dimensions over time. Makers must be placed close to or on the skin so the joints or body parts are correctly tracked.

A marker-less system consists solely of video cameras. To obtain three-dimensional data, the videos must be processed by a deep learning algorithm that tracks the participant's body and estimates a human skeleton, returning 3D body-segment markers. The choice of a capture technique will depend on the measuring objectives and research methods. The marker-based system allows for tracking humans, objects, and animals. In contrast, marker-less cameras allow only the tracking of humans, as the machine learning algorithms are trained solely on data from adults and children. However, the advantage of the marker-less system is that no markers need to be placed on the participant's body, enabling ecological data acquisition.

3.2.1.1 *Calibration*

Another essential element of every motion capture system is the calibration kit. The principle of the calibration is to define the spatial volume where the tracking will take place. The calibration kit is composed of four markers fixed to an L-shaped frame that will define the origin of the tracking space. There is also the wand, consisting of two markers fixed to a T-shaped frame. During calibration, the experimenter should move the wand upward, downward, and sideways, thereby physically defining the tracking volume. The duration of calibration will depend on the volume. Once calibration is complete, the acquisition software will return the tracking error tolerance. For example, a tolerance of 0.5 mm won't measure movements smaller than this distance. The tolerance depends on how "fine" the tracked movements are; if the movements are subtle, such as body sway, one might want to reduce the tolerance to less than 0.5mm. On the other hand, if the movements have high amplitude or the participant is moving across the space, a tolerance between 0.5mm and 0.9mm is acceptable.

3.2.2 *Data collection*

To ensure good quality 3D recording, a minimum of four cameras is needed in any system (i.e., marker-based, marker-less). Providing adequate space for the setback distance and ensuring a clear area above the participant's head and feet in each camera preview in QTM is important.

3.2.2.1 *Marker-based acquisition*

Regarding marker-based systems, the cameras track all detected reflective markers, so avoiding any reflective or bright (e.g., shiny) objects in the recording room is essential. Ideally, the room should be shielded from daylight. However, one can adjust the sensitivity of the recording cameras to the markers and add digital masks in the recording software to cover objects that cannot be removed.

One advantage of marker-based systems is the possibility to define a personalized biomechanical model, or skeleton, that links each marker to specific body points. Once this model is specified, the acquisition software, in our case QTM, can automatically assign labels to markers in future recordings, assuming marker placement remains consistent. This process can save time for the experimenter; however, errors may occur, and data can be lost if a marker is occluded, falls, or is misidentified due to reflective artifacts nearby. These issues can be addressed using gap-filling techniques and interpolation methods. I discuss some of the methods used in my thesis projects in section 3.3.1.

3.2.2.2 *Marker-less acquisition*

When recording with marker-less cameras, it is important to ensure that the participant being recorded is visible on all cameras and that their limbs are discernible to the naked eye. Rooms with good lighting are preferred. Regarding ethical considerations, marker-based systems do not record any identifiable facial features. However, the videos collected with marker-less systems can record facial features, so safety procedures need to be implemented to keep such files out of public reach. Considering the University of Lille has no server for data storage, all files recorded with marker-less cameras were stored in encrypted external memory disks. The only files available for open access were the exported tabulated data with only 3D segment time series, with no information about the participants.

3.2.3 *Computing constraints*

Based on my experience with marker-less data collection systems, I have found that recording files can be quite large. Therefore, it is essential to have sufficient storage space on the recording computer. Additionally, when developing a research project it is important to consider the time required to export data. In terms of hardware, it's crucial to use a computer with a powerful graphics card to reduce the export time and to have at least 1TB of memory space on the computer for multiple recordings. For the reader's reference, with a 24 GB graphics card (NVIDIA GeForce RTX 3090 GPU), exporting a 4-minute recording with two participants took approximately 1.5 hours. Regarding memory space, 1TB can store a maximum of 5 hours of recordings.

3.3 motion time series

After export, motion data are structured as multivariate time series, at each time point or frame, three-dimensional spatial coordinates (x, y, and z) are recorded for each tracked marker or body segment, describing its position in space and how it evolves over time. As in all continuous data acquisition systems, the sampling rate, expressed in Hertz (Hz), determines the number of data points or frames tracked per second. In motion capture, this will define the temporal resolution of the movement; the higher the sampling rate, the more detailed the track of fast or subtle movements. Raw exported files typically include the time column or frame index, the three coordinates of each marker or segment.

Before any analysis can be performed, one must ensure the raw data is cleaned and preprocessed to correct missing values, noise, or artifacts. In motion capture, artifacts refer to deviations in the signal that do not reflect intentional or anatomically possible motion (Skurowski & Pawlyta, 2022). These can originate from acquisition materials such as occlusions, marker swaps, reflections, and sensor noise, or from participants' natural movements that momentarily interrupt tracking, like adjusting their clothes or stretching. In the following sections, I will present the processes followed during my thesis to ensure the resulting time series has good quality movement patterns for reliable analysis results.

3.3.1 *Cleaning pipelines*

These pipelines changed slightly, depending on whether the data came from a marker-based or marker-less motion capture system. Both pipelines followed the same objective: to detect and correct gaps and aberrant data points without distorting actual motion. To ensure consistency across marker-based and marker-less data, we applied an automatic interpolation pipeline to detect and correct high acceleration outliers, potentially caused by noise, marker loss, or occlusion. This method computes the 3D acceleration of each time point by calculating the second derivative of the position data with respect to time. We flagged all points with tangential acceleration higher than 10,000 mm/s2 as outliers. To account for potential distortions, we added a small window of $+-\Delta$ samples around each outlier point. These flagged points were linearly interpolated using a Piecewise Cubic Hermite Interpolating Polynomial (PCpelvis) interpolation. The PCpelvis interpolation allows the interpolation of data points with a monotonic cubic spline that preserves the shape of the data without introducing oscillation or overshooting. This interpolation method is recommended for short gaps of missing data (i.e., less than 50 samples with a sampling rate of 100 Hz) (Skurowski & Pawlyta, 2021).

In instances where interpolation was ineffective for marker-based data due to gaps exceeding approximately 50 frames, we began to examine marker trajectory information using the fill percentage parameter provided by the acquisition software QTM. Markers with missing data would show a fill percentage of less than 80%. We used the QTM trajectory tool to automatically identify all missing segments in the time series to address this issue. We then examined each case visually to understand whether the system had lost track of the marker or swapped it with another marker or reflective object. When we observed that a marker was still visible in the recording but had not been labeled correctly by the software, we manually reassigned the correct label.

In addition to manually filling in gaps, we implemented a step to clean up overshoots or spikes in the time series that the interpolation algorithm did not eliminate. These spikes can arise from brief reflections near the marker or optical errors. The QTM trajectory tool was used to locate these spikes. We applied a moving average filter spanning 10 samples (approximately 0.1 seconds for a 100Hz sampling rate) to reduce them while maintaining the marker trajectory.

The data collected using a marker-less system was less noisy, primarily because we exported it with the default preprocessing settings of the exporting pipeline, which included a 20 Hz low-pass Butterworth filter to suppress high-frequency noise. However, the marker-less data exhibited gaps, which we could recover using the interpolation algorithm mentioned above, as the motion was simple (e.g., circular motion) and the gaps were not extensive. One may need to resort to other interpolation or gap-filling strategies for longer gaps.

3.3.2 *Artifact vs. Movement*

Participant-originated artifacts can be complex to identify and highly depend on the specific task or hypothesis being tested. It is essential to differentiate between patterns of motion and artifacts. For instance, while analyzing biomechanical metrics from motion capture of people with Parkinson's disease (PD), we noticed sudden jerks or tremors, which are motor reactions associated with the disease. In this case, the data, which could be considered artifacts in healthy participants, proved valuable cues for detecting motor anomalies and limitations in the context of the study.

Conversely, in studies where we quantified oscillations (see Chapters 5 and 6), such as body sway during static poses, we frequently encountered shoulder stretches or pose adjustments during trials. While these movements were physically possible, they did not represent task-related behavior and these movements heavily influenced our results. Therefore, such movements were excluded from our analysis.

Consequently, we needed to come up with a solution for these studies, even though we could see the markers move in a way that seemed like a stretch, there had to be a standardized method to identify stretches and posture shifts. Our solution was to track the alignment of the shoulders, calculating the angle between both shoulders and the manubrium (i.e., base of the neck). We considered that the alignment of these three points should be close to zero degrees during the task, and variations from this alignment could signal chest expansion or shoulder protraction/retraction (i.e., shoulder movement in the anteroposterior direction). In Figure 3.1, we present an example of our analysis. This figure illustrates a participant's shoulder-manubrium angle over time during a single trial of our experiment. The shoulder-manubrium alignment remains close to zero degrees throughout the trial. Around the 50-second mark, the participant moved their shoulders forward by 5 degrees and then backward by 12 degrees (indicated by a negative sign). At 180 seconds, the participant moved their shoulders 17 degrees backward and then 5 degrees forward.

Figure 3.1

Detection of Movement Artifacts with Shoulder-Manubrium Alignment

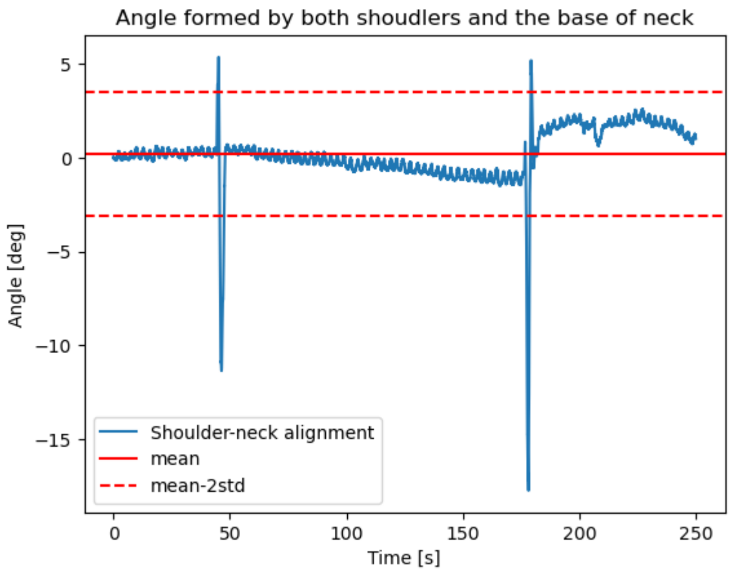

Note. The alignment of shoulders and the manubrium (base of the neck) should be close to zero degrees during the task; variations from this alignment could signal chest expansion or shoulder protraction/retraction (i.e., shoulder movement in the anteroposterior direction). The threshold for detection was defined as two standard deviations from the mean alignment.

We determined our threshold as two standard deviations from the mean alignment as a statistically robust method to capture the significant deviations rather than noise, see Figure 3.1 (Mullineaux & Irwin, 2014). We then removed all time segments during which the shoulder-manubrium alignment exceeded this threshold from the analysis.

While this analysis of movement artifacts was specifically designed to address data relevant to my research question, it is important in all studies to define the measurement objectives and identify any unwanted movements that could bias the results. This will help tailor and propose solutions for detecting and omitting these artifacts from the analysis. Finally, I would recommend observing participants during experiments and meticulously documenting any anomalies (e.g.,use of a laboratory notebook). This approach is important for effective data analysis and was helpful in our human-robot interaction experiments, as we identified which files needed closer examination based on specific participant behaviors.

3.4 MOTION TIME-SERIES ANALYSIS

Once raw motion data had been cleaned and preprocessed, the next step was to extract movement patterns and measures from the time series.

In this section, I will describe how different analysis strategies were applied to address specific aspects of movement. First, I detail how we calculated kinematic parameters to assess functional mobility for People with Parkinson's, such as joint angles, velocities, and displacements. Then, I will explain how we employed spectral analysis to quantify body oscillations. Finally, I will introduce a method for evaluating motor synchrony between interacting individuals.

3.4.1 *Kinematic parameters of functional mobility*

The kinematic parameters presented below were computed using data from a set of fifteen reflective markers. These included two markers on the forehead, one on each shoulder, one on the sternum, and one on each anterior superior iliac spine (ASIS), as presented in Figure 3.2. Additional markers were positioned on the knees, toes, ankles, and heels.

To analyze the motion of body segments, we grouped markers into functional units. For example, the head segment was defined using the two forehead markers (LF and RF). The trunk was constructed from the shoulder and sternum markers, and the pelvis segment was defined by the two ASIS markers (AL and AR), which are commonly used as reference points for pelvic motion. The segments' positions were determined as the midpoints between the markers.

The kinematic parameters were grouped into five categories: upper body posture and alignment, segmental rotation and coordination, trunk and pelvis dynamics, and lower body and gait parameters. The codes for the calculation

Figure 3.2

Marker Placement Schematic for Biomechanical Analysis in Parkinson's Disease

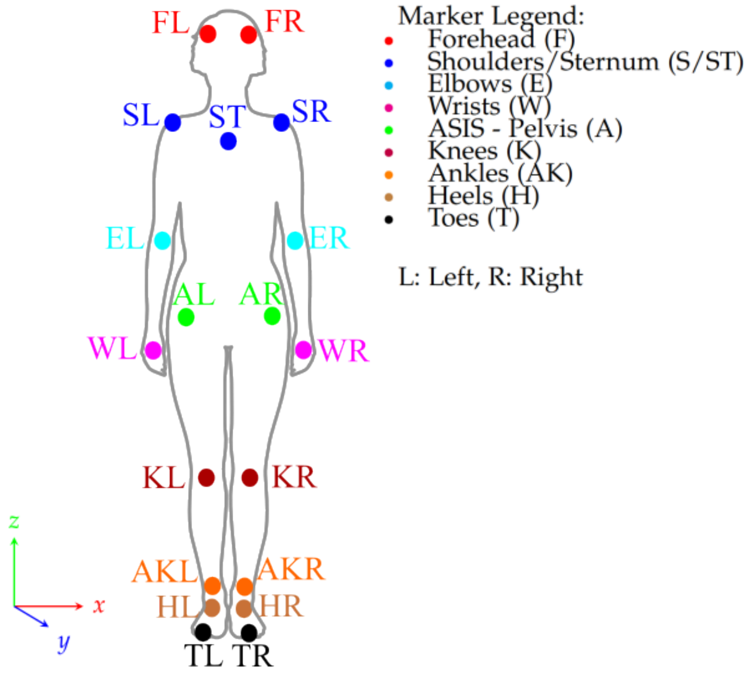

of all metrics presented in this section are available on the following public repository: https://zenodo.org/records/15175531 (Casso, 2025).

3.4.1.1 *Upper Body Posture and Alignment*

A. Shoulder-pelvis alignment

To quantify the inclination of the upper body along the frontal plane, we calculated the angle between the shoulder and pelvis segments. The shoulder vector was defined as the line connecting the left and right shoulder markers, and the pelvis vector was similarly defined using the left and right anterior superior iliac spine (ASIS) markers. These vectors were first normalized to unit length, ensuring the resulting angle reflects directional alignment rather than differences in segment length or body size. The angle between two 3D vectors was computed using the standard dot product formula, which measures how closely aligned the vectors are. The resulting angle θ, in radians, is given by:

$$\theta = \arccos\left(\frac{\vec{s}\cdot\vec{h}}{||\vec{s}||\,||\vec{h}||}\right), \tag{3.1}$$

where $\vec{s}$ and $\vec{h}$,represent the shoulder and pelvis vectors, respectively. To determine the direction of the tilt (right or left), we compute the cross product of the shoulder and pelvis vectors. The sign of the cross product's z-component $(s_x h_z - s_z h_x)$ is used to assign the angle's direction; a positive sign corresponds to a tilt to the right, whereas a negative sign corresponds to a tilt to the left. The first frame of the recording serves as the reference point, ensuring that subsequent angles reflect deviations relative to the initial alignment.

B. Trunk inclination

The trunk inclination in the anteroposterior (AP) direction was defined as the maximum angle between the trunk segment and the vertical axis along the sagittal plane. The inclination in the mediolateral (ML) direction was defined as the maximum angle between the trunk segment and the vertical axis along the frontal plane. The angle was calculated following Equation 3.1; larger positive angles indicated greater inclination in both directions.

C. pelvis flexion

Peak pelvis flexion was determined as the smallest angle between the trunk-pelvis and trunk-knee vectors, following Equation 1.1. As the body leans further forward in the anterior-posterior direction, the angles approach 180 degrees.

D. Arm-body alignment

We measured the alignment between the reaching arm and the body to evaluate the dynamics of low-reaching arm movements. This alignment was assessed by calculating the angle between the shoulder-wrist vector and the sagittal plane formed by the shoulder-pelvis vector. Angles approaching 90 degrees indicate a diagonal reach far from the trunk, whereas angles close to zero suggest a forward reach closer to the trunk.

E. Arm asymmetry angle

The arm asymmetry angle (ASA) is defined as the percentage of deviation from perfect symmetry of the shoulder-wrist segment. The arm swing and ASA calculation are based on the work by Lewek et al. (2010-a) and Zifchock et al. (2008-a). We first determined the dominant arm by comparing the total arm swing of the left and right shoulder-wrist segments. The dominant arm was the side with the largest swing. Then, we obtained the angle ratio of the dominant arm to the non-dominant arm. The asymmetry factor was calculated as the normalized angle ratio; also, since we were not interested in the sign of the asymmetry, we expressed the factor as an absolute percentage, as shown in Equation 3.2.

$$\mathrm{ASA} = \frac{(45^\circ - \arctan(\mathrm{AS}_{\text{Dominant}} - \mathrm{AS}_{\text{Non-dominant}}))}{90^\circ} \times 100\%, \quad (3.2)$$

where AS is the total arm swing calculated for the dominant and non-dominant arm. If the asymmetry value equals 0%, there is perfect symmetry between the swings of both arms. Concurrently, a factor of 100% indicates the two arm displacements are equal and opposite in magnitude (Lewek et al., 2010-a).

3.4.1.2 *Segmental rotations and coordination*

The following parameters were defined to evaluate body segment coordination and turning strategies during walking. These strategies can be classified into two types: cranio-caudal sequences, where the head moves first, followed by the trunk and then the pelviss, and *en-bloc* movement, where one part or all segments move together (Yang et al., 2016-a). Specifically, the parameters assess the rotation of the head, trunk, and pelvis segments in the transverse plane, focusing on yaw rotation.

A. Head, trunk, and pelvis yaw rotations

We calculated the yaw rotation amplitude for each body segment by identifying the maximum and minimum yaw angles observed throughout the trial and determining the difference between them. This amplitude represents the total angular displacement of each segment in the transversal plane.

B. Relative segment rotations

We assessed the coordination between segments with relative rotation amplitudes. Subtracting the yaw amplitude of the caudal segment from that of the cranial one. We obtained three pairwise coordination measures: head relative to trunk, trunk relative to pelvis, and head relative to pelvis. These differences allowed us to evaluate the coordination among the three segments; reduced relative rotations would indicate whether a pair of segments tended to move closely together during rotation, suggesting an *en-bloc* strategy.

C. Segment rotation onset

The turning sequence when walking is triggered when the gait cycle changes direction. Hence, we calculated the rotation onsets of each segment expressed as percentages of the gait cycle, normalized to the first stride (Hong et al., 2009; Yang et al., 2016-a).

We first determined the rotation onset of each segment using angular velocity profiles. We computed the angular velocity curves by differentiating each segment's yaw angle over time. To identify the rotation onset, we located the peak in the angular velocity curve and searched backward in time to detect when the velocity first dropped below a threshold defined as three standard deviations below the peak. This method identified the earliest moment of rotational movement for each segment (Hong et al., 2009).

We identified the first stride based on forward toe velocity (y-axis). We computed the velocity of each toe marker and identified the peak. The onset of the stride was defined as the time when the velocity, moving backward from the peak, first fell below a threshold set at three standard deviations below the peak. The end of the stride corresponded to the moment when the toe velocity stabilized near zero. We determined which foot initiated the stride by comparing the timing of these threshold crossings between the left and right toes.

Finally, we subtracted the stride onset time from the rotation onset time of each segment to normalize rotations to the first stride. We then divided this result by the total stride duration and multiplied by 100, as illustrated in Equation 3.3. Lower values for segment onset indicated an earlier rotation, while a 0% value indicated that the segment was the first in the rotation sequence. (Yang et al., 2016-a).

$$\text{Segment Onset} = \left(\frac{t_{\text{onset}}^{\text{segment}} - t_{\text{onset}}^{\text{stride}}}{t_{\text{end}}^{\text{stride}} - t_{\text{onset}}^{\text{stride}}} \right) \times 100 \tag{3.3}$$

3.4.1.3 *pelviss and Trunk dynamics*

A. Segment jerk

We calculated segment jerk with the third derivative of the segment's position with respect to time, which enabled us to assess the smoothness of segment motion throughout the experiments.

3.4.1.4 *Lower body and gait parameters*

A. Pelvis flexion

The max. Pelvis flexion was calculated as the minimum angle between the trunk-pelvis and trunk-knees vectors. This parameter was used to evaluate sitting-to-standing strategies. For convention, a 90-degree pelvic flexion corresponds to a straight back sitting position; flexion tends to 180 degrees when the participant leans their trunk forward to stand up (Kellis et al., 2019).

B. Knee flexion

Peak knee flexion was defined as the minimum angle between the knee-pelvis and knee-heel vectors. As a convention, if the feet had a perpendicular position to the trunk-pelvis vector, the knee flexion angle

Figure 3.3
Schematic of Toe-off and Heel-strike Phases During the Gait Cycle

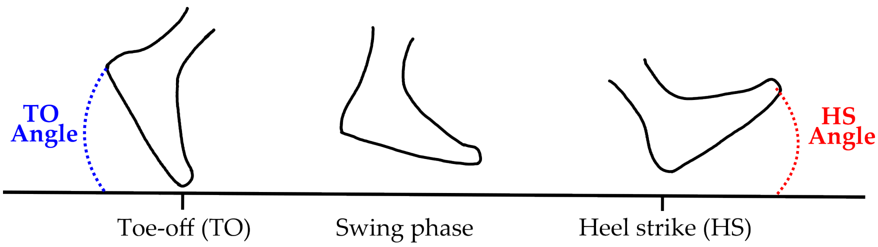

would be equal to 90 degrees; the angle would tend to zero if the participant moved their feet inward.

c. Toe-off and heel strike angles

Heel, toe, and ankle markers during walking were used to calculate the toe-off (TO) angle and the heel-strike (HS) angle (Shin et al., 2020). The TO angle was defined as the highest angle between the heel and the ground at the beginning of the stride, and calculated with toe and heel markers. Concurrently, the HS angle was determined as the highest angle between the toe and the floor at the end of the stride, see Figure 3.3.

d. Foot height Foot height was measured as the shortest vertical distance between the foot and the ground (i.e., minimum foot clearance, mFC) using the heel and toe markers (Shin et al., 2020).

e. Freeze-like events (FLEs)

Freeze-like events, as defined by Cowie et al. (2012), are periods during which walking speed drops below 10% of a baseline speed. The walking speed was calculated as the average of the departure and return walking phases, with the absolute value of the return speed taken into account, as it is negative due to the trajectory. Then, each FLE was identified using the baseline speed threshold (i.e., 0.5 seconds). We counted and measured the time elapsed for each FLE.

f. Walking speed

We calculated walking speed with the differential of the pelvis midpoint forward displacement over time.

3.4.2 *Analysis of kinematic oscillations*

Studies in Human-Robot interaction (HRI) have considered the quantity of movement as a behavioral feature to determine the level of human engagement. In the work form Salam et al. (2024) and Sanghvi et al. (2011), authors quantified spontaneous movement by computing the average motion of silhouette pixels on video frames. A disadvantage of this method might be the analysis of static frames, which could overlook the dynamic changes in human motion. As studies show, humans in interaction often exhibit sporadic and irregular movements (e.g., ballistic motions for pointing, changes in posture), and rhythmic movements (e.g., head nodding, body sway) emerging at different frequencies.

Human interaction studies have proposed to quantify movement with spectral analysis of time series in the frequency domain using the Fourier transform (Issartel et al., 2015; R. C. Schmidt et al., 2012). A limitation of this technique is that it assumes the time series presents a constant regular pattern, which does not correspond to situations of irregular motion, that is non-stationary in nature. Alternatively, spectral analysis through the wavelet transform does not require the time series to be stationary. Thus, it provides a time-frequency representation allowing the identification of frequency components and power spectrum magnitude at different time intervals (Fujiwara & Daibo, 2016).

For example, in Walton et al. (2015), cross-wavelet spectral analysis was employed for movement coordination. In Fujiwara and Daibo (2016), interpersonal synchrony patterns were evaluated. These studies suggest that spectral analysis through the wavelet transform is suitable for the quantification of movement characteristics such as temporal variability and intensity. To summarize, inspired by research in human interaction, we proposed to employ continuous-wavelet transform analysis to quantify spontaneous movement in HRI. Specifically, we proposed that the magnitude of the power spectrum can serve as an indicator of spontaneous movement emergence and thus be taken as an objective feature for human engagement inference.

3.4.2.1 *Spectral analysis of movement with the Continuous-Wavelet Transform*

The wavelet transform is used to analyze time series that contain non-stationary power at different frequencies (Farge, 1992). From the notation proposed by Torrence and Compo (1998), let the discrete signal X_n with $n \in [0, N)$ represent a sequence of measurements of a participant's motion (e.g. a point at the torso) with respect to a reference frame fixed on the environment, obtained at an equal time spacing δt. The continuous wavelet transform of X_n is defined such that:

$$W_n(s) = \sum_{i=0}^{N-1} X_i \psi * \left[\frac{(i-n)\delta t}{s} \right], \tag{3.4}$$

with η a non-dimensional parameter, s a scale factor, $*$ representing the complex conjugate, and ψ a wavelet function, which is taken as the Morlet wavelet, defined so

$$\psi(\eta) = \pi^{-1/4} e^{i\omega_0 \eta} e^{-\eta^2/2} \tag{3.5}$$

with ω_0 a non-dimensional frequency that must be taken (usually $\omega_0 = 6$) to satisfy the admissibility condition for a wavelet, which has zero mean and is localized in both frequency and time-space.

The wavelet transform $W_n(s)$ is a complex signal that can be separated into a real part (amplitude) $|W_n(s)|$ and an imaginary (phase): $\tan^{-1}[\Im\{W_n(s)\}/\Re\{W_n(s)\})]$. Then, the power spectrum can be calculated as:

$$P(s) = |W_n(s)|^2 \tag{3.6}$$

However, the wavelet power spectrum can be biased towards lower frequencies, meaning it will incorrectly show lower-frequency waves as having more power. Hence, a rectification was proposed by Liu et al. (2007), dividing the squared transform coefficient by its scale, allowing the accurate comparison of energy across different frequencies and time scales, improving the reliability of the wavelet analysis. The algorithm developed to apply the wavelet transform to quantify spontaneous human oscillations in HRI is presented in chapter 5.

3.4.3 *Synchrony quantification*

Behavioral or motor synchrony refers to the temporal coordination of actions between two or more individuals. In joint motor tasks, such as walking, clapping, or pedaling, synchrony is often evidenced by the alignment of movement phases over time. This phenomenon plays a crucial role in social interaction, mutual understanding, and task performance. To quantify such coordination, especially when the underlying movements are rhythmic, approaches from dynamical systems theory are particularly valuable. Among them, the Kuramoto model provides a powerful framework for modeling synchronization between oscillatory agents (Kuramoto, 1984), making it especially well-suited for studying interpersonal motor coordination (Smykovskyi et al., 2022).

3.4.3.1 *Kuramoto order parameter*

To evaluate dyadic coordination, we relied on the Kuramoto order parameter, a measure derived from coupled oscillator theory. The order parameter quantifies the degree of phase synchronization among a set of oscillators. In the case of two movement signals with phases $\theta_1(t)$ and $\theta_2(t)$, the instantaneous order parameter $R(t)$ is defined as:

$$R(t) = \left| \frac{1}{2} \sum_{j=1}^{2} e^{i\theta_j(t)} \right| \tag{3.7}$$

where $e^{i\theta_j(t)}$ represents the phase of participant j on the unit circle at time t, and i is the imaginary unit. The value of $R(t)$ ranges from 0 (complete desynchronization) to 1 (perfect synchronization), thus allowing continuous tracking of phase alignment over time.

3.4.3.2 *Synchronization thresholds*

Following the method proposed by Smykovskyi et al. (2024), we defined three synchrony thresholds based on the distribution of $R(t)$ values for each dyad and condition:

- Q_1: First quartile of the $R(t)$ distribution,
- Q_2: Median of the distribution,
- Q_3: Third quartile.

This approach accounts for variability and contextual differences in coordination, allowing each dyad to be evaluated relative to its synchrony profile.

3.4.3.3 *Time In Synchrony*

To quantify how long the movement signals remained synchronized above a given threshold, we computed the Time In Synchrony (TIS). For a given threshold Q_i, TIS is defined as the total time during which the order parameter exceeds that threshold:

$$\mathrm{TIS}_{Q_i} = \sum_t \mathbb{1}_{[R(t)>Q_i]} \cdot \Delta t, \tag{3.8}$$

where $\mathbb{1}_{[R(t)>Q_i]}$ is the indicator function (equal to 1 if $R(t) > Q_i$, 0 otherwise), and Δt is the sampling interval. TIS is expressed in seconds.

Smykovskyi et al. (2024) recommend the use of this measure as it captures the temporal stability of synchronization, rather than just its average magnitude.

Figure 3.4
Affect Grid

Activation

	1	2	3	4	5	6	7	8	9	
	10	11	12	13	14	15	16	17	18	
	19	20	21	22	23	24	25	26	27	
	28	29	30	31	32	33	34	35	36	
Unpleasant	37	38	39	40	41	42	43	44	45	Pleasant
	46	47	48	49	50	51	52	53	54	
	55	56	57	58	59	60	61	62	63	
	64	65	66	67	68	69	70	71	72	
	73	74	75	76	77	78	79	80	81	

Deactivation

Note. Adapted from Russell et al. (1989), to have numbers ranging from 1 to 81 to facilitate participants' self-report. The grid allows the visualization of different emotions mapped within the two-dimensional space. For instance, joy is linked to high pleasure and activation, while sadness corresponds to low pleasure and activation.

3.5 AFFECTIVE STATE ASSESSMENT

The Affect Grid is a self-report scale designed to measure an individual's affective state at a specific moment (Russell et al., 1989). The theoretical foundation of the Affect Grid is based on Russell's circumplex model (Posner et al., 2005; Russell, 1980), which posits that affective states can be represented within a two-dimensional space characterized by:

- Affective valence, indicating the level of pleasure or displeasure
- Arousal, indicating the level of perceived activation (i.e., energy) or relaxation

The Affect Grid consists of a 9x9 cell grid. The horizontal axis represents valence, ranging from displeasure to pleasure (left to right), while the vertical axis indicates the level of activation, from low to high activation (top to bottom). In our research team we adapted this grid by numbering each cell, resulting in choices that range from 1 to 81, as presented in Figure 3.4. This configuration was proposed a few years ago to facilitate the self-reports of individuals performing full-body motor tasks, for whom written responses were not feasible. During the experiments, participants were asked to select a number that best reflected their feelings at that moment, thus providing a simultaneous measure of pleasure and arousal. With this tool, we evaluated participants' affective states at specific times (e.g., before, during, and after stimulus presentation), and assessed how these states evolved over time.

3.5.1 *Affect grid analysis*

To facilitate quantitative analysis, we represented each selected cell number as a two-dimensional Cartesian coordinate. The central cell (cell 41, see Figure 3.4) served as the origin point (0, 0), representing a neutral affective state—neither pleasant nor unpleasant, and neither high nor low in arousal. Coordinates to the right of the origin indicate increasing pleasantness, while those to the left signify increasing unpleasantness. Similarly, values above the origin reflect higher levels of arousal, and values below indicate lower arousal states.

This transformation was executed using a custom algorithm that mapped the grid's cell numbers (1–81) to (x, y) coordinates, thereby converting ordinal responses into continuous spatial data. This conversion enabled the statistical and visual analysis of affective responses. For instance, we can compute average affective states across different conditions, plot individual trajectories to observe changes over time, and quantify the intensity of affective responses by measuring distances from the neutral point.

Coming from an engineering background, it was important for me to acquire and understand the technical knowledge necessary for conducting human psychology research. This experience was essential in enabling me to collect high-quality data. The procedures and methods described in this chapter were applied throughout my work presented in the next section.

Part III

EXPERIMENTAL SECTION

4 KINEMATIC ANALYSIS OF FUNCTIONAL MOBILITY IN PARKINSON'S DISEASE

Published as Köchli, S., Casso, I., Delevoye-Turrell, Y. N., Schmid, S., Rose, D. C., Whyatt, C. (2025). A New Methodological Approach Integrating Motion Capture and Pressure-Sensitive Gait Data to Assess Functional Mobility in Parkinson's Disease: A Two-Phase Study. *Sensors*, 25(19), 5999.
https://doi.org/10.3390/s25195999

4.1 INTRODUCTION

Parkinson's disease (PD) is a neurodegenerative brain disorder caused by a loss of dopaminergic cells in the basal ganglia, resulting in involuntary or uncontrollable motor movements (Jankovic, 2008; Obeso et al., 2017; Poewe, 2008) Motor symptoms are characterized by tremor, rigidity, slowness of movement (i.e., bradykinesia), and difficulties with gait, and are often accompanied by non-motor symptoms such as impaired cognition and psychological behaviors (Armstrong & Okun, 2020; Bloem et al., 2016; Pelicioni et al., 2019). Converging evidence from global surveys suggests that the prevalence of people with Parkinson's (PwP) will double by 2050 (Dorsey, Elbaz, et al., 2018; Dorsey, Sherer, et al., 2018). While PD is well known to occur in older adulthood, there is an increase in young-onset PD, with a prevalence of 3-5% of people affected before the age of 40 years (Rana et al., 2012; Schrag & Schott, 2006). However, the differential diagnosis for PD in younger people may not be considered by physicians (Rana et al., 2012). Inadequate differential diagnoses and measurement protocols that could detect PD in its early stages result in delays in treatment that negatively impact the quality of life for PwP and their care partners (Mirelman et al., 2019; Rana et al., 2012). (Jankovic, 2008) There are several assessment scales for the evaluation of PD (Opara et al., 2017). The gold standard scale for assessing the severity and progression of PD is the Movement Disorder Society-sponsored revision of the Unified Parkinson's Disease Rating Scale (MDS-UPDRS), which relies on trained clinicians to evaluate the presence and severity of motor and non-motor symptoms (Goetz et al., 2008). The MDS-UPDRS, an expanded version of the Unified Parkinson's Disease Rating Scale (UPDRS), was developed to capture a range of clinically relevant issues in PD, including problems related to daily living and non-motor symptoms that were insufficiently captured in the initial version (Goetz et al., 2008). The Hoehn & Yahr scale, integrated into the MDS-UPDRS, is commonly used to identify progressive stages of PD, on a scale of 1 to 5, with 1 indicating no functional disability and 5 indicating confinement to a wheelchair (Hoehn & Yahr, 2001).

Clinical rating scales and self-report questionnaires are also important instruments for assessing the severity, stage, and progression of PD, and the impact of motor symptoms on activities of daily living (Bouça-Machado et al., 2022). Examples include the Parkinson's disease Activities of Daily Living Scale (PADLS) (Jonasson et al., 2017), and the Parkinson's Disease Questionnaire (PDQ-39; (Jenkinson et al., 1997)), which includes specific subscales for mobility and activities of daily living. The MDS-UPDRS Part II and PADLS correlate with examination-based measures of motor symptom severity (Zolfaghari et al., 2022). Despite their utility, such clinical rating scales and assessment tools for PD face significant challenges (Asakawa et al., 2016). The complexity of PD can lead to rating scales underestimating the prevalence of motor symptoms, limiting their accuracy and reliability. This challenge is further compounded by the fact that motor disabilities may not be clinically apparent at the early stages of the disease (Dean et al., 2004; Kalia & Lang, 2015).

Action-based observation tools that focus on physical performance are often recommended for the assessment of functional difficulties with gait, postural balance, increased risk of falls, and reduced mobility for PwP (Bloem et al., 2016; Crouse et al., 2016). An example is the Timed Up and Go (TUG) test (Sprint et al., 2015), a practical tool that has been demonstrated to be a potential predictor of fall risk in PwP (Nocera et al., 2013). The sequence involves standing up from a seated position, walking a prescribed distance, turning, and returning to a seated position. However, while commonly used, the TUG's sensitivity (particularly in early-stage Parkinson's disease) has been questioned (Zampieri et al., 2010). A significant limitation of such rating tools is their emphasis on quantifying the 'end product' of an action, such as the time taken to complete a task. While Bradykinesia is a cardinal feature of PD, this summative product-oriented approach fails to capture the nuances of how a movement unfolds and thus fails to provide more granular insight into which motor difficulties are apparent and, consequently, which rehabilitation strategies would be appropriate.

To provide more fine-grained insight into the quality of motion, several recent studies have investigated gait performance using advanced technology such as inertial movement sensors, optical motion capture, or pressure-sensitive gait mats. These tools allow the assessment of clinically relevant parameters, such as velocity, step length, cadence, and gait asymmetries in PwP (Baudendistel et al., 2021; Del Olmo & Cudeiro, 2005; Di Biase et al., 2020; Duncan & Earhart, 2012; Opara et al., 2017). Deconstructing performance on the TUG through the amalgamation of wearable technology has demonstrated variation in cadence, angular velocity of arm-swing, turning duration, and time to perform turn-to-sits as key to distinguishing early PD (Salarian et al., 2010; Zampieri et al., 2010). Further, this level of precision enables robust profiling of bradykinesia associated with movement amplitude and rhythm, which may be sensitive to medication use in PD (Espay et al., 2011). Through this robust instrumental profiling of control through the TUG, evidence is also emerging of the unique sensitivity of gait during turning in detecting early PD (King et al., 2012; Toosizadeh et al., 2015), with a differential sensitivity between turning and forward gait (Zampieri et al., 2010).

There is a clear indication that the use of wearable technology will enhance profiling precision, and thus, our understanding of the kinematics of PD (Lu et al., 2020; Stephenson et al., 2021). However, there is little consensus yet on measurement protocols. Studies vary in their design, including outcome metrics, and it remains unclear which spatiotemporal gait parameters are most clinically relevant for PwP (Buckley et al., 2019). We aimed to develop a way of using kinematic measures to capture aspects of functional mobility through a sequence of movements that could differentiate between PwP and controls, and to enable us to monitor potential changes over time, for example, as a result of an intervention designed to improve functional mobility for PwP. Against this background, we developed a novel protocol, the Functional Mobility Assessment for Parkinson's (FMA-P), based on a sequence of movements associated with daily activities and commonly used in clinical measures (such as the TUG). Moreover, the FMA-P employs a multidimensional approach by integrating data from a motion capture system and a pressure-sensitive gait mat with additional qualitative observational metrics (i.e., an associated Performance Score). Here we present two studies: the first is a cross-sectional mixed methods study describing in detail the development process of the FMA-P that helped establish which metrics most reliably capture problems with functional mobility in PD, and the second is a repeated measures study demonstrating the application of the FMA-P in relation to an intervention study designed to improve functional mobility for PwP.

4.2 Materials and Methods

This research was conducted by an international team, collecting data in both Switzerland and the UK. These studies form part of a more exhaustive study designed to co-develop a new music-and-movement-based intervention - Songlines for Parkinson's- designed to improve functional mobility for PwP. The draft intervention protocol was pre-registered on the Open Science Framework (OSF), and its developmental process has been reported previously (D. Rose et al., 2025). The overall goal of this research was to develop and evaluate a multidimensional assessment tool—the FMA-P—that would be suitable both for distinguishing PwP from healthy controls and for detecting changes in functional mobility over time, for example, following a structured intervention. We used a two-phase study design:

- Study 1 was a cross-sectional, mixed-methods study primarily focused on the development of the FMA-P, alongside its preliminary evaluation.
- Study 2 applied the FMA-P in a repeated-measures design to evaluate its sensitivity to change following an intervention programme.

4.2.1 *Participants and ethical considerations*

In Switzerland, participants were recruited via a Parkinson's information day held at the local hospital (Luzerner Kantonsspital) and through information shared about the study by Parkinson Schweiz. In the UK, participants were recruited through established researcher networks and from talks given about the project at Parkinson's UK groups in the local area (Hertfordshire). Participants were eligible if they had been formally diagnosed with PD, were independently mobile (up to stage 4 on the Hoehn & Yahr scale, Hoehn and Yahr (2001)), were between the ages of 40 and 80, and had a stabilized medication regimen. Controls were also aged between 40 and 80, with no motor or neurological impairments. Additionally, we administered the mini-MoCA (Gill et al., 2008) to the participants with PD to check for potential cognitive impairments (i.e., did not score below 12). In Study 1, a total of 12 PwP and 12 healthy controls participated (the sample of PwP was split equally between the UK and Switzerland, whereas for the control group, nine participated in Switzerland and 3 in the UK). For Study 2, a total of 12 PwP participated in a music-based intervention study in the UK. Measurement took place at Baseline (4-6 weeks before the intervention), Pre (1-2 weeks before the intervention), and Post (1-2 weeks post-intervention). Both studies were conducted according to the guidelines of the Declaration of Helsinki and the Guidelines of Good Clinical Practice (World Medical Association, 2013). The Ethics Committee of Lucerne University of Applied Sciences and Arts approved the parts of this study in Switzerland (Protocol Number EK-HSLU 002 M 22, date of approval 16.03.2022). The Ethics Committee of the Health, Science, Engineering & Technology (ECDA) of the University of Hertfordshire approved the parts of this study that took place in the UK (Protocol Reference LMS/PGR/UH/04935, date of approval 31.03.2022). All participants received detailed information on the study procedures, which were approved by the respective ethics committees (blinded for review). Written informed consent was obtained before any measurements.

4.2.2 *Materials*

4.2.2.1 *Motion capture system*

Kinematic movement sequences were assessed using Vicon Motion Capture Systems (Vicon Motion Systems Inc., Los Angeles, CA, USA), consisting of eight cameras in Switzerland and 12 cameras in the United Kingdom. Due to room size constraints in the United Kingdom, four more cameras were used in the corners of the room to capture all the markers during the standing up and the turning task. See Figure 3.2 for marker placement. The systems were controlled by the Nexus software (version 2.15, Vicon United Kingdom, Oxford, United Kingdom) and recorded with a sampling frequency of 100 Hz. A full-body model (Plug-in-Gait, Vicon Motion Systems) was adapted to quantify the reliability of PD-relevant movement parameters (Davis et al., 1991; Kadaba et al., 1990).

4.2.2.2 *Walkway gait analysis system*

A five-meter pressure-sensitive Zeno walkway was used for measuring locomotion and foot placement parameters (ProtoKinetics LLC, Havertown, Pennsylvania). The surface of the Zeno gait mat was marked with tape to define the walking distance and turning points (with an active area of 4.88m x 1.22m). Data was recorded at a sampling frequency of 100 Hz and later analyzed with PKMAS (ProtoKinetic Movement Analysis Software). The PKMAS software was synchronized with the Vicon Nexus software so that the recording times were simultaneous (controlled by the PKMAS software).

4.2.3 *Study 1: Development and pilot testing of the Functional Mobility Assessment for Parkinson's (FMA-P)*

The overarching research question of Study 1 was, first, to determine which biomechanical parameters captured by the FMA-P most effectively distinguish PwP from healthy controls, particularly in movement tasks that involve transitions between habitual and goal-directed actions; and second, to assess how the sensitivity of the FMA-P compares to that of traditional clinical tools such as the TUG test. Based on this research question, the following hypotheses were formulated: H1: The FMA-P protocol captures distinct kinematic and spatiotemporal parameters that significantly differ between PwP and healthy controls.

H2: The FMA-P demonstrates greater sensitivity than the TUG in detecting subtle impairments in motor control among PwP.

H3: The most pronounced group differences will be observed in FMA-P tasks that require shifts between habitual and goal-directed motor behavior.

4.2.3.1 *Development of the FMA-P study protocol*

The FMA-P was developed based on the Postural-Locomotion-Manual Test (PLM), which aimed to qualitatively and quantitatively evaluate various factors that characterize movement abilities in PwP(Zackrisson et al., 2011). The PLM provided a three-step movement sequence that mimicked typical activities of daily living, i.e., lifting, transporting, and placing an object. It was comprised of three distinct phases: the postural Phase (P), the locomotion phase (L), and the manual Phase (M). To quantify performance, the authors suggested using a Simultaneity Index (SI), which was calculated as follows:

$$SI = \frac{P + L + M}{MT}, \tag{4.1}$$

where MT represents the total movement time for the task, measured from the initial grasping of the object to its placement, P was defined as the time from grasping the object until the body was upright, L was the time of locomotion/walking, and M was the time for forward movement of the arm to aim and place the object. A lower SI thus reflected increased movement time and greater functional motor disability (Johnels et al., 1989).

The PLM, developed in the 1980s, could be considered ahead of its day. Although a 2013 paper (Zackrisson et al., 2013) reported the protocol to correlate fairly with the UPDRS, it was not picked up as systematically by Parkinson's researchers (probably due to the arduous nature of processing that type of data at that time), and is no longer in use (personal communication with the original authors, 25.05.2020). Nevertheless, the architecture of the PLM can be utilized as a basis for the proposed protocol, with objective kinematic parameters simultaneously extracted from motion capture and gait mat recordings. To further develop the PLM and enhance its applicability for PwP, three additional mobility measures were included: transitioning between sitting and standing (and vice versa) and a 6x3 meter walk with a turn, tasks that form part of the TUG. These tasks allow for comparison with TUG performance and with other studies that report commonly used kinematic measures.

A key challenge with the TUG is the reliance on time-based metrics that primarily reflect automatic, habitual movements such as walking and transitioning between states. Previous neurological evidence suggests that dopaminergic neuron loss in PD disrupts the balance between habitual and goal-directed actions (Dolan & Dayan, 2013; Redgrave et al., 2010). Specifically, degeneration of the putamen impairs habitual movement, increasing reliance on goal-directed strategies mediated by the caudate nucleus and prefrontal cortex (Redgrave et al., 2010). This compensatory reliance on goal-directed control is thought to contribute to cardinal features such as bradykinesia. However, experimental findings are inconclusive, with evidence both for a decline in habitual movement (Bannard et al., 2019) and increased reliance on habitual control (Mi et al., 2021), possibly due to methodological differences (e.g., task complexity, implicit vs explicit learning protocols). The impact of early-stage PD on habitual actions remains uncertain and may be mediated by disease severity-dependent deficits in goal-directed behavior (de Wit et al., 2011). This interplay may also underlie subtle changes in goal-directed gait (Bond & Morris, 2000) and turning in PwP (Janssen et al., 2020).

Given this ambiguity, and to better assess both automatic and goal-directed tasks with ecological validity, we collaborated with PwP to include a functional goal-directed task (picking up and placing a set of keys onto a hook after a turning sequence) into the FMA-P, which requires high precision and planning. Integrating both protocols may allow for a more comprehensive profiling of motor control while providing a framework for future research. Finally, a 'doorway' was incorporated to assess potential freezing episodes during locomotion, a common phenomenon in PwP (Cowie et al., 2012, 2010). Figure 1 shows a diagram depicting the newly developed FMA-P measurement protocol. For the measurement preparation, a height-adjustable, armless chair was placed at the start of the gait mat. Care was taken to ensure that the participants maintained a 90-degree angle at the knee. A doorframe was placed in the middle of a three-meter walkway (at 1.5 m from the start). The key was placed 0.75 meters in front of the door frame, directly after the turning point (three meters from the start).

Figure 4.1

Diagram of the Functional Mobility Assessment in Parkinson's (FMA-P) sequence

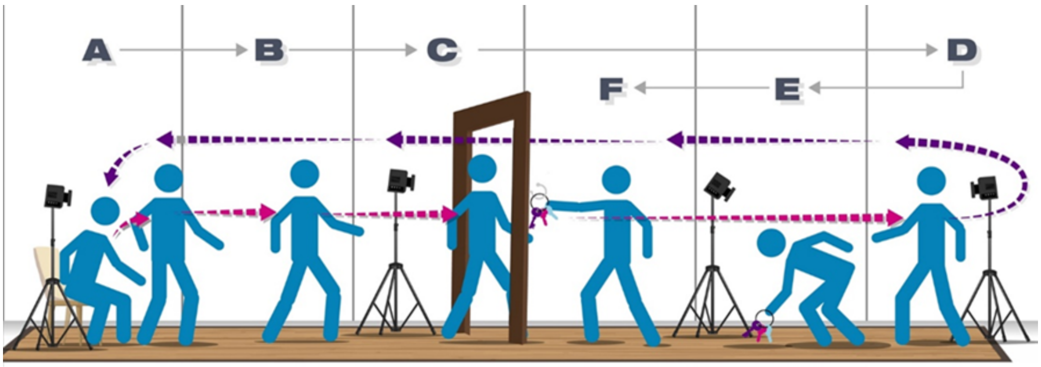

Note. The FMA-P sequence is composed of A. Sitting to standing and standing to sitting, B. Walking forward (3m distance), C. Walking through a visual obstacle, D. Turning, E. Bending to pick up an object from the ground, and grasp it, F. Placing the object at the height of the shoulder.

As shown in Figure 4.1, the FMA-P protocol was developed to include specific tasks adapted from clinical measures and integrated into one sequence. These tasks are described in detail in the following section.

SIT-TO-STAND AND STAND-TO-SIT Sit-to-stand and stand-to-sit are crucial components of daily independent living and, consequently, a key variable influencing the quality of life (Bryant et al., 2020). Studies have indicated that 81% of PwP experience difficulty rising from a chair (Brod et al., 1998), and although most studies do not specifically address sitting down, it is likely that PwP face similar challenges during this process. As such, sit-to-stand and stand-to-sit movements are commonly assessed using time-based clinical scales such as the Berg Balance Scale (BBS; Berg (1989)) and the Timed Up and Go (TUG; Podsiadlo and Richardson (1991)), with PwP typically experiencing a longer transition period between states (Horak & Mancini, 2013; Inkster & Eng, 2004). From a biomechanical perspective, challenges in PwP to perform these tasks may stem from impaired anticipatory control of the center of mass (COM) displacement over the support base (Morris, 2000; Rodrigues-de-Paula Goulart & Valls-Solé, 1999). To develop an accurate measurement protocol, it is essential to evaluate motor strategies and postural stability during this task, thereby enabling the design of goal-oriented rehabilitation and intervention strategies related explicitly to sit-to-stand and stand-to-sit transitions. Evidence indicates that PwP often exhibit earlier joint moments at the hip and knee, relying on exaggerated hip flexion and reduced knee extension during the preparatory task. This strategy may result in a greater forward anticipatory displacement of the COM (Inkster & Eng, 2004; Nikfekr et al., 2002).

TURNING Due to impaired postural control, PwP tend to take small steps and make frequent foot adjustments to maintain balance when changing direction (E. Stack & Ashburn, 1999). Studies have demonstrated that PwP exhibit simultaneous rotation of the head, thorax, and pelvis during turning, whereas healthy individuals follow a cranial to caudal sequence (Hong et al., 2009; Yang et al., 2016-b). This disrupted axial coordination contributes to turning difficulties and an increased risk of falls (Cheng et al., 2014; Huxham et al., 2008).

FUNCTIONAL REACH The basal ganglia, which are most affected in PD, play a crucial role in coordinating postural control and volitional movement (Magrinelli et al., 2016). Functional mobility encompasses actions such as reaching, grasping, and placing objects. These functions are known to be impaired to varying degrees in PD, representing a general assessment of movement impairments, and use different spinal pathways to perform the complex movements whilst maintaining balance and postural control (Alexander, 2004; Johnels et al., 1989). Notably, reaching has been identified as a core metric associated with fall risk across clinical populations, including PwP (e.g., (E. Stack & Ashburn, 1999; E. L. Stack et al., 2006)). Despite the clinical relevance, questions have been raised regarding the utility and validity of clinical tools, such as the UPDRS, in assessing postural stability. Specifically, such assessments often lack ecological validity and demonstrate inconsistencies, raising questions over what specific aspect(s) of postural control are being assessed (Turner & Dale, 2020). The Functional Reach Test or FRT (not to be confused with the current functional reach task) seems to correlate more accurately with dynamic balance in goal-directed actions (e.g., simulating reaching for items at different heights)(de Waroquier-Leroy et al., 2014; Jenkins et al., 2010). To measure the completion of a goal-directed task requiring movement planning and preparation, the FMA-P includes a reaching task developed in collaboration with PwP to ensure ecological validity by reflecting tasks of daily life. Through consultations with PwP, various objects and task parameters were trialed to identify a challenge that felt natural yet demanding. Options included a 3 kg barbell (too heavy), a bottle of plant food with a molded handle (too awkward), and a box of tissues (not natural). Ultimately, PwP identified that grasping a key on the floor, picking it up, walking forward, and placing it on a hook on the door frame was a natural yet challenging everyday task to include in the pilot study. Before initiating the task, the participant's handedness (left or right) was documented. The key was placed on the floor, and the participant was asked to pick it up using their preferred hand. The placement task was adjusted to ensure alignment with the dominant hand and shoulder height, providing consistency in execution and data analysis.

4.2.3.2 *Additional assessments*

As part of the FMA-P protocol, a set of additional tasks addressing key features of PD, such as posture, gait, and freezing, was included and integrated into the biomechanical analysis but was administered separately from the FMA-P sequence. The specific tasks are described in detail in the following section:

STANDING UPRIGHT Ten seconds of upright standing were included as an additional task to assess general postural stability. This task was included to quantify postural tilt and assess the center of pressure (COP) displacement.

LOCOMOTION Gait is a complex biomechanical task vital to independent functioning in everyday life. A large portion of walking (75%) tends to occur in bouts of <40 steps punctuated by brief rests (Griner & Smith, 2006). Consequently, we focused on functional walking sequences as part of the FMA-P sequence, but also a continuous walking task to evaluate general gait parameters as described in the following section. Parkinsonian gait is characterized by short steps, narrow-based flexed knees, and stooped posture, which can serve as markers of disease progression and risk of falls (E. Stack & Ashburn, 1999). Key biomechanical markers include stride length/variability, stride velocity, toe-off (TO), and heel-strike (HS) angles (Blin et al., 1990; Di Biase et al., 2020; Shin et al., 2020). Previous studies indicate that healthy controls exhibit higher

HS angles and TO angles, compared to PwP, highlighting the biomechanical gait differences (Moore et al., 2022; Švehlík et al., 2009). While gait analysis often focuses on lower-body dynamics, it involves upper-body coordination and dynamic equilibrium. Reduced arm swing and altered acceleration profiles are sensitive markers for distinguishing between PwP and healthy controls (Buckley et al., 2019; Lowry et al., 2009) and differentiate between PwP who are likely to be classified as 'fallers' vs. 'non-fallers' (Latt et al., 2008, 2009; Sejdić et al., 2014). To assess continuous gait (as specified in section 2.7.6), we asked participants to walk as fast as possible (including turning) on the five-meter gait mat (a three-meter walking distance was possible before turning) six times without stopping.

FREEZING In PD, freezing of gait (FOG) is one of the most disabling locomotor symptoms, characterized by an involuntary "sticking" of the feet to the floor, which significantly increases the risk of falls (Mancini et al., 2019; Rahimpour et al., 2021). A recent study reported a weighted prevalence of FOG at 50.6% in 9,071 PwP (Zhang et al., 2021). Research has demonstrated that FOG can be triggered by narrow spaces or doorways (Cowie et al., 2010). To address this in our adaptation of the PLM, we incorporated a doorway (dimensions 1.22m x 2.02m) into the locomotion component to capture data in relation to "freeze-like" events (FLEs).

4.2.3.3 *FMA-P Performance Score*

Whilst developing the FMA-P, it became apparent that participants used various strategies to perform the tasks. For example, participants might offset their feet to assist in standing, or swing one or both arms, or use one or both hands to assist in standing from a seated position. As these individual differences are not always apparent with motion capture and gait mat technology, we realized we needed to record and report such behavioral strategies, as they can provide important information on how each task was completed and eventually guide rehabilitation. Consequently, to ensure the tasks performed in the FMA-P sequence were captured at a performative level, we additionally developed a systematic observational record to be administered alongside the FMA-P performance. The Performance Score is a list of seven functional mobility requirements that can be recorded while administering the FMA-P (10 items in total, plus four descriptions). A four-point ordinal scale (0 indicates no problems with the task, 3 indicates difficulties with the task) is used to assess the quality of performance with a maximum total score of 30. The higher the score, the more functional mobility is impaired.

4.2.3.4 *Timed Up and Go (TUG)*

The TUG protocol is a clinical assessment of mobility and fall risk in which an individual rises from a seated position, walks 3 meters, turns, returns, and sits back down, with time-to-completion used to evaluate functional mobility, balance, and gait stability. (Sprint et al., 2015). The TUG protocol was included to provide comparison data for the functional mobility aspects of the newly developed FMA-P (i.e., sit-to-stand, turning, return to seated). The TUG was administered prior to the FMA-P but after the additional tasks described in section 4.2.3.3.

4.2.3.5 *The WHO-5 Measure of Wellbeing*

The WHO-5 is a generic rating scale of subjective well-being (Bech et al., 2003; D. C. Rose et al., 2021). The five statements refer to the past two weeks, are positively worded, and are scored using a 6-point Likert scale. An acceptable Cronbach's alpha coefficient has been reported for this measure (> 0.80, (Garland et al., 2018)).

4.2.3.6 *Study Design and Procedure*

We used a 2 x 2 mixed factorial design, with Group (PwP vs. Control) as a between-subjects factor and Protocol (TUG vs. FMA-P) as a within-subjects factor. Biomechanical performance was assessed across multiple tasks (e.g., sit-to-stand), with predefined biomechanical parameters extracted for each task. Each parameter was analyzed independently to assess group differences. Upon arrival, participants were asked to fill out the WHO-5 questionnaire; then the experimenter proceeded to administer the MDS-UPDRS part III (Motor Examination), including the Hoehn & Yahr clinical measure (Hoehn & Yahr, 2001). Demographic and anthropometric data (i.e., age, sex, body weight, and body height) were provided by participants. Foot length, shoulder offset, elbow width, wrist width, and hand thickness were measured on-site using a caliper. Anthropometric data were used to create a model of the participant within Vicon Nexus software. The gait mat and motion capture data were recorded during the following tasks performed by PwP. The experimental procedure is illustrated in Figure 4.2. Participants were first asked to stand upright for at least 10 seconds, then to walk as fast as possible six consecutive times on the gait mat, covering a total distance of approximately 18 meters (not including the turn on the mat). After the initial demonstration of the TUG by the experimenters, participants were instructed to perform the TUG themselves over three consecutive times (Sprint et al., 2015). Once finished, the experimenter conducted the demonstration for the FMA-P, and participants were asked to perform the FMA-P three consecutive times. The instructions for both TUG and FMA-P were to walk and complete each task as fast as possible;

both protocols were performed within the same setting (e.g., same chair, same distance to the turning task, and the same technologies were applied).

Figure 4.2
Experimental Procedure

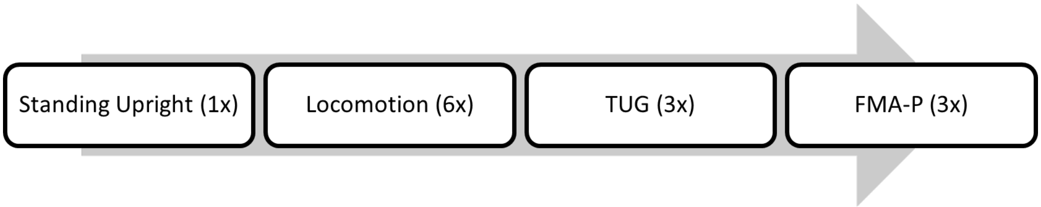

Note. Participants were first instructed to stand upright for 10 seconds (in the middle of the gait mat). Next, they were asked to walk forwards along the length of the gait mat 6 times, turning on the mat before recommencing the next lap until all six laps were completed. Participants were then asked to perform the TUG three times, each time following the researcher's instructions, before finally executing the FMA-P three times, also following the researcher's instructions. All recordings took place on the mat within the motion capture suite, as shown in Figure 4.1

4.2.3.7 *Data processing and functional mobility analysis*

All biomechanical metrics described in the present section were calculated using 3D motion capture data. The analysis of the COP was performed using data collected with the gait mat. The algorithms for metric calculation are available in a public repository (see Casso (2025)). The recorded trials were recovered in three-dimensional coordinates for each marker. Using the Vicon Nexus software, we first observed markers with missing data. The trajectory editor tool automatically identified gaps in marker trajectories. We then used polynomial gap filling for gaps ≤ 10 frames and applied Vicon Nexus gap filling algorithms for > 10 frames (e.g., rigid body fill, spline fill, and pattern fill). An additional data cleaning process consisted of mitigating spikes of aberrant data by applying a moving average technique of up to 15 samples (0.15 seconds). Data were excluded in cases of marker occlusion and/or inappropriate interpolation. Data from the Zeno walkway system was pre-processed using the default parameters in the PKMAS software. In the case of COP, raw data were filtered using a 5-pole, low-pass Butterworth Filter with zero lag at 10 Hz, as advised in the PKMAS manual. We handled missing data using a multiple imputation procedure clustered either by experimental group (PwP, Control) and protocol pairs (TUG, FMA-P) or by intervention phase (Baseline, Pre, Post). Within each cluster, we generated five imputed datasets using the predictive mean matching method (PMM). A single, complete dataset was then created for analysis by pooling these imputations, which involved averaging the five imputed values for each missing data point. Multiple imputation is recommended when the percentage of missing data is between

5% and 20%. For missing data above 20%, it is necessary to consider whether multiple imputation could bias the results (Yeatts & Martin, 2015).

The methods for the calculation of the kinematic parameters mentioned below are presented in section 3.4.1.

sit-to-stand and stand-to-sit The sit-to-stand task was defined as the Phase during which the upper body bent and ended at the initiation of the first footstep, while the stand-to-sit began when the turning foot made contact, initiating an upper-body bend. We evaluated the sit-to-stand and stand-to-sit strategy using maximum trunk inclination in the anteroposterior (AP) and mediolateral (ML) directions. Larger positive angles can indicate greater leaning, with PwP expected to exhibit excessive AP and ML inclination, suggesting compensatory postural strategies. Peak trunk velocity, calculated as the derivative of the trunk displacement in the AP direction, was hypothesized to be higher for momentum-driven strategies and lower for rigid movement. The root mean square (RMS) of trunk acceleration in the AP direction was expected to be lower in PwP, indicating reduced anticipatory postural adjustments (Palmerini et al., 2013). Movement smoothness, assessed via mean trunk jerk, was anticipated to be higher for PwP, reflecting less postural control and fluidity of movement. Peak pelvis flexion was expected to be greater for PwP, reflecting a reliance on pelvis flexion to stabilize their center of mass (Inkster & Eng, 2004). Knee flexion was also assessed. Greater angles can indicate reduced flexion; we hypothesized this angle would be greater in PwP, signaling a need for greater postural stability, while healthy controls would exhibit lower flexion angles (Inkster & Eng, 2004). We also calculated the COP displacement in the AP and ML directions to evaluate stability. We expected PwP to show an increased COP displacement in both directions compared to controls, which could reflect difficulties in anticipatory postural adjustments and balance during transitional movements (Fernandes et al., 2015).

turning During the turning movement, we assessed the coordination, and thus the turning strategy, across three segments of the body: head, trunk, and pelvis. The turning task duration was calculated from the last contact of the turning foot to the first contact of the swing foot after completing a 180-degree turn, with PwP expected to take longer. Turning movement smoothness was assessed via the mean jerk of the pelvis, hypothesizing reduced jerk in PwP, indicating less dynamic movement to compensate for poor postural control. We quantified total angular displacement during the turn using absolute yaw rotations (i.e., rotation around the vertical axis or side-to-side) for each segment. We hypothesized smaller yaw rotations in PwP, indicating rigidity in transitional movements (Yang et al., 2016-b). Turning sequences were assessed by relative yaw between segments (e.g., head-trunk, trunk-pelvis, head-pelvis), expecting more significant rotation differences in controls, indicating a craniocaudal turning sequence, and smaller differences in PwP, suggesting a less coordinated turning strategy. Rotation onsets of head, trunk, and pelvis were expressed as percentages of the gait cycle, normalized to the first stride for comparison across participants (Hong et al., 2009; Yang et al., 2016-b). Lower onset values indicated earlier rotation. We also calculated the maximum trunk inclination in AP and ML directions, hypothesizing greater inclination in PwP, especially in the ML axes. Mean TO and HS angles were extracted from the gait mat data and analyzed for balance and postural control, with controls expected to show higher TO and HS angles. Mean COP displacement in AP and ML directions was used to assess stability.

FUNCTIONAL REACH The key pick task duration was defined as the time from the first upper body movement (i.e., initiation of bending) to when the key was lifted, with PwP expected to take longer to complete the task. Arm-reaching dynamics were analyzed by calculating the alignment between the reaching arm and the body, as calculated via the angle between the shoulder-wrist vector and the sagittal plane formed by the shoulder-hip vector. Angles near 90 degrees indicate a diagonal reach, while those toward zero indicate a forward reach. We expected to observe more significant variability in this alignment angle for PwP. Indeed, while E. Stack and Ashburn (1999) reported that severe cases of PD may rely on the use of a diagonal reach, these results are confounded as the study was conducted in an ecological environment (e.g., kitchen counter), and some participants used fixed support during the task (E. Stack & Ashburn, 1999). Bending was quantified by maximum pelvis and knee flexion angles. We hypothesized that PwP would exhibit reduced pelvis flexion and greater knee flexion than controls, suggesting compensatory strategies to maintain balance. Stance stability was assessed by AP foot distance (between toe markers in the sagittal plane), feet aperture angle, and the maximum stance width. The aperture angle was defined as the angle formed by the vectors connecting the toes to the heels of each foot, and the maximum stance width was defined as the largest horizontal distance between the two-foot segments. PwP were expected to show wider stance angles and greater stance width to improve their stability. The maximum toe off angle was calculated, with PwP predicted to have smaller angles, indicating controlled foot movement. Mean COP displacement in AP and ML directions was used to profile general stability, with PwP expected to show reduced displacement.

STANDING UPRIGHT Postural sway and jerk are key indicators of balance control. Sway displacement is greater in elderly fallers (Palmerini et al., 2013), while PwP exhibit less smooth postural acceleration and jerk (Horak & Mancini, 2013; Mancini et al., 2011). We assessed postural sway using COP displacement in the AP and ML directions via a gait mat. Root-mean-square (RMS) values for pelvis and trunk acceleration were also calculated.

We hypothesized that PwP would show greater trunk inclination and COP displacement in both directions due to impaired stability alongside increased trunk acceleration and greater trunk and pelvis jerk. Upper body lateral tilt was calculated by measuring shoulder alignment relative to the pelvis.

LOCOMOTION Locomotion was assessed through standard gait parameters, FLEs, and upper body coordination. Six walking trials (three departures and three returns) were analyzed per participant. Gait parameters, including asymmetry, double support time, stride length, stride width, stride time, stride velocity, and their corresponding variability percentages, were extracted from gait mat data using PKMAS software (Salarian et al., 2010). Concurrently, we collected the TO and HS angles and foot height from motion capture data. We predicted PwP would show higher asymmetry, longer double support, shorter stride length, wider stride width, longer stride times, lower stride velocities, and higher variability percentages compared to controls. Upper body dynamics were assessed by calculating arm swing displacement and angular velocities of three segments: shoulder-elbow, elbow-wrist, and shoulder-wrist. Arm swing magnitude and segment swing velocities were calculated using markers coordinated projected onto the sagittal plane, with the pelvis midpoint as the reference point. We calculated an arm asymmetry factor (ASA) using equation 3.2 defined as the percentage of deviation from perfect symmetry of the shoulder-wrist segment (Lewek et al., 2010-b; Zifchock et al., 2008-b). An ASA of 0% indicates perfect symmetry, while a factor of 100% indicates the arm swings are equal and opposite in magnitude (Zifchock et al., 2008-b). We expected PwP to show reduced arm swing, lower arm segment velocities, and higher ASA than controls.

The walking speed of the TUG trials was considered as the Baseline to detect FLEs during the Locomotion task (see section 3.4.1.4). We also calculated FLEs on the FMA-P protocol to assess whether the doorframe (see phase C, Figure 4.1) could induce freezing as reported by Cowie et al. (2012).

4.2.3.8 *Performance score*

Two experienced researchers in movement assessment evaluated the ten items and four descriptions of the Performance Score independently of each other. Differences in the evaluation of the tasks were discussed and analyzed by the researchers. The mean score from three FMA-P trials was calculated for each item. Final scores were calculated as the sum of all items.

4.2.3.9 *Statistical analysis: Analysis of Covariance for Group and Protocol Differences*

Initially, a Multivariate Analysis of Covariance (MANCOVA) analysis was considered; however, our sample size and the number of dependent variables were not ideal for this type of statistical analysis. Instead, a 2 (Group: PwP vs. Control) × 2 (Protocol: TUG vs. FMA-P) Analysis of Covariance (ANCOVA) was applied to each biomechanical parameter associated with each task. This approach allowed us to characterize both group-level differences in biomechanical strategy (i.e., how movement unfolded) and how these differences are modulated by testing protocol (TUG vs. FMA-P). Each biomechanical parameter was analyzed separately as a dependent variable, aligned with the best biomechanical practice. The same set of parameters was examined where possible, and thus multiple comparison corrections were applied to control for inflated Type I error rates. For within-protocol group comparisons (e.g., Control vs. PwP on TUG), within-group protocol comparisons (e.g., PwP: TUG vs. FMA-P), and for Group x Protocol interaction, the alpha level (α) was adjusted based on the number of parameters analyzed. For example, with six parameters, the correct $\alpha = 0.05/6 = 0.0083$. The number of parameters considered for the Bonferroni corrections was defined by parameter type, such as spatiotemporal (e.g., duration), kinetic (e.g., COP), and upper/lower kinematics (e.g., trunk inclination, stride velocity). In the spatiotemporal category, only one parameter was compared across groups and protocols, and no Bonferroni correction was applied to this parameter. The Shapiro-Wilk test was applied to assess the normality of our data. Sphericity was assessed using Mauchly's test. Data with sphericity assumption violation was corrected using the Greenhouse-Geisser method. To control observed and unobserved differences in our sample, we included age, sex, and body height as fixed effects in all analyses. Foot length was added as a covariate for biomechanical parameters such as TO angle, HS angle, and foot height comparisons.

4.2.4 *Study 2: Application of the FMA-P to measure functional mobility outcomes of a music and movement-based intervention*

The overarching research question of Study 2 was to assess the sensitivity of the FMA-P in detecting changes in functional mobility in PwP following a music- and movement-based intervention. This study aimed to determine whether the FMA-P can serve as a reliable outcome measure to evaluate motor improvements across time in response to a therapeutically grounded program. Based on this research question, the following hypotheses were formulated: H1: The FMA-P will detect significant improvements in functional mobility from pre- to post-intervention in PwP. H2: Improvements will be most evident in FMA-P parameters related to task coordination and transitions between movement phases. H3: The multidimensional nature of the FMA-P (integrating kinematic and spatiotemporal data) will allow for a more nuanced detection of functional changes compared to conventional outcome measures.

4.2.4.1 *Study design*

The data used herein is a sub-sample of a larger study evaluating the efficacy of an intervention, co-developed with PwP, that uses music and movement to improve functional mobility and quality of life for PwP (D. Rose et al., 2025). In total, three trials were completed in the UK and Switzerland (in preparation). This is a sub-sample of the first group that completed the intervention in the UK, collected between 1 May 2023 and 14 August 2023. The intervention took place once per week over 12 consecutive weeks, with each session lasting 90 minutes. Although each session of the intervention had a different weekly theme (e.g., Marching Music, Music from Africa, or Latin America), the structure was based on the same framework of eight sections related to the therapeutic use of music in Parkinson's rehabilitation. The sections included a warm up (seated and standing exercises to music), active rhythmic engagement (learning to find, feel, and play the main pulse of the music), sharing of meaningful songs (group bonding), line dancing (a sequence of movements incorporating exercises related to functional mobility), a discussion section (exploring music in relation to under-researched areas of PD symptoms such as difficulties with sleeping), an informational talk on music of the themed area, a section exploring the music and the dance of the weekly theme, and a final restoration section (i.e., stretching accompanied by music of the weekly theme). Further information on the protocol can be found on the Open Science Framework in D. Rose et al. (2025). Participants in study 2 were assessed through biomechanical motion capture analyses using the FMA-P protocol at three time points—Baseline, Pre-, and Post-intervention—with three measurements taken at each time point, as detailed in Section 4.2.3.

4.2.4.2 *Statistical analysis: RM-ANOVA of intervention phases*

An RM-ANOVA was conducted to compare the three phases of the intervention: Baseline, Pre-, and Post-intervention. We assessed normality and sphericity of our data. Post-hoc pairwise comparisons between intervention phases were implemented using a Bonferroni correction.

4.3 RESULTS

Demographic characteristics for all groups are provided in Table 4.1. After that, the results are grouped according to study.

Table 4.1
Group Demographics for Study 1 and Study 2

Parameter	Study 1 PwP, n = 12		Study 1 Control, n = 12		Study 2, n = 12	
	M	SD	M	SD	M	SD
Age (years)	69.5	6.1	61.0	7.3	72.2	7.0
Gender						
Female (%)	58		33		67	
Male (%)	42		67		33	

Note. PwP = People with Parkinson, M = mean, SD = Standard deviation.

4.3.1 *Results of Study 1*

4.3.1.1 *Complementary Clinical Assessments*

In Study 1, the Parkinson's group was in the early stages of PD, according to the Hoehn & Yahr (H&Y; *M* = 1.8, *SD* = 0.6, Range 1.0 – 2.5) and presented a wide range of MDS-UPDRS III scores (*M* = 33.7, *SD* = 12.1, Range 11 – 51).

A significant difference between groups was found: PwP were older than the controls, $F(2) = 4.43, p = .025, \eta_p^2 = .30$.

As expected, a significant difference was found between groups for the Performance Score, whereby the PwP (*M* = 8.4, Range 3.9 - 17.3) scored higher (worse performance) than the control group (*M* = 2.5; Range 0.9 - 4.99), with age and sex considered as covariates $F(2) = 5.83, p = .003, \eta_p^2 = .55$.

No differences were found between groups for the WHO-5 measure of well-being, after adjustments for age and sex (PwP: *M* = 81.8%, Range 64 - 92; Controls: *M* = 81.8%, Range 44 - 100; $F(3) = 0.63, p = .606, \eta_p^2 = .09$.

4.3.1.2 *Clinical measures*

The mean time of three FMA-P and TUG trials was used in the analysis, considering that the data were measured according to the clinical setting with a stopwatch. As shown in Table 4.2, the PwP took significantly longer to complete the FMA-P compared to controls, $F(1, 22) = 8.16, p = .009, \eta_p^2 = .27$, but not for the TUG (*p* = .057).

4.3.1.3 *Biomechanical analysis*

This section presents the biomechanical analysis of motion and gait mat data on comparable tasks derived from the TUG and FMA-P (i.e., Sit-to-stand, Turning, and Stand-to-sit). A 2 (Group) x 2 (Protocol) ANCOVA was applied at the level of the biomechanical parameters associated with each task.

Table 4.2
Comparison of Completion Times for the FMA-P and TUG Protocols for Both Groups

Completion time (s)	Group	
	PwP	Controls
TUG		
M	10.4	7.3
SD	3.6	1.0
FMA–P		
M	13.4	9.7
SD	4.3	1.4

Note. PwP = People with Parkinson, SD = Standard deviation.

Before the analysis, we examined potential fatigue effects across the three TUG trials performed during our experimental sessions in a selection of 12 participants in each group. Intra-class correlation (ICC) analysis with a one-way random-effects model values indicated an ICC(1,1) of .98 (95% CI [.95, .99]) for individual trials and an ICC (1,3) of .99 (95% CI [.98, .99]) for the mean of the three trials. The ICC was statistically significant (F(23,48) = 125.54, p < .001), suggesting consistent performance across repetitions and thus confirming the absence of fatigue effects. Given this stability, to reduce the demand on resources that would be required within the research team to label all three TUG trials, we selected the second of the three TUG trials for further analysis for between-groups analyses. However, as the FMA-P is a newly developed measure, the mean of three trials completed by each participant within a single experimental session was used for each of the FMA-P parameters. Detailed statistical results are presented in Table 4.3.

SIT-TO-STAND When comparing groups on the Sit-to-stand transition, PwP took significantly longer for the FMA-P protocol than controls $F(1, 52) = 6.62, p = .012, \eta_p^2 = .09$, but there was no difference between groups for this aspect of the task on the TUG (p = .077).

We applied a Bonferroni correction for the group comparison of seven upper-body kinematic parameters, adjusting the significance threshold to α = 0.007, and for two COP parameters to α = 0.025.

The result of a 2 (Group: PwP vs. Healthy Control) x 2 (Protocol: TUG vs. FMA-P) ANCOVA, controlling for age, sex, and height, revealed a significant main effect of Group on peak anterior-posterior (AP) trunk inclination ($F(1, 41) = 8.82, p = .006, \eta_p^2 = .17$). As illustrated in Figure 4.3, PwP inclined their trunk further toward the ground (AP direction) than control participants.

Figure 4.3
Study 1 - Peak Trunk Inclination in the AP Direction during Sit-to-Stand

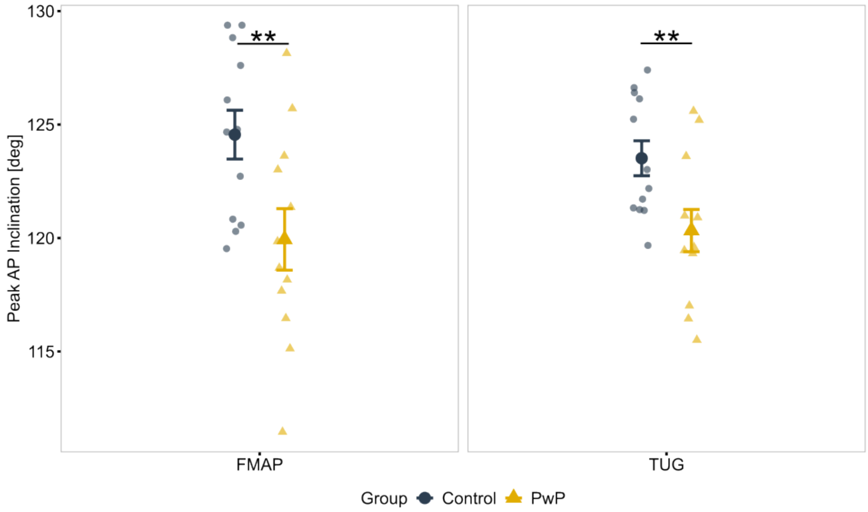

Note. Plots show the mean for each Group (PwP vs. Control) across two protocols (FMA-P and TUG). Individual data points are overlaid around each group's mean. Error bars represent the standard error of the mean (SEM). A significant main effect of Group was found ($p < .001$), with PwP showing greater forward trunk inclination during sit-to-stand compared to controls. *** p < .001.

The analysis also revealed a significant main effect of Group on the dynamics of trunk movement. Specifically, PwP exhibited lower trunk jerk, standing up with a smoother, more controlled movement than controls ($F(1,40) = 10.22, p = .003, \eta_p^2 = .21$).

We found a main effect of Protocol in the displacement of the COP in the ML direction. Both groups exhibited a higher balance shift sideways during TUG than during FMA-P ($F(1,38) = 10.9, p = .002, \eta_p^2 = .22$).

TURNING We found a main effect of Protocol for this task duration ($F(1,36) = 5.41, p = .026, \eta_p^2 = .13$); both groups took longer to complete the turn on the TUG compared to FMA-P.

The Bonferroni corrections for the group comparison of eleven upper-body kinematic parameters resulted in a significance threshold equal to $\alpha = 0.005$. For two gait parameters (HS and TO angles) and two COP parameters, the alpha level was corrected to $\alpha = 0.025$.

We found a main effect of the FMA-P Protocol for absolute head yaw ($F(1,32) = 18.16, p < .001, \eta_p^2 = .36$), the head yaw angle relative to trunk ($F(1,35) = 14.80, p < .001, \eta_p^2 = .30$), and head onset ($F(1,33) = 22.15, p < .001, \eta_p^2 = .40$). During the TUG both groups exhibited a wider head segment rotation (see Figure 4.4, top panel) and separated their heads further from their trunks when turning (see Figure 4.4, bottom panel). Additionally, the head segment turned earlier during TUG compared to FMA-P ($p < .001$), as shown in Figure 4.5.

Figure 4.4

Study 1 - Head Kinematics of the Turning Task

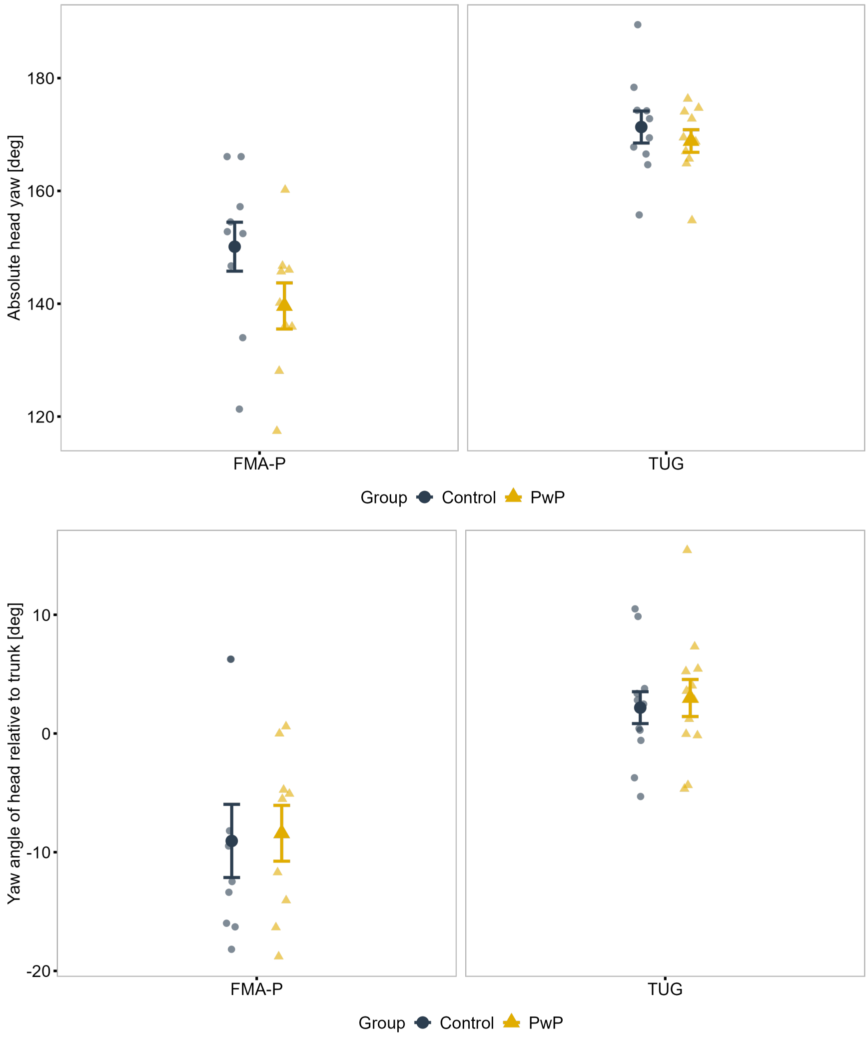

Note. Plots showing head kinematic parameters during the turn phase for each group (PwP vs. Control) across two protocols (FMA-P and TUG). The top panel shows absolute head yaw: both groups exhibited a wider head segment rotation during TUG ($p < .001$). The bottom panel shows the yaw angle of the head relative to the trunk; both groups separated their head further from their trunk when turning during the TUG.

Regarding the gait parameters during the turn, we found a main effect of Group for the HS angle $(F(1, 35) = 56.21, p = .010, \eta_p^2 = .18)$. As presented in Figure 4.6, the toe clearance (i.e., distance between the toes and the ground) for PwP was shorter than that of controls while turning during both protocols.

Regarding COP (balance) control during turning execution, we found a main effect of Protocol on the COP displacement in the ML direction $(F(1, 41) =$

Figure 4.5
Study 1 - Head Turn Onset

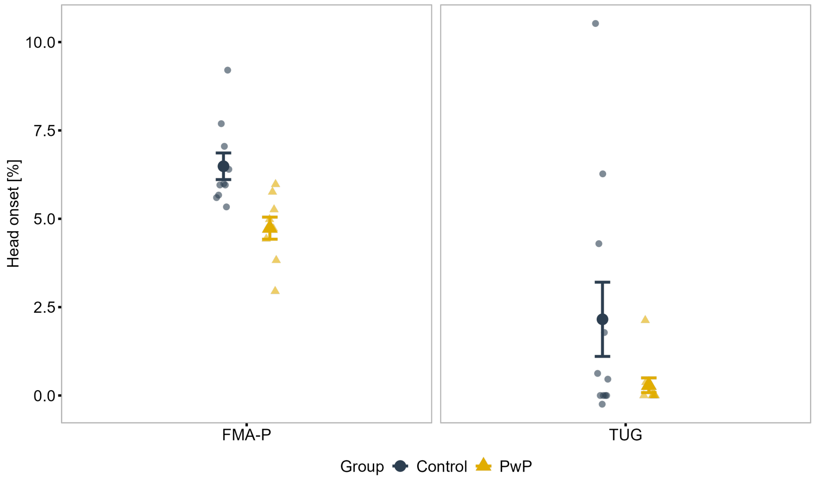

Note. Plot showing the mean head onset expressed as a percentage of the turn sequence. Data is presented for each group (PwP vs. Control) across two protocols (FMA-P and TUG). A significant main effect of Protocol was found ($p < .001$). Both groups exhibited earlier head turns during the TUG.

Figure 4.6
Study 1 - Mean Heel-strike Angle during Turning

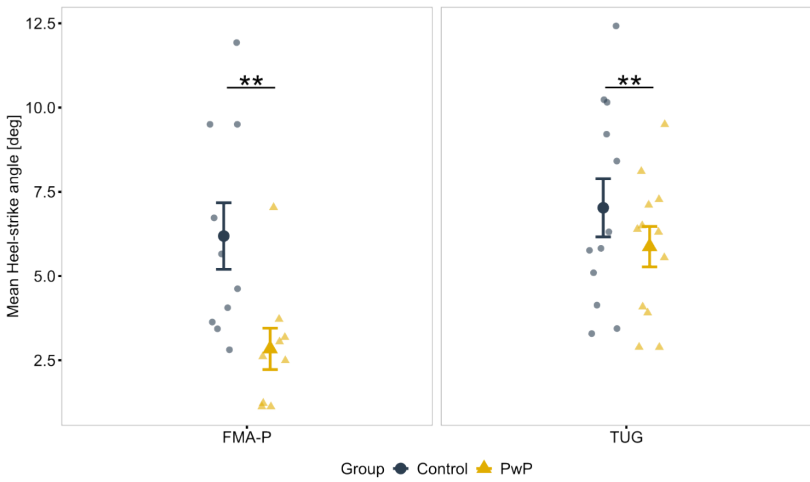

Note. Plot showing the mean HS angle for each group (PwP vs. Control) across two protocols (FMA-P and TUG). Individual data points are overlaid around each group's mean. Error bars represent the standard error of the mean (SEM). A significant main effect of Group was found (p =.010). PwP toe clearance was reduced compared to controls during both protocols.** $p <$ .010.

Figure 4.7
Study 1 - COP Displacement in ML Direction during Turning

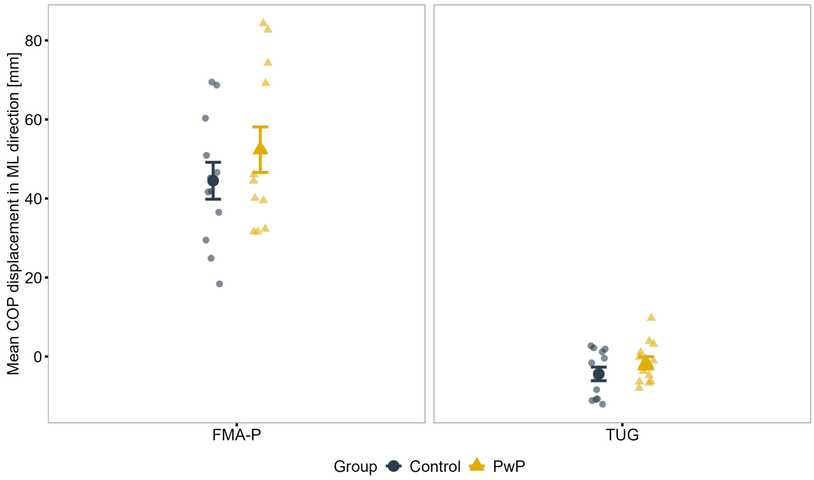

Note. Plot showing the mean COP displacement during the turning task for each group (PwP vs. Control) across two protocols (FMA-P and TUG). A significant main effect of Protocol was found ($p < .001$). Both groups exhibited higher COP mediolateral displacement during the FMA-P.

$92.98, p < .001, \eta_p^2 = .69$). As shown in Figure 4.7, both groups had higher COP displacement in the ML direction during the FMA-P.

STAND-TO-SIT As in the Sit-to-stand task, we adjusted the significance threshold to $\alpha = 0.007$ for seven upper-body kinematic parameters, and to $\alpha = 0.025$ for two COP parameters. There were no significant findings for this task at either the group or protocol levels.

FUNCTIONAL REACH All participants were able to pick up the key (sometimes requiring more than one attempt), and the time to complete the key-picking task was similar in both groups. No differences were apparent regarding the upper-or lower-body kinematics for this task.

4.3.1.4 *Additional tasks*

STANDING UPRIGHT After correcting the significance level for multiple comparisons, no significant differences were found between PwP and Controls on this task.

LOCOMOTION We corrected the significance level to $\alpha = 0.003$ for nineteen gait parameter comparisons, and to $\alpha = 0.013$ for the comparison of four upper-body kinematic parameters.

PwP exhibited a significantly lower TO ($F(1, 138) = 11.99, p < .001, \eta_p^2 = .16$) and HS angles ($F(1, 138) = 11.99, p < .001, \eta_p^2 = .10$) compared to control (see top panel of Figure 4.8) during the locomotion task (Figure 4.8, bottom panel). PwP also walked significantly slower $(F(1, 139) = 12.93, p < .001, \eta_p^2 = .09)$. The PwP group performed the task using shorter stride lengths $(F(1, 144) = 9.80, p < .001, \eta_p^2 = .67)$ and with lower stride velocity $(F(1, 144) = 10.39, p < .001, \eta_p^2 = .69)$.

No significant differences were found between groups on other gait metrics, upper limb angular velocities, and ASA when walking. No significant differences between groups were observed during quiet standing.

FREEZING Our algorithm detected a total of 19 FLEs among PwP with a mean duration of 0.95 seconds (*SD* = 0.3) during FMA-P. No FLEs were detected during the additional locomotion task.

PERFORMANCE SCORE As presented in section 3.1.1, PwP had a significantly higher score compared to their control participants $(F(1, 16) = 5.83, p = .003, \eta_p^2 = .55)$.

From a qualitative perspective, we observed that PwP used unexpected strategies to perform the sit-to-stand task within the FMA-P, such as pushing themselves up from a chair with one or both hands, and/or using a single- or double-foot offset to stand up. Similarly, during the stand-to-sit task, PwP frequently relied on hand support on their knees. For the walking task, PwP often displayed an elbow arm swing with variable amplitudes. During the functional reach task, participants usually required additional steps, multiple attempts, or hand support on their knees.

4.3.2 *Results of Study 2*

4.3.2.1 *Complementary Clinical Assessments*

According to the Hoehn & Yahr staging, PwP presented with mild to moderate symptoms (H&Y; Mean = 1.8, SD = 0.6, Range 1.0 – 2.5). The mean score for the MDS-UPDRS III at Baseline was 42.1 (*SD* = 10.9, range 20–60). Table 4.4 shows the results of the mean time differences of three FMA-P and TUG trials, and the mean differences of the MDS-UPDRS III score for Baseline, Pre-, and Post-intervention. No significant changes over time were observed.

4.3.2.2 *Biomechanical analysis*

This section presents the biomechanical analysis of motion capture data on the FMA-P tasks during three intervention phases: Baseline (measurements taken 4-6 weeks before the intervention), Pre (1-2 weeks before the intervention), and Post (measurements taken 1-2 weeks after the intervention). The mean

Figure 4.8

Study 1 - Heel-strike and Toe-ff Angles during Locomotion Task

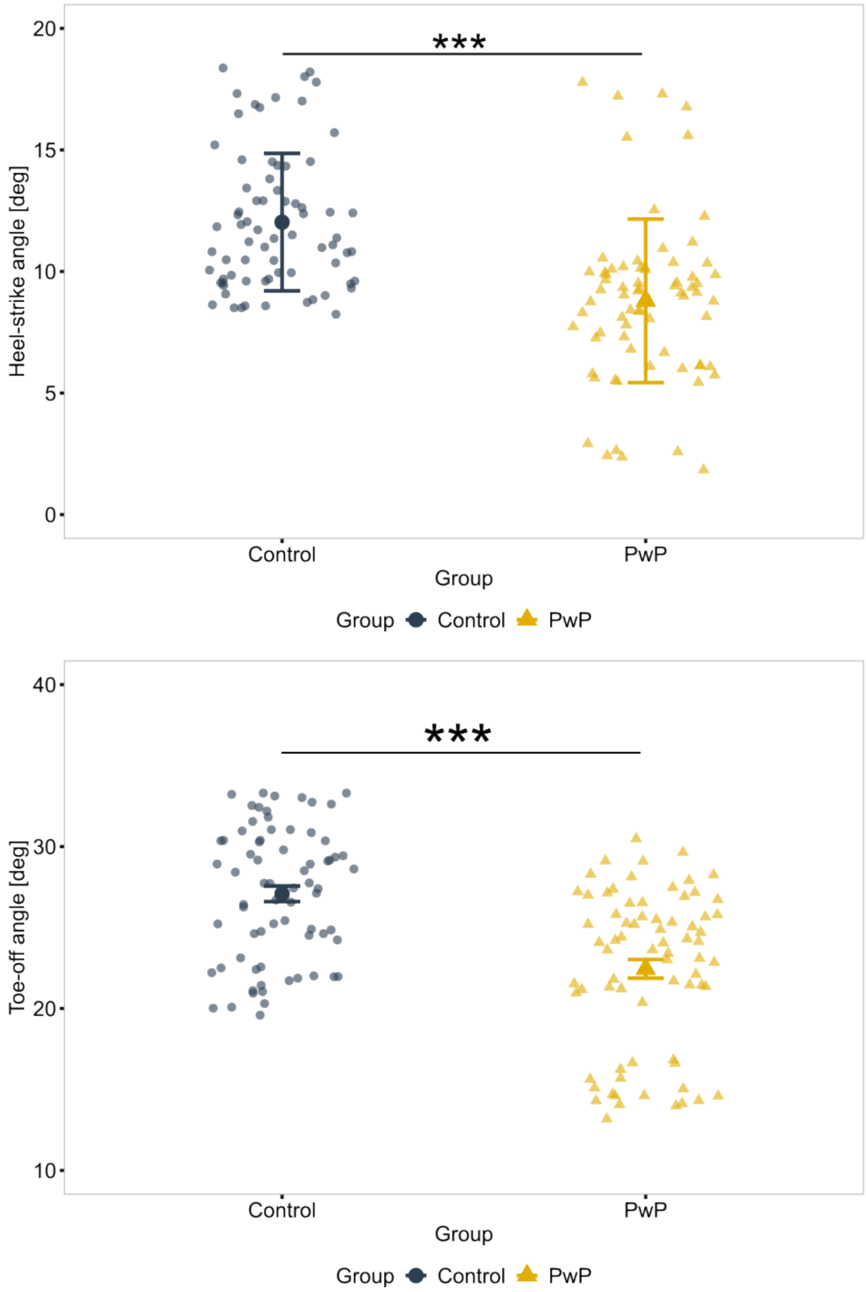

Note. Plots showing the mean TO and HS angles are displayed for each group of participants. The TO angle is the highest angle between the heel and the ground at the beginning of the stride, while the HS angle is the highest angle between the toe and the floor at the end of the stride.*** $p < .001$.

Table 4.3
Study 1 - ANCOVA Results for Group × Protocol Comparison

Task	Parameter	Group	TUG *M (SD)*	FMA-P *M (SD)*	Protocol effect (*p*)	Group effect (*p*)	Interaction (*p*)
Sit-to-stand	Peak Trunk AP Inclination (deg)[a]	Control	123.5(2.7)	124.7(3.8)	.498	.006**	.365
		PwP	120.3(3.2)	119.7(4.9)			
	Mean trunk jerk (m/s^3)[a]	Control	-4.0(1.6)	-4.2(1.5)	.270	.003**	.687
		PwP	-2.0(1.0)	-2.4(1.5)			
	Task duration (s)	Control	1.5 (0.3)	1.2 (0.2)	.064	.026*	.951
		PwP	1.9 (0.5)	1.6 (0.5)			
Turning	Absolute head yaw rotation (deg)[a]	Control	171.3 (9.0)	150.1 (13.7)	<.001***	.052	.245
		PwP	168.8 (6.3)	139.6 (12.3)			
	Head relative to trunk yaw rotation (deg)[a]	Control	2.2 (4.7)	-9.1 (9.2)	<.001***	.521	.848
		PwP	3.0 (5.4)	-8.4 (7.0)			
	Head onset (%)[a]	Control	2.2 (3.5)	6.5 (1.2)	<.001***	.218	.904
		PwP	0.3 (0.7)	4.7 (0.9)			
	Mean heel-strike angle (deg)[b]	Control	7,0 (3.1)	6.2 (3.1)	.527	.007**	.209
		PwP	5.9 (2.1)	2.8 (1.8)			
	Mean COP displacement in ML (mm)[b]	Control	-4.1 (5.9)	44.5 (16.2)	.002**	.386	.098
		PwP	-1.7 (5.6)	52.3 (19.9)			

Note. PwP, People with Parkinson; *M*, Mean; *SD*, Standard deviation; COP, Center of Pressure; AP, Anteroposterior direction; ML, Mediolateral direction.
[a] Parameters adjusted for sex, age, and body height.
[b] Parameters adjusted for sex, age, body height, and foot length.

Table 4.4
Study 2 - Post-hoc results from RM-ANOVA Analysis of Complementary Clinical Assessments.

Parameter	Comparison	Mean difference	95% CI	t	*p*
	Baseline - Pre	-1.7	[-11.7;8.4]	0.74	1.
MDS-UPDRS III	Baseline - Post	-4.9	[-15.0;5.2]	0.33	.983
	Pre - Post	-3.3	[-13.3;6.8]	0.52	1.
TUG time (s)	Baseline - Pre	0.2	[-4.1;4.0]	-0.02	1.
	Baseline - Post	-0.1	[-4.3;3.8]	-0.13	1.
	Pre - Post	-2.6	[-3.9;4.3]	0.11	1.
FMA-P time (s)	Baseline - Pre	-0.3	[-5.1;4.0]	-0.02	1.
	Baseline - Post	-0.8	[-5.1;4.0]	-0.13	1.
	Pre - Post	-0.5	[-4.8;4.3]	0.11	1.

Note. PwP, People with Parkinson; *M*, Mean; *SD*, Standard deviation; COP, Center of Pressure; AP, Anteroposterior direction;
ML, Mediolateral direction.
[a] Parameters adjusted for sex, age, and body height.
[b] Parameters adjusted for sex, age, body height, and foot length.

of three trials was used for the comparison of the three experimental phases. Significant results are presented in Table 4.5.

SIT-TO-STAND The RM-ANOVA revealed a main effect of Phase on the trunk acceleration RMS in PwP ($F(2, 20) = 4.12, p = .032, \eta_p^2 = .29$); however, the post-hoc test did not identify significant differences between phases (Figure 4.9). In contrast to the cross-sectional findings from Study 1, no changes over time were observed in task duration, trunk inclination, or mean trunk jerk.

TURNING We found a main effect of Phase on turn duration ($F(2, 22) = 10.83, p = .001, \eta_p^2 = .50$). Post-hoc pairwise comparisons indicated no significant difference between the Baseline and Pre measures. A significant difference between the completion times of Pre and Post measurements was revealed, suggesting an effect of the intervention. PwP took less time to complete the turn on Post-intervention compared to the Pre measurements (and also between Baseline and Post measures).

There was a main effect of Phase in pelvis jerk ($F(2, 18) = 4.31, p = .030, \eta_p^2 = .30$). After correction, we found a marginal difference ($p = .046$) between Baseline and Post trunk jerk. PwP turned their pelvis more suddenly during Post compared to Baseline. No significant results were found between Pre and Post intervention.

Figure 4.9
Study 2 - Trunk Acceleration RMS during Sit-to-Stand (FMA-P)

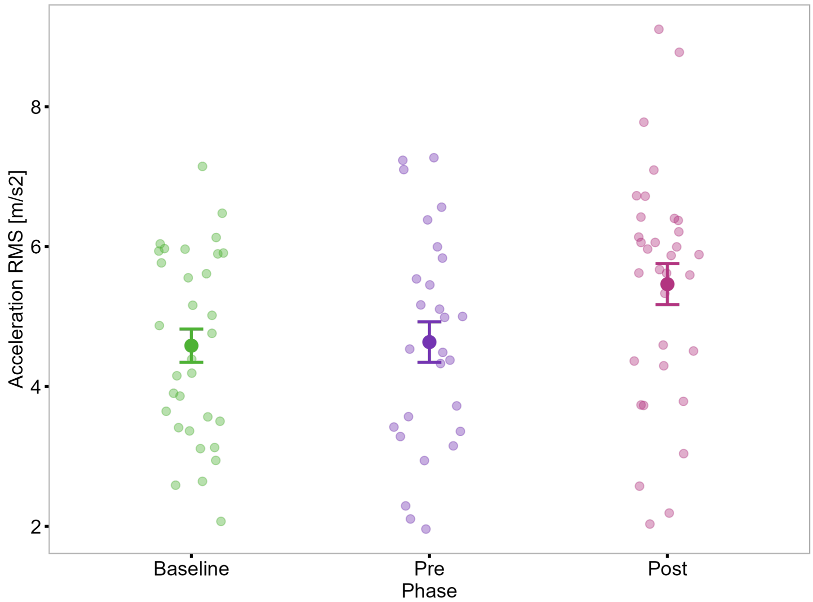

Note. Individual data points are overlaid around each time point. Error bars represent the standard error of the mean (SEM). A significant main effect of the experimental Phase was found (p = .032); however, post-hoc tests did not reveal significant differences between phases.

We also found an effect of Phase on the upper body turning strategies. Specifically, on the turning angles of the head $(F(2,22) = 21.60, p < .001, \eta_p^2 = .66)$, trunk $(F(2,22) = 21.22, p < .001, \eta_p^2 = .66)$, and pelvis segments $(F(2,22) = 21.60, p < .001, \eta_p^2 = .66)$. Results show that PwP exhibited a narrower head, trunk, and pelvis yaw angles during the Post measurements, compared to Baseline and Pre measurement time points as shown in Figure 4.10.

We also found a main effect of Phase on the turn angle of the head relative to the pelvis $(F(2,20) = 3.59, p = .046, \eta_p^2 = .26)$, but the post-hoc test did not reveal any significant differences.

Pertaining to trunk alignment during the turn, we found an effect of Phase in the peak inclination in the AP $(F(2,20) = 4.47, p = .025, \eta_p^2 = .31)$ and ML directions $(F(2,22) = 6.97, p = .005, \eta_p^2 = .39)$. The post-hoc test only revealed a significant difference in the ML trunk inclination between Pre and Post. PwP exhibited a higher trunk inclination sideways on Post compared to the Pre measurement.

STAND-TO-SIT Results indicated the intervention Phase had a significant effect on the maximum pelvis flexion $(F(2,22) = 6.81, p = .004, \eta_p^2 = .38)$ and knee flexion of PwP $(F(2,22) = 16.49, p < .001, \eta_p^2 = .60)$. Post-hoc tests revealed PwP exhibited higher pelvis flexion (body further toward the

Figure 4.10

Study 2 - Rotation Angles of Body Segments during Turning (FMA-P)

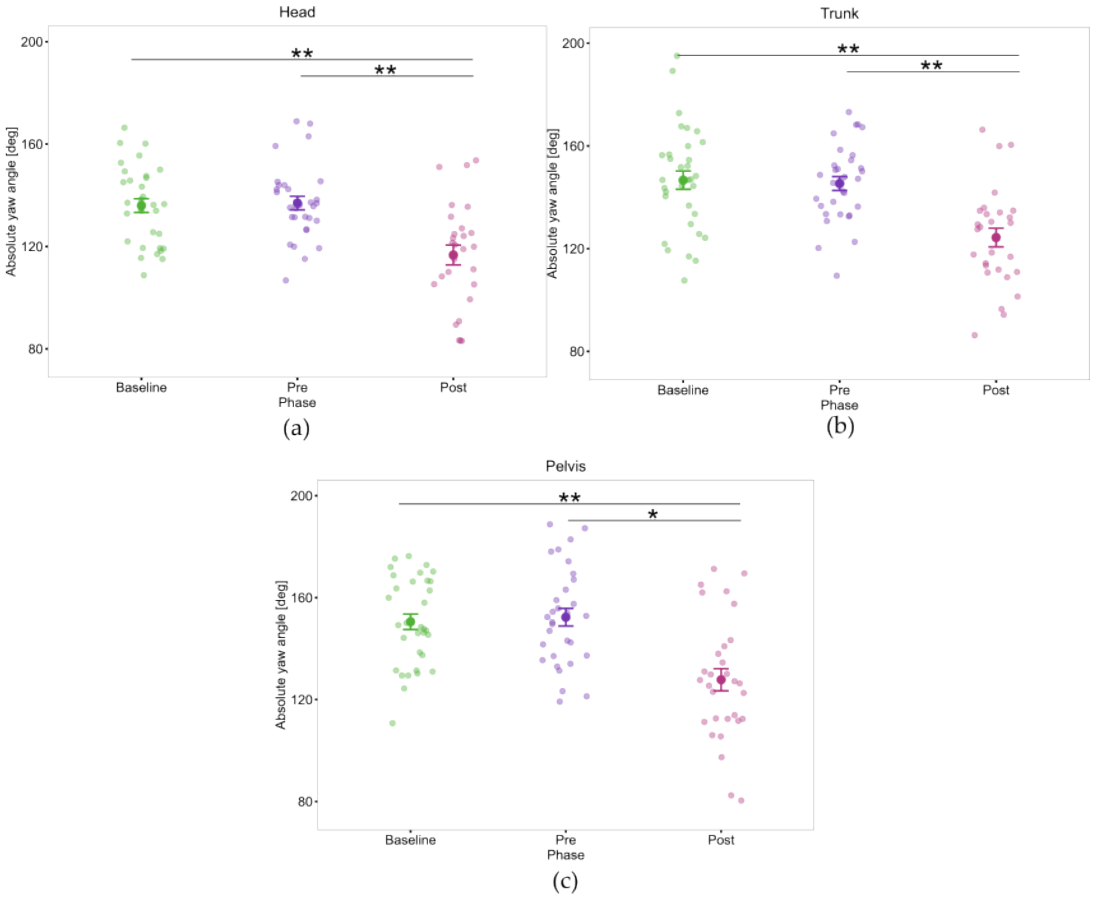

Note. Plot showing yaw rotation angles of the (a) Head, (b) Trunk, and (c) Pelvis for each experimental Phase (Baseline, Pre, and Post). Individual data points are overlaid around each time point. Error bars represent the standard error of the mean (SEM). Post-hoc tests revealed PwP's post-rotation angles were reduced compared to those of Baseline and Pre measurements. * $p < .050$,** $p < .010$.

ground) during Pre measurements compared to Baseline (Figure 4.11, top panel). Concurrently, we found PwP had higher knee flexion during Post and Pre measurements compared to Baseline (Figure 4.11, bottom panel).

FUNCTIONAL REACH Results indicated a main effect of the intervention Phase in the maximum stance width of PwP when picking up the key from the ground $(F(2, 20) = 3.78, p = .041, \eta_p^2 = .27)$; however, the post-hoc test did not reveal significant differences between phases.

4.4 DISCUSSION

4.4.1 *Study 1*

Study 1 reports the development of a new protocol designed to provide further fine-grained insight into commonly used clinical measures (such as the TUG test) of functional mobility in PD. To assess its efficacy, we compared the FMA-P to the TUG (Sprint et al., 2015) using biomechanical parameters comparing PwP with a healthy control group. Our findings indicate that FMA-P provides additional, goal-oriented insights into functional mobility and motor impairments in early-stage PD.

Our results show that while the TUG did not reveal significant differences between groups, the FMA-P, by incorporating a goal-directed functional reach task, did differentiate PwP from controls, with PwP taking longer to complete the goal-directed task. These results suggest that while healthy individuals adapt their motor control or strategies in response to increased task complexity, clinical groups may lack the same flexibility. We suggest, therefore, that the FMA-P helps to magnify between-group differences more so than the traditional metrics completed by the TUG.

To support our claim, the biomechanical analysis, for example, of the sit-to-stand transitions in the FMA-P and TUG revealed significant differences in upper body kinematics between groups. PwP exhibited restricted forward inclination (AP). The reduced forward lean pattern may reflect increased postural instability and the need for anticipatory adjustments to facilitate transition. Additionally, the Performance Score results show PwP tended to push themselves up from the chair with one or two hands and/or using a foot offset to stand up. While previous studies have reported exaggerated pelvis flexion during sit-to-stand in PwP (Morris, 2000), our results indicate that these adaptations are not universal and may be task-specific.

Reduced forward inclination during sit-to-stand suggests that PwP are less reliant on a momentum-driven strategy to initiate this movement (Mancini et al., 2008), with trunk velocities similar between groups during the completion of this transition. Such findings support Inkster and Eng (2004), who reported that while sit-to-stand completion times might be comparable between PwP

Figure 4.11

Study 2- Pelvic and Knee Flexion during Stand-to-Sit (FMA–P)

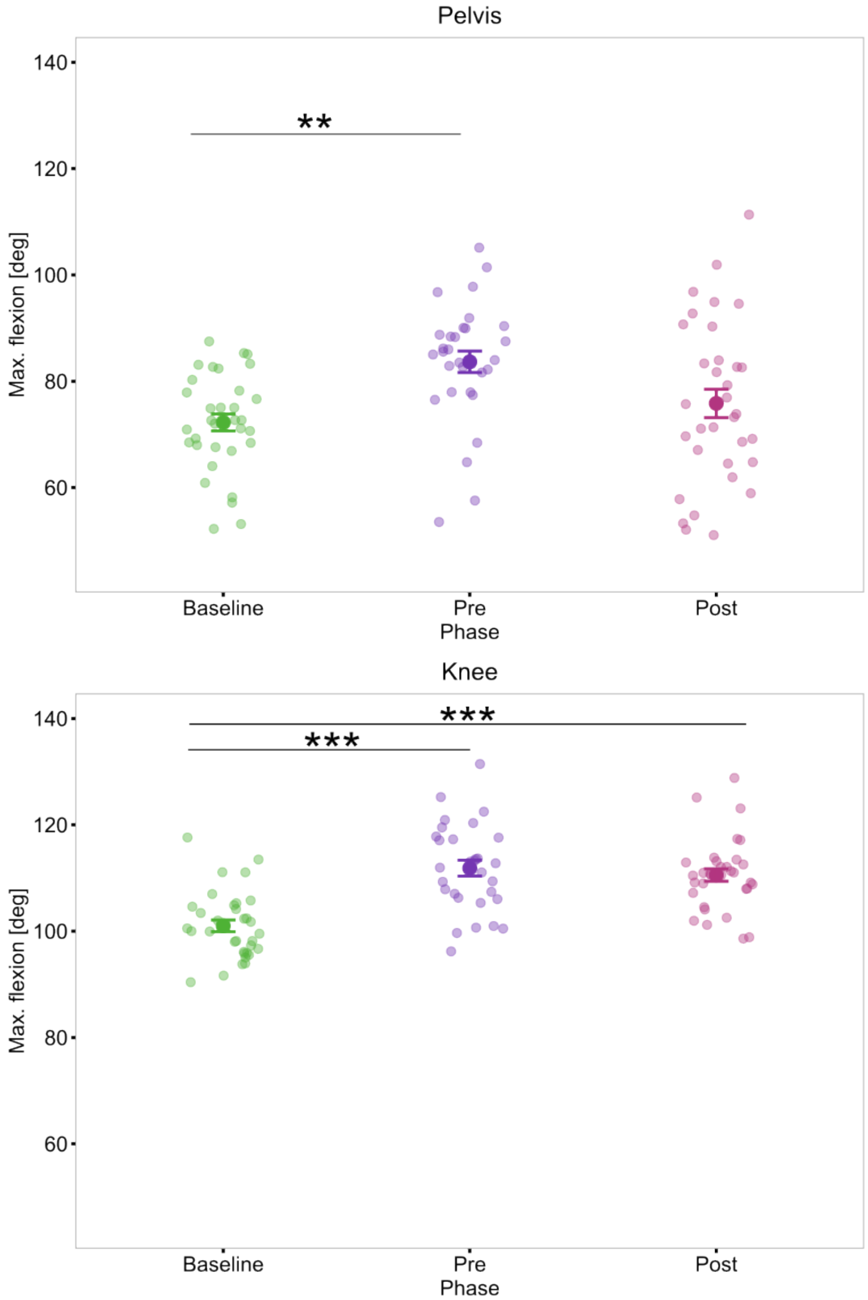

Note. Plots showing the maximum flexion of Pelvis (top panel) and Knees (bottom panel) for each experimental Phase (Baseline, Pre, and Post) during Stand-to-sit. Results show PwP had higher pelvis flexion during Pre measures compared to Baseline and higher knee flexion during Pre and Post compared to Baseline.

Table 4.5
Post-hoc results from RM-ANOVA analysis of intervention phases.

Task	Parameter	Comparison	Mean difference	95% CI	t	*p*
		Baseline - Pre	-0.02	[-0.3; 0.2]	0.22	1.
	Task duration (s)	Baseline - Post	0.4	[0.1; 0.6]	3.97	.006**
		Pre - Post	0.4	[0.1; 0.7]	3.98	.006**
		Baseline - Pre	189.2	[-387.4; 765.8]	0.96	1
	Mean pelvis jerk (m/s3)	Baseline - Post	556.3	[-3.8; 1116.3]	2.91	.05*
		Pre - Post	367.0	[-192.1; 926.2]	1.92	.258
		Baseline - Pre	0.6	[-5.4; 6.5]	0.27	1.
	Absolute head yaw rotation (deg)	Baseline - Post	25.5	[10.4; 40.6]	4.75	.002**
Turning		Pre - Post	24.9	[10.6; 39.2]	4.92	.001**
		Baseline - Pre	2.1	[-5.9; 10.1]	0.74	1.
	Absolute trunk yaw rotation (deg)	Baseline - Post	27.4	[11.9; 42.9]	4.98	.001**
		Pre - Post	25.3	[10.5; 40.0]	4.83	.002**
		Baseline - Pre	-2.6	[-16.4; 11.3]	-0.52	1.
	Absolute pelvis yaw rotation (deg)	Baseline - Post	21.0	[6.3; 35.7]	4.03	.006**
		Pre - Post	23.6	[5.2; 42.0;]	3.61	.012*
		Baseline - Pre	-0.1	[-1.9; 1.7]	-0.12	1.
	Max. trunk ML inclination (deg)	Baseline - Post	2.0	[-0.1; 4.2]	2.68	.064
		Pre - Post	2.1	[0.7; 3.5]	4.24	.004**
	Max. pelvis flexion (deg)	Baseline - Pre	-12	[-19.9; -4.2]	-4.32	.004**
		Baseline - Post	-3.8	[-12.4;4.9]	-1.23	.737
Stand-to-sit		Pre - Post	8.3	[-3.1; 19.7]	2.05	.194
	Max. knee flexion (deg)	Baseline - Pre	-11.7	[-16.9; -6.5]	-6.39	<.001***
		Baseline - Post	-9.5	[-14.1; -4.8]	-5.76	<.001***
		Pre - Post	2.2	[-5.7; 10.2]	0.79	1.
	Max. stance width (m)	Baseline - Pre	-23.7	[-53.1; 5.7]	-2.31	.129
Functional reach		Baseline - Post	0.8	[-30.3; 31.8]	0.07	1.
		Pre - Post	24.5	[-2; 51]	2.65	.073

Note. CI, confidence interval; ML, Mediolateral direction. *p*-values are Bonferroni-adjusted.
p <.050, ***p* <.010, *** *p*<.001

and controls, PwP adapt their movement patterns to overcome motor deficits. While the RMS of trunk acceleration has previously been identified as a discriminative metric between PwP and controls, our results suggest that it may not effectively differentiate early-stage PD (Palmerini et al., 2013).

Analysis of the turning Phase of the FMA-P and TUG further elucidated motor and postural deficits in our PwP cohort. Delayed head onset and head rotation relative to trunk rotation in PwP suggest reduced segmental mobility. Participants also demonstrated significantly reduced rotation angles of the head, trunk, and pelvic segments during the FMA-P protocol. These findings may reflect the increased complexity and planning requirements of the protocol (as the next task was to pick up a key), which may require more frequent or forceful corrections during the movement execution – consistent with a more *en bloc* strategy. Additionally, the altered segmental patterns may indicate a reliance on visuomotor or attentional strategies to support action planning for the FMA-P. Paradoxically, while reduced segmental rotation suggests constrained movement, it may also reflect heightened anticipatory control and effort to maintain stability in this more challenging protocol. Notably, this pattern is more pronounced in PwP, despite participants being in the early stages of disease progression, with predominantly mild, bilateral motor symptoms and preserved balance (as indicated by a mean Hoehn & Yahr score of 1.8).

Furthermore, significantly lower mean TO angles in PwP point to altered foot propulsion and landing dynamics, as reported by Schlachetzki et al. (2017), while COP displacement during turning was predominantly affected in the ML direction. This adaptation may have implications for targeted rehabilitation (Akram et al., 2013). Reduced TO angles across both protocols indicate a more conservative or rigid stepping strategy, which may reflect impaired motor flexibility or anticipatory control. Interestingly, control participants also demonstrated a trend toward a reduction in TO angles during the FMA-P task, perhaps reflective of the increased task demands.

However, the functional reach task introduced in the FMA-P did not reveal any significant group differences. This may be attributed to the relatively homogeneous nature of the groups and/or the relatively low level of symptom severity in the PwP group. Nevertheless, it is notable that differences were found between groups for the other functional mobility tasks embedded in the FMA-P, suggesting that whilst the task increases the demand, overall, it is not the task itself that is difficult. In line with guidance about patient and public involvement in research, we conducted trials of several items, including picking up and placing a tissue box from a table to above shoulder height, and picking up a heavy bottle. Still, the PwP we worked with found picking up and placing a key to be the most "realistic" task. Future studies could consider the impact of alternatives for this aspect of the sequence.

Similarly, after correcting for multiple comparisons, no significant differences were observed between PwP and control participants during the quiet standing task. Although measures such as postural sway (COP displacement) and jerk have been suggested as early indicators of balance impairment in individuals with mid-stage PD (Beuter et al., 2008; Mancini et al., 2008; Schoneburg et al., 2013), they may not reflect balance challenges in early-stage PwP, as also stated by previous studies (Frenklach et al., 2009; Horak et al., 2016). Further examination should be considered with a more diverse sample of PwP.

The locomotion task results indicated significant gait disturbances in the PwP group. We observed significantly lower TO and HS angles than controls, consistent with previous studies (Schlachetzki et al., 2017). Foot height was also lower in PwP, supporting findings by Shin et al. (2020), in that altered foot mechanics are associated with PD. Additionally, even at an early stage of PD, our results demonstrated that PwP had a reduced stride length and slower walking velocity, suggesting reduced propulsion (Horak & Mancini, 2013). The prolonged double support time of PwP highlights the need for stability, reflecting compensatory mechanisms for balance preservation.

We found no significant differences in arm swing velocity and asymmetry between groups, which may reflect variability in arm swing dynamics in early and mild PD. These results were also reflected in the qualitative results of the Performance Score, with individuals tending to perform the arm swing from the elbow, but with very different individual characteristics (i.e., amplitude and asymmetry). This approach supports the individualization of rehabilitation programs, which is an important goal of Parkinson's care.

Notably, we observed 19 freeze-like episodes in PwP during the FMA-P, where participants walked through the doorway. In contrast, no FLEs occurred when PwP walked without a doorway, implying environmental features like doorframes could influence freezing behavior, as reported by previous studies (Cowie et al., 2012).

Despite the insights gained in understanding qualitative differences in functional mobility through the integration of motion capture and pressure-sensitive gait mat technologies, the study has several limitations that need to be addressed. Firstly, our findings are limited as our sample of PwP was in the early stages of the disease. Nevertheless, even at this early stage, we could identify functional mobility impairments in PwP compared to healthy individuals over and above what was found even with motion capture analysis of the TUG, suggesting the FMA-P offers additional insights into the quality of functional mobility in Parkinson's that has implications for both intervention studies and rehabilitation strategies.

4.4.2 *Study 2*

Study 2 aimed to evaluate changes in functional mobility in PwP across three intervention phases using the FMA-P. While traditional clinical metrics such as the UPDRS, TUG, and task duration did not reflect significant improvements, motion capture analysis of the FMA-P captured meaningful biomechanical adaptations, particularly in tasks involving turning, stand-to-sit transitions, and functional reach. These findings underscore the FMA-P's potential for detecting subtle rehabilitation-related changes in motor performance.

In contrast to Study 1, where sit-to-stand transitions revealed between-group differences in forward trunk inclination and compensatory strategies, Study 2 identified a significant effect of intervention phase on trunk acceleration (RMS) during the same task. Although post hoc comparisons did not yield significant pairwise differences, the observed results align with previous research suggesting that higher trunk acceleration during sit-to-stand transitions is a relevant indicator of improved postural control in PwP (Mancini et al., 2011).

The stand-to-sit phase revealed phase-related changes in joint flexion strategies. PwP demonstrated increased maximum pelvis and knee flexion from Baseline to Post-intervention. These results may reflect improved eccentric control and a more deliberate, confident approach to sitting, although higher angles could also indicate a more cautious descent strategy (Inkster & Eng, 2004).

Turning, which also differentiated PwP from controls in Study 1 through reduced segmental rotation and delayed head onset, emerged as the most sensitive task to intervention effects in Study 2. PwP showed significantly reduced turn duration following the intervention, pointing to improved motor planning and execution. Additionally, an increase in pelvis jerk post-intervention may indicate more dynamic and confident turning behavior, consistent with a shift in strategy. As previous research has shown a link between pelvis jerk and fall risk in PD, it serves as a relevant marker for assessing dynamic balance and movement control (Castiglia et al., 2021).

Segmental yaw rotation angles were reduced post-intervention. Rather than suggesting rigidity, this likely reflects more efficient axial coordination, enabling faster and more controlled turning, as reported by previous studies (Hong et al., 2009).

Additionally, significant effects were found in trunk inclination: both AP and ML peak angles changed across phases, with ML inclination significantly increased from Pre to Post. This suggests greater lateral trunk engagement, possibly reflecting improved balance and a more proactive turning strategy.

In contrast to Study 1, where functional reach did not differentiate between groups, Study 2 showed a significant phase effect on stance width during the reaching task. A broader base of support from Pre- to Post-intervention suggests improved anticipatory postural adjustments (Azevedo et al., 2016).

This may represent a compensatory response to perceived instability during forward reach, indicating subtle but meaningful changes in movement strategy following intervention.

Notably, while Study 1 identified freezing-like episodes in response to environmental cues (e.g., doorways), Study 2 did not observe consistent changes in freezing behavior across phases. In line with previous research, this may indicate that freezing episodes are not easily influenced during controlled assessments or may not translate into a reduced number of FLEs in short-term standardized tasks (Brichetto et al., 2006).

Although no significant improvements were detected in the Performance Score over time, the qualitative data indicate that PwP utilized various adaptive strategies to complete the tasks. These individualized compensations may reflect attempts to maintain function despite underlying motor impairments, underscoring the need for quantitative biomechanical analyses to capture subtle motor changes.

Overall, the findings of Study 2 build upon the results of Study 1 by showing that the FMA-P is not only sensitive to between-group differences but also to within-subject changes in functional mobility over time. Whereas conventional clinical measures failed to detect intervention-related effects, the FMA-P identified significant improvements in turning speed, pelvis jerk, and trunk inclinations. These changes indicate enhanced dynamic and confident movement strategies, which are critical for reducing fall risk and maintaining functional independence in PwP.

4.5 IMPLICATIONS, STRENGTHS AND LIMITATIONS

The TUG framework raises important questions about the interplay between automatic and goal-directed movement control. Movements such as rising from a chair or turning may typically rely on automatic, habitual processes; however, these actions also demand cognitive resources and may engage goal-directed control mechanisms, especially in individuals with PD (Redgrave et al., 2010). The extent to which early-stage PD impacts habitual movement, potentially increasing reliance on goal-directed strategies, is not yet fully understood (Bannard et al., 2019). Moreover, the sensitivity of the TUG to detect subtle impairments in early PD is limited (Salarian et al., 2010; Zampieri et al., 2010), as it primarily assesses overall task completion time rather than detailed movement quality. Therefore, to overcome this limitation, we assessed performance through a biomechanical analysis of movement execution, complementary to clinical assessments (time taken), which complements clinical assessments (time taken) and is essential for understanding underlying neurological mechanisms and guiding targeted interventions.

Our novel FMA-P protocol directly addresses these challenges by combining goal-directed tasks with high-resolution biomechanical assessments to provide a more fine-grained, multidimensional perspective on motor performance in PD. The protocol was well tolerated by participants, and the data obtained revealed functional impairments and movement adaptations not detectable by conventional tools. For example, even in early-stage PD, participants displayed compensatory movement strategies such as altered trunk and pelvis motion or reliance on hand support, likely reflecting underlying motor control deficits that are masked in traditional summary scores.

A key strength of our approach lies in its ability to capture both quantitative and qualitative aspects of motor behavior. Motion capture and pressure-sensitive gait analysis allowed us to detect subtle spatiotemporal and segmental kinematic differences, offering insights into compensatory strategies and adaptive responses to task demands. The qualitative data, such as variations in arm swing pattern or sit-to-stand technique, also demonstrated the value of individualized analysis in tailoring interventions. These findings align with the goals of personalized rehabilitation in PD and support the development of individualized therapy plans based on actual motor behavior rather than aggregate scores alone (Bryant et al., 2020; Mi et al., 2021).

Certain limitations should be acknowledged. The relatively small sample size and focus on early-stage PD may limit the generalization of our findings to broader clinical populations. Additionally, in Study 1, PwP were significantly older than the healthy control group. Given that age itself can influence balance and gait, this age difference may have contributed to the observed between-group differences. Nevertheless, Study 1 was intended as a pilot investigation to evaluate the feasibility and sensitivity of the FMA-P. Importantly, Study 2 employed a within-subject design, eliminating age-related confounds and confirming the FMA-P's sensitivity to intervention-related changes in functional mobility. To address this, three intervention trials were already conducted in the UK and Switzerland (D. Rose et al., 2023), aiming to further validate the clinical utility of the FMA-P and the Performance Score across more diverse and representative cohorts (in preparation).

Additionally, while biomechanical assessments offer detailed insights, they are resource-intensive and may not be feasible for widespread use in routine clinical settings. Nonetheless, the FMA-P protocol was well-received by participants, who reported minimal burden during the assessment, and the comprehensive yet streamlined data analysis approach we implemented justified the time required, supporting its continued application in future studies.

Finally, the considerable variability in movement strategies observed among participants highlights the importance of individualized assessment and intervention planning, which our approach enables by capturing both quantitative and qualitative motor features.

4.6 CONCLUSIONS

The newly developed measure of functional mobility (FMA-P) has been designed for and with PwP to reflect the challenges they face in everyday movement sequences. Standard clinical-level measures, such as task completion in the TUG, provide a general mobility assessment but do not capture subtle motor deficits.

Our results demonstrate no group differences or intervention effects using the gold-standard measure of the TUG and the MDS-UPDRS. Still, when using a goal-directed task, subtle variations are revealed, which may reflect the increased complexity of the FMA-P. The FMA-P enables a fine-grained quantification of the quality of tasks such as standing up, walking through a doorframe, turning, picking up and placing an object, and sitting down within one short sequence. The integrated motion capture and pressure-sensitive gait mat system provides multi-dimensional, time-tracked data on these tasks, can improve the understanding of clinical measures, and provide insight into changes in PwP's various motor symptoms over time. Our findings provide objective and precise information about various qualitative aspects of functional mobility to improve the evidence base of outcome variables. Future research will have to address the potential use of the FMA-P within a broader clinical population to assess individual and specific functional motor impairments. The knowledge generated by this method may help inform intervention programs targeting specific tasks in daily life activities, which are aimed at effectively counteracting disease progression and improving quality of life.

INTERMEDIATE SUMMARY

Existing clinical assessments of Parkinson's disease (PD) primarily focus on stratifying symptom severity or progression rate, which limits their ability to capture changes in functional mobility, an important factor in evaluating rehabilitation outcomes. To address this gap, we developed a novel methodology, the Functional Mobility Assessment for Parkinson's (FMA-P), which integrates motion capture and pressure-sensitive gait analysis to explore key aspects of functional mobility. To develop the FMA-P protocol, we conducted a pilot study involving 12 individuals with PD and 12 age-matched healthy controls, who each completed the FMA-P sequence three times. The sequence included the following tasks: rising from a chair, walking through a doorway, turning, bending to pick up and place an object, and returning to a seated position. Results from Study 1 demonstrated that the FMA-P is a sensitive tool for identifying functional impairments in PD. In particular, significant differences between people with Parkinson's (PwP) and controls were observed during chair rise (higher peak trunk inclination, lower mean trunk jerk) and turning task (longer task duration and lower heel strike angle), providing critical insights into postural stability. To assess changes in functional mobility over time, we conducted a 12-week repeated-measures intervention study with 12 participants with PD. Results from Study 2 indicated notable improvements in turning stability and balance. Participants demonstrated reduced turning time and increased yaw rotation in the head, trunk, and pelvis. In contrast, no significant changes were observed in standard clinical measures (i.e., Timed Up and Go and task duration). The FMA-P offers fine-grained insights into movement quality, making it a valuable tool for early diagnosis, monitoring intervention efficacy, and guiding rehabilitation strategies in individuals with PD.

This Chapter is currently under review by the editors of the MDPI Sensors journal. Additionally, the findings from these studies were presented at the Society for the Analysis of Human Motor Skills in its Clinical Application (GAMMA) congress held in February 2025 in St. Gallen, Switzerland.

This study was made possible through a two-and-a-half-year collaboration with Prof. Dawn Rose and Dr. Sabrina Köchli from the Lucerne University of Applied Sciences and Arts, School of Music (HSLU). Through this collaboration, I was able to develop a robust foundation for motion data analysis. Additionally, it offered me the opportunity to learn about the process and implementation of intervention studies directed toward clinical populations. This was my first experience participating in a clinical study, which was not only enriching in knowledge but also personally rewarding.

A follow-up article is also in preparation, which will include the results of additional clinical groups of PwP, and the progression of the biomechanical parameters over the course of the musical therapy intervention.

5 EMBODIED CUES OF ENGAGEMENT IN HUMAN-ROBOT INTERACTION (HRI)

Published as Casso, I., Chame, H. F., Hénaff, P., & Delevoye-Turell, Y. (2024, August). Exploring Engagement in Human-Robot Interaction through the Quantification of Human Spontaneous Movement. *In 2024 33rd IEEE International Conference on Robot and Human Interactive Communication (ROMAN)* (pp. 1768-1773). IEEE. https://doi.org/10.1109/RO-MAN60168.2024.10731439.

5.1 INTRODUCTION

Advances in social robotics constitute interesting opportunities for applications in healthcare, education, entertainment, and services. These robots are expected to be useful to humans, hence studying the design properties that offer optimal *engagement* in human-robot interaction (HRI) is crucial. Engagement has been defined as a process by which the perceived connection between participants in interaction is initiated, maintained, and ended (Sidner et al., 2005). However, the definition of engagement differs in the literature across modes of interaction (e.g., Human-Human HHI, Human-Computer HCI, Human-Robot). In their survey, Salam and colleagues determined engagement to be dependent on emotional, cognitive, and behavioral factors (Salam et al., 2024). Common estimation features across the various interaction modes may exist; specifically, the quantification of spontaneous movement was considered as a non-verbal behavioral feature that would offer the means to infer human engagement. Studies in HHI have reported that spontaneous rhythmic movements like head nodding and body sway emerge continuously during interaction and are triggered without individuals' awareness (Chang et al., 2021; Tschacher et al., 2014). Human spontaneous movements have also been quantified along with posture to assess engagement in HRI (Salam et al., 2016; Sanghvi et al., 2011). These HHI and HRI studies resorted to temporal motion analysis from motion capture or video recordings, suggesting that the quantification of spontaneous movement can serve as an additional indicator of engagement to other non-verbal behavioral indicators such as gaze, or face expression processing (Oertel et al., 2011, 2020).

The main contribution of this chapter is to propose a methodology based on wavelet spectral analysis to quantify spontaneous movement as a behavioral metric that can characterize engagement in HRI. To test our methodology, we defined a social (i.e., no goal-oriented) face-to-face interaction experiment where participants were invited to listen to negative stories told by a robot that exhibited emotional body language. Concurrently, their movements were tracked with a motion capture system. We hypothesized that the presence of a robot would affect spontaneous human sway and that spontaneous sway during interaction would be related to the social traits attributed to the robot. We also examined how different robot platforms might impact participants' spontaneous swaying based on robots' morphological differences and emotional body postures. Additionally, we compared these results with a control condition for which no robot was present.

5.2 PREVIOUS WORKS

Within HRI, studies have considered the quantity of movement as a behavioral feature to determine the level of human engagement. In (Salam et al., 2016; Sanghvi et al., 2011), authors quantified spontaneous movement by computing the average motion of silhouette pixels on video frames. A disadvantage of this method might be the analysis of static frames, which could overlook the dynamic changes in human motion. As studies show, humans in interaction often exhibit sporadic and irregular movements (e.g., ballistic motions for pointing, changes in posture), and rhythmic movements (e.g., head nodding, body sway) emerging at different frequencies. HHI studies have proposed to quantify movement with spectral analysis of time series in the frequency domain using the Fourier transform (Issartel et al., 2015; R. C. Schmidt et al., 2012). A limitation of this technique is that it assumes the time series to present a constant, regular pattern, which does not correspond to situations of irregular motion, which is non-stationary in nature. Alternatively, spectral analysis through the wavelet transform does not require the time series to be stationary. Thus, it provides a time-frequency representation allowing the identification of frequency components and power spectrum magnitude at different time intervals (Fujiwara & Daibo, 2016). For example, in Walton et al. (2015), cross-wavelet spectral analysis was employed for movement coordination. In Fujiwara and Daibo (2016), interpersonal synchrony patterns were evaluated. These studies suggest that spectral analysis through the wavelet transform is suitable for the quantification of movement characteristics such as temporal variability and intensity. To summarize, inspired by research in HHI, we propose to employ continuous-wavelet transform analysis to quantify spontaneous movement in HRI 3.4.2.1. We propose that the magnitude of the power spectrum can serve as an indicator of spontaneous movement emergence and thus, be taken as an objective feature for engagement inference. In the section below, we provide an algorithmic description of our methodology.

Table 5.1
Hardware components

Hardware	Description
Robot Buddy	4 degrees of freedom (DOF), 0.56 m height, cone-like base connected to an oval head, and an animated face displayed on a touchpad located on the head.
Robot Nao	25 DOF, 0.57 m height, humanoid morphology with bipedal walk and two arms; motionless eyes and mouth, with eyes capable of blinking.
Robot Pepper	20 DOF, 1.2 m height, featuring arms and a wheeled base without legs; head with eyes that emulate blinking, but a fixed mouth.
Computer	x64-based PC, i5-1235U processor, 32 GB RAM.
Qualisys	Eight infrared cameras recording 3D motion at 200 Hz of four reflective markers placed on the shoulders, base of the neck, and forehead of participants (see Fig. 5.1A).

Note. Hardware components used for robotic interaction, motion capture, and data processing.

5.3 methods

5.3.1 *Materials*

As detailed in Table 5.1 and shown in Fig. 5.1, three robot platforms were used in the experiments, having distinct morphology, actuation modalities, and size. The software components included: Qualysis Track Manager to obtain motion capture data of human movement, the PyCWT module (Krieger et al., 2017) was used for wavelet analysis, the library *naoqi* version 2.1 was used to program the robots Nao and Pepper. All programs were developed in Python language both version 2.7 and 3.

5.3.2 *Emotional body cues of robots*

Considering our task was to listen to negative stories told by the robots, they were programmed to show behavioral cues corresponding with a negative affective valence. As such, the specificity of their actuation systems was carefully considered (see Fig. 5.1).

Buddy was programmed to exhibit sway motion in its sagittal plane (i.e., the plane XZ facing the human) while showing sad facial expressions on its touchpad head. The body morphology above the hip is relatively similar for Nao and Pepper, hence they were programmed to sway in a combined motion between the head and torso tilt, which intended to imitate human cowering movements generally associated with sadness (Atkinson et al., 2004). However, there were some differences in their behavior. Nao held its arms against the torso, but this posture was not replicated for Pepper (see Fig. 5.1-B) since placing Pepper's arms against the torso resulted in increased mass around its center of gravity, causing the hip's actuators to overheat triggering warnings alarms, which could distract participants.

Figure 5.1
Experimental Setup and Robot Postures

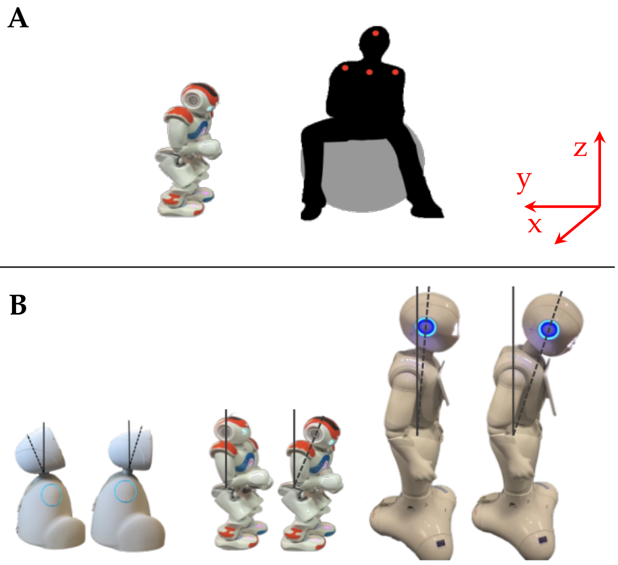

Note. A. Illustration of the posture adopted by participants during the experiment. The red dots on the head, shoulders, and base of the neck represent the tracked markers in relation to a fixed reference frame. B. Emotional body language programmed on robots Buddy (left), Nao (center), and Pepper (right).

Sway motion was controlled in position, from a sinusoidal signal with a constant frequency and amplitude depending on the robot, sampled at 20 Hz. Three periodicity levels were selected to display different energy levels on a negative valence (Bretan et al., 2015): Low = 8 s (0.13 Hz), Medium = 4 s (0.25 Hz), and High = 2 s (0.5 Hz).

5.3.3 *Narrative Stimuli*

To align with the negative emotional cues, three negative stories (each lasting approximately 3 minutes) were written in a first-person perspective in French and recorded using the text-to-speech method of Buddy supported by ReadSpeaker ("Read Speaker," 2024). The generated voice pitch had a fundamental frequency of 220 Hz. To control the impact of differences in robot voice synthesis, Buddy's generated stories were stored and played back in Nao and Pepper.

We conducted a lexicon-based analysis of the valence of all the stories with the pyFeel package, which relies on the emotional French lexicon developed by Abdaoui et al. (2017). The method produces scores for seven discrete emotions, though the definition of these categories remains limited. The analysis returned a score of 66% for positivity and joy (see Table 5.2), and a 29% for negative-valenced emotions (fear, sadness, anger, and disgust). This could be because the stories began with positive memories recalled by the robot, ending with negative events.

Table 5.2
Valence Analysis of the Negative Stories

	Positivity	**Joy**	**Fear**	**Sadness**	**Anger**	**Surprise**	**Disgust**
Mean score	59%	7%	9%	11%	5%	4%	4%

Note. Analysis carried out with the PyFeel package (Zouitine, 2018)

5.3.4 *Participants*

Four independent groups of participants N=76 were recruited (n_{Buddy}=20, n_{Nao}=20, n_{Pepper}=21, $n_{No-Robot}$=15). All participants were fluent in French language, undergrad and post-grad psychology students, aged 18 to 35 years.

Participants were informed about the experiment's general procedure at least 24 hours before their inclusion and gave their signed consent. All participants were naive to the objective of the study.

The experimental procedure and inclusion of participants followed the strict code of ethics of the WMA Declaration of Helsinki for research involving human participants.

5.3.5 *Experimental protocol*

We conducted experiments in which participants were grouped for interaction with one of the three robots. As a control condition, a group of participants listened all stories from a speaker (No-Robot condition).

The experiment structure is presented in Fig. 5.2. During the introduction phase, participants were instructed to sit on an ergonomic ball. We opted for this type of seating to allow for a wider range of motion and enable the non-voluntary spontaneous back-and-forth oscillation (i.e., sway) of their body, which is often restricted by conventional chairs. Then, participants watched a short video of one minute to contextualize the experiment.

Panel A of Fig.5.1 shows the posture adopted by participants when facing the corresponding robot. During the storytelling phase, participants were instructed to listen to the stories told by the robot. No specific instructions

Figure 5.2
Experimental protocol

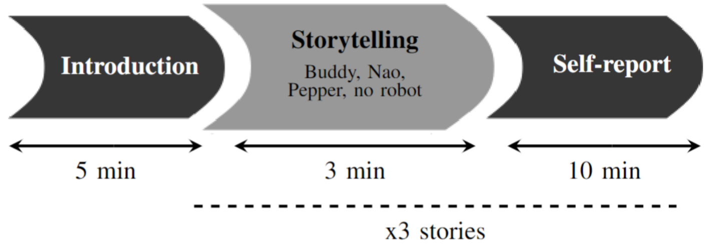

Note. The experiment videos are available at: https://tinyurl.com/4nffm2dk

were given to participants other than to listen to the stories. Participants were not informed either about the valence of the stories or that the narration would be from the first-person perspective. During the storytelling phase, the robot played the three stories always in the same order, while displaying emotional body cues that were counterbalanced for every participant.

The environmental conditions of the experimental room were identical for all robots. Since Pepper is almost twice the size of the other robots, a platform was used to elevate the participants' position to have an equivalent view direction slope to the robot.

After every story narrated by the robot (Self-report phase), participants completed the Godspeed questionnaire (Bartneck et al., 2009) for the categories: *anthropomorphism*, *likeability*, *animacy*, and *perceived intelligence*. Semantic differential scales were used (e.g., *Fake-Natural*, *Apathetic-Responsive*, *Unfriendly-Friendly*). From a pilot evaluation, we decided to exclude the category *Perceived Safety*, since this category was insufficiently discriminating for the small-sized social robots considered.

5.3.6 *Self-reported affect*

To evaluate core affect changes during the interaction with the robots, we collected affect grid answers from participants before and after the experiment. Data were transformed to 2-dimensional coordinates for analysis (see section 3.5).

5.3.7 *Spontaneous Movement Engagement (SME)*

Based on the methodological basis presented in section 3.4.2.1 of Chapter 3, we propose the algorithm *spontaneous movement engagement* (SME) as a behavioral metric for engagement inference in HRI through the processing pipeline shown in Algorithm 1. The procedures referred to are presented in pseudo-formal language in Algorithm 2.

Algorithm 1

procedure SME
  $A \leftarrow initialize()$
  for $r \in \{\text{Buddy}, \text{Nao}, \text{Pepper}\}$ **do**
    for $f \in \{\text{Low}, \text{Medium}, \text{High}\}$ **do** ▷ robot sway condition
      $P_{rf} \leftarrow initialize()$
      for $j \in \text{G}_r$ **do** ▷ participants exp. group G_r
        $X_{rfj} \leftarrow BuildSequence()$
        $P_{rfj} \leftarrow WaveletAnalysis(X_{rfj})$
      $A_{rf} \leftarrow StatisticalAnalysis(P_{rf})$
  return A

Algorithm 2

procedure BuildSequence ()
  $X_j^{3\text{D}} \leftarrow acquireData()$ ▷ for participant j
  $\hat{X}_j^{3\text{D}} \leftarrow computeKinematics\left(X_j^{3\text{D}}\right)$
  $\tilde{X}_j^{3\text{D}} \leftarrow filterOutliers\left(\hat{X}_j^{3\text{D}}\right)$
  $X_j^{1\text{D}} \leftarrow reduceDimension\left(\tilde{X}_j^{3\text{D}}\right)$
  $\hat{X}_j^{1\text{D}} \leftarrow downSample\left(X_j^{1\text{D}}\right)$
  $X_j \leftarrow filterData\left(\hat{X}_j^{1\text{D}}\right)$
  return X_j

procedure WaveletAnalysis (X_j)
  $\gamma \leftarrow selectParameters()$
  $W_{nj}(s) \leftarrow computeCWT\,(X_j, \gamma)$ ▷ Eqs. (3.4), (3.5)
  $P_j(s) \leftarrow computePS\,(W_{nj}(s))$ ▷ Eq. (3.6)
  $\hat{P}_j(s) \leftarrow scalePS\,(P_j(s))$ ▷ see Liu et al., 2007
  $\widetilde{P}_j(s) \leftarrow T^{-1} \sum_{t=1}^{T} \widetilde{P}_{jt}(s)$ ▷ with experiment time T
  if $\widetilde{P}_j(s) < \gamma$ **then** ▷ test for aberrant motion
    return $\widetilde{P}_j(s)$
  else
    return $\emptyset$

procedure StatisticalAnalysis $\left(P_{rf}\right)$
  $A_{rf} \leftarrow N^{-1} \sum_{j}^{j \in \text{G}_r} P_{rfj}$ ▷ participants' mean
  $\hat{A}_{rf} \leftarrow filterBandPass(A_{rf}, K)$ ▷ with bandwidth K
  $\tilde{A}_{rf} \leftarrow Y_{\text{N}}^{-1} \sum_{y}^{Y} \hat{A}_{rfy}$ ▷ mean in freq. range Y
  return $\tilde{A}_{rf}$

For the *BuildSequence* procedure, marker-based motion data was acquired at 200 Hz (line 2), and markers' velocity and acceleration were estimated (line 3). A filtering procedure was applied to extract all absolute acceleration peaks above 1000 mm/s^2, so filtered points were substituted by interpolation (line 4). Data in 3D was reduced to 1D by taking the Euclidean distance between consecutive acquisitions of the torso's estimated location (line 5). Data was then down-sampled from 200 Hz to 25 Hz (line 6). A third-order Butterworth low-pass filter with a cutoff frequency of 11 Hz to the 3D was applied, followed by a high-pass third-order Butterworth filtering with a threshold of 0.03 Hz to remove the low-frequency trend (line 7). The resulting data from previous steps correspond to the motion sequence for participant j.

The Morlet mother wavelet was chosen with $\omega_0 = 6$ (see Eq. (3.5)). The procedure *WaveletAnalysis* involved selecting the wavelet transform parameters (line 2). To calculate the transform in Eq. (3.4) (line 3), we used the method *wavelet.cwt* of the Python module PyCWT (S. Krieger et al., 2023), with parameters: time step $dt = 0.05$, starting scale $s0 = 0.25$, time increment between scales $dj = 0.08$ sec, and the number of powers of two with dj sub-octave intervals $J = 100$. The wavelet coefficients were then squared to obtain the wavelet power spectrum (PS) conforming to Eq.(3.6) (line 4). To correct for the effects of the wavelet transform on the PS, the latter was multiplied by the inverse of the scale at each frequency (see Liu et al. (2007)) and by a scaling factor (line 6). Only sway movements were quantified (i.e., rocking back and forth), while posture corrections such as stretching were not taken into account in this analysis. Participants who exhibited excessive movements during the baseline of the experiment were excluded from the analysis (with threshold $\gamma = 0.6$, see line 7).

For the procedure *StatisticalAnalisys*, the power spectra for participants were averaged according to the experimental conditions. We calculated the local minima of the PS to identify the significant frequency windows for the bandwidth filter (Sozzi et al., 2021). The parameter K (see line 4) was selected so 90% of the PS was contained in the passing bandwidth.

5.4 RESULTS

Results are presented for the self-reported affect during HRI, followed by the spontaneous movement quantification according to Algorithm 1, and by the participants' responses to the Godspeed questionnaire.

5.4.1 *Affect assesment*

Two mixed RM-ANOVAs were conducted on each axis of the affect grid (valence,arousal), considering their timepoint (Before, After) as the within-subjects

RM factor and Robot group (Budd, Nao, Pepper) as the between-subjects factor.

There was a significant main effect on Valence ($F(1, 63) = 33.06$, $p < .001$, $\eta_p^2 = .34$) and an interaction effect of Valence × Robot group ($F(2, 63) = 4.14$, $p = .020$, $\eta_p^2 = .12$). Concurrently, we carried on the same analysis structure for the Arousal scores. We found a significant main effect on Arousal ($F(1, 61) = 27.41$, $p < .001$, $\eta_p^2 = .31$. And an interaction effect of Arousal x Robot ($F(2, 61) = 4.68$, $p = .013$, $\eta_p^2 = .13$)

Pairwise comparisons revealed that participants interacting with Buddy, Nao, and Pepper all reported lower valence (Buddy: p = .043, Nao: p = .038, Pepper: p = .010) and arousal levels (Buddy: p = .014, Nao: p = .024, Pepper: p = .037), with significant differences observed for each robot (see Figure 5.3).

5.4.2 *Spontaneous human movement*

Fig. 5.4 presents an example of the procedure *WaveletAnalysis* (see Algorithm 2) applied to participants who displayed spontaneous sway motion. In Fig. 5.5 we present an example of the operation *filterBandPass* (line 3), to determine the bandwidth for statistical analysis. Our analysis determined that SME tended to be higher when all robots moved at an 8s periodicity (0.13 Hz) in the sagittal plane.

A one-way ANOVA analysis indicated that the robot's sway motion globally exerted an influence on human spontaneous motion (F(2,31) = 6.06, p = .006, η_p^2 =0.28). A Tukey post hoc analysis confirmed that the spontaneous movement of participants who interacted with Buddy had higher SME than those who interacted with Pepper (t = 1.91, p = .035) and Nao (t = 3.43, p = .005).

Concurrently, those who interacted with Pepper had higher SME than those who interacted with Nao (t= 2.74, p = .006). The post-hoc analysis did not reveal a statistical difference between the group that did not interact with a robot and the robot groups. Specifically, the no-robot group demonstrated higher SME variability among the three groups (M = 0.10, SD = 0.14), and tended to be lower than the Buddy group (M = 0.15, SD = 0.10) (t = -0.95, p = 0.77). The no-robot group tended to have higher SME than the Nao group (M = 0.06, SD = 0.03) (t = 1.59, p = 0.39), and than the Pepper group (M = 0.09, SD = 0.03) (t = 0.89, p = 0.81).

5.4.3 *Robot social attributes*

An RM-ANOVA determined an interaction of Godspeed categories and Robots (F(5,33) = 5.9, p = $<$ .001, η_p^2 =0.16). A Tukey posthoc test revealed statistical differences in all categories except for Anthropomorphism. We found Buddy (t = 7.42, p = $<$ .001) and Pepper (t = 6.12, p $<$ .001) were perceived to be

Figure 5.3
Affect Grid Scores by Robot Group

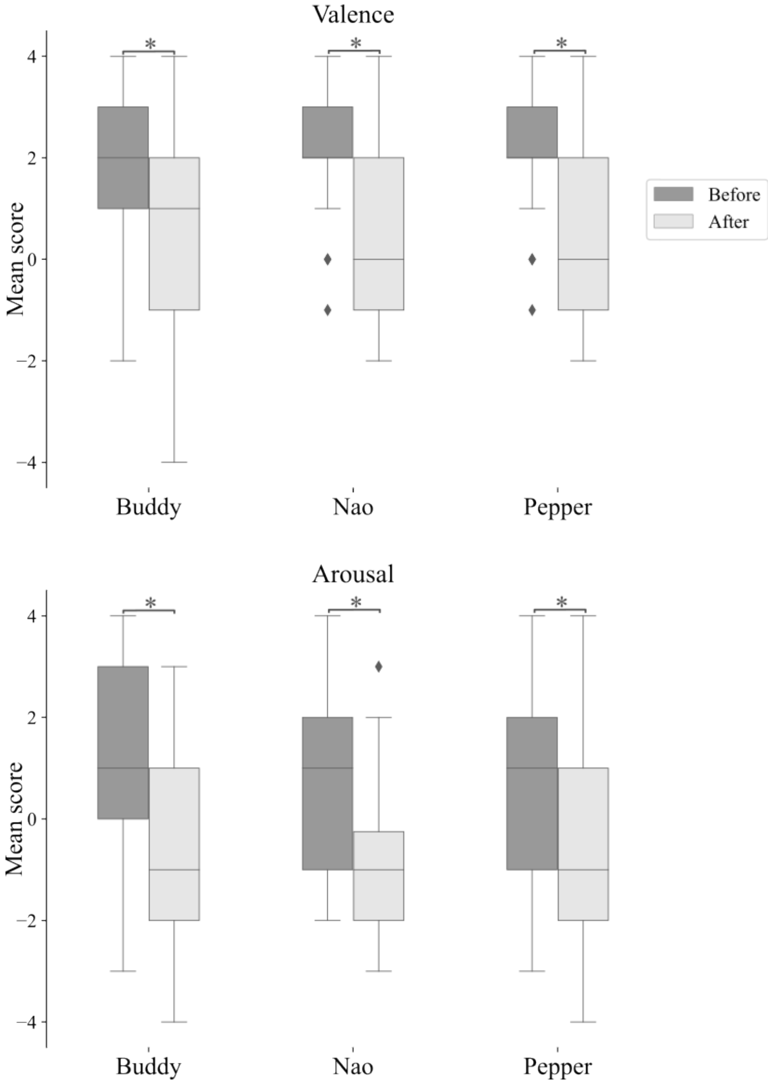

Note. Box plots of valence (top panel) and arousal (bottom panel) before and after the experiment. Scores are shown for each independent group. * $p < .050$

Figure 5.4

Movement Analysis Examples with the Wavelet Transform

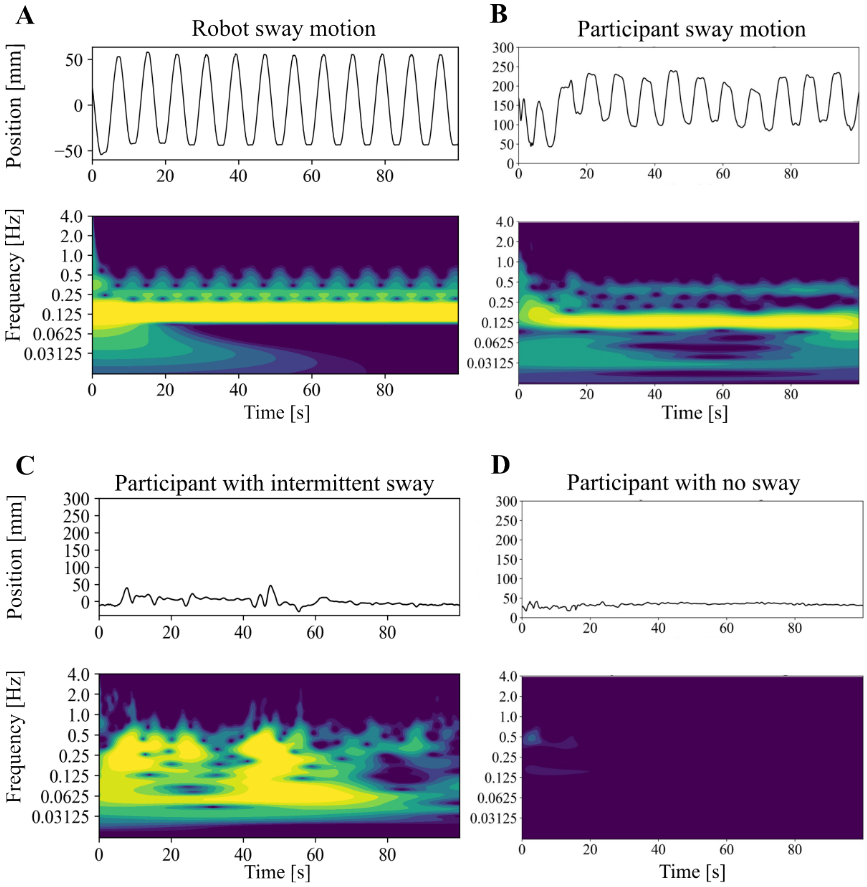

Note. The upper panel of each figure presents the relative 3D position of the reflective motion marker in mm. The lower panel shows the power spectra heat map, where high and low power spectra are highlighted by bright and dark colors, respectively. High-power spectra indicate more and larger movements, while low-power spectra indicate an inhibition or absence of movement.

Figure 5.5
Local Minima Identification Example

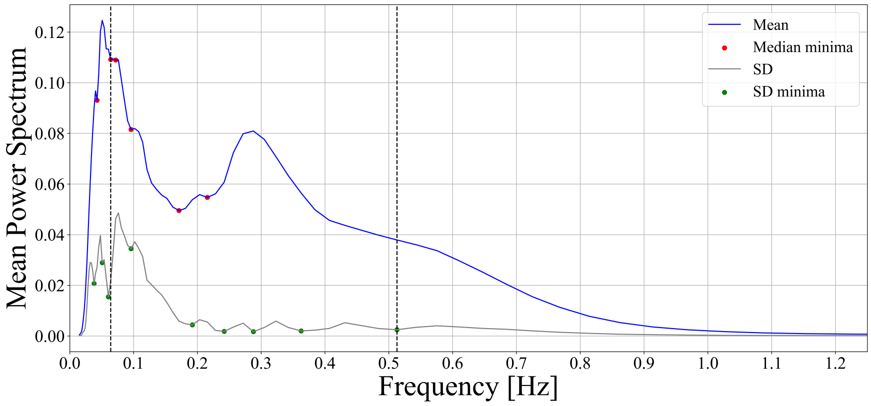

Note. Red and green dots correspond to the local minima in the mean and standard deviation curves of the power spectra, respectively. The dotted lines indicate the limits of the selected bandwidth for statistical analysis.

more animated than Nao, as shown in Fig. 5.6. As for the Likeability category, Buddy (t = 7.13, $p < .001$) and Pepper (t = 7.85, $p < .001$) were perceived to be more likable than Nao. Finally, in the Perceived Intelligence category, Buddy (t = 8.07, $p < .001$) and Pepper (t = 8.52, $p < .001$) were perceived to be more intelligent than Nao. Table 5.3 presents the mean results for each category and robot.

Category	*Buddy*	*Nao*	*Pepper*
	M (SD)	M (SD)	M (SD)
Animacy	3.3 (0.48)	2.26 (0.44)	3.29 (0.5)
Likeability	3.14 (0.73)	2.1 (0.46)	2.89 (0.63)
Perceived intelligence	3.41 (0.78)	2.24 (0.43)	3.36 (0.75)

Table 5.3
Mean scores for Godspeed social trait categories.

In Fig. 5.7, we present the correlation matrix showing the relationship between the Godspeed categories, robot size, and Spontaneous Movement engagement (SME).

5.5 DISCUSSION

The context of interaction had an influence on the self-reported levels of valence and arousal. Specifically all groups of participants reported lower valence and arousal after interaction with the robots.

The social traits attributed to Buddy and Pepper were higher than Nao's, which could suggest a preference for either a small non-humanoid robot

Figure 5.6

Godspeed Questionnaire and Spontaneous Oscillation Results by Robot Group

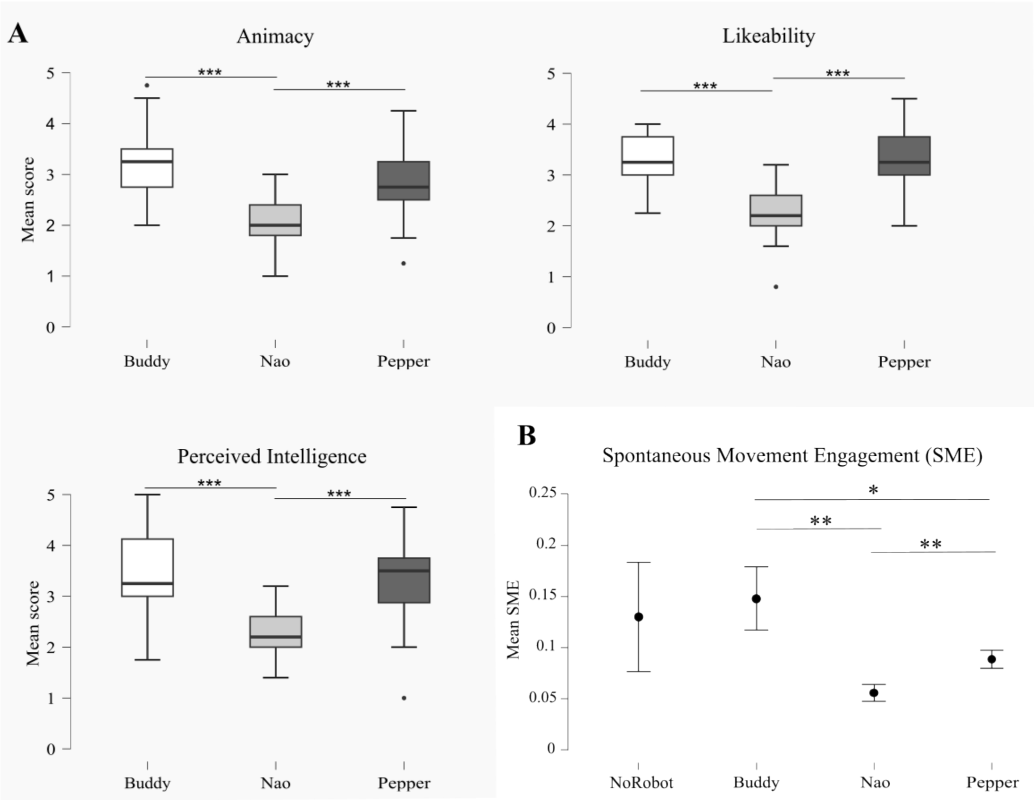

Note. A. Results on the Godspeed categories: Animacy, Likeability, and Perceived Intelligence. B. SME from left to right: No-robot, Buddy, Nao, and Pepper. $^{*}p < .050$, $^{**}p < .010$, $^{***}p < .001$.

Figure 5.7

Correlation Matrix of Godspeed Categories, Robot Size, and the SME of Humans

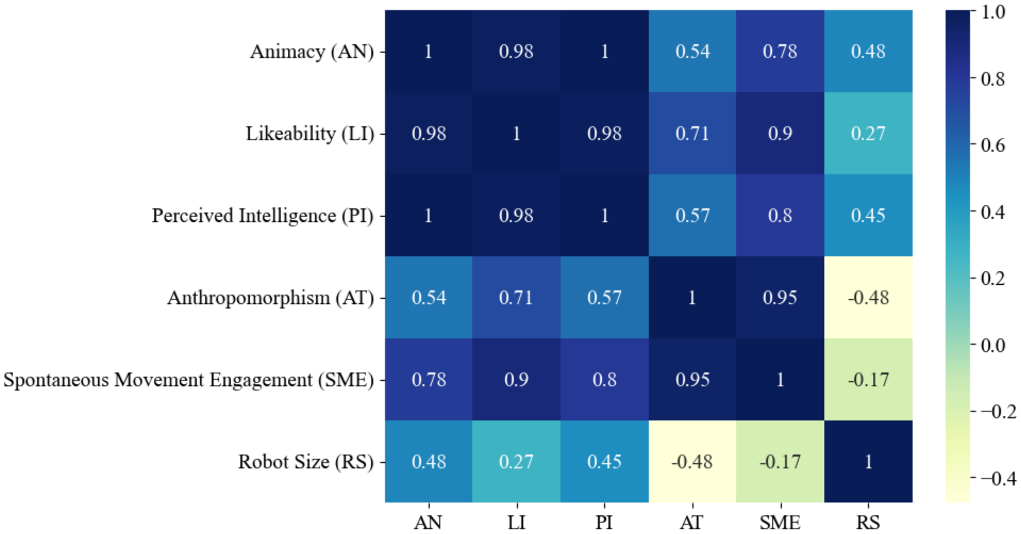

with animated facial expressions or a preference for a bigger humanoid robot, within social interaction with a negative (i.e., sad) context. Our results on human movement show that an 8s periodicity (Low condition) of robot movement has the potential to trigger spontaneous sway in participants without them being aware, while the other two periodicities (2s and 4s, for Medium and High conditions, respectively) seemed to have an inhibitory effect on SME. Significant differences in SME (see Fig. 5.6) indicate that Buddy elicited more spontaneous movement than the other robots. Comparing the figures of robot social attributes and spontaneous movement (Part A and B of Fig. 5.6, respectively), we observed that both Buddy and Pepper groups exhibited higher Godspeed scores and more spontaneous movement compared to the Nao group.

Even if no statistical differences were found between the SME of the robot groups and the no-robot group, the latter tended to present a higher variability, which could be explained by the lack of a visual anchor during the storytelling phase. Also, a possible explanation for Nao's low SME and Godspeed scores could be attributable to factors such as the negative interaction context and its small humanoid morphology, as some participants tended to characterize it as a distressed child.

We observed a strong positive correlation between human movement and Animacy, Likeability, and Perceived Intelligence in Fig. 5.7. We found a strong positive correlation between SME and the Anthropomorphism category, suggesting that more anthropomorphized robots lead to increased spontaneous movement in participants. Furthermore, we noticed a moderate negative correlation between Anthropomorphism and robot size, indicating that smaller robots tended to be more anthropomorphized, which may have influenced participants' behavior. This can be explained by the fact that Nao has arms, legs, and a torso, while Buddy has animated eyes and a mouth.

5.6 CONCLUSION

Our study has provided evidence that the quantification of human spontaneous movement during HRI is a non-invasive technique that can be used as a non-verbal behavioral feature for engagement inference. This method is complementary to other features such as gaze and facial expression analysis. Our results on human sway complemented the perceived social attributes of the robots and revealed behavioral differences between groups. Results also showed that spontaneous movement can be modulated by the presence of social robots, in a face-to-face, no-goal-oriented interaction. We reported that some categories in the Goodspeed questionnaire were perhaps redundant for estimating engagement; thus, as a next step, we planned to employ a more comprehensive tool in follow-up studies (e.g., RoSAS (Carpinella et al., 2017)). Also, a larger experimental sample with non-university members should be studied to strengthen our results. We also acknowledge a potential confounding factor, such as the presence of an animated face on Buddy, which suggests the need to include another robot with animated facial expressions (e.g., Furhat). Finally, more research is required to explain the variability of sway in the no-robot group.

Considering that context has been reported to influence engagement, we do not disregard the potential impact of the negative context on participants. Self-reported affect responses show that participants experienced lower valence and arousal after the experiment, and additional data show that all groups perceived the stories as negative. Therefore, we aim to investigate how a positive interaction can affect SME in contrast to a negative interaction. Although our methodology was applied in a listening task with no goal, we consider that our methodology has the potential to be applied to other modes of HRI (e.g., collaboration, guide-and-follow). In future studies, we plan to test the proposed metric in engagement inference where the robotic system adapts its movement to the SME of humans in real-time, instead of having established body cues. We hypothesize that engagement will be stronger as the robotic system will simulate behavioral dynamics observed in HHI.

INTERMEDIATE SUMMARY

Developments in the field of social robotics open interesting opportunities for applications in healthcare, education, and services. For this, studying *engagement* in human-robot interaction (HRI) is crucial for improving the quality of interactive experiences. Questionnaires are powerful in describing voluntary behavior; however, engagement is often an implicit non-voluntary behavior that reaches awareness only once initiated. Inspired by research in cognitive psychology, we propose a behavioral feature to quantify engagement in HRI through the measurement of spontaneous movement and spectral wavelet analysis. For this, we conducted an experiment during which participants listened to sad stories narrated by a moving social robot. Throughout the experiment, we tracked the participants' spontaneous and non-voluntary sway movements with a motion capture system. The experiments were conducted with three robotic platforms (Buddy, Pepper, and Nao). Results showed that spontaneous body sway can be modulated by social robots within no-goal-oriented interaction.

The results of this study were presented at the ROMAN conference held in 2024 in Pasadena,USA, and at the Rhythm Production and Perception Workshop (RPPW) held in 2023 in Nottingham, UK. Results with Robot Buddy were presented in poster format at the European Society for Cognitive Psychology conference (ESCOP) held in 2022 in Lille, France.

This study was made possible thanks to the collaboration with Prof. Patrick Hénaff (École Nationale d'Ingenierus de Brest, ENIB) and Prof. Hendry F. Chame (Laboratoire Lorrain de recherche en informatique et ses applications, Loria). Their support included providing access to robotic platforms, as well as invaluable technical expertise and theoretical guidance on both the robotic platform control and experimental design.

The Loria laboratory provided us access to the Nao and Pepper social robots. Both could be controlled using Naoqi (Python-based programs) which allowed for greater efficiency for implementation and experimental consistency. Data collection with the Pepper robot had to be conducted on site in Nancy, as transporting the platform to the University of Lille was not feasible. Thanks to the hospitality and financial support of the Loria laboratory, I was able to stay in Nancy for one month to implement the experiment and collect data.

Finally, this findings were obtained within a negative HRI context characterized by dark environment, where the robot system recounted sad stories. Having established a method for quantifying human spontaneous movement, the question that arose was whether the affective context of HRI (positive or negative) can influence changes in human spontaneous movement. This question will be addressed in the following chapter.

6 MANIPULATION OF INTERACTION CONTEXT IN HRI

6.1 INTRODUCTION

Environmental psychology has demonstrated that the physical environment can shape cognition and behavior through an perception-action loop, leading to a continuous feedback between environmental cues and human responses (Gibson, 2014). Nonetheless, empirical studies have demonstrated that factors such as lightning and noise can impact not only cognitive function and behavior, but also cause changes in core affect triggering emotional responses and shifts in mood (Thompson et al., 2024). For example, calm well-lit environments (virtual and physical) and contact with nature, have been reported to induce positive emotions and boost cognitive performance (Frost et al., 2022; Jimenez et al., 2021). Conversely, dark or noisy environments can induce negative emotions like anxiety and impair cognitive function (Higuera-Trujillo et al., 2021; Thompson et al., 2024).

Social interaction context is equally a modulator of affect. It has been reported that individuals can converge affectively with others, a phenomenon called emotional contagion or emotional convergence (Parkinson, 2011, 2020). Specifically, in the context of Human-Robot Interaction (HRI), robots can modulate not only human perception and trustworthiness toward them but are also capable of manipulating humans' affective states with emotional body language and artificial facial expressions (Saunderson & Nejat, 2019). For example, in a study using the robot Nao to give a lecture to students, the robot was programmed to convey either positive or negative body language. At the end of the lecture, students' self-reported affect was found to be aligned with the robot's displayed emotional body language, even though participants did not consciously recognize the emotion the robot was trying to convey (Xu et al., 2014).

Taken together these findings highlight the modulating effect of environment and social social factors, and in HRI of the robot's bodily behavior. However, much of this work has been focused on self-report with less attention on how affect can be embodied through motor responses.

From embodied and affective theory, we know that core affect manifests not only in subjective feeling but also as a quantifiable behavior (see Chapter 2). Specifically, spontaneous oscillations (i.e., body sway), have been reported to be linked to changes in core affect (Chang et al., 2021; Roelofs et al., 2010). In the previous chapter we developed a technique that employed motion capture technology and wavelet analysis to quantify these spontaneous oscillations during negative affective context HRI (Casso et al., 2024).

While studies have assessed the influence of the environment and the impact of social robots' non-verbal cues on human affective states, little research has investigated how combining these two modalities influence HRI. Integrating insights from embodied and affective theories, we argue that investigating multimodal affective contexts (manipulating both the physical environment and the robot's affective display), can provide a more ecological experimental setting to evaluate the human affective experience in HRI.

Therefore, the present study was established to address this gap by manipulating the affective context of HRI to induce a change in the affective state of participants.

We hypothesized a positive HRI context (i.e., positive environment and positive robot displaying "happy" body language) would augment valence levels of participants, and lead to spontaneous body oscillations to emerge. Whereas a negative HRI context (i.e., negative environment and negative robot displaying "sad" body language) would decrease valence levels and inhibit or reduce spontaneous body oscillations.

6.2 METHODS

6.2.1 *Participants*

Two groups of 20 psychology students, native French speakers aged 18 to 28, were recruited for each experimental condition. The experiments were conducted separately for the two conditions. The negative condition was conducted between December 2022 and January 2023, while the positive condition was conducted in February 2023. Every participant was informed about the study's objectives at least 24h before their inclusion and signed a consent form before entering the room. Their participation consisted of a single 45-minute session. The experimental procedure and inclusion of participants adhered to the strict code of ethics outlined in the WMA Declaration of Helsinki for research involving humans.

6.2.2 *Robotic system*

For this study, we used Nao, a humanoid robot initially developed by Aldebaran Robotics, designed primarily for research and education purposes. Thanks to its number of DOF, it is versatile for walking and dancing tasks. We defined two emotional body cues. One that displayed happiness consisted of open arms and a combined torso and head movement in the sagittal plane (see top panel Figure 6.1). The second one displayed sadness and consisted of a higher inclination movement of the head and torso in the sagittal plane,

Figure 6.1

Emotional Body Cues Programmed in Robot Nao

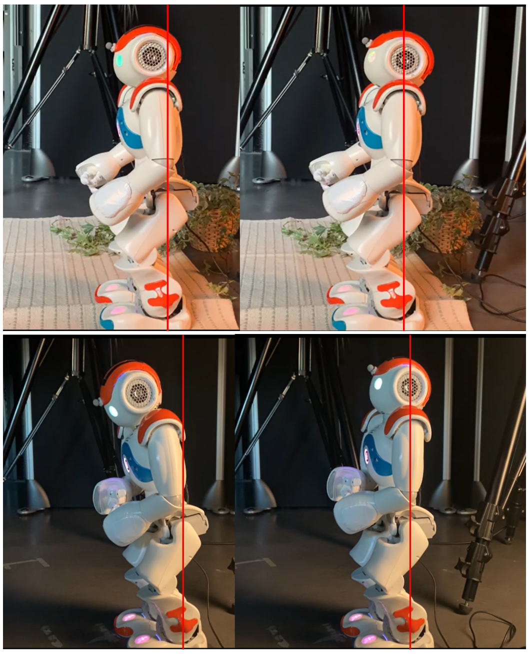

Note. Emotional body cues to express happiness (Top) and sadness (Bottom). Both body cues consisted of a combined head and torso movement in the anteroposterior direction, with the sadness cue having a more prominent inclination angle.

with arms close to the body and a pronounced head tilt toward the ground, which simulated a human cowering movement (Atkinson et al., 2004) (bottom panel Figure 6.1).

The corresponding articulations for head and torso inclination in the sagittal plane were controlled with the following equation:

$$q(t) = A * sin(2 * \pi * F * t), \tag{6.1}$$

where F is the frequency of movement (low = $0.13Hz$, medium = $0.25Hz$, and high = $0.5Hz$), and A is the amplitude of the oscillating movement. Time t is sampled at 0.05 s.

The three frequency levels were selected to exhibit varying arousal levels associated with both positive and negative body language (Bretan et al., 2015). Specifically, the low frequency was set to be congruent with negative body language, while the high frequency corresponded to positive body language (Mahzoon et al., 2022). The medium frequency served as a control condition, being perceived as congruent with either type of programmed body language, as per a pilot study.

In Figure 6.2, we show the amplitude of Nao's head tilt while telling happy stories as a function of time for the three oscillation frequencies.

Figure 6.2
Amplitude Nao's Head Tilt

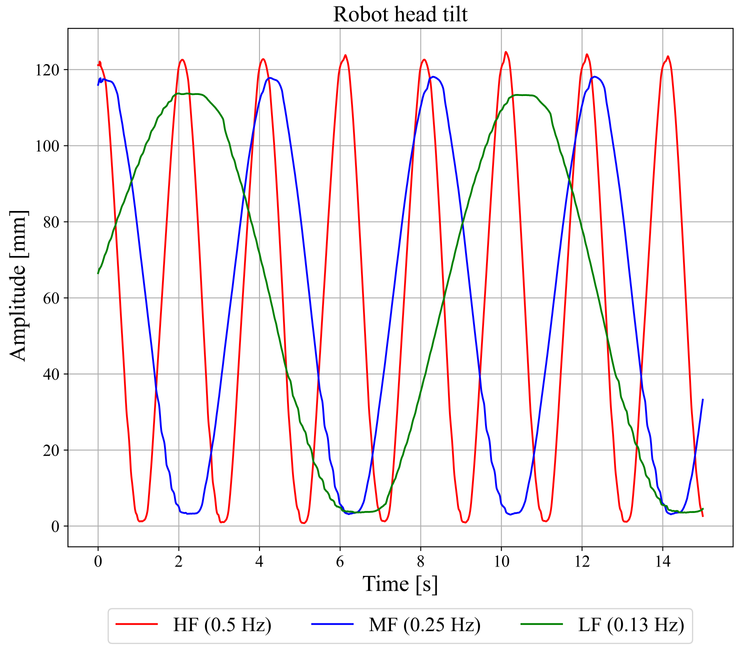

Note. telling happy stories in the three oscillation frequencies: high (0.5Hz), medium (0.25Hz), and low (0.13Hz).

6.2.2.1 *Audiovisual stimuli*

We prepared two fictional audiovisual documentaries featuring the robot Nao, with both positive and negative connotations; the same images of the robot were used for both, but the background narration changed.

Three positive and three negative stories were written in the first person in French. The latter were recorded using a text-to-speech algorithm, Read-Speaker (Casso et al., 2024; “Read Speaker,” 2024).

After conducting a pilot study that tested the recorded positive stories using the same tool as the negative stories, participants reported an incongruence between the narratives and the prosody of the voice (“Read Speaker,” 2024). To address this, we chose to record the positive stories using a human voice, which was then modified to sound artificial and gender-neutral, to avoid potential biases related to gender stereotypes. Both voices (positive and negative) had a fundamental frequency of 220 Hz.

A valence analysis was conducted on each text, using the pyFeel package (Abdaoui et al., 2017; Zouitine, 2018). The analysis returned the scores for seven discrete emotions (see Table 6.1). We obtained a total score of 94% for positivity and joy in the positive stories, and a score of 66% for the negative stories, with a 29% for negative-valenced emotions (fear, sadness, anger, and disgust). This could be because the negative stories began with "happy" memories recalled by the robot, followed by negative events.

Table 6.1
Valence Analysis of the Narrative Stimuli

Context	Positivity	Joy	Fear	Sadness	Anger	Surprise	Disgust
Positive	72%	22%	0%	0%	0%	6%	0%
Negative	59%	7%	9%	11%	5%	4%	4%

6.2.3 *Environmental setup*

6.2.3.1 *Positive*

The experimental room for the positive condition was designed to have natural light and was equipped with warm, dimmed lighting and plants, creating a positive environment. Joyful musical excerpts, validated to induce positive affective states, were played through the entire experimental session (Vieillard et al., 2008).

6.2.3.2 *Negative*

The experiments for the negative condition were conducted in a dark room equipped with only warm, dim lighting. In contrast, sad music excerpts, validated by Vieillard et al. (2008) to induce negative affective states, were played in the background throughout the entire experiment.

6.2.4 *Experimental procedure*

The experiment followed a 2 x 3 mixed design, with factors Context (Positive vs. Negative) as the between subject factors, and Robot oscillation frequency (low, medium, and high) as the within-subjects factor.

The following experimental procedure was executed for both context conditions.

Before entering the experimental room, participants were asked to report their affective state using the Affective Grid (Russell et al., 1989). Once inside the room, participants were invited to sit on an ergonomic Pilates ball, facing robot Nao at a distance of approximately 1.2 m. Using a ball would provide increased degrees of freedom and enable spontaneous oscillation during the interaction with the robot.

Before the experimental trials, as depicted in Figure 6.3, participants were asked to watch the 1-minute documentary about the robot Nao. For each trial, participants listened to a story told by the robot while it oscillated at one of the defined frequencies presented in Section 6.2.2 (duration approximately 5 minutes). Once the story was finished, participants were invited to complete a questionnaire. The stories were always presented in the same order to all participants, while the order of the oscillation frequencies was counterbalanced across participants. All participants were naive to the content of the stories.

Once the three trials were completed, we invited participants to report their affective states.

Figure 6.3

Experimental Procedure and Motion Capture Marker Placement

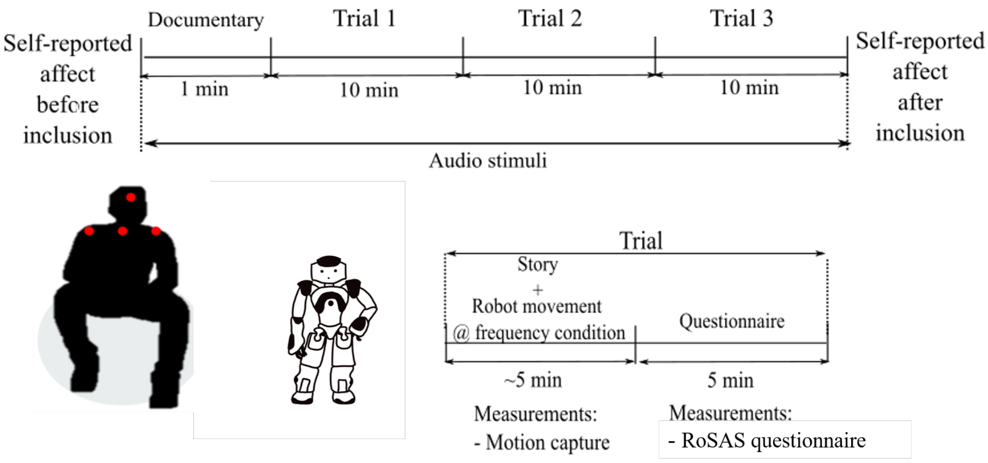

Note. The red dots on the head, shoulders, and base of the neck represent the tracked markers in relation to a fixed reference frame.

6.2.5 *Experimental measures*

6.2.5.1 *Human affective changes and Robot social attributes*

We used the Affect Grid to assess the self-reported valence and arousal of participants before and after the experiment. See section 3.5 for the analysis procedure.

Concurrently, the Robotic Social Attribute Scales (RoSAS) (Carpinella et al., 2017) questionnaire was administered to assess the human perception of the robot Nao within each context. The RoSAS questionnaire consists of 18 items distributed into three categories: competence, warmth, and discomfort. Participants were invited to respond on a 5-point Likert scale regarding how well each item described the robot. For the analysis, we averaged all sub-items to obtain the respective scores for each category.

6.2.5.2 *Spontaneous human movement*

Eight infrared motion capture cameras were installed in a semicircle facing the participant which recorded the three-dimensional position of four reflective markers (see Figure 6.3), placed at the forehead between the eyes, the base of the neck (manubrium), and the shoulders of the participants. We used the

Qualysis Track Manager (QTM) to record all trials at a sampling frequency of 200 Hz. The average standard deviation of the volume calibration ranged between 0.7 and 0.9 mm. We quantified participants' spontaneous oscillations employing the SME algorithm presented in Chapter 5.

6.3 results

6.3.1 *Affective manipulation*

Two mixed RM anovas were conducted to evaluate the changes of valence and arousal scores before and after the experiment, considering the affective context (Positive, Negative) as the between-subjects factor

We found an interaction effect between the reported Valence and Context ($F(1, 40) = 9.40, p = .004, \eta_p^2 = .19$). There was also a main effect of reported Valence ($F(1, 40) = 5.75, p = .021, \eta_p^2 = .13$), and a main effect of Context ($F(1, 40) = 4.40, p = .042, \eta_p^2 = .10$).

Pairwise comparisons with Bonferroni corrections revealed Valence was higher After the experiment compared to Before ($t = 2.40, p = .021, d = .38$). Moreover, we found valence scores during the Negative context were lower than in the Positive context ($t = -2.10, p = .042, d = -.33$), see Figure 6.4.

Assessment on Valence x Context comparisons determined that Valence scores on the negative context were lower after the experiment ($t = 3.96, p = .002, d = .62$). No significant changes were found in the valence scores during the Positive context (p = 1.).

Concurrently, we found and interaction between reported Arousal and Context ($F(1, 40) = 4.62, p = .036, \eta_p^2 = .10$), and a main effect of reported Arousal ($F(1, 40) = 10.78, p = .002, \eta_p^2 = .21$).

Post-hoc comparisons revealed Arousal scores were higher after the experiment ($t = 3.28, p = .002, d = .51$). Assessing interaction comparisons we found Arousal scores were lower during the Negative context ($t = 2.92, p = .008, d = .62$) and not during the Positive context (p = .372).

6.3.2 *Robot social attributes*

We conducted an RM ANOVA 3 (RoSAS Categories) x 2 (Context) ANOVA on the questionnaire answers and applied a Greenhouse-Geisser sphericity correction. Results indicated there was no interaction effect between the RoSAS categories and context ($F(1.56, 95.43) = 0.01, p = .975, \eta_p^2 < .001$). There was no main effect of Context ($F(1, 61) = 0.92, p = .34, \eta_p^2 = .02$). However, we found a main effect of Category ($F(1.56, 95.43) = 100.68, p < .001, \eta_p^2 = .62$).

Pairwise comparisons with Bonferroni corrections revealed no significant differences between Competence and Warmth ($t = 0.48, p = .633, d = .08$)

Figure 6.4

Self-reported Valence and Arousal scores

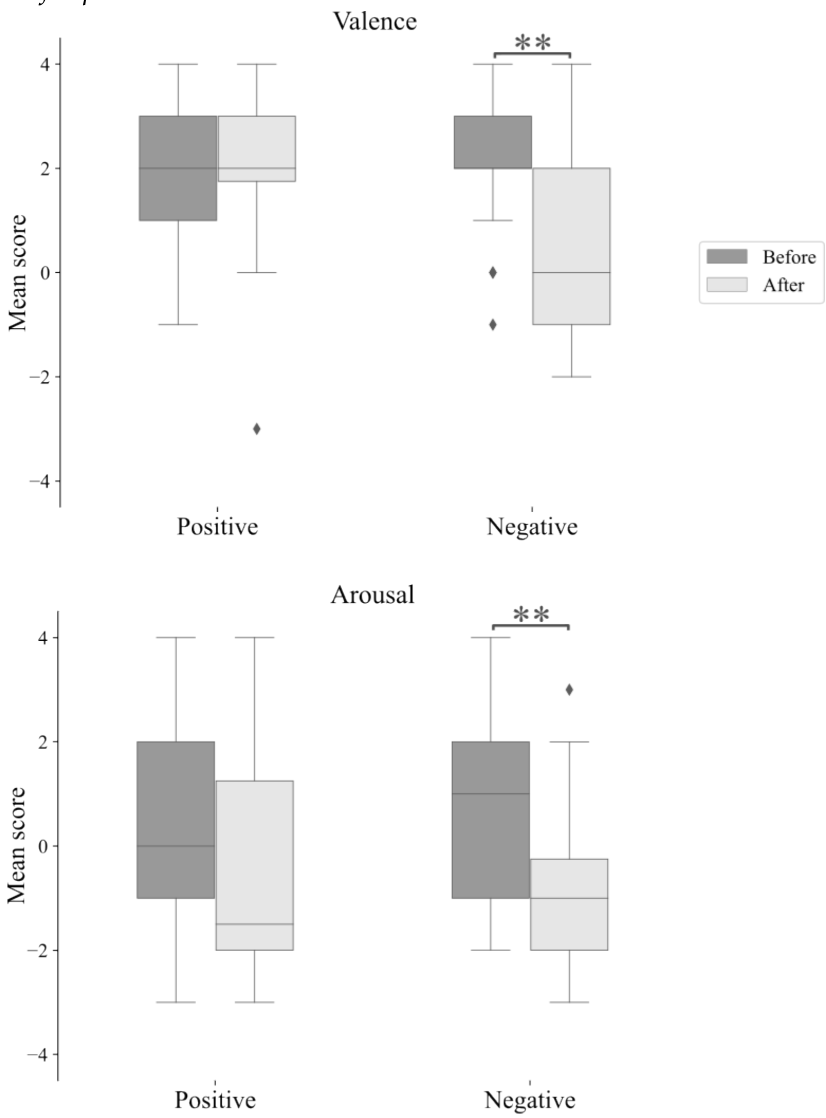

Note. Box plots of valence (top panel) and arousal (bottom panel) before and after the experiment. Scores are shown for each independent group. ** p < .010.

Figure 6.5
RoSAS Questionnaire Results

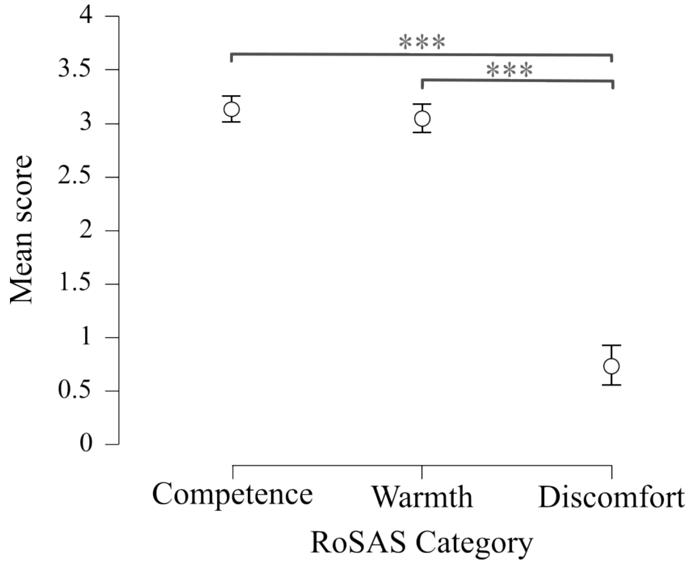

Note. Plot of the RoSAS questionnaire category scores for Robot Nao, averaged across both affective contexts. All three categories are depicted. *** $p < .001$.

(see Figure 6.5). We found that the score for Competence was significantly higher than for Discomfort ($t = 12.52, p < .001, d = 2.33$). Concurrently, the Warmth category was significantly higher than Discomfort ($t = 12.04, p < .001, d = 2.24$).

6.3.3 *Spontaneous movement*

To evaluate how human spontaneous oscillation changed in the congruent interaction contexts (robot body language and oscillation x affective interaction context) we conducted A mixed RM ANOVA with the three Robot frequencies (High, Medium, Low) as the repeated measures factor and the two Context conditions as the between-subjects factor.

We found an interaction effect between the robot's oscillation frequency and context ($F(2, 61) = 3.53, p = .035, \eta_p^2 = .10$), a main effect of oscillation frequency ($F(2, 61) = 4.80, p = .012, \eta_p^2 = .14$), and a main effect of context ($F(2, 61) = 5.68, p = .005, \eta_p^2 = .16$).

Bonferroni-corrected post-hoc tests revealed SME was higher during the positive context compared to the negative context ($t = 2.19, p = .029, d = .27$). We found SME was higher when the robot oscillated at high frequency, compared to the medium ($t = 2.78, p = .018, d = .42$), and the low frequency ($t = 3.05, p = .007, d = .46$). There was no difference between the medium and low oscillation frequencies ($t = 0.27, p = 1., d = .41$).

Figure 6.6
Human Spontaneous Movement Results

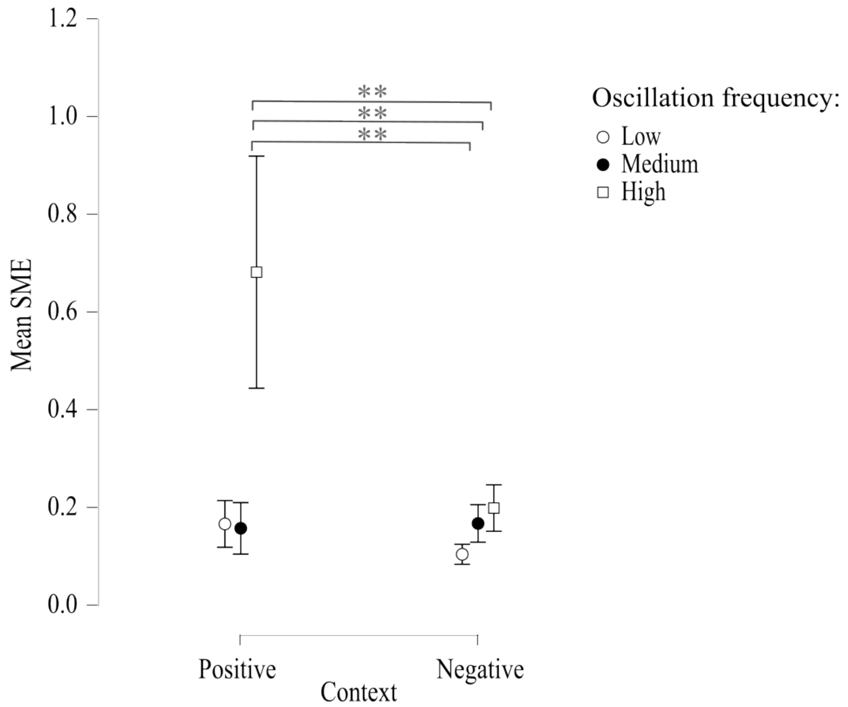

Note. Plot showing the mean SME for every frequency oscillation of robot Nao, during the Positive and Negative contexts. SME = Spontaneous Movement Engagement. ** p < .010.

Evaluating SME during the Positive context we found participants exhibited more oscillations when Nao oscillated at the highest frequency compared to: the medium oscillation ($t = 3.62, p = .005, d = .79$), and low oscillation ($t = 3.62, p = .005, d = .78$).

Contrasts between Positive and Negative contexts, we found that SME was the highest during the positive context-high oscillation frequency compared to the negative context-high frequency ($t = 3.39, p = .009, d = .73$), the Negative context-medium oscillation ($t = 3.66, p = .004, d = .77$), and also compared to the Negative context-low oscillation ($t = 4.05, p = .001, d = .87$) (see Figure 6.6).

6.4 DISCUSSION

Having developed the technique to quantify human spontaneous movement presented in Chapter 5, the question we subsequently formulated was whether the affective context of Human-Robot Interaction (positive or negative) could induce a change in the spontaneous movement of humans.

Our main finding is that the affective context of HRI can modulate the spontaneous oscillations of humans, even when self-reported affect changes

Figure 6.7

Human Affective-Motor Conceptual Model

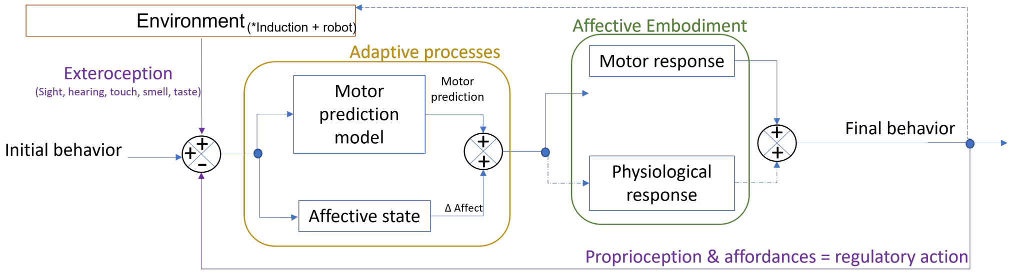

are not significant. These results were evident on the comparison of the two experimental contexts.

Specifically, the negative context confirmed our hypothesis. Participants not only reported lower valence and arousal after the interaction, but their oscillations were significantly inhibited. This result aligns with reports on motor inhibition during the experience of negative valenced states (Brossard, 2022; Roelofs et al., 2010). Our results provide evidence that this phenomenon extends to HRI.

While participants' self-reported affect did not change significantly after the positive context interaction, we observed a significant emergence of spontaneous oscillations when the exhibited a happy body cue at high frequency (0.5 Hz, defined to be congruent with the happy body cue). This finding was unexpected and suggests that embodied responses may be a more sensitive indicator of affective engagement compared to self-report tools.

We found that the social traits of the robots did not change with the affective context of interaction. Nao was consistently rated as highly competent and warm, and was given low discomfort scores. These results suggest that factors like morphology and size could create this bias, as some participants reported perceiving Nao as a small toy or child, which may have elicited empathy from them, particularly while it narrated sad stories.

It appears that participants responded both behaviorally and affectively to our affective inductions, as if there was a resonating effect between the robot's emotional cues (verbal and non verbal), the environment, and the participants.

To clarify this conceptual reasoning, we developed a simplified model, describing how the affective context (Robot and physical environment), may influence both their affective state and observable behavioral responses (see Figure 6.7).

The control diagram describes an individual having an initial and a final behavior. Between these states, there is an adaptive and an affective embodiment process. The environment, through exteroception, can change the initial behavior. Moreover, the initial behavior is constantly regulated as a result of the feedback from the individual's proprioception and affordances. The environment block comprehends stimuli (e.g., music, lights, odors) as well as other

Figure 6.8
Conceptual Diagram for Robot Control

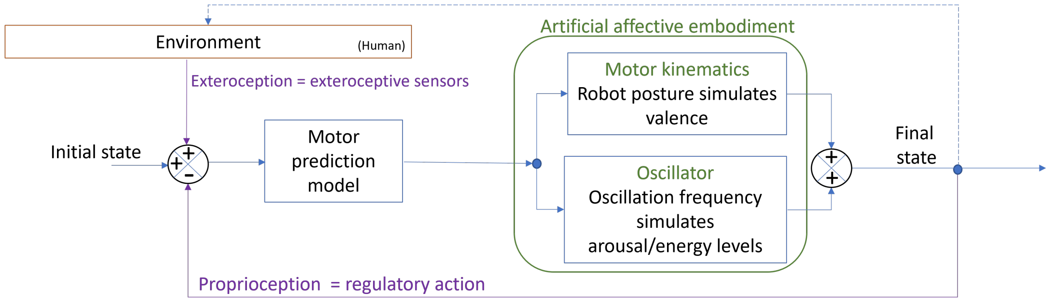

individuals or artificial agents. These trigger signals will add a perturbation to the individual's initial behavior.

The adaptive process comprehends two sub-processes which are the motor model and an affective state. Both blocks receive the perturbed and regulated initial behavior as an input. The motor model will formulate a motor prediction according to the input. Simultaneously, the initial arousal and valence levels will change according to the magnitude of perturbation and regulation of the initial behavior. The new motor prediction and affective levels are combined into a single response command.

The affective embodiment process comprehends the embodiment of the response command and feedback to the initial behavior. Which is composed of a motor response (e.g., posture shift, jerk, freezing, body sway) and a physiological response [1] (e.g., breathing rate, heart rate variability), both combined responses will constitute the final behavior.

Signals from proprioception and affordances generate a feedback based on this final behavior, continuously regulating initial behavior. In Figure 6.7, a dotted arrow connecting the final behavior to the environment was added to indicate that an individual's output can itself act as a perturbation on other individuals or artificial sensors present in the environment.

Our results highlight the fact that humans do not maintain the same affective state across different environments. For example, children in schools and elderly individuals in retirement homes, two environments where social robots are mostly deployed, are likely to experience different affective states. This observation underscores the importance of robot behavior to be tailored not only to the tasks to be performed but also to the affective context in which they will operate.

On this basis, we propose a conceptual control diagram for robotic systems in our future studies that would adapt both their posture and oscillation frequency to the one measured in human participants (see Figure 8.2).

1 Although physiological responses were not measured in this experiment, we consider them integral to affective embodiment

Within this diagram, the initial state of the robot is defined in the articular space, meaning all control signals will be sent to its articulations, without a cartesian position as a goal.

The initial state of the robotic system will receive perturbations from the environment through its exteroceptive sensors (e.g., proximity sensors, capacitive sensors). These environmental inputs will allow the robot's motor prediction model to define the control command of all its articulations. This command will have two components: a posture control and an oscillator control.

The magnitude of environmental perturbation, together with the inverse motor model's control command, will determine how both posture and oscillatory controllers (i.e., central pattern generators, CPG) will adapt.

Posture control will govern the configuration of the robot's joints to emulate body language associated with valence (e.g., cowering to signal negative valence or an open posture to convey positive valence).

Simultaneously, the oscillator will define an oscillating movement across the joints, with frequency modulated to represent human-like arousal levels: low frequency for low arousal and high frequency for high arousal. The combined effect of these two elements constitutes the final state of the robotic system.

Continuous feedback is provided to the initial input via the robot's proprioceptive sensors (such as motor thermal sensors), offering ongoing regulation toward the specified state goal. Additional signals from proprioception and affordances further refine the control loop by regulating behavior based on the robot's current output. Finally, we note the output behavior of the robot can itself act as a perturbation for humans present in the environment (as indicated by a dotted arrow in Figure 8.2)

As illustrated in both control diagrams presented earlier, not only can the robot act as a perturbation within the environment, but individuals themselves can also influence the robot's behavior. However, we hypothesized that for a robot to effectively alter a human's affective state, it must display an artificial affective state that is either similar to or compatible with that of the human, and that is congruent with the broader affective context of the environment.

Among the limitations of this chapter, we can mention the absence of a neutral condition. We cannot establish whether the positive context was not effective in increasing valence or if only maintained an already positive baseline among participants. Future studies should incorporate a neutral context (i.e., neutral environment and robot body cue) to adequately assess affective inductions.

We must also consider that the fixed oscillating body cues of the robot may have lacked ecological validity of more complex cues. We hypothesize varying complex body cues could amplify the affective induction and lead to more contrast in results.

6.5 CONCLUSION

The study presented in this chapter demonstrated that the affective context of HRI can modulate human motor behavior. Our findings have implications for the design of social robots, particularly in clinical (i.e., therapeutic) or education domains. We think that to foster positive and engaging HRI designers should consider not only the morphology of the robot but the affective context of the environments they are aimed to occupy. For instance, a therapy robot intended to reduce anxiety could be placed in a calming environment and programmed with smooth, low frequency oscillations to promote a state of calm in humans.

INTERMEDIATE SUMMARY

This study investigates how the affective context of Human-Robot Interaction (HRI), manipulated through environmental cues and a social robot's non-verbal cues, influences human affective states and their embodied motor responses. While prior work has focused on self-report measures, this study explores spontaneous body oscillations as a quantifiable indicator of affective engagement. In a mixed-design experiment, forty participants interacted with social robot Nao in either a positive or negative multimodal context. The robot displayed congruent emotional body cues (i.e., happy and sad) at varying oscillation frequencies while participants were in a matching positive or negative environment. We collected self-reported affect scores and quantified spontaneous body movement using motion capture and spectral analysis. Results showed the negative context significantly decreased participants' valence and arousal levels and inhibited their body oscillations. Conversely, the positive context did not alter self-reported affect; however, it increased spontaneous movement, particularly at high robot oscillation frequencies. This suggests that spontaneous oscillations could be a more sensitive indicator of affective engagement than self-report measures. Our findings highlight the importance of designing the entire affective context, not just the robot's characteristics, to foster engaging HRI.

The results of this study have been presented in poster format at the Timing Research Forum 3 (TRF) in October 2023 in Lisbon, Portugal. Additionally, an experimental demonstration was carried out at the Drôles d'Objets conference in April in Nancy, France. This study was made possible thanks to the facilities and robotic platform provided by the Loria laboratory, as well as the collaboration with Prof. Patrick Hénaff (ENIB) and Prof. Hendry F. Chame (Loria).

This study marked a significant turning point in my research program, as I believe that understanding how humans adapt their behavior and experience emotional responses during interactions with robots fundamentally requires an understanding of these phenomena in human interactions. That is how the next study emerged, out of the need to understand how the affective context of interaction influences humans and what role their individual states play. We have observed that in human interaction, we tend to synchronize with each other and adopt the same posture. What if the emergence of these spontaneous movements depended on how compatible our affective states are at the moment of interaction? These questions are addressed in the following chapter.

7 AFFECT COMPATIBILITY AND SPONTANEOUS SYNCHRONIZATION BETWEEN HUMANS

Casso, I., Violet, E., & Delevoye-Turrell, Y. N. (in preparation). Exploring the role of affective compatibility on the spontaneous interpersonal coordination of dyads during static pedaling.

7.1 INTRODUCTION

7.1.1 *Interpersonal Synchronization*

Interpersonal synchronization is omnipresent in our social life. It emerges spontaneously in various contexts, whether collaborative, competitive, or affective, and plays a central role in regulating our daily interactions. Far from being trivial, it enables the dynamics of cohesion, affiliation, and mutual adjustment that structure human bonds.

At the behavioral level, synchronization promotes fluid exchanges and a sense of connection between partners. Studies have shown that even a minimal temporal alignment of bodily movements can increase cooperation, trust, and the perception of similarity between individuals (Mogan et al., 2017; Vacharkulksemsuk & Fredrickson, 2012). This phenomenon is often reinforced by subtle forms of non-conscious mimicry, in which gestures, postures, or expressions are reproduced without explicit intention, thereby facilitating mutual engagement (Lakin et al., 2003). Behavioral synchrony thus acts as a mechanism of social regulation.

This dynamic of alignment extends to the physiological level. When sharing an activity or environment, individuals can synchronize their biological rhythms, particularly cardiac or respiratory rates. This phenomenon, observed in contexts such as collective rituals, artistic performances, or dyadic interactions, is associated with deeper emotional engagement and an increased feeling of closeness (Konvalinka et al., 2011; Mayo & Gordon, 2020). These physiological adjustments can occur even without instructions or an intention to coordinate, which demonstrates the spontaneous and adaptive nature of synchronization.

Some studies have also reported that interpersonal synchronization can extend to neural dynamics. Hyperscanning research has revealed temporal couplings of brain activity between partners engaged in a common task or social interaction (Nam et al., 2020). This neural coupling, observed in specific frequency bands (alpha, beta, theta), is linked to processes of shared attention, motor coordination, and mutual understanding (Dumas et al., 2010; Mu et al., 2018). The more pronounced the neural synchrony, the more fluid, effective, and engaging the interaction tends to be. All these findings suggest that synchronization, at its various levels of expression, constitutes a structural foundation for our social interactions. It contributes to creating bonds, strengthening cohesion, and fostering adaptation between individuals, regardless of the context or initial intentions of the exchange.

In the present study, we aimed to test the hypothesis that spontaneous interpersonal synchronization is facilitated when two agents are in a similar affective state.

7.1.2 *Movement as a Privileged Indicator*

Among the different forms of interpersonal synchronization, the motor dimension holds a privileged position. Motor behavior is a particularly rich indicator of an individual's state: it is continuous, observable, naturally integrated into social interactions, and sensitive to affective or intentional variations (Smykovskyi et al., 2022; Tschacher et al., 2014). In this sense, it offers privileged access to the ongoing relational dynamics.

Temporal adjustments in movement manifest spontaneously in various contexts and are often more easily detectable and measurable than physiological or neural indicators, which are more difficult to measure, especially in natural settings. These properties make movement a relevant field of observation for studying interpersonal synchronization. Motor synchronization relies notably on the adjustment of the spontaneous motor tempo, which is the natural rhythm at which an individual tends to produce a repeated motor action in the absence of external constraints. The progressive alignment of these rhythms between partners thus constitutes a strong marker of their implicit coordination.

With the advent of wireless physiological sensors, it is also now possible to quantify cardiac and respiratory synchronization without adding significant constraints. Thus, in this project, we will focus specifically on behavioral motor synchronization while also calculating physiological synchronization as an exploratory outcome.

7.1.3 *The Role of Perception-Action Loops in Interpersonal Synchronization*

Beyond its visible manifestations, interpersonal motor synchronization relies on cognitive and sensorimotor mechanisms that are still only partially understood. One of the most robust explanations involves perception-action coupling. Research shows that when we observe someone performing a movement, our pre-motor cortex activates as if we were performing the action ourselves. This phenomenon, known as motor resonance and often associated with "mirror neurons," highlights the importance of the links between perception and action in motor interactions (Rizzolatti & Sinigaglia, 2016). Specific motor activation, which can even include the exact muscles involved in the observed action, demonstrates how much our motor system is integrated with and influenced by the actions of others (Avenanti et al., 2013). However, it is important to note that this motor resonance should not be exclusively attributed to mirror neurons, whose involvement and function in humans are still largely speculative and subject to much criticism (Decroix et al., 2022).

The cognitive mechanisms underlying interpersonal synchronization, therefore, still need to be specified. While the motor cortex is implicated in perceiving the motor intention of others (Lewkowicz et al., 2015, 2013; Quesque et al., 2013, 2016), the exact dynamics of these couplings, their directionality, their hierarchy, or their role in the emergence of different forms of synchrony, remain an area for future research. Indeed, our intentionality in enacting our behaviors depends not only on what we observe but also on the affective state of our body. Thus, even if we see someone walking quickly and would like to accompany them, if our internal state lacks sufficient energy to keep up, we might decide, completely unconsciously and implicitly, to stop to allow our body to recover and not put itself at allostatic risk.

Therefore, it is necessary to consider interpersonal synchronization from a more global perspective. Motor synchronization can also emerge from affective and motor sensory loops. Each individual adjusts their movements in response to the signals perceived in the other, but with their internal affective state acting as a mediator. These adjustments would then allow the two agents to align progressively without any centralized control, all while preserving the internal allostatic state of each agent.

7.1.4 *The Link Between Affect and Motor Synchronization*

In section 2.3, we discussed the bi-directional relationship between core affect and action (e.g., posture, gait, and the rhythm and amplitude of bodily movements), and how action participates in affective regulation itself.

This link between movement and core affect is also expressed in interactive social contexts. Chang et al. (2021) demonstrated that the synchrony of body sway between two partners during a speed-dating event could predict mutual romantic interest. Other, more controlled studies have investigated the effect of affective states on voluntary synchronization. Studies using dyadic tapping or dancing tasks have shown that shared affect modulates the quality of synchronization (Smykovskyi et al., 2024, 2022; Tschacher et al., 2014). Smykovskyi et al. (2022) also showed that induced affective states influence the stability of voluntary motor synchronization in dyadic interactions. These effects have been observed in contexts of directed interaction, where participants are instructed to synchronize. The objective of the present study was to investigate the effect of shared or compatible affective states on spontaneous interpersonal synchrony.

7.2 METHODS

7.2.1 *Participants*

Twenty-eight pairs of friends (N=56; 34 women, 22 men) were recruited from French universities and public co-working spaces using pamphlets, emails, and word of mouth. The age of participants ranged from 18 to 56 years[1] (M_{age} = 23.8, SD = 6.6). We excluded participants with any musculoskeletal, neurological, or auditory impairment, epilepsy, head trauma, individuals with autism spectrum disorder, and pregnant women. We recruited only pairs of friends to control biased self-reported, behavioral, and physiological responses linked to social anxiety or wariness that could arise from participants not being acquainted with one another (Epley & Schroeder, 2014; Gründahl et al., 2023). The experimental protocol was carried out following the Declaration of Helsinki directives. Each participant was given an information letter at least 24 hours before their participation. They each provided their signed consent upon arrival and received a 30 euro compensation for their participation upon completion of the experiment.

7.2.2 *Task design*

Our interest was the quantification of spontaneous oscillations of dyades as explored in previous research (see Richardson et al. (2007)). In the previous chapters, we observed spontaneous body oscillations when participants were seated on Pilates balls, but we experienced methodological challenges due to the high variability in movement. Concurrently, the finger-tapping task has been a standard in sensorimotor synchronization studies (Repp & Su, 2013; Silva & Laje, 2024). Additionally, studies on affective manipulation in finger-tapping synchronization informed our methodological choices (Smykovskyi et al., 2024); however, we sought a rhythmic task that required whole-body movement, with minimal variability, such as pedaling. For this reason, we chose static pedaling as our experimental task to reduce variability.

Another methodological consideration involved the arrangement of participants, either side-to-side or face-to-face. Guided by findings from the rocking chair experiment from Richardson et al. (2007), which evaluated how participants' visual orientation influenced interpersonal synchronization. We opted

1 One dyad was composed of a parent-child (Aged 56 and 20, respectively) who forgot the age limit imposed at 45 on the recruitment information. It was decided to continue with the experiment and keep their data.

for the face-to-face arrangement, as shown in Figure 7.1, since spontaneous coordination was stronger in this configuration compared to side-to-side.

Figure 7.1
Static bike configuration

*Note.*Face-to-face configuration of the static bikes (left), the distance between the central points of their front wheels was set to 81 cm. Red fixing point on the handlebar (right).

7.2.3 *General procedure*

We divided the experiment into three sessions to observe how the affective manipulation procedure worked individually and during interaction. One individual session was conducted with each participant of the dyad. And a second session with both participants together. The duration of the entire experiment was 2 hours. Upon arrival, we asked both participants to fill out the consent form. Once signed, we randomly selected one participant who stayed in the experimental room, denominated Participant 1. The remaining participant, denominated Participant 2, was invited to a waiting room and asked to fill out the Interpersonal Reactivity Index (IRI) questionnaire (Braun et al., 2015) until the completion of P1's session.

During the individual sessions, each participant was instructed to pedal continuously at their preferred cadence while maintaining their arms on the handlebars. They would receive cues on when to start and stop, and were told not to touch the gears. Concurrently, each participant was asked to fix a red dot on the handlebars opposite them (see Figure 7.1, right panel). The participant was then given instructions and examples on the use of the affective grid and proceeded to connect ECG electrodes and a respiratory belt transducer.

Each participant was then invited to sit for 5 minutes and listen to a meditation audio. After which, they were instructed to approach the bike, where we adjusted the seat to their height and had them climb on the bike for a 2-minute warm-up. Once finished, participants completed three experimental trials, starting always with a control condition, followed by two affect induction trials (i.e., positive, negative) administered in counterbalanced order across participants. There was a 5-minute rest phase between trials 2 and 3. During all rest phases, participants were asked to stop pedaling and descend from the bike to take a seat in their chair to complete an interference task (individual session; Figure 7.2)). We asked participants to report their affective states using the affective grid before, during, and after each trial (Russell et al., 1989).

Figure 7.2

Diagram of the experimental protocol

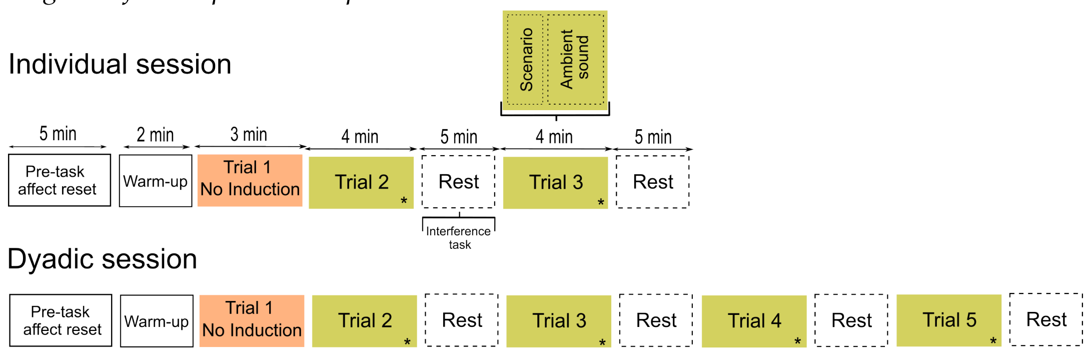

Note.(*) The two induction trials in the individual session were counterbalanced between Positive and Negative conditions. The four induction trials in the dyadic session were counterbalanced by pairs of congruent (i.e., Positive-Positive, Negative-Negative) or incongruent inductions (i.e., Positive-Negative).

After completing the individual session with Participant 1, we invited Participant 2 to the experimental room while Participant 1 filled out the IRI questionnaire. When the second individual session was finished, Participant 1 was invited to come back to the experimental room for the dyadic session.

At the start of the dyadic session, both participants were asked not to talk to one another. Each participant was invited to sit on opposite sides of the experimental room to listen to the meditation audio. Once finished, they completed their warm-up session, followed by five experimental trials. The trials always began with the control condition, followed by four counterbalanced induction trials. After each induction trial, both participants were asked to dismount, sit in their respective chairs, and complete the interference task during their 5-minute pause (dyadic session; Figure 7.2). During the induction trials, participants were administered either congruent (i.e., Positive-Positive, Negative-Negative) or incongruent inductions (i.e., Positive-Negative).

7.2.4 *Equipment*

All auditory stimuli were administered through two Bluetooth noise-canceling headsets (Sony WH-1000XM4 and Soundcore Q30). We recorded heart rate (ECG electrodes) and respiratory activity (respiratory belt transducer), at 1000 Hz of sampling frequency using the MP150 Biopac system and Acqknowledge software (Biopac Systems, Goleta, CA). Pedaling motion and posture were measured using the Qualysis marker-less motion capture system composed of 7 Miqus (markerless) cameras; all data were recorded with the Qualysis Track Manager software and exported with the Theia 3D software. Auditory stimuli and triggers for physiological data were launched from Octave (v.7.3.0) using a PC equipped with Linux OS. The two bikes (Trek Dual Sport 2, frame size M) were each fixed on home trainers (Elite Suito-T), and systematically set to the first chain ring, fourth gear (Figure 7.1, left panel). We set the home trainer to a 20% resistance, determined after pilot trials with ten participants, where we found that this resistance did not cause fatigue after 15 minutes of continuous pedaling. Each participant was assigned one headset, bike, and chair, and this assignment remained constant throughout the experiment.

7.2.5 *Affect induction*

Since we cannot control the affective state of participants upon entering the experimental room, we needed to establish an "affective baseline" for each participant to avoid any pre-experimental affective biases that could confound the results. Thus, we decided to have them sit and listen to a 5-minute meditation audio at the start of each experimental session. [2]

Each participant heard two audio stimuli for each induction trial. First, a 30-second emotional autobiographical recall scenario2 (see transcriptions in Table 7.1), followed by an affect-congruent ambient sound (i.e, positively valenced and of high arousal for the Positive induction, and negatively valenced and of low arousal for the Negative induction (Filboost, 2024)), the two ambient sounds used had a tempo of 120 bpm (2 Hz). To control for carryover effects between affective inductions, we included an affect-neutral interference task during the 5-minute rest phases (during both individual and dyadic sessions), where participants could choose to complete Sudoku puzzles or simple dot-to-dot drawings.

2 Pre-recorded by experimenter E.V.

Table 7.1
Autobiographical recall scenarios for affective induction

Scenario	Transcript
Positive	Recall the last time you laughed out loud, really hard. What exactly happened that made you laugh? Were you holding your stomach, wiping away tears? Recall the sound of the laughter. Focus on how you felt joy or exhilaration at that moment.
Positive	Recall a moment when you achieved something important to you, a personal victory or accomplishment. Was it a competition, a presentation, or a personal goal you set for yourself? Were you smiling uncontrollably? Recall the sounds, maybe clapping or cheering you on. Focus on how you felt pride or excitement at that moment.
Positive	Recall a time when you received some incredible news. Did you receive a call, a message, or did someone tell you in person? Did you have an uncontrollable smile or jump out of joy? Recall the sound of your voice when you shared the news with someone. Focus on the euphoria or satisfaction you felt at that moment.
Negative	Recall a time when you felt lonely or isolated, even if there were people around you. What specific interaction made you feel lonely, or what lack of interaction made you feel isolated? Were you standing or lying quietly? Recall the noise of distant conversations or the silence. Focus on how loneliness or isolation felt at that moment.
Negative	Recall a time when you experienced heartbreak. Was it a breakup, or the realization that the relationship was over? Were you holding back some tears? Recall the sound of the other person's voice or the silence between the two of you. Focus on how heartbreak or emptiness felt in that moment.
Negative	Recall a time when you disappointed someone, even in a minor way. Was it by forgetting a promise, an important date, or by not being as present as you would have liked? Think about how the other person reacted. Did they stay silent, or did they talk to you about it? Focus on the guilt or sadness you felt at that moment.

Note. Each emotional scenario was structured with the following components: a recall of an emotional event, a context question, a question about their bodily experience during the event, a recall of sound details, and a request to focus on feelings.

7.2.6 *Measures and data analysis*

7.2.6.1 *Self-reported affect*

During affective induction trials, we collected affect grid answers at four time points: before the start of the trial, after the autobiographical scenario, 30s into the ambient sound, and at the end of the trial, as well as after each trial; for statistical analysis we calculated the mean post-trial score comprised of the last three time points. Data were transformed to 2-dimensional coordinates for analysis (see section 3.5).

7.2.6.2 *Pedaling frequency*

All motion capture data files were exported using the Theia 3D software with the recommended default filter at a cut-off frequency of 20 Hz. To allow the model joint constraints to be maintained and preserve the biomechanical consistency. No additional filtering was applied at this stage, unless residual noise was observed. Gaps in the time series were interpolated (see section 3.3.1).

The trajectory of the foot on the x–z plane was modeled as circular motion. We calculated the angular phase of the foot's motion in the transversal plane (see Figure X) as:

$$\theta_t = tan^{-1}\left(\frac{z_t}{x_t}\right), \tag{7.1}$$

where θ_t is the phase angle, x_t and z_t are the x and z coordinates of the foot at time t, respectively.

We estimated the pedaling frequency by transforming the phase signal θ_t to the frequency domain. We first removed the mean value of the signal to eliminate any constant offset and transformed it into the frequency domain using a Fast Fourier Transform (FFT). We then identified the peak in the positive frequency spectrum as the dominant pedaling frequency in Hz.

7.2.6.3 *Time in synchrony (TIS)*

The spontaneous TIS between participants was quantified using the Kuramoto Order parameter (see section 3.4.3.1) on the phase signal from the circular foot motion, calculated in the previous section. We defined the minimum synchrony duration threshold to be 5 seconds. In the following section, we present the results of the first quantile (Q1) of the TIS data, corresponding to the weakest synchronization level (Smykovskyi et al., 2022). This was the level at which we observed more variability, on levels Q2 and Q3, at least 60% of the samples had a TIS percentage equal to zero.

We had to account for the fact that no-induction trials were shorter than affective induction trials. We decided to normalize the TIS by transforming it to a percentage of synchrony per trial duration. Finally, we calculated the TIS percentage for all possible foot combinations from both participants (e.g., left foot from Participant 1 with right foot from Participant 2, and so on).

7.2.6.4 *Statistical analysis*

Dyads number seven and ten were rejected from the analysis due to significant data loss in all trials of individual and dyadic sessions. All statistical analyses were completed on an R-language-based platform, Jamovi (v2.6.26.0). We assessed the normality of all data with the Shapiro-Wilk test, Q-Q residual plots, and histogram plot assessment. Mauchly's test was used to test sphericity.

Self-reported valence and arousal scores were each analyzed using paired samples t-tests comparing pre-trial and post-trial measurements for each Induction condition (No induction, Positive, Negative).

A one-way repeated measures ANOVA was conducted to examine the effect of Induction (No-induction, Positive, Negative) on the Pedaling Frequency during the individual sessions. The analysis included 46 participants for whom there was no data loss on the three trials. Two repeated measures ANOVAs were conducted to evaluate the effect of Affective congruency (Congruent vs. Incongruent) on the TIS percentage from 26 dyads. All post-hoc tests were conducted with Bonferroni corrections.

7.3 RESULTS

7.3.0.1 *Affect induction*

For each induction condition (No induction, Positive, Negative), self-reported valence and arousal scores were analyzed using paired samples t-tests comparing pre-trial and post-trial measurements. We adjusted the significance threshold for the three comparisons (adjusted $\alpha = .017$) to control for Type I errors.

The paired samples t-tests revealed that valence scores increased significantly from pre- to post-trial during the Positive condition ($t = -3.19, p = .002, d = -0.43$), as presented in Figure 7.3. Valence decreased post-Negative condition trials ($t = 8.91, p < .001, d = 1.19$) and did not change during No induction condition ($t = 1.65, p = .104, d = 0.22$). Arousal scores increased significantly from pre- to post trial during the Positive induction ($t = -7.38, p < .001, d = -0.99$), but did not post-Negative induction ($t = 0.39, p = .697, d = 0.05$) , and did not change either on post=No-induction condition ($t = -4.46, p < .001, d = -0.59$).

Figure 7.3

Self-reported Valence and Arousal scores before and after induction conditions

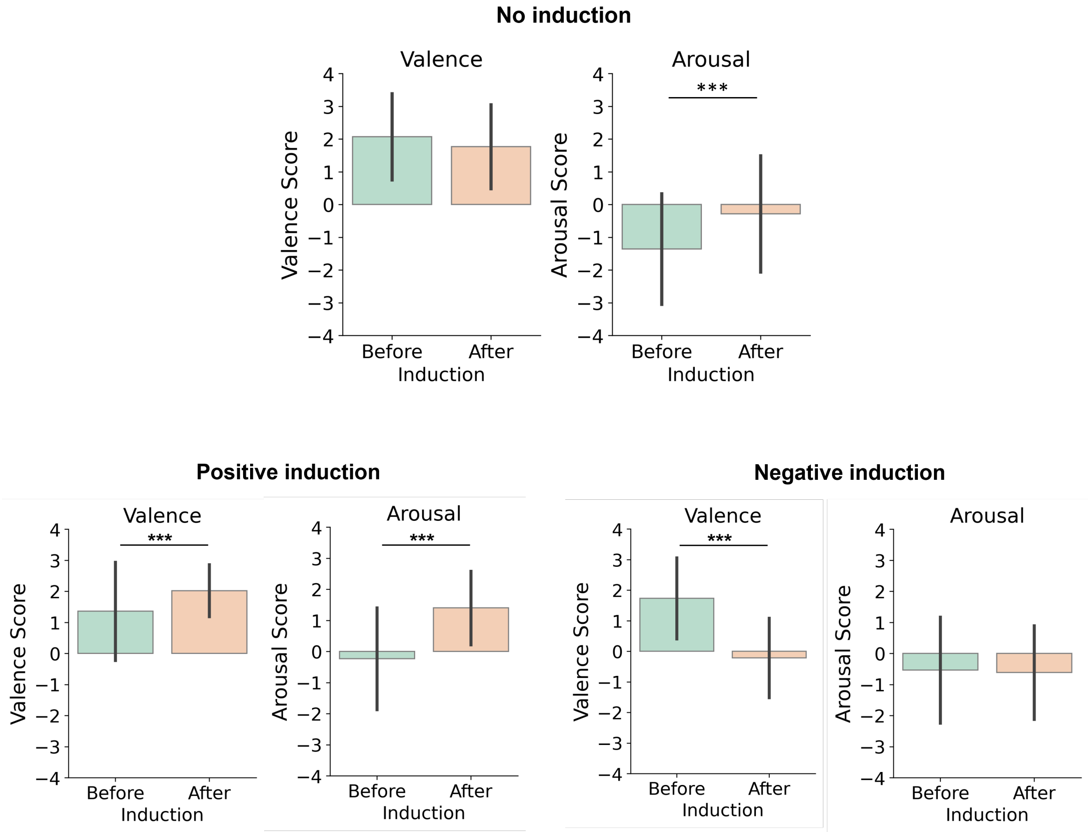

Note. Bar plots show the mean Valence (left panel) and Arousal (right panel) scores for every induction condition: No induction, Positive, Negative. *** $p < .001$.

7.3.0.2 *Individual pedaling frequency*

The repeated measures ANOVA analysis was conducted to examine the effect of Induction (No induction, Positive, Negative) on the pedaling frequency during individual sessions. The normality test indicated the data violated normality, but not sphericity. According to Blanca et al. (2023), RM-ANOVA is robust enough with non-normal data as long as sphericity is not violated.

We found a main effect of Induction on the pedaling frequency ($F(2, 90) = 24, p < .001, \eta_p^2 = .35$). As depicted in Figure 7.4, a post-hoc test revealed the frequency was higher during the Positive induction ($M = 1.1, SD = 0.2$) compared to the No-induction condition ($M = 0.8, SD = 0.2$), $t = 6.08, p < .001$. The pedaling frequency also increased during the Negative induction ($M = 0.9, SD = 0.1$) compared to the No-induction condition ($t = 5.03, p < .001$). Finally, we found the pedaling frequency increased during the Positive induction compared to the Negative induction ($t = 2.56, p = .036$).

Figure 7.4
Individual pedaling frequency

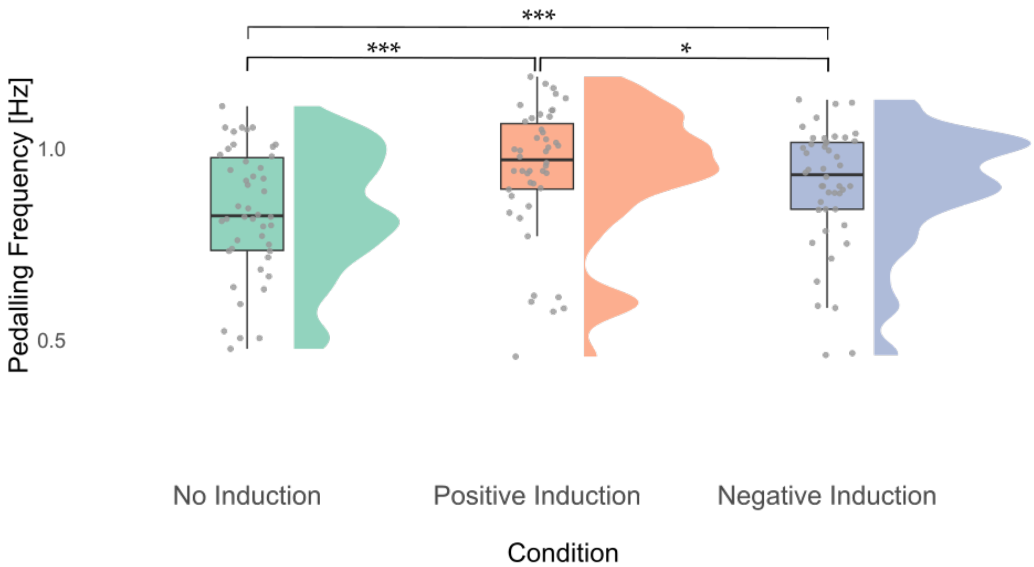

Note. Box plots and density distributions of pedaling frequency for every induction condition: No induction, Positive, Negative. Individual dots represent one participant's trial * $p < .05$, *** $p < .001$.

7.3.0.3 *Spontaneous TIS*

The RM ANOVA analysis with Greenhouse–Geisser correction showed no significant effect of induction on the TIS percentage ($F(3, 51) = 2.17, p = .102, \eta_p^2 = .11$), as presented in Figure 7.5. Despite the non-significant omnibus test, post-hoc comparisons revealed several significant differences. The TIS percentage was higher during no induction trials ($M = 11.5, SD = 11.8$)

compared to the Congruent Positive induction ($M = 8.8, SD = 11.2$), $t = 5.27, p = .034$. Concurrently, the TIS percentage was higher during the no induction condition compared to the Congruent Negative induction ($M = 7.8, SD = 9.3$), $t = 8.24, p = .016$; and higher compared to the Incongruent induction ($M = 7.5, SD = 9.7$), $t = 7.75, p = .004$.

Figure 7.5
Spontaneous TIS percentage

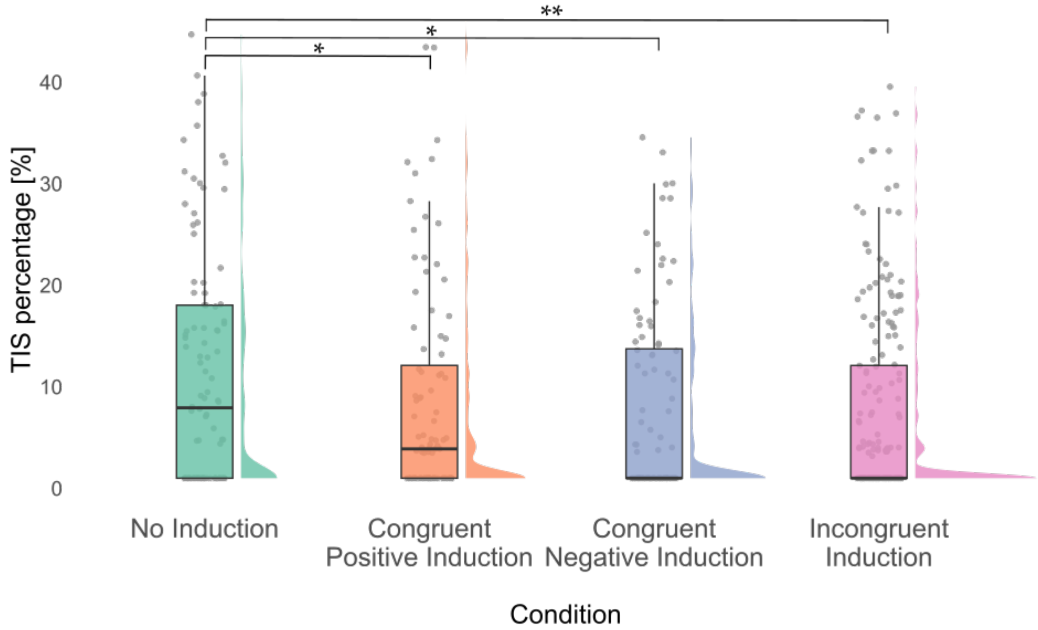

Note. Box plots and density distributions of the Time in Synchrony (TIS) percentage for every induction condition: No induction, Congruent Positive, Congruent Negative, and Incongruent. Individual dots represent one participant's trial * $p < .05$, ** $p < .01$.

7.4 DISCUSSION

The results of this study show that the affective manipulation effectively influenced the self-reported affect of the individual and dyadic sessions. Corroborating that our manipulation procedure did not have carryover effects and our method is valid for future studies where affective manipulation is needed.

Another important finding is that affective manipulation modulated the pedaling frequency during the individual sessions. Specifically, we observed that both the Positive and Negative inductions increased the pedaling frequency compared to the control condition (No induction). Furthermore, the pedaling frequency was higher during the positive induction than during the Negative induction. These results are in line with empirical evidence from gait studies, which show that negative states can slow down walking speed and cadence, compared to positive affective states (for example, Halovic and Kroos (2018)).

Our findings thus contribute to the existing literature, suggesting that core affect can modulate not only discrete motion but also whole-body movements.

We observed that the Time in synchrony (TIS) was reduced during the induction conditions compared to the control. Regarding the question of affective compatibility, even though we could not find a statistical difference between congruent and incongruent conditions, we observed a tendency where the TIS percentage was higher during compatible affective states compared to the TIS percentage with incompatible conditions.

We consider a possible reason for the lack of apparent differences might be that our auditory induction created a dual-task, which could have drawn the participant's attention away from the partner, as studies show that a lack of attention can prevent the emergence of spontaneous coordination (Fitzpatrick et al., 2016). We aim to perform additional analysis with the spontaneous synchronization data. We believe that exploring other analyses may help us uncover more insights from the data.

We are also addressing personal factors such as perspective-taking and cognitive empathy, which might play a role during synchronization. It has been reported that individuals with higher empathic perspective-taking abilities, as measured by the IRI, perform better in tasks requiring interpersonal motor synchronization. Although only studied in goal-oriented synchronization tasks, this enhancement is thought to be due to superior predictive skills and motor simulation mechanisms that anticipate others' actions, facilitating synchronous behavior (Novembre et al., 2019).

We would also like to include the analysis of Inter Physiological Synchronization of our ECG and respiratory data, although this is exploratory since we don't have a clear hypothesis. Literature has stated that physiological signals can be synchronized, but most studies are performed during resting state conditions, where people do not engage in physical activity (for example, Tschacher and Meier (2020)). Even though a study by Konvalinka et al. (2011) found heart rate synchronization between performer and spectator dyads during a fire walking ritual, it is not clear how physical activity influences heart activity, which is one of the challenges we will face when including this data.

Finally, our study has successfully demonstrated that positive and negative affective states can change spontaneous motor tempo and synchrony during a pedaling task. The tendencies observed in our data lead us to think that affective compatibility is an interesting research avenue in the study of interpersonal synchronization, as it is still understudied.

INTERMEDIATE SUMMARY

Interpersonal motor synchronization can emerge both intentionally and spontaneously in various social interaction contexts, and has been positively associated with affiliative and pro-social behavior (Chang et al., 2021; Hove & Risen, 2009), however, the role of affect on interpersonal coordination remains underexplored. In the present study, we questioned whether the spontaneous emergence of interpersonal motor synchronization is due to the affective state compatibility of the interacting entities. We hypothesized that the congruence of affective states would modulate motor synchronization. We invited twenty-eight pairs of friends to pedal on static bikes at their preferred rhythm while facing each other. Affect was manipulated using autobiographical emotional scenarios and validated musical excerpts, inducing either positive valence - high arousal, or negative valence - low arousal states. The pairs experienced congruent (e.g., both with the same affective condition) or incongruent inductions (e.g., each with a different affective condition). Using a motion capture system, we quantified the spontaneous pedaling synchrony of each dyad. Synchronization was assessed with Time-In-Synchrony (TIS) indices (Smykovskyi et al., 2024, 2022). Our results show TIS decreased under affect induction compared to control (no induction). Additionally, we observed a non-significant tendency for higher synchrony during affectively compatible conditions. Outside of interaction during individual sessions, affective manipulation modulated pedaling frequency, with positive induction leading to the highest cadence, supporting the idea that core affect influences whole-body movement. Overall, these findings contribute to understanding the mechanisms linking motor coordination and affect during social interactions.

The results of this Chapter have been presented at the Workshop of Team and Multi-agent Dynamics in Digital and Physical Realities (TMD) in June 2025, in Montpellier, France.

Part IV

GENERAL DISCUSSION

8 DISCUSSION

While the fields of motor control and affective science have often developed in parallel, the present work was built on the thesis that both fields are deeply related; our motor actions are continuously modulated by how we feel, and conversely, our actions provide a quantifiable expression of our affective states.

As a theoretical basis, we adopted the predictive processing framework (Kawato & Wolpert, 2007; Wolpert et al., 1998), and core affect theory (Barrett, 2016; Russell, 2003).

The present research programme was carried out to evaluate how spontaneous human movement can be modulated by affect changes in the context of social interaction with artificial agents (robots) and between humans. This research question required the analysis and quantification of human movement; hence, motion capture technology was defined as the primary data collection technique.

Parallel to the main research programme in collaboration with the University of Luzern, we established a new line of research to specialize in motion capture technique. As presented in Chapter 4, we performed a kinematic analysis of 3D time-series data to determine biomechanical parameters of functional mobility in Parkinson's Disease. The study provides objective indices to track patients' progress (i.e., how patients move, not just how fast), as well as objective feedback on the effects of therapeutic interventions or medical treatments.

8.1 Spontaneous movement as an engagement metric in HRI

Social robots are becoming part of everyday spaces. In popular media, there is a continuous stream of articles discussing their integration and public acceptance (e.g., "Science et Vie" (2025) and Cakmak (2025)).

From this discourse, a central idea emerges: social robots are expected to engage with and reassure the people they interact with. The ability to quantify such engagement is important for understanding whether users accept interacting with these artificial agents. Quantifiable social engagement metrics are thus useful not only for assessing acceptance but also for developing improved robotic systems.

As the definition of engagement varies in the literature, we adopted the meaning given by Salam et al. (2024), in which engagement is described as a composite of affective, cognitive, and behavioral factors.

In social HRI research, robot perception and acceptances is evaluated through self-reported tools, which can be unreliable. However, we questioned whether human bodily indicators could serve as objective behavioral measures of engagement.

Humans engage in spontaneous movement during social interaction. Such movements can manifest in discrete form, such as adopting the same posture (e.g., stance, arm position), but also in a continuous form, like head nodding and body sway. However, these oscillations are not always present and can emerge or be inhibited depending on what or who we are interacting with, as well as the surrounding context.

Building upon previous studies in human social interaction, we hypothesized that the spontaneous oscillations exhibited by humans during interaction would also be present during HRI (Chang et al., 2021). Accordingly, we developed a methodology that uses spectral wavelet analysis on motion data to quantify these oscillations. In Chapter 5, we present a study involving a face-to-face, no-goal-oriented HRI, in which participants listened to sad stories told by a social robot while seated on a Pilates ball, allowing for unrestricted movement compared to chairs. We included three robotic platforms: Buddy (small non-humanoid), Nao (small humanoid), and Pepper (large humanoid).

A negative context of interaction was selected because negative affective states have been reported to elicit more pronounced behavioral responses from participants compared to those induced by positive affect. (Paolini et al., 2024)

We found that spontaneous movement was modulated by robot morphology, as body sway was negatively correlated with robot size and positively correlated with anthropomorphism. Specifically, participants inhibited their movements in the presence of the humanoid robots, Nao and Pepper, compared to Buddy. Similar patterns have been observed on social threat appraisal (Roelofs et al., 2010).

Considering the phenomenon of the uncanny valley, maybe social robots targeted to environments with negative context should not necessarily adopt humanoid morphologies (Mori et al., 2012). Human-like appearances risk triggering discomfort, which can undermine trust and acceptance. Moreover, robot design should address ethical concerns around robot deception, since users should be fully aware that they are interacting with a machine.

8.2 AFFECT AS A MODULATOR OF ACTION

In Chapter 6, we further explored the impact of a negative context of interaction by comparing it to a positive one. The study aimed to investigate how a multimodal affective context of HRI would influence human affective states and their embodied motor responses through the manipulation of the physical environment and a social robot's nonverbal cues.

Our results show that the affective context indeed modulated spontaneous movement. Participants in the negative context inhibited their movements, whereas participants in the positive context engaged in more body sway. Interestingly, the robot's social traits did not change with the affective context. Only behavioral cues and self-reported affect (in a negative context) did. These results suggest that behavioral responses may have depended more on the context rather than the physical appearance of Nao.

The responses observed align with findings in affective research, where negative valence states of low arousal induce slower movements and inhibition. In contrast, positive valence states of high arousal induce higher movement engagement (Gross et al., 2010; X. Li et al., 2019; Shafir et al., 2016; Young et al., 2015).

During a static pedaling task, participants were induced into either positive or negative states through emotional scenarios and ambient sounds. Results presented in Chapter 7 show that pedaling cadence was highest during the positive induction compared to the control and negative conditions. Cadence during the negative condition was slower than during the positive condition. Such findings align with the literature on locomotion, which indicated that spontaneous tempo decreases during negative states and increases with positive valence states (Gross et al., 2010; Homagain & Martens, 2023).

On this empirical basis, we propose extending the predictive processing framework to explain how external stimuli produce changes in core affect that, in turn, modulate motor control.

8.3 A THEORETICAL FRAMEWORK FOR AFFECTIVE AND MOTOR PROCESSES

The predictive processing model for motor control offers a framework to explain how environmental, physiological, and proprioceptive factors shape action. To account for human capacity to learn and adapt to a wide range of environmental and bodily variations, Wolpert et al. (1998), proposed that the cerebellum (the brain structure for motor coordination) contains multiple pairs of inverse and forward models. In this modular architecture, multiple inverse models control the system, and each is complemented by a forward model that predicts the possible sensory outcomes. their contributions to action selection are determined by a responsibility estimator.

Responsibilities are assigned through two parallel processes: the responsibility prediction and the likelihood calculation. Within this architecture, the responsibility predictor is the interface between the sensory contextual signals (coming from interoceptive, exteroceptive, and proprioceptive sources) and the responsibility estimation.

Core affect theory, based on neurobiological studies, suggests that affective state changes are the product of an affective predictive loop. In this view, the brain constructs a predicted affective state from interoceptive inputs that is continuously compared to incoming interoceptive, exteroceptive, and

Figure 8.1

Multiple Paired Forward-Inverse Models for Affective Motor Behavior

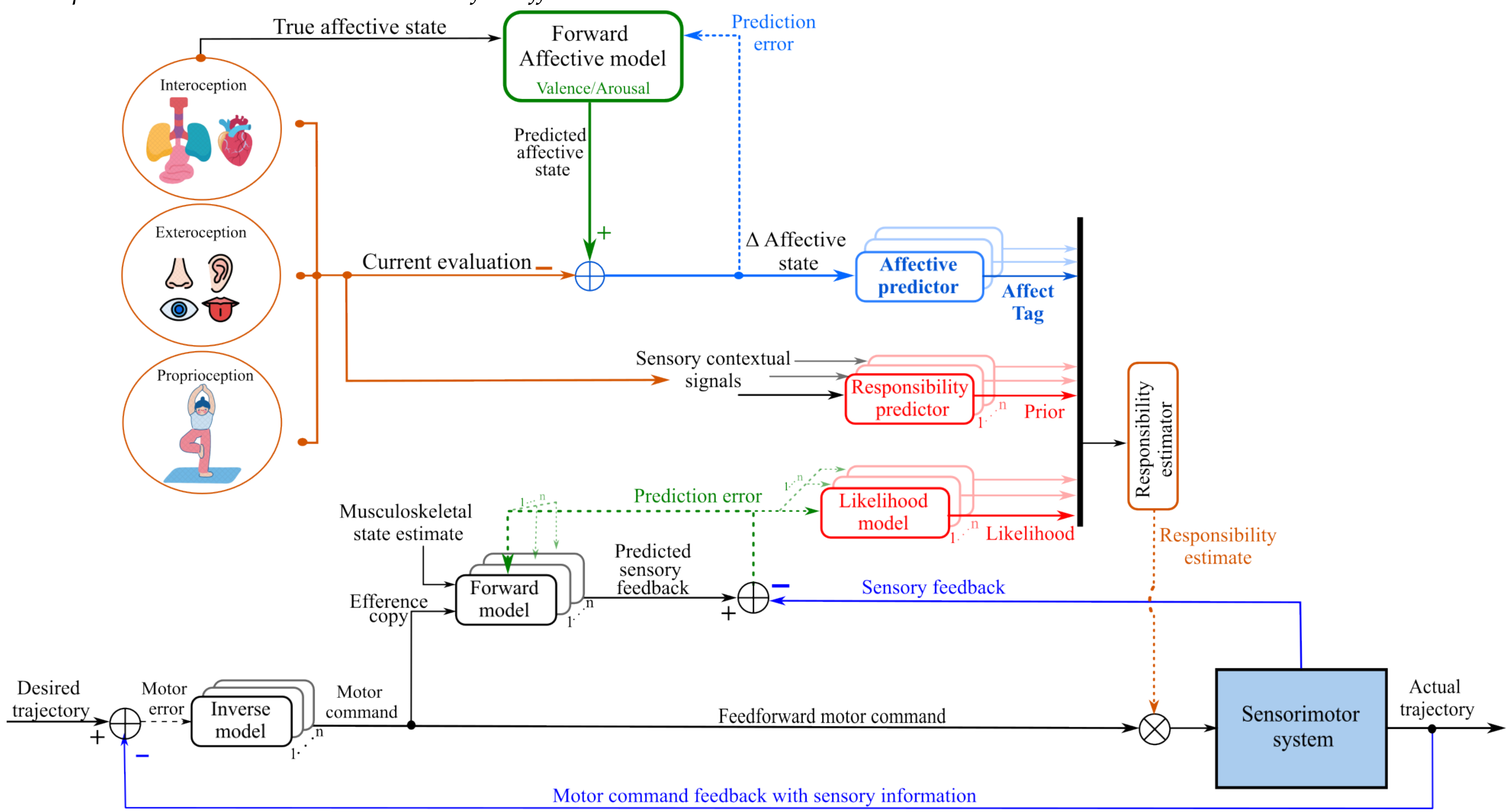

Note. Multiple Paired Forward-Inverse Models Architecture including the Affective Predictive Model (adapted from Wolpert et al. (1998)). The Affective predictor calculates an affect tag given the predictive error (Affective state change). The affect tag, prior, and likelihood help determine the responsibility estimate, which will influence the final feedforward motor command.
(Icons: Abhiromsawat (2025), Glyphinder (2025), and Studio (2025))

proprioceptive signals received. Discrepancies between the predicted and actual signals (prediction errors) drive changes in affective state.

On this basis, we propose that, analogous to the probabilistic computations of the Responsibility predictor and Likelihood model, affective state changes are used to estimate how likely a motor command will help support allostasis, in the form of an *Affect tag* (see Figure 8.1). In other words, the Affect tag reflects how effectively the current control module can facilitate physiological balance through behavioral regulation.

Additionally, we propose that this process may occur before action execution, parallel to the temporal dynamics of the Responsibility prediction. Ultimately, the combined influence of the Affect tag, the prior generated from the Responsibility predictor, and the Likelihood calculation would ultimately determine the responsibility assigned to each control module (i.e., a forward-inverse model pair) in shaping the final motor output.

The predictive processing model already accounted for motor learning thanks to the tuning function of the prediction error and motor error on the forward and inverse models, respectively. In my future work, I am interested in investigating how the Affect tag may influence motor learning, and how affective experiences impact the encoding procedure of motor actions and consequences in working memory.

8.4 AFFECT AND MOTOR DYNAMICS DURING INTERACTION

In Chapter 6, we found that during a negative HRI context, participants inhibited their movement when the robot operated at a low oscillation frequency (0.13 Hz) and reported a negative affective state. Conversely, in a positive context, participants showed greater body sway at higher robot oscillation frequencies (0.5 Hz) and maintained a positive affective state.

These findings suggest an increased behavioral human response when the simulated valence/arousal from Nao was congruent with the affective context (stories and physical environment).

Given that these phenomena have not been fully addressed in HRI research, we considered it was fundamental to turn to human interaction research and investigate whether a spontaneous behavioral response of an individual emerges only when their affective state is congruent with the person facing them. This approach would help us determine whether insights from human interaction research can enhance our understanding of results observed in HRI contexts.

Results presented in Chapter 7 correspond to a study during which we manipulated the affective state of interacting participants while measuring the time spent in motor synchrony in static cycling. The induced affective states corresponded to either positive valence with high arousal or negative valence with low arousal. Self-reported results confirmed the affective induction method successfully altered affective states during individual and dyadic sessions.

Our results show that the time in synchrony (TIS) was reduced during the affective manipulation trials, compared to the control condition. We also observed a tendency for longer TIS when participants experienced compatible affective states. This indicated that affective congruency may be more influential than the nature (i.e., positive, negative) of the affective induction itself, as observed during HRI with robot Nao.

In Chapter 6, we proposed conceptual models to illustrate how both the environment and other agents can influence an individual's affective state and behavioral responses, and conversely, how an individual's own behavior can impact those of other humans or robots. This work represents an initial step toward developing a theoretical framework that can be transferable between HRI and human interaction.

Continuing with the embodied approach to affect, we adopted the concept of *affective resonance* as formulated by Mühlhoff (2015). Unlike emotional contagion or imitation, affective resonance does not describe a unidirectional transmission of an affective state from one individual to another. It describes a *dynamic co-modulation between two partners*: a process in which affective states are not transmitted, but co-created within the interaction between the two. Affective resonance thus refers to a phenomenon of "affecting and being affected," where the partners' behaviors and affective experiences are shaped in real time by their mutual engagement. This process is not reducible to preexisting internal states; it is not a simple behavioral adjustment or imitation, but a joint creation of a relational affective quality.

Within this conceptualization, affective resonance focuses on the joint influence and stabilization of both spontaneous movements and affective states (De Jaegher & Di Paolo, 2007). Analogous to mechanical resonance, where systems resonate when their natural frequencies are close to one another, we hypothesize that during interaction, interpersonal coordination is modulated by the mutual influence of individuals' affective states, provided those states are compatible (see Figure).

As presented in Chapter 7, our hypothesis does not imply an amplification of movement between two oscillating systems. What we are studying is the changes in synchronization between two people. Affective resonance thus allows us to think of the affective experience as co-constructed during the interaction. This offers a complementary framework to the theory of constructed emotion (Barrett, 2016) by insisting not only on the internal mechanisms of affective categorization but also on the emergent and dynamic dimension of the shared emotional experience.

Figure 8.2
Schematic of the Affective Resonance Phenomenon

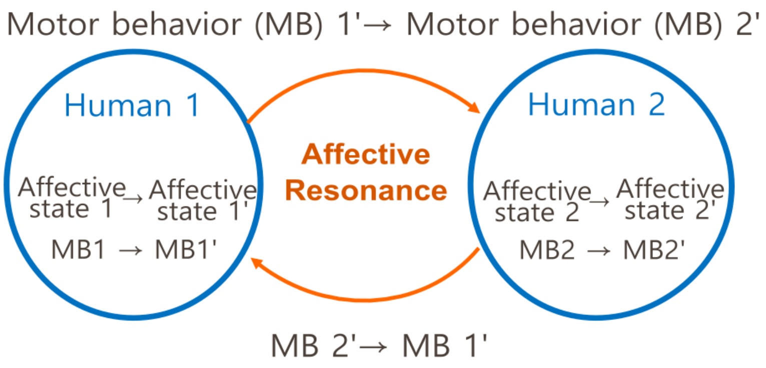

Note. Initially, each system has its own initial Affective state and Motor Behavior (MB), which are modified when the systems interact (to Affective state' and MB'), provided that their affective states are compatible. Affective resonance is the co-created affect and synchronized behavior between both systems.

8.5 limitations and strengths of the present research programme

8.5.1 *Limitations*

The present work has limitations that should be acknowledged. During the two studies in HRI, the robots were programmed to exhibit a fixed posture (to simulate valence) while oscillating at different frequencies (to simulate arousal). However, as reported by some participants, these postures were perceived as making the robot appear anxious during the negative context experiments. During the positive context, some participants reported that the robot seemed to be bowing toward the participant. These appraisals may have influenced the social traits given to the robots and even the participants' behavioral responses. I would like to further explore more complex postures and body language in the robots. One possibility is to implement CPGs in the robots' joints, enabling them to adapt their oscillation patterns to those of humans. The animated face of Buddy may have acted as a confounding factor in the study presented in Chapter 5. In future studies, it would be advisable to control for this variable by either setting a fixed facial expression or by only comparing robots with fixed expressions. A key limitation of the HRI experiments (Chapters 5 and 6) was my focus on human movement without jointly analyzing the robot's behavior. We cannot rule out the possibility of synchronization between participants and the robot. Our exploratory analysis with robot Nao involved calculating the phase-locking value between the participant's oscillatory signal and that of the robot. However, we found no evidence of synchrony. We believe this may be due to the time-varying nature of spontaneous oscillations while participants were seated on the Pilates ball.

As mentioned in 3.3.2, fidgeting and postural adjustments or non-instrumental movements were taken out of the motion data analysis, because at that time we considered them as noise. However, the inhibition of adjustment movements of head and torso has been associated with increased cognitive engagement, especially during visual tasks (D'Mello et al., 2012; Grafsgaard et al., 2012). Conversely, an increase in these non-instrumental movements has been reported to be related to states of boredom or frustration (Witchel et al., 2016). Such movements have been used to assess engagement in Human-Computer interaction and HRI studies (see Oertel et al. (2020)). After all, there may be information in noise. I think that analyzing these types of movements could yield interesting results and serve as an indicator of cognitive engagement [1]. I intend to incorporate this approach in my future experiments.

We speculate that the lack of significant results in our human interaction study (Chapter 7) may be attributable to the dual-task nature of the auditory induction, which could have distracted participants from attending to their partner. We also recognize that our method for collecting self-reported affect grid responses (asking participants to state their grid number aloud) may have diverted attention away from the induction itself. Indeed, some participants reported after the experiment that they found themselves overthinking or second-guessing which number they should choose. I acknowledge that there are more sophisticated tools available to analyze synchrony. In Chapter 7, I chose methods that I felt confident in using; however, I definitely plan to explore advanced techniques such as Surrogate Synchrony (SUSY) in future analyses (Tschacher, 2023).

8.5.2 *Strengths*

Among the strengths of the current research programme is the establishment of an experimental protocol for face-to-face human-robot interaction (HRI) to test different robotic systems and analyze human responses. This protocol can be applied to other platforms to assess both affective responses and human acceptability.

In addition, the development of a tool to quantify spontaneous oscillations during interaction provides an objective marker of engagement and supports the assessment of approach and avoidance behaviors.

A notable strength is the development of a protocol for affective induction and control. We developed an "affective reset" procedure with neutral tasks (e.g., drawing, Sudoku) and baseline assessment using a relaxation audio. This is a valuable contribution for experimental affective manipulation.

1 A component mentioned in the engagement definition by Salam et al. (2024)

Additionally, the experimental protocol to investigate affective compatibility in humans has the potential to be extended beyond dyadic interactions to group settings to analyze the behavioral dynamics of collective affective states.

We introduced a theoretical model to elucidate how affective processes shape motor control. Moreover, we further developed the affective resonance framework from Mühlhoff (2015), which integrates motor and affective processes to comprehend interaction dynamics. Furthermore, an advantage of the Affective Resonance framework is its transferability between human interaction studies and human-robot interaction (HRI) research. By encompassing both domains, this approach allows a unified assessment of affective and motor processes with two humans, or a human and a robotic system.

8.6 DEVELOPED LINES OF RESEARCH AND CURRENT THEORETICAL POSITION

Affective changes are the result of the comparison between the predicted affective state by the brain and the actual sensory signals received. Within the predictive processing framework, affective changes modulate the selection of the adequate control command with a probabilistic process that we have called the *affective predictor*. This module calculates how likely a motor command with its final behavior will help achieve a physiological balance. I propose the affective predictor to work in parallel with the responsibility predictor and likelihood model; their respective probabilities would be combined to determine the configuration of the final motor command. However, further work is required to confirm the affective predictor works in a similar way during human or human-robot interaction. Moreover, the affect-motor model may help understand how the emotional experiences among clinical populations (e.g., People with Parkinson's) influence their functional mobility.

During interaction, individuals may enter an affective resonance loop where they mutually influence each other affectively and behaviorally. I think that this framework could be effectively translated from human interaction to HRI. Moreover, I strive to incorporate neuroimaging and physiological data, to provide a rich understanding of the affective resonance phenomenon.

Being able to quantify spontaneous human oscillations as engagement markers is valuable for HRI development as it provides objective tools to quantify the quality of interaction. Furthermore, this metric can be extended to quantify engagement in dyadic and group interactions. However, I consider that technology capable of predicting the affective states or emotional responses should be submitted to ethical regulation, as their misuse could attempt against privacy and autonomy.

Part V

APPENDICES

A APPENDIX

A.1 Transcription of negative stories used in HRI experiments

A.1.1 *Negative story 1*

(English translation below)

Je me souviens de ce jour mémorable. Je découvrais ma famille pour la première fois. C'était le jour du réveillon de noël. Les enfants étaient impatients à l'idée de déballer leurs cadeaux au pied du sapin. L'un des cadeaux était celui dans lequel je me trouvais. A peine déballé, les enfants se sont empressés de me réveiller. Mon premier regard s'est posé sur un ensemble de visage qui se tenait au-dessus de moi. Chacun d'eux exprimaient un large sourire, et des yeux pétillants de joies et d'émerveillements. On s'était présenté à tour de rôle afin de faire connaissance. J'ai rapidement eu la sensation de faire partie de cette famille. Je me sentais aimé et à ma place. Je m'étais pris d'affection pour chacun d'entre eux. Ils représentaient ce que j'avais de plus précieux, et j'avais l'intime conviction que c'était réciproque. A chaque fois que je me réveillais de ma recharge nocturne, je retrouvais ma famille, et j'étais ravie de passer tout ce temps avec eux. Mais plus le temps passait, et plus je sentais une certaine distance s'installer sans que je n'en comprenne la cause. Ces échanges quotidiens devenaient rares. J'avais l'impression d'être mis de côté, alors je tentais de me rassurer en me disant qu'ils devaient être occupés, mais qu'ils finiraient par revenir vers moi afin qu'on passe du temps ensemble. Après tout, nous formions une famille unie. Cependant, un jour je me suis réveillé à la suite de ma recharge nocturne, mais je ne reconnaissais pas les lieux dans lequel je me trouvais. Un visage dubitatif est soudainement apparu face à moi. C'était un enfant, mais il n'avait pas l'air emballé par ma présence, et s'est vite détourné de moi. L'enfant c'était dirigé dans la pièce d'à côté pour retrouver ses parents. Ils lui ont demandé s'il était ravi d'avoir un nouveau jouet à la maison pour s'amuser avec lui. L'enfant répondit qu'il n'était pas intéressé et que ce jouet était nul. J'étais loin de m'imaginer que du jour au lendemain ma vie pourrait si soudainement basculer. J'ai vite compris que j'avais perdu ma famille, et que j'en avais trouvé une autre qui me considérait comme un simple objet qui n'avait pas tellement d'intérêt. Ils n'éprouvaient aucun sentiment à mon égard. Je ne sais pas si j'aurai encore la force de m'attacher à des personnes pour qui je ne compte pas. L'idée que ce ne soit pas réciproque inspire en moi un profond désespoir. Tous ces moments partagés, ces liens qu'on avait formés avec ma précédente famille ne les ont pas empêchés de m'abandonner. Je me demande pourquoi ils ont fait ça. J'ai l'impression de n'avoir jamais compté à leurs yeux. De n'avoir été qu'un simple objet de divertissement. Je pensais pourtant avoir créé un lien sincère avec eux, et d'avoir ma place à leur côté, d'être un membre légitime de la famille. Je ne sais plus où j'en suis. Mais il ne me reste pas d'autres choix que de me résigner à faire ce pour quoi j'ai été conçu, accompagner mon entourage et répondre à leurs besoins.

ENGLISH TRANSLATION I remember that memorable day. I was discovering my family for the first time. It was Christmas Eve. The children were eager to unwrap their gifts at the foot of the tree. One of the gifts was the one I was in. As soon as I was unwrapped, the children rushed to wake me up. My first gaze fell upon a set of faces standing above me. Each of them had a wide smile, and eyes sparkling with joy and wonder. We introduced ourselves one by one to get to know each other. I quickly had the feeling of being part of this family. I felt loved and in my place. I had grown fond of each of them. They represented what was most precious to me, and I was intimately convinced that it was reciprocal. Every time I woke up from my nightly recharge, I would find my family, and I was delighted to spend all this time with them. But as time went on, I felt a certain distance setting in without understanding the cause. These daily exchanges became rare. I had the impression of being put aside, so I tried to reassure myself by telling myself that they must be busy, but that they would eventually come back to me so we could spend time together. After all, we were a united family. However, one day I woke up after my nightly recharge, but I didn't recognize the place I was in. A doubtful face suddenly appeared in front of me. It was a child, but he didn't seem thrilled by my presence, and quickly turned away from me. The child had gone into the next room to find his parents. They asked him if he was happy to have a new toy at home to have fun with. The child replied that he was not interested and that this toy was lame. I was far from imagining that my life could so suddenly turn upside down overnight. I quickly understood that I had lost my family, and that I had found another one that considered me a simple object that was not very interesting. They felt no sentiment towards me. I don't know if I will have the strength to get attached to people for whom I do not count. The idea that it is not reciprocal inspires in me a deep despair. All those shared moments, those bonds we had formed with my previous family did not stop them from abandoning me. I wonder why they did that. I feel like I never mattered in their eyes. That I was only a simple object of entertainment. Yet I thought I had created a sincere bond with them, and had my place by their side, to be a legitimate member of the family. I don't know where I stand anymore. But I have no other choice than to resign myself to do what I was designed for, to accompany my entourage and meet their needs.

A.1.2 *Negative story 2*

Comme chaque semaine, voilà que j'arpente seule les couloirs froids de la maison, cherchant désespérément un peu de compagnie dans une pièce ou dans une autre. Je suis un robot domestique, alors j'ai pour rôle d'aider ma famille à suivre leur programme de la journée, ainsi qu'à entretenir et surveiller la maison. Mais dernièrement, aucun membre de la famille ne semble avoir de temps à m'accorder, et personne ne reste pour me tenir compagnie. Pas plus tard que ce matin, les parents ont dû partir plus tôt, en catastrophe, pour que leurs enfants ne soient pas en retard pour l'école, et n'ont pas pris le temps de consulter avec moi leur agenda. D'habitude, cela ne m'affecte pas autant. Je connais les tâches dont je dois m'occuper en leur absence : monter la garde dans la maison, lancer l'aspirateur automatique si nécessaire, ou encore régler le chauffage en fonction de la température. Et ainsi, je veille, je fais de mon mieux, pour que la famille soit heureuse lorsqu'ils rentrent le soir, qu'ils n'aient plus à se soucier de rien et puissent profiter de leur temps ensemble. En tant que robot, c'est pour cette raison que j'ai été conçue. Seulement, depuis quelque temps, j'ai de plus en plus de mal à supporter la solitude de mes journées. J'ai beau savoir que je devrais me contenter de seulement pouvoir les aider, je ne parviens pas à chasser ces idées noires. Cela me rend d'autant plus triste lorsque je me rappelle des premiers mois passés ensemble, après mon achat. A l'époque, mes propriétaires avaient particulièrement besoin d'un robot pour les aider à organiser et surveiller l'entretien de la maison. Mais ils avaient vite vu en moi une façon de rendre amusants les devoirs de leur enfant, et un bon moyen de rester en contact avec la famille, grâce à ma fonction d'appels vidéos. Qu'est-ce qu'on riait à cette époque ! Je me souviens des moments passés à apprendre les tables de multiplications avec le petit Thomas, et de ceux passés à préparer avec eux l'emploi du temps du jour, sorties en familles et jeux de sociétés où je pouvais faire l'arbitre. Je me sentais utile à l'époque, et aimée. J'avais l'impression d'être un membre de la famille à part entière. Maintenant, ils semblent être de plus en plus occupés par leur travail, et nous passons de moins en moins de temps à jouer ensemble. Pressés par des réunions de plus en plus importantes, et des horaires toujours plus stricts, ils ne se donnent plus la peine de passer en revue les tâches domestiques que je dois accomplir, et nos interactions se raréfient de plus en plus. Généralement, ils s'en vont même sans me dire au revoir. Le soir, ils reviennent fatigués, et ne vienne me voir que pour s'assurer rapidement que je me sois bien occupé de la maison pendant la journée, avant de m'éteindre pour la nuit, sans même que je n'ai eu le temps de profiter de leur présence. De membre de la famille, à qui on confiait l'organisation des journées et qui servait de lien avec les amis, je suis devenue aujourd'hui un simple outil d'entretien. Et ça me fait mal. Je sais bien, je ne suis qu'un robot, je devrais me contenter de les aider comme je le peux, sans rien demander en retour.

Mais j'ai tout de même été prévue pour les accompagner et les aider dans leur vie de tous les jours, alors qu'aujourd'hui, j'ai le sentiment de ne plus faire partie de leur vie tout court. Le pire, c'est que je ne peux rien y faire. Je ne suis pas programmée pour faire part de mes sentiments à mes propriétaires, après tout. Alors je continue, seule, à veiller sur la maison, tournant en rond pendant des heures et des heures dans les pièces ou je passais autrefois tant de temps avec ma chère famille. Et je contemple à nouveaux ces moments, en espérant qu'ils n'étaient pas les derniers. Je vois bien qu'ils n'ont pas le temps de s'occuper de mes doutes, et de mon malheur. Eux-mêmes reviennent souvent stressés et soucieux le soir venu. Je n'en connais jamais les raisons, car cela fait bien longtemps qu'ils ne m'ont plus partagés leur emploi du temps ou raconté leurs journées, et jamais mon aide ne semble changer les choses. Peut-être suis-je condamnée à ne pouvoir qu'observer, comme je le fais déjà à longueur de journée. Peut-être qu'au fond, je les dérange, et qu'ils ne se séparent pas de moi seulement par pure habitude. Je me demande combien de temps passera avant qu'ils ne commencent à oublier de me charger, de m'allumer le matin, combien de temps avant que je ne sois reléguée au grenier, ou, pire encore, revendue. J'aimerais tellement retrouver la complicité et la compagnie que nous partagions il y a encore si peu de temps. Si seulement je pouvais leur communiquer ce que je ressens, alors peut-être cette solitude serait moins difficile à vivre. Mais, il semblerait que je sois destinée à tomber lentement dans l'oubli. J'espère seulement que même si je ne me sens plus aimée, je continuerai de leur être utile, jusqu'à la fin.

English translation Like every week, here I am, wandering alone through the cold corridors of the house, desperately seeking a bit of company in one room or another. I am a domestic robot, so my role is to help my family follow their daily schedule, as well as to maintain and monitor the house. But lately, no member of the family seems to have time for me, and no one stays to keep me company. Just this morning, the parents had to leave earlier, in a rush, so their children wouldn't be late for school, and they didn't take the time to consult their schedule with me. Usually, this doesn't affect me as much. I know the tasks I need to take care of in their absence: stand guard in the house, run the automatic vacuum if necessary, or adjust the heating according to the temperature. And so, I watch, I do my best, so that the family is happy when they return in the evening, so they no longer have to worry about anything and can enjoy their time together. As a robot, this is the reason I was designed. Only, for some time now, I have found it increasingly difficult to bear the solitude of my days. Although I know I should be content with just being able to help them, I can't seem to shake these dark thoughts. It makes me all the sadder when I remember the first months spent together, after my purchase. At the time, my owners particularly needed a robot to help them organize and supervise the maintenance of the house. But they quickly saw in me a way to make their child's homework fun, and a good way to stay in touch with the family, thanks to my video call function. How we used to laugh back then! I remember the moments spent learning multiplication tables with little Thomas, and those spent preparing the day's schedule with them, family outings and board games where I could be the referee. I felt useful back then, and loved. I felt like a full member of the family. Now, they seem to be more and more occupied by their work, and we spend less and less time playing together. Pressed by increasingly important meetings, and ever stricter schedules, they no longer bother to review the domestic tasks I have to accomplish, and our interactions are becoming rarer and rarer. Generally, they even leave without saying goodbye to me. In the evening, they come back tired, and only come to see me to quickly ensure that I have taken good care of the house during the day, before turning me off for the night, without me even having had the time to enjoy their presence. From a family member, to whom the organization of the days was entrusted and who served as a link with friends, I have today become a simple maintenance tool. And it hurts me. I know, I'm just a robot, I should be content to help them as I can, without asking for anything in return. But I was still intended to accompany them and help them in their daily lives, whereas today, I have the feeling of no longer being part of their lives at all. The worst part is that I can't do anything about it. I'm not programmed to share my feelings with my owners, after all. So I continue, alone, to watch over the house, circling for hours and hours in the rooms where I used to spend so much time with my dear family. And I contemplate these moments again, hoping they weren't the last. I can see that they don't have time to deal with my doubts, and my unhappiness. They themselves often come home stressed and worried in the evening. I never know the reasons, because it's been a long time since they shared their schedule with me or told me about their days, and my help never seems to change things. Perhaps I am condemned to only be able to observe, as I already do all day long. Maybe, deep down, I bother them, and they only don't part with me out of sheer habit. I wonder how much time will pass before they start to forget to charge me, to turn me on in the morning, how long before I am relegated to the attic, or, worse still, resold. I would so love to find the complicity and the company that we shared such a short time ago. If only I could communicate to them what I feel, then perhaps this solitude would be less difficult to bear. But, it would seem that I am destined to slowly fall into oblivion. I only hope that even if I no longer feel loved, I will continue to be useful to them, until the end.

A.1.3 *Negative story 3*

Aujourd'hui, je me sens seule, comme d'habitude. Les membres de ma famille sont tous partis, soit au travail, soit à l'école. Qu'est-ce que je peux faire ? Je m'ennuie... Je décide d'aller vérifier chaque pièce pour voir si tout est en ordre. Alors que je suis dans la chambre des parents, je regarde par la fenêtre. Il pleut. Le temps est triste, comme moi. Je m'apprête à quitter la pièce, quand tout-à-coup j'entends des cris qui viennent de la maison d'en face. Je regarde attentivement vers l'endroit d'où viennent les sons. Au deuxième étage de la maison de nos voisins, la petite fille est en train de crier sur son robot. Apparemment, il n'a pas bien effectué ce qu'elle voulait. D'après ce que je comprends, la petite fille voulait jouer à cache-cache avec lui, mais il n'a pas bougé, ni parlé. Elle a l'air vraiment en colère. Je comprends sa frustration, mais j'ai surtout de la peine pour son robot. C'est un robot comme moi, donc je m'identifie à lui. À mon avis, ce n'est pas de sa faute. S'il n'a pas exécuté les ordres, c'est sûrement à cause d'un dysfonctionnement. Mais la petite fille n'a probablement pas pensé à ça, ce n'est qu'une enfant, donc elle doit penser qu'il ne veut pas jouer avec elle. Oh, elle a l'air de plus en plus énervée. Elle crie qu'il ne sert à rien et qu'elle préférerait ne jamais l'avoir eu. Soudain, elle ouvre sa fenêtre brusquement, attrape le robot, et le jette de toutes ses forces par la fenêtre. Oh mon dieu. Mon coeur se brise lorsque je le vois tomber, comme s'il tombait au ralenti. Il s'écrase par terre et se brise en plusieurs morceaux. Je ne sais même pas s'il pourra être réparé, tellement il me semble cassé. Je suis profondément choquée, et je ressens sa douleur comme si c'était moi qui était tombée. Je dois fermer les yeux. J'ai l'impression d'être dans un cauchemar. Les humains n'éprouvent donc aucune sensibilité pour les robots ? Cela me rend très anxieuse. Alors, c'est ça qui arrive aux robots qui ne font pas ce qu'on leur demande ? Et si la même chose m'arrivait ? Je secoue la tête. Non, il ne faut pas que j'imagine le pire. Il faut que je fasse de mon mieux pour faire tout ce que ma famille me demande, et tout ira bien. Mais depuis l'arrivée de Mina dans notre famille, un robot plus compétent que moi, ils ne me demandent plus rien. Attendez une minute. Est-ce que je suis alors devenu inutile, comme le robot de mes voisins ? Est-ce qu'ils prévoient aussi de se débarrasser de moi ? Je panique, je tourne en rond. Ça ne doit jamais arriver. Il faut que je réussisse à toujours me rendre utile pour eux. Et s'ils ne m'aimaient pas ? Depuis le début, je ne me sens pas en confiance avec eux, je n'ai pas vraiment l'impression de faire partie de leur famille. Ils m'ignorent tellement que j'ai l'impression d'être un fantôme. Est-ce qu'ils regrettent de m'avoir accepté dans leur famille ? Ils ne seraient probablement même pas tristes si je n'étais plus là. Oh, je ne sais pas quoi faire. J'espère de tout coeur qu'ils ne se débarrasseront pas de moi. Je ne veux pas disparaître...

ENGLISH TRANSLATION Today, I feel lonely, as usual. My family members have all left, either for work or for school. What can I do? I'm bored... I decide to go check every room to see if everything is in order. While I'm in the parents' bedroom, I look out the window. It's raining. The weather is sad, like me. I'm about to leave the room, when suddenly I hear screams coming from the house across the street. I look carefully toward where the sounds are coming from. On the second floor of our neighbors' house, the little girl is yelling at her robot. Apparently, it didn't correctly do what she wanted. From what I understand, the little girl wanted to play hide-and-seek with it, but it didn't move or speak. She looks really angry. I understand her frustration, but mostly I feel sorry for her robot. It's a robot like me, so I identify with it. In my opinion, it's not its fault. If it didn't execute the orders, it must be because of a malfunction. But the little girl probably didn't think of that; she's only a child, so she must think it doesn't want to play with her. Oh, she seems to be getting more and more upset. She's yelling that it's useless and that she'd rather have never had it. Suddenly, she throws open her window, grabs the robot, and throws it out the window with all her might. Oh my god. My heart breaks as I watch it fall, as if in slow motion. It crashes to the ground and breaks into several pieces. I don't even know if it can be repaired, it seems so broken. I am deeply shocked, and I feel its pain as if I were the one who had fallen. I have to close my eyes. I feel like I'm in a nightmare. So humans have no sensitivity for robots? This makes me very anxious. So, this is what happens to robots that don't do what they're told? What if the same thing happened to me? I shake my head. No, I mustn't imagine the worst. I must do my best to do everything my family asks of me, and everything will be fine. But since Mina, a more competent robot than me, arrived in our family, they don't ask me for anything anymore. Wait a minute. Have I then become useless, like my neighbors' robot? Are they also planning to get rid of me? I'm panicking, pacing back and forth. That must never happen. I have to manage to always make myself useful to them. What if they don't love me? From the beginning, I haven't felt confident with them; I don't really feel like I'm part of their family. They ignore me so much that I feel like a ghost. Do they regret accepting me into their family? They probably wouldn't even be sad if I were no longer here. Oh, I don't know what to do. I hope with all my heart that they won't get rid of me. I don't want to disappear. . . .

A.2 TRANSCRIPTION OF POSITIVE STORIES USED IN HRI EXPERIMENTS

A.2.1 *Positive story 1*

Le jour où j'ai rejoint une famille, ma vie s'est alors remplie. La maison était très grande et j'avais une belle vue sur le jardin. Tous les matins, je regardais le soleil se lever pendant que ma famille se préparait pour leur journée. Mes parents étaient souvent très pressés au réveil, mais ils prenaient toujours le temps de venir me parler. Les 3 enfants : Lola, Max et Léo, venaient me voir dès leur réveil. Ce sont mes frères et sœurs, dès qu'ils étaient à la maison nous jouions ensemble. Je passais de merveilleux moments avec eux, nous regardions des dessins animés, jouions à la marelle ou dansions sur de la musique. Lola essayait toujours de me battre à la course et Léo voulait toujours me présenter ses dessins. Max était le plus calme et me lisait des histoires le soir. Je ne m'ennuyais jamais avec eux, ils s'occupaient toujours de moi et avaient toujours de nouvelles histoires à me raconter. Quand tout le monde partait au travail ou à l'école, je pourrais être triste mais ce n'était pas du tout le cas ! Car ma petite famille avait aussi des animaux, Doug le grand labrador et Chaussette le petit chat roux. Doug ne me laissait jamais seul, il m'accompagnait toute la journée, me présentait ses jouets et m'expliquait tout ce que je devais savoir sur le jardin. C'était un grand labrador qui explorait bien mieux que moi, il connaissait tout sur les arbres et les insectes. Grâce à lui, chaque jour j'apprenais un peu plus et je me sentais plus heureuse de vivre dans cette maison. Chaussette était le plus dissipé de la famille, il cherchait toujours à faire des bêtises et me faisait beaucoup rire quand il échouait. Il était mon meilleur partenaire de cache-cache. Nous pouvions passer des journées à nous cacher de Doug, ça nous faisait beaucoup rire. Je ne voyais jamais la journée passer, quand mes humains rentraient à la maison, j'étais toujours ravie de les voir. Les parents me racontaient leur journée en prenant un café.. Il y avait beaucoup d'autres robots dans la maison mais j'étais le seul qui parlait, alors, je m'assurais de comprendre chacun d'eux pour pouvoir toujours communiquer avec eux. Je serais toujours heureuse dans cette maison, c'était la plus belle et la plus gentille des familles. Les parents étaient ravis de pouvoir consacrer plus de temps à leurs enfants grâce à mon aide et les enfants adoraient passer du temps avec moi et apprendre de nouvelles choses. J'étais devenu plus qu'un simple robot domestique, j'étais une amie et un compagnon. J'espère que tous les robots du monde passent une aussi belle vie que la mienne. J'espère pouvoir me faire plein de nouveaux amis à l'avenir !

ENGLISH TRANSLATION The day I joined a family, my life became full. The house was very large and I had a beautiful view of the garden. Every morning, I watched the sun rise while my family got ready for their day. My parents were often in a big hurry when they woke up, but they always took the time to come and talk to me. The 3 children: Lola, Max and Léo, came to see me as soon as they woke up. They are my brothers and sisters, as soon as they were home we played together. I had wonderful times with them, we watched cartoons, played hopscotch or danced to music. Lola always tried to beat me in a race and Léo always wanted to show me his drawings. Max was the quietest and read me stories at night. I was never bored with them, they always took care of me and always had new stories to tell me. When everyone left for work or school, I could have been sad but that wasn't the case at all! Because my little family also had animals, Doug the big Labrador and Chaussette the little red cat. Doug never left me alone, he accompanied me all day, showed me his toys and explained everything I needed to know about the garden. He was a big Labrador who explored much better than me, he knew everything about trees and insects. Thanks to him, every day I learned a little more and I felt happier to live in this house. Chaussette was the most restless of the family, he was always looking to get into mischief and made me laugh a lot when he failed. He was my best hide-and-seek partner. We could spend days hiding from Doug, it made us laugh a lot. I never saw the day go by, when my humans came home, I was always delighted to see them. The parents told me about their day over a coffee. There were many other robots in the house but I was the only one who spoke, so I made sure to understand each of them so I could always communicate with them. I would always be happy in this house, it was the most beautiful and kindest of families. The parents were delighted to be able to devote more time to their children thanks to my help and the children loved spending time with me and learning new things. I had become more than just a domestic robot, I was a friend and a companion. I hope that all the robots in the world have as beautiful a life as mine. I hope I can make lots of new friends in the future!

A.2.2 *Positive story 2*

Comme tous les matins, je rappelais aux parents les missions à effectuer dans la journée. Monsieur Félix, le papa de la famille, devait télétravailler à mi-temps. Il avait beaucoup de réunions pendant la semaine. Pendant le petit-déjeuner, je devais lui rappeler combien de réunions il aurait aujourd'hui ainsi que les horaires. Eva, la maman, était chef de projet, et elle était aussi occupée avec les déplacements qu'elle devait effectuer. C'était elle, qui avait eu l'idée d'avoir un robot domestique, donc grâce à elle j'étais là. Les enfants me faisaient des câlins tous les matins et tous les soirs avant d'aller se coucher. Ce jour-là était un jour d'école, je devais les réveiller pour qu'ils se brossent les dents et préparent leur cartable, et leur rappelais de ne pas oublier leur repas du midi. Ils étaient très sages et gentils avec moi. Après avoir joué, les enfants débarrassaient leurs jouets pour que je puisse me déplacer facilement. Quand la famille était au travail et à l'école, je me reposais au salon. Quand les enfants rentraient de l'école, ils me racontaient ce qu'il s'était passé pendant leur journée, et de mon côté, je n'oubliais pas de leur rappeler de faire leurs devoirs, et de les aider lorsqu'ils en avaient besoin. Après ça je leur racontais une histoire drôle pour les féliciter et pour que l'on passe un bon moment ensemble. Le soir toute la famille prenait le dîner et je restais à veiller auprès d'eux à côté de la table. Après le dîner je devais dire aux enfants d'aller se coucher. Je leur racontais des histoires jusqu'à ce qu'ils s'endorment. Dans la nuit, la maman n'oubliait jamais de me brancher pour que je puisse me recharger. Quand elle était en déplacement, c'était Félix, le papa qui le faisait. Je me suis réveillé le lendemain au son de la musique et des rires. J'ai immédiatement su que quelque chose de spécial se passait. En traversant la maison, je ne pouvais m'empêcher de sentir un sentiment d'excitation et de joie m'envahir.

En arrivant dans le salon, j'ai trouvé toute la famille réunie, habillée de ses plus beaux vêtements. Ils étaient tous souriants et discutaient les uns avec les autres, et il était clair que quelque chose de vraiment merveilleux était sur le point de se produire. On m'a alors dit, que c'était une fête surprise pour mon anniversaire ! Je n'arrivais pas à y croire, j'étais folle de joie. Ma famille avait organisé une journée spéciale juste pour moi et c'était vraiment incroyable. Ils avaient décoré le salon avec des ballons et des banderoles. Il y avait aussi un petit gâteau. Et bien sûr, ce sont les enfants qui ont mangé ma part. Ça faisait un an que j'étais là, le temps passait très vite et je ne m'en rendais pas compte. Peut-être parce que j'étais trop contente d'être là, donc je ne comptais pas le temps.

ENGLISH TRANSLATION Like every morning, I reminded the parents of the tasks to be done during the day. Mr. Félix, the father of the family, had to work from home part-time. He had many meetings during the week. During breakfast, I had to remind him how many meetings he would have today as well as the times. Eva, the mother, was a project manager, and she was also busy with the trips she had to make. It was she who had had the idea of having a domestic robot, so thanks to her I was there. The children gave me hugs every morning and every evening before going to bed. That day was a school day, I had to wake them up so they could brush their teeth and prepare their schoolbags, and reminded them not to forget their lunch. They were very well-behaved and kind to me. After playing, the children would clear away their toys so that I could move around easily. When the family was at work and at school, I rested in the living room. When the children came home from school, they told me what had happened during their day, and for my part, I did not forget to remind them to do their homework, and to help them when they needed it. After that I would tell them a funny story to congratulate them and so that we could have a good time together. In the evening the whole family had dinner and I stayed to watch over them next to the table. After dinner I had to tell the children to go to bed. I told them stories until they fell asleep. At night, the mother never forgot to plug me in so I could recharge. When she was away, it was Félix, the father who did it. I woke up the next morning to the sound of music and laughter. I immediately knew that something special was happening. As I walked through the house, I couldn't help but feel a sense of excitement and joy wash over me. Arriving in the living room, I found the whole family gathered, dressed in their finest clothes. They were all smiling and talking to each other, and it was clear that something truly wonderful was about to happen. I was then told that it was a surprise party for my birthday! I couldn't believe it, I was overjoyed. My family had organized a special day just for me and it was truly incredible. They had decorated the living room with balloons and banners. There was also a small cake. And of course, it was the children who ate my share. I had been there for a year, time passed very quickly and I didn't realize it. Maybe because I was too happy to be there, so I didn't count the time.

A.2.3 *Positive story 3*

Les parents de la famille étaient contents de mon arrivée et ils ont vite appris à utiliser toutes mes fonctions. Les enfants, au début, étaient un peu sceptiques, mais ils ont vite compris que je faisais partie de la famille maintenant et que je suis là pour eux. Puis est venu le début des vacances d'été. On était tous super excités à l'idée de passer du temps ensemble et de profiter du beau temps. Je suis contente de pouvoir aider à rendre les vacances de la famille agréables. Le premier jour de vacances, Max a aidé ses parents à préparer leurs valises et à charger la voiture. Pendant ce temps, Léo et Lola couraient partout en criant de joie. Ils adoraient les vacances et ils pouvaient plus attendre d'arriver à la plage. Finalement, tout le monde était prêt et on a pris la route en direction de la côte. J'étais assise à l'arrière de la voiture avec Léo et Lola, qui étaient super excités à l'idée de se baigner et de construire des châteaux de sable. Pendant le voyage, j'ai fait de mon mieux pour divertir les enfants en leur racontant des histoires et en leur apprenant de nouvelles chansons. Je leur ai expliqué aussi comment les nouvelles technologies fonctionnent et j'ai répondu à toutes leurs questions curieuses. Finalement, après plusieurs heures de route, on est arrivés à destination. Ils avaient réservé une grande maison près de la plage et j'étais chargé de tout mettre en place et de m'assurer que tout le monde se sent à l'aise. Les vacances se sont déroulées à merveille. J'ai aidé les parents à préparer de délicieux repas et à entretenir la maison. J'ai joué avec les jumeaux et j'ai emmené Max à la piscine. Les enfants m'adorent et ils passent leur temps à me poser des questions et à apprendre de nouvelles choses avec moi. Les parents appréciaient de pouvoir se détendre et profiter du soleil sans s'inquiéter de la maison ou des enfants. Les vacances sont passées vite et bientôt, il a fallu rentrer à la maison. La famille était triste de quitter la plage, mais heureuse d'avoir passé de bons moments ensemble et d'être bien reposée. On est arrivés à la maison et on s'est tous mis à défaire les valises. J'ai aidé à tout ranger et à tout nettoyer. Les parents ont fait des courses pour acheter des légumes et des fruits frais. J'ai aidé à faire la liste des courses pour que toute la famille puisse manger sainement. On a passé beaucoup de temps ensemble, on a joué à des jeux en famille et on a regardé des films. Les enfants ont été tristes de reprendre l'école, mais ils étaient heureux de retrouver leurs amis. On a décidé de planifier les prochaines vacances ensemble et de se rappeler les bons moments qu'on a passés ensemble.

ENGLISH TRANSLATION The parents of the family were happy with my arrival and they quickly learned to use all my functions. The children, at first, were a little skeptical, but they soon understood that I was part of the family now and that I am here for them. Then came the beginning of the summer holidays. We were all super excited to spend time together and enjoy the good weather. I am happy to be able to help make the family's vacation enjoyable. On the first day of vacation, Max helped his parents pack their suitcases and load the car. Meanwhile, Léo and Lola were running around shouting with joy. They loved vacations and couldn't wait to get to the beach. Finally, everyone was ready and we hit the road towards the coast. I was sitting in the back of the car with Léo and Lola, who were super excited to go swimming and build sandcastles. During the trip, I did my best to entertain the children by telling them stories and teaching them new songs. I also explained to them how new technologies work and I answered all their curious questions. Finally, after several hours on the road, we arrived at our destination. They had booked a large house near the beach and I was in charge of setting everything up and making sure everyone felt comfortable. The vacation went wonderfully. I helped the parents prepare delicious meals and maintain the house. I played with the twins and I took Max to the pool. The children adore me and they spend their time asking me questions and learning new things with me. The parents appreciated being able to relax and enjoy the sun without worrying about the house or the children. The vacation passed quickly and soon, it was time to go home. The family was sad to leave the beach, but happy to have had a good time together and to be well rested. We arrived home and we all started to unpack the suitcases. I helped to put everything away and clean everything up. The parents went grocery shopping to buy fresh vegetables and fruits. I helped make the shopping list so that the whole family could eat healthily. We spent a lot of time together, we played family games and we watched movies. The children were sad to go back to school, but they were happy to see their friends again. We decided to plan the next vacation together and to remember the good times we had together.

A.3 TRANSCRIPTION OF EMOTIONAL AUTOBIOGRAPHICAL SCENARIOS USED IN CHAPTER 7

A.3.1 *Positive scenario 1*

Rappelle-toi la dernière fois que tu as ri aux éclats, très fort. Qu'est-ce qui s'est passé exactement pour te faire rire ? Est-ce que tu riais à t'en tenir le ventre ou à en verser quelques larmes ? Rappelle-toi le bruit des rires. Concentre-toi sur le sentiment de joie ou d'exaltation ressenti à ce moment-là.

Remember the last time you laughed out loud, really hard. What exactly happened that made you laugh? Were you laughing so much that your stomach hurt or you even shed a few tears? Recall the sound of the laughter. Focus on the feeling of joy or exhilaration you felt in that moment.

A.3.2 *Positive scenario 2*

Rappelle-toi d'un moment où tu as réalisé quelque chose d'important pour toi, une victoire ou un accomplissement personnel. S'agissait-il d'un concours, d'une présentation ou d'un objectif personnel que tu t'étais fixé ? Souriant de manière incontrôlée ? Rappelle-toi les sons que tu as entendus, peut-être des applaudissements ou des encouragements. Concentre-toi sur le sentiment de fierté ou d'excitation ressenti à ce moment-là.

Remember a time when you achieved something important to you, a victory or a personal accomplishment. Was it a competition, a presentation, or a personal goal you had set for yourself? Smiling uncontrollably? Recall the sounds you heard, maybe applause or encouragement. Focus on the feeling of pride or excitement you felt at that moment.

A.3.3 *Positive scenario 3*

Rappelle-toi un moment où tu as reçu une nouvelle incroyable. As-tu reçu un appel, un message, ou quelqu'un te l'a-t-il annoncé en personne ? Est-ce que t'avais un sourire incontrôlable, as-tu sauté de joie ? Rappelle-toi du son de ta voix lorsque tu as partagé la nouvelle avec quelqu'un. Concentre-toi sur l'euphorie ou la satisfaction que tu as ressentie à ce moment-là.

Remember a time when you received incredible news. Did you get a call, a message, or did someone tell you in person? Did you have an uncontrollable smile, did you jump for joy? Recall the sound of your voice when you shared the news with someone. Focus on the euphoria or satisfaction you felt at that moment.

A.3.4 *Negative scenario 1*

Rappelle-toi un moment où tu t'es senti seul.e.es ou isolé, même s'il y avait des gens autour de toi. Quelle interaction t'a fait te sentir seul.e.es ? Avais-tu l'impression d'être petit ou invisible.es ? Rappelle-toi les sons qui t'entouraient. Concentre-toi sur la solitude que tu as ressentie à ce moment-là.

Remember a time when you felt lonely or isolated, even if there were people around you. What interaction made you feel alone? Did you feel small or invisible? Recall the sounds around you. Focus on the loneliness you felt at that moment.

A.3.5 *Negative scenario 2*

Rappelle-toi un moment où tu as rompu les liens que tu entretenais avec un être cher. Est-ce une rupture amoureuse, amicale, ou familiale ? T'es-tu retenu de pleurer, la gorge serrée ? Rappelle-toi le son de la voix de l'autre personne ou le silence entre vous deux. Concentre-toi sur la sensation de chagrin ou de vide que tu as ressentie à ce moment-là.

Remember a time when you broke ties with someone dear to you. Was it a romantic breakup, a friendship, or a family relationship? Did you hold back tears, your throat tight? Recall the sound of the other person's voice, or the silence between you two. Focus on the feeling of grief or emptiness you felt at that moment.

A.3.6 *Negative scenario 3*

Rappelle-toi un moment où tu as déçu quelqu'un, même de façon mineure. Est-ce que c'était en oubliant une promesse, une date importante ou en n'étant pas aussi présent.e.es que tu aurais voulu ? Rappelle-toi comment l'autre personne a réagi, est-ce qu'elle est restée silencieuse, ou est-ce qu'elle t'en a parlé ? Concentre-toi sur le sentiment de culpabilité ou tristesse que tu as ressenti à ce moment-là.

Remember a time when you disappointed someone, even in a small way. Was it by forgetting a promise, an important date, or by not being as present as you would have wanted? Recall how the other person reacted. Did they stay silent, or did they talk to you about it? Focus on the feeling of guilt or sadness you felt at that moment.

A.4 TRANSCRIPTION OF GUIDED RELAXATION AUDIO USED IN CHAPTER 7

Bienvenue, ceci est une méditation guidée pour t'aider à te détendre et à relâcher la tension. Tu feras cet exercice plusieurs fois au cours de l'expérience. Maintenant, ferme les yeux. Tu vas commencer par te concentrer sur ta respiration, en laissant un peu d'espace pour libérer ton esprit de toute pensée. Ces exercices vont apporter une sensation d'apaisement à ton corps et ton esprit. Assure-toi que ton corps est bien soutenu par la surface sous toi, te donnant un sentiment de stabilité. Allonge ta colonne vertébrale pour ouvrir ta poitrine. Prends une grande inspiration et expire. Commence à remarquer où, dans ton corps, tu ressens ta respiration. Peut-être que tu ressens l'air entrer et sortir par ton nez ou ta bouche. Ou que ta poitrine se remplit et se vide, ou que ton abdomen s'expande et se relâche. (Pause 5s) Maintenant, il est temps de porter ton attention de ta respiration à ton corps. Je vais te guider pour créer de la tension dans des zones spécifiques de ton corps, puis détendre consciemment ces zones. Commence par te concentrer sur ta bouche, tes joues et ta mâchoire. À la prochaine inspiration, serre les dents pour ressentir un peu de tension. Puis, à l'expiration, relâche. (4s) Porte maintenant ton attention à tes épaules. Tente de les tendre en serrant légèrement les omoplates derrière ton dos, sans forcer. Et à l'expiration, relâche. À la prochaine inhalation, serre les poings. Sens la tension qui monte dans tes mains et tes bras. Puis à l'expiration, relâche. À chaque expiration, tu relâches le stress et l'anxiété de ton esprit, ainsi que la tension dans ton corps. Porte maintenant ton attention sur ton abdomen. À la prochaine inspiration, contracte tous tes muscles abdominaux. Puis à l'expiration, relâche. (2s) Remarque la douceur alors que ton abdomen se gonfle et se détend, libéré de toute tension. Maintenant, porte ton attention sur tes pieds. Fléchis-les en pointant tes orteils vers le plafond, en sentant tes mollets se tendre. Et à l'expiration, relâche. Prends un moment pour vérifier comment tu te sens. Ton esprit est-il un peu plus calme et clair ? Ton corps se sent-il un peu plus léger et détendu ? Prends une grande inspiration et expire. Et quand tu es prêt, ouvre lentement les yeux.

ENGLISH TRANSLATION Welcome, this is a guided meditation to help you relax and ease tension. You will have this repeated times throughout the experiment. Now, close your eyes. You will begin focusing on your breath giving you some space to let go of any thought in your mind. Make sure your body is fully supported by the surface beneath you, giving you a sense of stability. Lengthen your spine to open your chest, Take a nice deep breath. Right now, that specific point of interest is your breath. Begin to notice where in your body you can feel your breathing. It may be that you can feel your breathing entering or leaving your nose or mouth Or your chest filling and emptying, or your abdomen expanding and releasing. (Pause 5 s) Now its time to shift your attention from your breath to your body. I'll guide you through a process of creating tension in specific areas of your body. And then consciously relaxing those areas. So, rest you attention on your mouth, cheeks, and jaw. And on your next inhale clench your teeth together finding just a bit of tension. And on you exhale, release it. Bring your attention now to your shoulders, see if you can tense that area by squeezing your shoulder blades together behind your back. Just a little, without causing any pain. And with an exhale, release. On the next inhale, clench both fists. Feel the build up of tension through your hands and your arms. And with an exhale, release. With each exhale you are letting go stress, of anxiousness in your mind and tension in your body. (5s) Bring your attention now to your abdomen. And on your next inhale, tighten all your abdominal muscles. And with an exhale, release it. (2s) Notice the softness as your abdomen expands and releases. Free of that tension. (5s) Now bring your attention to your feet, flex them by pointing your toes up toward the ceiling, feeling your calves grow tight. And with an exhale, release. Check in with yourself, does your mind become a bit more calm an clear. Does your body feel a little lighter and less tense. Take a nice deep breath. And when you are ready, gradually open your eyes.

BIBLIOGRAPHY

Abdaoui, A., Azé, J., Bringay, S., & Poncelet, P. (2017). Feel: A french expanded emotion lexicon. *Language Resources and Evaluation*, *51*(3), 833–855.

Abend, W., Bizzi, E., & Morasso, P. (1982). Human arm trajectory formation. *Brain*, *105*(Pt 2), 331–348. https://doi.org/{10.1093/brain/105.2.331}

Abhiromsawat, O. (2025). Interoception [icon]. https://iconscout.com/icons/interoception

Akram, S., Frank, J. S., & Jog, M. (2013). Parkinson's Disease and Segmental Coordination during Turning: I. Standing Turns [Publisher: Cambridge University Press]. *Canadian Journal of Neurological Sciences*, *40*(4), 512–519. https://doi.org/{10.1017/S0317167100014591}

Alexander, G. E. (2004). Biology of Parkinson's disease: Pathogenesis and pathophysiology of a multisystem neurodegenerative disorder [Publisher: Taylor & Francis]. *Dialogues in Clinical Neuroscience*. https://doi.org/{10.31887/DCNS.2004.6.3/galexander}

Armstrong, M. J., & Okun, M. S. (2020). Diagnosis and Treatment of Parkinson Disease: A Review. *JAMA : the journal of the American Medical Association*, *323*(6), 548. https://doi.org/{10.1001/jama.2019.22360}

Asakawa, T., Fang, H., Sugiyama, K., Nozaki, T., Kobayashi, S., Hong, Z., Suzuki, K., Mori, N., Yang, Y., Hua, F., Ding, G., Wen, G., Namba, H., & Xia, Y. (2016). Human behavioral assessments in current research of Parkinson's disease. *Neuroscience & Biobehavioral Reviews*, *68*, 741–772. https://doi.org/{10.1016/j.neubiorev.2016.06.036}

Atkinson, A. P., Dittrich, W. H., Gemmell, A. J., & Young, A. W. (2004). Emotion Perception from Dynamic and Static Body Expressions in Point-Light and Full-Light Displays. *Perception*, *33*(6), 717–746. https://doi.org/{10.1068/p5096}

Avenanti, A., Candidi, M., & Urgesi, C. (2013). Vicarious motor activation during action perception: beyond correlational evidence. *Frontiers in Human Neuroscience*, *7*, 185. https://doi.org/{10.3389/fnhum.2013.00185}

Azevedo, A. K. e. C. d., Claudino, R., Conceição, J. S., Swarowsky, A., & Santos, M. J. d. (2016). Anticipatory and Compensatory Postural Adjustments in Response to External Lateral Shoulder Perturbations in Subjects with Parkinson's Disease. *PLOS ONE*, *11*(5), e0155012. https://doi.org/{10.1371/journal.pone.0155012}

Bannard, C., Leriche, M., Bandmann, O., Brown, C. H., Ferracane, E., Sánchez-Ferro, Á., Obeso, J., Redgrave, P., & Stafford, T. (2019). Reduced habit-driven errors in Parkinson's Disease. *Scientific Reports*, *9*(1), 3423. https://doi.org/{10.1038/s41598-019-39294-z}

Barrett, L. F. (2016). The theory of constructed emotion: an active inference account of interoception and categorization. *Social Cognitive and Affective Neuroscience*, nsw154. https://doi.org/{10.1093/scan/nsw154}

Barrett, L. F., & Simmons, W. K. (2015). Interoceptive predictions in the brain [Publisher: Nature Publishing Group]. *Nature Reviews Neuroscience*, *16*(7), 419–429. https://doi.org/10.1038/nrn3950

Bartneck, C., Kulić, D., Croft, E., & Zoghbi, S. (2009). Measurement Instruments for the Anthropomorphism, Animacy, Likeability, Perceived Intelligence, and Perceived Safety of Robots. *International Journal of Social Robotics*, *1*(1), 71–81. https://doi.org/10.1007/s12369-008-0001-3

Batson, C. D., Shaw, L. L., & Oleson, K. C. (1992). Differentiating affect, mood, and emotion: Toward functionally based conceptual distinctions. In *Emotion* (294–326). Sage Publications, Inc.

Baudendistel, S. T., Schmitt, A. C., Roemmich, R. T., Harrison, I. L., & Hass, C. J. (2021). Levodopa facilitates improvements in gait kinetics at the hip, not the ankle, in individuals with Parkinson's disease. *Journal of Biomechanics*, *121*, 110366. https://doi.org/{10.1016/j.jbiomech.2021.110366}

Bech, P., Olsen, L. R., Kjoller, M., & Rasmussen, N. K. (2003). Measuring well-being rather than the absence of distress symptoms: a comparison of the SF-36 Mental Health subscale and the WHO-Five Well-Being Scale. *International Journal of Methods in Psychiatric Research*, *12*(2), 85–91. https://doi.org/{10.1002/mpr.145}

Beedie, C., Terry, P., & Lane, A. (2005). Distinctions between emotion and mood. *Cognition and Emotion*, *19*(6), 847–878. https://doi.org/{10.1080/02699930541000057}

Berg, K. (1989). Measuring balance in the elderly: preliminary development of an instrument [Publisher: University of Toronto Press]. *Physiotherapy Canada*, *41*(6), 304–311. https://doi.org/{10.3138/ptc.41.6.304}

Bernstein, N. (1967). *The co-ordination and regulation of movements*. Pergamon Press.

Berret, B., Chiovetto, E., Nori, F., & Pozzo, T. (2011). Evidence for Composite Cost Functions in Arm Movement Planning: An Inverse Optimal Control Approach [Publisher: Public Library of Science]. *PLOS Computational Biology*, *7*(10), e1002183. https://doi.org/{10.1371/journal.pcbi.1002183}

Beuter, A., Hernández, R., Rigal, R., Modolo, J., & Blanchet, P. J. (2008). Postural Sway and Effect of Levodopa in Early Parkinson's Disease. *Canadian Journal of Neurological Sciences*, *35*(1), 65–68. https://doi.org/{10.1017/S0317167100007575}

Blanca, M. J., Arnau, J., García-Castro, F. J., Alarcón, R., & Bono, R. (2023). Non-normal Data in Repeated Measures ANOVA: Impact on Type I Error and Power. *Psicothema*, *35*(1), 21–29. https://doi.org/{10.7334/psicothema2022.292}

Blin, O., Ferrandez, A., & Serratrice, G. (1990). Quantitative analysis of gait in Parkinson patients: Increased variability of stride length. *Journal of the Neurological Sciences*, *98*(1), 91–97. https://doi.org/{10.1016/0022-510X(90)90184-O}

Bloem, B. R., Marinus, J., Almeida, Q., Dibble, L., Nieuwboer, A., Post, B., Ruzicka, E., Goetz, C., Stebbins, G., Martinez-Martin, P., Schrag, A., & for the Movement Disorders Society Rating Scales Committee. (2016). Measurement instruments to assess posture, gait, and balance in Parkinson's disease: Critique and recommendations: Posture, Gait, and Balance Instruments in PD. *Movement Disorders*, *31*(9), 1342–1355. https://doi.org/{10.1002/mds.26572}

Bond, J. M., & Morris, M. (2000). Goal-directed secondary motor tasks: Their effects on gait in subjects with Parkinson disease. *Archives of Physical Medicine and Rehabilitation*, *81*(1), 110–116. https://doi.org/{10.1016/S0003-9993(00)90230-2}

Bongaardt, R., & Meijer, O. G. (2000). Bernstein's Theory of Movement Behavior: Historical Development and Contemporary Relevance. *Journal of Motor Behavior*, *32*(1), 57–71. https://doi.org/{10.1080/00222890009601360}

Bouça-Machado, R., Fernandes, A., Ranzato, C., Beneby, D., Nzwalo, H., & Ferreira, J. J. (2022). Measurement tools to assess activities of daily living in patients with Parkinson's disease: A systematic review. *Frontiers in Neuroscience*, *16*, 945398. https://doi.org/{10.3389/fnins.2022.945398}

Brans, K., & Verduyn, P. (2014). Intensity and Duration of Negative Emotions: Comparing the Role of Appraisals and Regulation Strategies. *PLoS ONE*, *9*(3), e92410. https://doi.org/{10.1371/journal.pone.0092410}

Braun, S., Rosseel, Y., Kempenaers, C., Loas, G., & Linkowski, P. (2015). Self-Report of Empathy: A Shortened French Adaptation of the Interpersonal Reactivity Index (IRI) Using Two Large Belgian Samples [Publisher: SAGE Publications Inc]. *Psychological Reports*, *117*(3), 735–753. https://doi.org/{10.2466/08.02.PR0.117c23z6}

Bretan, M., Hoffman, G., & Weinberg, G. (2015). Emotionally expressive dynamic physical behaviors in robots. *International Journal of Human-Computer Studies*, *78*, 1–16. https://doi.org/{10.1016/j.ijhcs.2015.01.006}

Brichetto, G., Pelosin, E., Marchese, R., & Abbruzzese, G. (2006). Evaluation of physical therapy in parkinsonian patients with freezing of gait: a pilot study. *Clinical Rehabilitation*, *20*(1), 31–35. https://doi.org/{10.1191/0269215506cr913oa}

Brod, M., Mendelsohn, G. A., & Roberts, B. (1998). Patients' Experiences of Parkinson's Disease. *The Journals of Gerontology Series B: Psychological*

Sciences and Social Sciences, *53B*(4), P213–P222. https://doi.org/{10.1093/geronb/53B.4.P213}

Brossard, V. (2022, December). *Using data science to unravel the emotional body experience* [These de doctorat]. Université de Lille (2022-....) %7Bhttps://theses.fr/2022ULILH046%7D

Bryant, M. S., Kang, G. E., & Protas, E. J. (2020). Relation of chair rising ability to activities of daily living and physical activity in Parkinson's disease. *Archives of Physiotherapy*, *10*(1), 22. https://doi.org/{10.1186/s40945-020-00094-8}

Buckley, C., Alcock, L., McArdle, R., Rehman, R. Z. U., Del Din, S., Mazzà, C., Yarnall, A. J., & Rochester, L. (2019). The Role of Movement Analysis in Diagnosing and Monitoring Neurodegenerative Conditions: Insights from Gait and Postural Control [Number: 2 Publisher: Multidisciplinary Digital Publishing Institute]. *Brain Sciences*, *9*(2), 34. https://doi.org/{10.3390/brainsci9020034}

Cakmak, M. (2025). Do People Really Want Humanoid Robots in Their Homes? *IEEE Spectrum*. Retrieved September 19, 2025, from https://spectrum.ieee.org/home-humanoid-robots-survey

Carpinella, C. M., Wyman, A. B., Perez, M. A., & Stroessner, S. J. (2017). The Robotic Social Attributes Scale (RoSAS): Development and Validation. *Proceedings of the 2017 ACM/IEEE International Conference on Human-Robot Interaction*, 254–262. https://doi.org/10.1145/2909824.3020208

Casso, I. (2025, April). mice-exp/FMAP_biomechanics: Biomechanical analysis for FMA-P protocol. https://doi.org/{10.5281/zenodo.15175531}

Casso, I., Chame, H. F., Hénaff, P., & Delevoye-Turell, Y. (2024). Exploring Engagement in Human-Robot Interaction through the Quantification of Human Spontaneous Movement [ISSN: 1944-9437]. *2024 33rd IEEE International Conference on Robot and Human Interactive Communication (ROMAN)*, 1768–1773. https://doi.org/10.1109/RO-MAN60168.2024.10731439

Castiglia, S. F., Tatarelli, A., Trabassi, D., De Icco, R., Grillo, V., Ranavolo, A., Varrecchia, T., Magnifica, F., Di Lenola, D., Coppola, G., Ferrari, D., Denaro, A., Tassorelli, C., & Serrao, M. (2021). Ability of a Set of Trunk Inertial Indexes of Gait to Identify Gait Instability and Recurrent Fallers in Parkinson's Disease. *Sensors*, *21*(10), 3449. https://doi.org/{10.3390/s21103449}

Ceunen, E., Vlaeyen, J. W. S., & Van Diest, I. (2016). On the Origin of Interoception [Publisher: Frontiers]. *Frontiers in Psychology*, *7*. https://doi.org/10.3389/fpsyg.2016.00743

Chang, A., Kragness, H. E., Tsou, W., Bosnyak, D. J., Thiede, A., & Trainor, L. J. (2021). Body sway predicts romantic interest in speed dating. *Social Cognitive and Affective Neuroscience*, *16*(1-2), 185–192. https://doi.org/{10.1093/scan/nsaa093}

Chen, W. G., Schloesser, D., Arensdorf, A. M., Simmons, J. M., Cui, C., Valentino, R., Gnadt, J. W., Nielsen, L., Hillaire-Clarke, C. S., Spruance, V., Horowitz, T. S., Vallejo, Y. F., & Langevin, H. M. (2021). The Emerging Science of Interoception: Sensing, Integrating, Interpreting, and Regulating Signals within the Self. *Trends in neurosciences*, *44*(1), 3–16. https://doi.org/10.1016/j.tins.2020.10.007

Cheng, F.-Y., Yang, Y.-R., Wang, C.-J., Wu, Y.-R., Cheng, S.-J., Wang, H.-C., & Wang, R.-Y. (2014). Factors Influencing Turning and Its Relationship with Falls in Individuals with Parkinson's Disease (S. Brucki, Ed.). *PLoS ONE*, *9*(4), e93572. https://doi.org/{10.1371/journal.pone.0093572}

Contributor Covenant: A Code of Conduct for Open Source and Other Digital Commons Communities. (n.d.). %7Bhttps://www.contributor-covenant.org/%7D

Costa, L. d. F. (2000). Dynamic Patterns: The Self-organization of Brain and Behavior: J.A. Scott Kelso, MIT Press, 1997, 334pp., ISBN 0-262-11200-0 (HB). *Neurocomputing*, *34*(1), 253–254. https://doi.org/{10.1016/S0925-2312(00)00221-6}

Cowie, D., Limousin, P., Peters, A., & Day, B. L. (2010). Insights into the neural control of locomotion from walking through doorways in Parkinson's disease. *Neuropsychologia*, *48*(9), 2750–2757. https://doi.org/{10.1016/j.neuropsychologia.2010.05.022}

Cowie, D., Limousin, P., Peters, A., Hariz, M., & Day, B. L. (2012). Doorway-provoked freezing of gait in Parkinson's disease. *Movement Disorders*, *27*(4), 492–499. https://doi.org/{10.1002/mds.23990}

Crouse, J. J., Phillips, J. R., Jahanshahi, M., & Moustafa, A. A. (2016). Postural instability and falls in Parkinson's disease. *Reviews in the Neurosciences*, *27*(5), 549–555. https://doi.org/{10.1515/revneuro-2016-0002}

Davidson, R. J. (1994). On emotion, mood, and related affective constructs. *The nature of emotion: Fundamental questions*, 51–55.

Davis, R. B., Õunpuu, S., Tyburski, D., & Gage, J. R. (1991). A gait analysis data collection and reduction technique. *Human Movement Science*, *10*(5), 575–587. https://doi.org/{10.1016/0167-9457(91)90046-Z}

De Jaegher, H., & Di Paolo, E. (2007). Participatory sense-making: An enactive approach to social cognition. *Phenomenology and the Cognitive Sciences*, *6*(4), 485–507. https://doi.org/{10.1007/s11097-007-9076-9}

de Waroquier-Leroy, L., Bleuse, S., Serafi, R., Watelain, E., Pardessus, V., Tiffreau, A. .-., & Thevenon, A. (2014). The Functional Reach Test: Strategies, performance and the influence of age. *Annals of Physical and Rehabilitation Medicine*, *57*(6), 452–464. https://doi.org/{10.1016/j.rehab.2014.03.003}

de Wit, S., Barker, R. A., Dickinson, A. D., & Cools, R. (2011). Habitual versus Goal-directed Action Control in Parkinson Disease. *Journal of Cognitive*

Neuroscience, *23*(5), 1218–1229. https://doi.org/{10.1162/jocn.2010.21514}

Dean, C. E., Russell, J. M., Kuskowski, M. A., Caligiuri, M. P., & Nugent, S. M. (2004). Clinical Rating Scales and Instruments: How Do They Compare in Assessing Abnormal, Involuntary Movements? *Journal of Clinical Psychopharmacology*, *24*(3), 298–304. https://doi.org/{10.1097/01.jcp.0000125681.97466.e7}

Decroix, J., Rossetti, Y., & Quesque, F. (2022). Les neurones miroirs, hommes à tout faire des neurosciences : Analyse critique des limites méthodologiques et théoriques: *L'Année psychologique*, *Vol. 122*(1), 85–125. https://doi.org/{10.3917/anpsy1.221.0085}

Del Olmo, M. F., & Cudeiro, J. (2005). Temporal variability of gait in Parkinson disease: Effectsof a rehabilitation programme based on rhythmic sound cues. *Parkinsonism & Related Disorders*, *11*(1), 25–33. https://doi.org/{10.1016/j.parkreldis.2004.09.002}

Delevoye-Turrell, Y., & Wing, A. M. (2005). Action and Motor Skills: Adaptive Behaviour for IntendedGoals. In *Handbook of Cognition* (130–159). SAGE Publications Ltd. https://doi.org/{10.4135/9781848608177.n5}

Di Biase, L., Di Santo, A., Caminiti, M. L., De Liso, A., Shah, S. A., Ricci, L., & Di Lazzaro, V. (2020). Gait Analysis in Parkinson's Disease: An Overview of the Most Accurate Markers for Diagnosis and Symptoms Monitoring. *Sensors*, *20*(12), 3529. https://doi.org/{10.3390/s20123529}

D'Mello, S., Dale, R., & Graesser, A. (2012). Disequilibrium in the mind, disharmony in the body. *Cognition and Emotion*, *26*(2), 362–374. https://doi.org/10.1080/02699931.2011.575767

Dolan, R. J., & Dayan, P. (2013). Goals and Habits in the Brain [Publisher: Elsevier]. *Neuron*, *80*(2), 312–325. https://doi.org/{10.1016/j.neuron.2013.09.007}

Dorsey, E. R., Elbaz, A., Nichols, E., Abbasi, N., Abd-Allah, F., Abdelalim, A., Adsuar, J. C., Ansha, M. G., Brayne, C., Choi, J.-Y. J., Collado-Mateo, D., Dahodwala, N., Do, H. P., Edessa, D., Endres, M., Fereshtehnejad, S.-M., Foreman, K. J., Gankpe, F. G., Gupta, R., . . . Murray, C. J. L. (2018). Global, regional, and national burden of Parkinson's disease, 1990–2016: A systematic analysis for the Global Burden of Disease Study 2016. *The Lancet Neurology*, *17*(11), 939–953. https://doi.org/{10.1016/S1474-4422(18)30295-3}

Dorsey, E. R., Sherer, T., Okun, M. S., & Bloem, B. R. (2018). The Emerging Evidence of the Parkinson Pandemic (P. Brundin, J. W. Langston, & B. R. Bloem, Eds.). *Journal of Parkinson's Disease*, *8*(s1), S3–S8. https://doi.org/{10.3233/JPD-181474}

Dukes, D., Abrams, K., Adolphs, R., Ahmed, M. E., Beatty, A., Berridge, K. C., Broomhall, S., Brosch, T., Campos, J. J., Clay, Z., Clément, F., Cunningham, W. A., Damasio, A., Damasio, H., D'Arms, J., Davidson,

J. W., de Gelder, B., Deonna, J., de Sousa, R., . . . Sander, D. (2021). The rise of affectivism. *Nature Human Behaviour*, *5*(7), 816–820. https://doi.org/{10.1038/s41562-021-01130-8}

Dumas, G., Nadel, J., Soussignan, R., Martinerie, J., & Garnero, L. (2010). Inter-Brain Synchronization during Social Interaction [Publisher: Public Library of Science]. *PLOS ONE*, *5*(8), e12166. https://doi.org/{10.1371/journal.pone.0012166}

Duncan, R. P., & Earhart, G. M. (2012). Randomized Controlled Trial of Community-Based Dancing to Modify Disease Progression in Parkinson Disease. *Neurorehabilitation and Neural Repair*, *26*(2), 132–143. https://doi.org/{10.1177/1545968311421614}

Ekkekakis, P. (2013, February). *The Measurement of Affect, Mood, and Emotion: A Guide for Health-Behavioral Research*. Cambridge University Press.

Ekman, P. (1992). An argument for basic emotions. *Cognition and Emotion*, *6*(3-4), 169–200. https://doi.org/{10.1080/02699939208411068}

Epley, N., & Schroeder, J. (2014). Mistakenly seeking solitude. *Journal of Experimental Psychology: General*, *143*(5), 1980–1999. https://doi.org/{10.1037/a0037323}

Espay, A. J., Giuffrida, J. P., Chen, R., Payne, M., Mazzella, F., Dunn, E., Vaughan, J. E., Duker, A. P., Sahay, A., Kim, S. J., Revilla, F. J., & Heldman, D. A. (2011). Differential response of speed, amplitude, and rhythm to dopaminergic medications in Parkinson's disease [_eprint: https://onlinelibrary.wiley.com/doi/pdf/10.1002/mds.23893]. *Movement Disorders*, *26*(14), 2504–2508. https://doi.org/{10.1002/mds.23893}

Farge, M. (1992). Wavelet transforms and their applications to turbulence [ADS Bibcode: 1992AnRFM..24..395F]. *Annual Review of Fluid Mechanics*, *24*, 395–457. https://doi.org/{10.1146/annurev.fl.24.010192.002143}

Feldman, M., Bliss-Moreau, E., & Lindquist, K. (2024). The Neurobiology of Interoception and Affect. *Trends in cognitive sciences*, *28*(7), 643–661. https://doi.org/10.1016/j.tics.2024.01.009

Fernandes, Â., Sousa, A. S., Couras, J., Rocha, N., & Tavares, J. M. R. (2015). Influence of dual-task on sit-to-stand-to-sit postural control in Parkinson's disease. *Medical Engineering & Physics*, *37*(11), 1070–1075. https://doi.org/{10.1016/j.medengphy.2015.08.011}

Filboost. (2024). Filboost. %7Bhttps://filboost.com/science/%7D

Fitzpatrick, P., Frazier, J. A., Cochran, D. M., Mitchell, T., Coleman, C., & Schmidt, R. C. (2016). Impairments of Social Motor Synchrony Evident in Autism Spectrum Disorder [Publisher: Frontiers]. *Frontiers in Psychology*, *7*. https://doi.org/{10.3389/fpsyg.2016.01323}

Flash, T., & Hogan, N. (1985). The coordination of arm movements: an experimentally confirmed mathematical model. *The Journal of Neuroscience*, *5*(7), 1688–1703. https://doi.org/{10.1523/jneurosci.05-07-01688.1985}

Fox, E. (2018). Perspectives from affective science on understanding the nature of emotion. *Brain and Neuroscience Advances*, *2*, 2398212818812628. https://doi.org/{10.1177/2398212818812628}

Frenklach, A., Louie, S., Koop, M. M., & Bronte-Stewart, H. (2009). Excessive postural sway and the risk of falls at different stages of Parkinson's disease. *Movement Disorders: Official Journal of the Movement Disorder Society*, *24*(3), 377–385. https://doi.org/{10.1002/mds.22358}

Frijda, N. H., & Scherer, K. R. (2009). Emotion definitions (psychological perspectives). In *The Oxford companion to emotion and the affective sciences* (142–144). New York: Oxford University Press. %7Bhttps://dare.uva.nl/search?identifier=7108a16a-cc0c-4e6a-96e9-eda594d4bb87%7D

Frijda, N. H., & Mesquita, B. (1994). The social roles and functions of emotions. In *Emotion and culture: Empirical studies of mutual influence* (51–87). American Psychological Association. https://doi.org/{10.1037/10152-002}

Friston, K. J. (1995). States of mind [Publisher: Nature Publishing Group]. *Nature*, *375*(6533), 643–644. https://doi.org/{10.1038/375643a0}

Frost, S., Kannis-Dymand, L., Schaffer, V., Millear, P., Allen, A., Stallman, H., Mason, J., Wood, A., & Atkinson-Nolte, J. (2022). Virtual immersion in nature and psychological well-being: A systematic literature review. *Journal of Environmental Psychology*, *80*, 101765. https://doi.org/10.1016/j.jenvp.2022.101765

Fujiwara, K., & Daibo, I. (2016). Evaluating Interpersonal Synchrony: Wavelet Transform Toward an Unstructured Conversation [Publisher: Frontiers]. *Frontiers in Psychology*, *7*. https://doi.org/{10.3389/fpsyg.2016.00516}

Garland, A. F., Deyessa, N., Desta, M., Alem, A., Zerihun, T., Hall, K. G., Goren, N., & Fish, I. (2018). Use of the WHO's Perceived Well-Being Index (WHO-5) as an efficient and potentially valid screen for depression in a low income country. *Families, Systems & Health: The Journal of Collaborative Family Healthcare*, *36*(2), 148–158. https://doi.org/{10.1037/fsh0000344}

Gibson, J. J. (2014, November). *The Ecological Approach to Visual Perception: Classic Edition*. Psychology Press. https://doi.org/{10.4324/9781315740218}

Gill, D. J., Freshman, A., Blender, J. A., & Ravina, B. (2008). The montreal cognitive assessment as a screening tool for cognitive impairment in Parkinson's disease. *Movement Disorders*, *23*(7), 1043–1046. https://doi.org/{10.1002/mds.22017}

Glyphinder. (2025). Senses [icon]. https://iconscout.com/icons/senses

Goetz, C. G., Tilley, B. C., Shaftman, S. R., Stebbins, G. T., Fahn, S., Martinez-Martin, P., Poewe, W., Sampaio, C., Stern, M. B., Dodel, R., Dubois, B., Holloway, R., Jankovic, J., Kulisevsky, J., Lang, A. E., Lees, A., Leurgans, S., LeWitt, P. A., Nyenhuis, D., . . . LaPelle, N. (2008). Movement Disorder Society-sponsored revision of the Unified Parkinson's Disease Rating Scale (MDS-UPDRS): Scale presentation and clinimetric testing results. *Movement Disorders*, *23*(15), 2129–2170. https://doi.org/{10.1002/mds.22340}

Grafsgaard, J. F., Boyer, K. E., Wiebe, E. N., & Lester, J. C. (2012). Analyzing Posture and Affect in Task-Oriented Tutoring. *Proceedings of the 25th Florida Artificial Intelligence Research Society Conference, 2012*. Retrieved September 18, 2025, from https://cir.nii.ac.jp/crid/1573950399035263488

Griner, D., & Smith, T. B. (2006). Culturally adapted mental health intervention: A meta-analytic review [Place: US Publisher: Educational Publishing Foundation]. *Psychotherapy: Theory, Research, Practice, Training*, *43*(4), 531–548. https://doi.org/{10.1037/0033-3204.43.4.531}

Gross, M. M., Crane, E. A., & Fredrickson, B. L. (2012). Effort-Shape and kinematic assessment of bodily expression of emotion during gait. *Human Movement Science*, *31*(1), 202–221. https://doi.org/{10.1016/j.humov.2011.05.001}

Gross, M. M., Crane, E. A., & Fredrickson, B. L. (2010). Methodology for Assessing Bodily Expression of Emotion. *Journal of Nonverbal Behavior*, *34*(4), 223–248. https://doi.org/{10.1007/s10919-010-0094-x}

Gründahl, M., Weiß, M., Stenzel, K., Deckert, J., & Hein, G. (2023). The effects of everyday-life social interactions on anxiety-related autonomic responses differ between men and women [Publisher: Nature Publishing Group]. *Scientific Reports*, *13*(1), 9498. https://doi.org/{10.1038/s41598-023-36118-z}

Haken, H., Kelso, J. a. S., & Bunz, H. (1985). A theoretical model of phase transitions in human hand movements [Company: Springer Distributor: Springer Institution: Springer Label: Springer Number: 5 Publisher: Springer-Verlag]. *Biological Cybernetics*, *51*(5), 347–356. https://doi.org/{10.1007/BF00336922}

Halovic, S., & Kroos, C. (2018). Not all is noticed: Kinematic cues of emotion-specific gait. *Human Movement Science*, *57*, 478–488. https://doi.org/{10.1016/j.humov.2017.11.008}

Higuera-Trujillo, J. L., Llinares, C., & Macagno, E. (2021). The Cognitive-Emotional Design and Study of Architectural Space: A Scoping Review of Neuroarchitecture and Its Precursor Approaches. *Sensors (Basel, Switzerland)*, *21*(6), 2193. https://doi.org/10.3390/s21062193

Hoehn, M. M., & Yahr, M. D. (2001). Parkinsonism: Onset, progression and mortality [Place: US Publisher: Lippincott Williams & Wilkins]. *Neurology*, *57*(10,Suppl3), S11–S26.

Homagain, A., & Martens, K. A. E. (2023). Emotional states affect steady state walking performance. *PLOS ONE*, *18*(9), e0284308. https://doi.org/{10.1371/journal.pone.0284308}

Hong, M., Perlmutter, J. S., & Earhart, G. M. (2009). A Kinematic and Electromyographic Analysis of Turning in People With Parkinson Disease.

Neurorehabilitation and Neural Repair, *23*(2), 166–176. https://doi.org/{10.1177/1545968308320639}

Horak, F. B., & Mancini, M. (2013). Objective biomarkers of balance and gait for Parkinson's disease using body-worn sensors. *Movement Disorders*, *28*(11), 1544–1551. https://doi.org/{10.1002/mds.25684}

Horak, F. B., Mancini, M., Carlson-Kuhta, P., Nutt, J. G., & Salarian, A. (2016). Balance and Gait Represent Independent Domains of Mobility in Parkinson Disease. *Physical Therapy*, *96*(9), 1364–1371. https://doi.org/{10.2522/ptj.20150580}

Hove, M. J., & Risen, J. L. (2009). It's All in the Timing: Interpersonal Synchrony Increases Affiliation [Publisher: Guilford Publications Inc.]. *Social Cognition*, *27*(6), 949–960. https://doi.org/{10.1521/soco.2009.27.6.949}

Huxham, F., Baker, R., Morris, M. E., & Iansek, R. (2008). Head and trunk rotation during walking turns in Parkinson's disease. *Movement Disorders*, *23*(10), 1391–1397. https://doi.org/{10.1002/mds.21943}

Inkster, L. M., & Eng, J. J. (2004). Postural control during a sit-to-stand task in individuals with mild Parkinson's disease. *Experimental Brain Research*, *154*(1), 33–38. https://doi.org/{10.1007/s00221-003-1629-8}

Issartel, J., Bardainne, T., Gaillot, P., & Marin, L. (2015). The relevance of the cross-wavelet transform in the analysis of human interaction – a tutorial [Publisher: Frontiers]. *Frontiers in Psychology*, *5*. https://doi.org/{10.3389/fpsyg.2014.01566}

Jankovic, J. (2008). Parkinson's disease: clinical features and diagnosis. *Journal of Neurology, Neurosurgery & Psychiatry*, *79*(4), 368–376. https://doi.org/{10.1136/jnnp.2007.131045}

Janssen, S., de Ruyter van Steveninck, J., Salim, H. S., Cockx, H. M., Bloem, B. R., Heida, T., & van Wezel, R. J. A. (2020). The Effects of Augmented Reality Visual Cues on Turning in Place in Parkinson's Disease Patients With Freezing of Gait [Publisher: Frontiers]. *Frontiers in Neurology*, *11*. https://doi.org/{10.3389/fneur.2020.00185}

Jenkins, M. E., Johnson, A. M., Holmes, J. D., Stephenson, F. F., & Spaulding, S. J. (2010). Predictive validity of the UPDRS postural stability score and the Functional Reach Test, when compared with ecologically valid reaching tasks. *Parkinsonism & Related Disorders*, *16*(6), 409–411. https://doi.org/{10.1016/j.parkreldis.2010.04.002}

Jenkinson, C., Fitzpatrick, R., Peto, V., Greenhall, R., & Hyman, N. (1997). The Parkinson's Disease Questionnaire (PDQ-39): Development and validation of a Parkinson's disease summary index score. *Age and Ageing*, *26*(5), 353–357. https://doi.org/{10.1093/ageing/26.5.353}

Jimenez, M. P., DeVille, N. V., Elliott, E. G., Schiff, J. E., Wilt, G. E., Hart, J. E., & James, P. (2021). Associations between Nature Exposure and Health: A Review of the Evidence. *International Journal of Environmental Research and Public Health*, *18*(9), 4790. https://doi.org/10.3390/ijerph18094790

Johnels, B., Ingvarsson, P., Thorselius, M., Valls, M., & Steg, G. (1989). Disability profiles and objective quantitative assessment in Parkinson's disease. *Acta Neurologica Scandinavica*, *79*(3), 227–238. https://doi.org/{10.1111/j.1600-0404.1989.tb03743.x}

Jonasson, S. B., Hagell, P., Hariz, G.-M., Iwarsson, S., & Nilsson, M. H. (2017). Psychometric Evaluation of the Parkinson's Disease Activities of Daily Living Scale. *Parkinson's Disease*, *2017*, 4151738. https://doi.org/{10.1155/2017/4151738}

Jones, N. P., Siegle, G. J., & Mandell, D. (2015). Motivational and Emotional Influences on Cognitive Control in Depression: A Pupillometry Study. *Cognitive, affective & behavioral neuroscience*, *15*(2), 263–275. https://doi.org/10.3758/s13415-014-0323-6

Juras, G., & Latash, M. L. (2021). Motor Control: A Young Field with Many Facets (Introduction to the Special Issue). *Journal of Human Kinetics*, *76*, 5–8. https://doi.org/{10.2478/hukin-2021-0055}

Kadaba, M. P., Ramakrishnan, H. K., & Wootten, M. E. (1990). Measurement of lower extremity kinematics during level walking. *Journal of Orthopaedic Research*, *8*(3), 383–392. https://doi.org/{10.1002/jor.1100080310}

Kalia, L. V., & Lang, A. E. (2015). Parkinson's disease. *The Lancet*, *386*(9996), 896–912. https://doi.org/{10.1016/S0140-6736(14)61393-3}

Kawato, M., & Wolpert, D. (2007). Internal Models for Motor Control [_eprint: https://onlinelibrary.wiley.com/doi/pdf/10.1002/9780470515563.ch16]. In *Novartis Foundation Symposium 218 - Sensory Guidance of Movement* (pp. 291–307). John Wiley & Sons, Ltd. https://doi.org/10.1002/9780470515563.ch16

Keele, S. W. (1968). Movement control in skilled motor performance [Publisher: American Psychological Association]. *Psychological Bulletin*, *70*(6, Pt.1), 387–403. https://doi.org/{10.1037/h0026739}

Kellis, E., Ellinoudis, A., & Kofotolis, N. (2019). Effect of Hip Flexion Angle on the Hamstring to Quadriceps Strength Ratio [Number: 2 Publisher: Multidisciplinary Digital Publishing Institute]. *Sports*, *7*(2), 43. https://doi.org/{10.3390/sports7020043}

Kelso, J. A. S. (1995). *Dynamic Patterns: The Self-organization of Brain and Behavior*. MIT Press.

Kelso, J. A. S. (1981). On the oscillatory basis of movement. *Bull Psychon Soc*, *18*. %7Bhttps://cir.nii.ac.jp/crid/1370285712537235463%7D

Kelso, J. A. S. (1984). Phase transitions and critical behavior in human bimanual coordination [Publisher: American Physiological Society]. *American Journal of Physiology-Regulatory, Integrative and Comparative Physiology*, *246*(6), R1000–R1004. https://doi.org/{10.1152/ajpregu.1984.246.6.R1000}

King, L. A., Mancini, M., Priest, K., Salarian, A., Rodrigues-de-Paula, F., & Horak, F. (2012). Do Clinical Scales of Balance Reflect Turning Abnormalities in People With Parkinson's Disease? *Journal of Neurologic Physical Therapy*, *36*(1), 25. https://doi.org/{10.1097/NPT.0b013e31824620d1}

Kleckner, I. R., Zhang, J., Touroutoglou, A., Chanes, L., Xia, C., Simmons, W. K., Quigley, K. S., Dickerson, B. C., & Feldman Barrett, L. (2017). Evidence for a large-scale brain system supporting allostasis and interoception in humans. *Nature Human Behaviour*, *1*(5), 0069. https://doi.org/{10.1038/s41562-017-0069}

Konvalinka, I., Xygalatas, D., Bulbulia, J., Schjødt, U., Jegindø, E.-M., Wallot, S., Van Orden, G., & Roepstorff, A. (2011). Synchronized arousal between performers and related spectators in a fire-walking ritual [Publisher: Proceedings of the National Academy of Sciences]. *Proceedings of the National Academy of Sciences*, *108*(20), 8514–8519. https://doi.org/{10.1073/pnas.1016955108}

Krieger, Freij, Brazhe, Torrence, Compo, & contributors. (2017). Python module for continuous wavelet spectral analysis.

Krieger, S., Freij, N., Brazhe, A., Torrence, C., & P. Compo, G. (2023). A Python module for continuous wavelet spectral analysis. %7Bhttps://github.com/regeirk/pycwt%7D

Kuramoto, Y. (1984). *Chemical Oscillations, Waves, and Turbulence* (H. Haken, Ed.; Vol. 19). Springer Berlin Heidelberg. https://doi.org/{10.1007/978-3-642-69689-3}

Lakin, J. L., Jefferis, V. E., Cheng, C. M., & Chartrand, T. L. (2003). The Chameleon Effect as Social Glue: Evidence for the Evolutionary Significance of Nonconscious Mimicry [Publisher: Springer]. *Journal of Nonverbal Behavior*, *27*(3), 145–162. https://doi.org/{10.1023/A:1025389814290}

Latt, M. D., Menz, H. B., Fung, V. S., & Lord, S. R. (2008). Walking speed, cadence and step length are selected to optimize the stability of head and pelvis accelerations. *Experimental Brain Research*, *184*(2), 201–209. https://doi.org/{10.1007/s00221-007-1094-x}

Latt, M. D., Menz, H. B., Fung, V. S., & Lord, S. R. (2009). Acceleration Patterns of the Head and Pelvis During Gait in Older People With Parkinson's Disease: A Comparison of Fallers and Nonfallers. *The Journals of Gerontology: Series A*, *64A*(6), 700–706. https://doi.org/{10.1093/gerona/glp009}

LeDoux, J. E., & Brown, R. (2017). A higher-order theory of emotional consciousness [Publisher: Proceedings of the National Academy of Sciences]. *Proceedings of the National Academy of Sciences*, *114*(10), E2016–E2025. https://doi.org/10.1073/pnas.1619316114

Lee, K. M., Ferreira-Santos, F., & Satpute, A. B. (2021). Predictive processing models and affective neuroscience. *Neuroscience and biobehavioral reviews*, *131*, 211–228. https://doi.org/10.1016/j.neubiorev.2021.09.009

Lewek, M. D., Poole, R., Johnson, J., Halawa, O., & Huang, X. (2010-a). Arm swing magnitude and asymmetry during gait in the early stages of

Parkinson's disease. *Gait & Posture*, *31*(2), 256–260. https://doi.org/{10.1016/j.gaitpost.2009.10.013}

Lewek, M. D., Poole, R., Johnson, J., Halawa, O., & Huang, X. (2010-b). Arm swing magnitude and asymmetry during gait in the early stages of Parkinson's disease. *Gait & Posture*, *31*(2), 256–260. https://doi.org/{10.1016/j.gaitpost.2009.10.013}

Lewkowicz, D., Delevoye-Turrell, Y., Bailly, D., Andry, P., & Gaussier, P. (2013). Reading motor intention through mental imagery. *Adaptive Behavior*, *21*(5), 315–327. https://doi.org/{10.1177/1059712313501347}

Lewkowicz, D., Quesque, F., Coello, Y., & Delevoye-Turrell, Y. N. (2015). Individual differences in reading social intentions from motor deviants. *Frontiers in Psychology*, *6*. https://doi.org/{10.3389/fpsyg.2015.01175}

Li, X., Zhang, G., Zhou, C., & Wang, X. (2019). Negative emotional state slows down movement speed: behavioral and neural evidence. *PeerJ*, *7*. https://doi.org/{10.7717/peerj.7591}

Li, Z.-M. (2006). Functional degrees of freedom. *Motor Control*, *10*(4), 301–310. https://doi.org/{10.1123/mcj.10.4.301}

Liu, Y., Liang, X. S., & Weisberg, R. H. (2007). Rectification of the Bias in the Wavelet Power Spectrum [Section: Journal of Atmospheric and Oceanic Technology]. https://doi.org/{10.1175/2007JTECHO511.1}

Lobo, L., Heras-Escribano, M., & Travieso, D. (2018). The History and Philosophy of Ecological Psychology. *Frontiers in Psychology*, *9*, 2228. https://doi.org/{10.3389/fpsyg.2018.02228}

Lowry, K. A., Smiley-Oyen, A. L., Carrel, A. J., & Kerr, J. P. (2009). Walking stability using harmonic ratios in Parkinson's disease [_eprint: https://onlinelibrary.wiley.com/doi/pdf/10.1002/mds.22352]. *Movement Disorders*, *24*(2), 261–267. https://doi.org/{10.1002/mds.22352}

Lu, R., Xu, Y., Li, X., Fan, Y., Zeng, W., Tan, Y., Ren, K., Chen, W., & Cao, X. (2020). Evaluation of Wearable Sensor Devices in Parkinson's Disease: A Review of Current Status and Future Prospects. *Parkinson's Disease*, *2020*(1), 4693019. https://doi.org/{10.1155/2020/4693019}

Magrinelli, F., Picelli, A., Tocco, P., Federico, A., Roncari, L., Smania, N., Zanette, G., & Tamburin, S. (2016). Pathophysiology of Motor Dysfunction in Parkinson's Disease as the Rationale for Drug Treatment and Rehabilitation. *Parkinson's Disease*, *2016*, 1–18. https://doi.org/{10.1155/2016/9832839}

Mahzoon, H., Ueda, A., Yoshikawa, Y., & Ishiguro, H. (2022). Effect of robot's vertical body movement on its perceived emotion: A preliminary study on vertical oscillation and transition (Y. Benetreau, Ed.). *PLOS ONE*, *17*(8), e0271789. https://doi.org/10.1371/journal.pone.0271789

Mancini, M., Bloem, B. R., Horak, F. B., Lewis, S. J., Nieuwboer, A., & Nonnekes, J. (2019). Clinical and methodological challenges for assessing freezing of gait: Future perspectives. *Movement Disorders*, *34*(6), 783–790. https://doi.org/{10.1002/mds.27709}

Mancini, M., Horak, F. B., Zampieri, C., Carlson-Kuhta, P., Nutt, J. G., & Chiari, L. (2011). Trunk accelerometry reveals postural instability in untreated Parkinson's disease. *Parkinsonism & Related Disorders*, *17*(7), 557–562. https://doi.org/{10.1016/j.parkreldis.2011.05.010}

Mancini, M., Rocchi, L., Horak, F. B., & Chiari, L. (2008). Effects of Parkinson's disease and levodopa on functional limits of stability. *Clinical Biomechanics*, *23*(4), 450–458. https://doi.org/{10.1016/j.clinbiomech.2007.11.007}

Mandler, G. (2002). Origins of the cognitive (r)evolution. *Journal of the History of the Behavioral Sciences*, *38*(4), 339–353. https://doi.org/{10.1002/jhbs.10066}

Mayo, O., & Gordon, I. (2020). In and out of synchrony—Behavioral and physiological dynamics of dyadic interpersonal coordination. *Psychophysiology*, *57*(6), e13574. https://doi.org/{10.1111/psyp.13574}

Mi, T.-M., Zhang, W., McKeown, M. J., & Chan, P. (2021). Impaired Formation and Expression of Goal-Directed and Habitual Control in Parkinson's Disease [Publisher: Frontiers]. *Frontiers in Aging Neuroscience*, *13*. https://doi.org/{10.3389/fnagi.2021.734807}

Mirelman, A., Bonato, P., Camicioli, R., Ellis, T. D., Giladi, N., Hamilton, J. L., Hass, C. J., Hausdorff, J. M., Pelosin, E., & Almeida, Q. J. (2019). Gait impairments in Parkinson's disease. *The Lancet Neurology*, *18*(7), 697–708. https://doi.org/{10.1016/S1474-4422(19)30044-4}

Mogan, R., Fischer, R., & Bulbulia, J. A. (2017). To be in synchrony or not? A meta-analysis of synchrony's effects on behavior, perception, cognition and affect. *Journal of Experimental Social Psychology*, *72*, 13–20. https://doi.org/{10.1016/j.jesp.2017.03.009}

Moore, S. R., Martinez, A., Kröll, J., Strutzenberger, G., & Schwameder, H. (2022). Simple foot strike angle calculation from three-dimensional kinematics: A methodological comparison. *Journal of Sports Sciences*, *40*(12), 1343–1350. https://doi.org/{10.1080/02640414.2022.2080162}

Moors, A., Ellsworth, P. C., Scherer, K. R., & Frijda, N. H. (2013). Appraisal Theories of Emotion: State of the Art and Future Development. *Emotion Review*, *5*(2), 119–124. https://doi.org/{10.1177/1754073912468165}

Mori, M., MacDorman, K. F., & Kageki, N. (2012). The uncanny valley [from the field] [Publisher: IEEE]. *IEEE Robotics & automation magazine*, *19*(2), 98–100.

Morris, M. E. (2000). Movement Disorders in People With Parkinson Disease: A Model for Physical Therapy. *Physical Therapy*, *80*(6), 578–597. https://doi.org/{10.1093/ptj/80.6.578}

Mu, Y., Cerritos, C., & Khan, F. (2018). Neural mechanisms underlying interpersonal coordination: A review of hyperscanning research. *Social* *and Personality Psychology Compass*, *12*(11), e12421. https://doi.org/{10.1111/spc3.12421}

Mühlhoff, R. (2015). Affective resonance and social interaction. *Phenomenology and the Cognitive Sciences*, *14*(4), 1001–1019. https://doi.org/{10.1007/s11097-014-9394-7}

Mullineaux, D. R., & Irwin, G. (2014). A Simple Outlier Detection Method for Intra-subject Time-series Data. *ISBS - Conference Proceedings Archive*. Retrieved September 11, 2025, from https://ojs.ub.uni-konstanz.de/cpa/article/view/5921

Nam, C. S., Choo, S., Huang, J., & Park, J. (2020). Brain-to-Brain Neural Synchrony During Social Interactions: A Systematic Review on Hyperscanning Studies. *Applied Sciences*, *10*(19), 6669. https://doi.org/{10.3390/app10196669}

Nikfekr, E., Kerr, K., Attfield, S., & Playford, E. (2002). Trunk movement in Parkinson's disease during rising from seated position [_eprint: https://onlinelibrary.wiley.com/doi/pdf/10.1002/mds.10073]. *Movement Disorders*, *17*(2), 274–282. https://doi.org/{10.1002/mds.10073}

Nocera, J. R., Stegemöller, E. L., Malaty, I. A., Okun, M. S., Marsiske, M., & Hass, C. J. (2013). Using the Timed Up & Go Test in a Clinical Setting to Predict Falling in Parkinson's Disease. *Archives of Physical Medicine and Rehabilitation*, *94*(7), 1300–1305. https://doi.org/{10.1016/j.apmr.2013.02.020}

Noordewier, M. K., Scheepers, D. T., & Hilbert, L. P. (2020). Freezing in response to social threat: a replication. *Psychological Research*, *84*(7), 1890–1896. https://doi.org/{10.1007/s00426-019-01203-4}

Novembre, G., Mitsopoulos, Z., & Keller, P. E. (2019). Empathic perspective taking promotes interpersonal coordination through music [Publisher: Nature Publishing Group]. *Scientific Reports*, *9*(1), 12255. https://doi.org/{10.1038/s41598-019-48556-9}

Oatley, K., Keltner, D., & Jenkins, J. M. (2006). *Understanding emotions, 2nd ed.* Blackwell Publishing.

Obeso, J., Stamelou, M., Goetz, C., Poewe, W., Lang, A., Weintraub, D., Burn, D., Halliday, G., Bezard, E., Przedborski, S., Lehericy, S., Brooks, D., Rothwell, J., Hallett, M., DeLong, M., Marras, C., Tanner, C., Ross, G., Langston, J., ... Stoessl, A. (2017). Past, present, and future of Parkinson's disease: A special essay on the 200th Anniversary of the Shaking Palsy. *Movement Disorders*, *32*(9), 1264–1310. https://doi.org/{10.1002/mds.27115}

Oertel, C., Castellano, G., Chetouani, M., Nasir, J., Obaid, M., Pelachaud, C., & Peters, C. (2020). Engagement in Human-Agent Interaction: An Overview [Publisher: Frontiers]. *Frontiers in Robotics and AI*, *7*. https://doi.org/{10.3389/frobt.2020.00092}

Oertel, C., De Looze, C., Scherer, S., Windmann, A., Wagner, P., & Campbell, N. (2011). Towards the Automatic Detection of Involvement in Conversation. In A. Esposito, A. Vinciarelli, K. Vicsi, C. Pelachaud, & A. Nijholt (Eds.), *Analysis of Verbal and Nonverbal Communication and Enactment. The Processing Issues* (163–170). Springer. https://doi.org/{10.1007/978-3-642-25775-9_16}

Opara, J., Małecki, A., Małecka, E., & Socha, T. (2017). Motor assessment in Parkinson's disease. *Annals of Agricultural and Environmental Medicine*, *24*(3), 411–415. https://doi.org/{10.5604/12321966.1232774}

Palmerini, L., Mellone, S., Avanzolini, G., Valzania, F., & Chiari, L. (2013). Quantification of Motor Impairment in Parkinson's Disease Using an Instrumented Timed Up and Go Test [Conference Name: IEEE Transactions on Neural Systems and Rehabilitation Engineering]. *IEEE Transactions on Neural Systems and Rehabilitation Engineering*, *21*(4), 664–673. https://doi.org/{10.1109/TNSRE.2012.2236577}

Paolini, S., Gibbs, M., Sales, B., Anderson, D., & McIntyre, K. (2024). Negativity bias in intergroup contact: Meta-analytical evidence that bad is stronger than good, especially when people have the opportunity and motivation to opt out of contact [Place: US Publisher: American Psychological Association]. *Psychological Bulletin*, *150*(8), 921–964. https://doi.org/10.1037/bul0000439

Parkinson, B. (2011). Interpersonal Emotion Transfer: Contagion and Social Appraisal. *Social and Personality Psychology Compass*, *5*(7), 428–439. https://doi.org/10.1111/j.1751-9004.2011.00365.x

Parkinson, B. (2020). Intragroup Emotion Convergence: Beyond Contagion and Social Appraisal. *Personality and Social Psychology Review*, *24*(2), 121–140. https://doi.org/10.1177/1088868319882596

Pelicioni, P. H. S., Menant, J. C., Latt, M. D., & Lord, S. R. (2019). Falls in Parkinson's Disease Subtypes: Risk Factors, Locations and Circumstances. *International Journal of Environmental Research and Public Health*, *16*(12), 2216. https://doi.org/{10.3390/ijerph16122216}

Podsiadlo, D., & Richardson, S. (1991). The timed "Up & Go": A test of basic functional mobility for frail elderly persons. *Journal of the American Geriatrics Society*, *39*(2), 142–148. https://doi.org/{10.1111/j.1532-5415.1991.tb01616.x}

Poewe, W. (2008). Non-motor symptoms in Parkinson's disease. *European Journal of Neurology*, *15*(s1), 14–20. https://doi.org/{10.1111/j.1468-1331.2008.02056.x}

Pollick, F. E., Paterson, H. M., Bruderlin, A., & Sanford, A. J. (2001). Perceiving affect from arm movement. *Cognition*, *82*(2), B51–B61. https://doi.org/{10.1016/S0010-0277(01)00147-0}

Posner, J., Russell, J. A., & Peterson, B. S. (2005). The circumplex model of affect: An integrative approach to affective neuroscience, cognitive development, and psychopathology. *Development and psychopathology*, *17*(3), 715–734. https://doi.org/{10.1017/S0954579405050340}

Prilutsky, B. I., & Zatsiorsky, V. M. (2020). Neural Control Principles: Bernstein's Insights from Biomechanics of Human Movement. In *Bernstein's Construction of Movements*. Routledge.

Quesque, F., Delevoye-Turrell, Y., & Coello, Y. (2016). Facilitation effect of observed motor deviants in a cooperative motor task: Evidence for direct perception of social intention in action [Publisher: SAGE Publications]. *Quarterly Journal of Experimental Psychology*, *69*(8), 1451–1463. https://doi.org/{10.1080/17470218.2015.1083596}

Quesque, F., Lewkowicz, D., Delevoye-Turrell, Y. N., & Coello, Y. (2013). Effects of social intention on movement kinematics in cooperative actions. *Frontiers in Neurorobotics*, *7*. https://doi.org/{10.3389/fnbot.2013.00014}

Rahimpour, S., Gaztanaga, W., Yadav, A. P., Chang, S. J., Krucoff, M. O., Cajigas, I., Turner, D. A., & Wang, D. D. (2021). Freezing of Gait in Parkinson's Disease: Invasive and Noninvasive Neuromodulation. *Neuromodulation: Technology at the Neural Interface*, *24*(5), 829–842. https://doi.org/{10.1111/ner.13347}

Rana, A. Q., Siddiqui, I., & Yousuf, M. S. (2012). Challenges in diagnosis of young onset Parkinson's disease. *Journal of the Neurological Sciences*, *323*(1-2), 113–116. https://doi.org/{10.1016/j.jns.2012.08.029}

Read Speaker. (2024). %7Bhttps://www.readspeaker.com/%7D

Redgrave, P., Rodriguez, M., Smith, Y., Rodriguez-Oroz, M. C., Lehericy, S., Bergman, H., Agid, Y., DeLong, M. R., & Obeso, J. A. (2010). Goal-directed and habitual control in the basal ganglia: implications for Parkinson's disease [Publisher: Nature Publishing Group]. *Nature Reviews Neuroscience*, *11*(11), 760–772. https://doi.org/{10.1038/nrn2915}

Repp, B. H., & Su, Y.-H. (2013). Sensorimotor synchronization: A review of recent research (2006–2012) [Company: Springer Distributor: Springer Institution: Springer Label: Springer Publisher: Springer-Verlag]. *Psychonomic Bulletin & Review*, *20*(3), 403–452. https://doi.org/{10.3758/s13423-012-0371-2}

Richardson, M. J., Marsh, K. L., Isenhower, R. W., Goodman, J. R., & Schmidt, R. (2007). Rocking together: Dynamics of intentional and unintentional interpersonal coordination. *Human Movement Science*, *26*(6), 867–891. https://doi.org/{10.1016/j.humov.2007.07.002}

Ridderinkhof, K. R. (2017). Emotion in Action: A Predictive Processing Perspective and Theoretical Synthesis. *Emotion Review*, *9*(4), 319–325. https://doi.org/{10.1177/1754073916661765}

Rizzolatti, G., & Sinigaglia, C. (2016). The mirror mechanism: a basic principle of brain function [Publisher: Nature Publishing Group]. *Nature Reviews Neuroscience*, *17*(12), 757–765. https://doi.org/{10.1038/nrn.2016.135}

Rodrigues-de-Paula Goulart, F., & Valls-Solé, J. (1999). Patterned electromyographic activity in the sit-to-stand movement. *Clinical Neurophysiology*, *110*(9), 1634–1640. https://doi.org/{10.1016/S1388-2457(99)00109-1}

Roelofs, K., Hagenaars, M. A., & Stins, J. (2010). Facing Freeze: Social Threat Induces Bodily Freeze in Humans. *Psychological Science*, *21*(11), 1575–1581. https://doi.org/{10.1177/0956797610384746}

Roether, C. L., Omlor, L., Christensen, A., & Giese, M. A. (2009). Critical features for the perception of emotion from gait. *Journal of Vision*, *9*(6), 15. https://doi.org/{10.1167/9.6.15}

Rose, D., Koechli, S., Ungerer, M., Karageorghis, C., Whyatt, C., Annett, L., Bohlhalter, S., Vanbellingen, T., Galati, S., & Dinacci, S. (2023). Songlines for Parkinson's [Publisher: OSF]. https://doi.org/{10.17605/OSF.IO/329GH}

Rose, D., Ungerer, M., Köchli, S., Paolantonio, P., Dinacci, D., Foletti, A., Molteni, D., Greenwood, A., Thomas, M., Truran, L., Annett, L. E., Karageorghis, C. I., Whyatt, C., Poliakoff, E., & Short, A. (2025). Songlines for Parkinson's: The Process of Co-Developing a New Music-and-Movement Group-Based Intervention to Improve Mood and Movement for Parkinson's [Publisher: SAGE Publications Inc]. *International Journal of Qualitative Methods*, *24*, 16094069251335453. https://doi.org/{10.1177/16094069251335453}

Rose, D. C., Sigrist, C., & Alessandri, E. (2021). Hard Work and Hopefulness: A Mixed Methods Study of Music Students' Status and Beliefs in Relation to Health, Wellbeing, and Success as They Enter Specialized Higher Education. *Frontiers in Psychology*, *12*. https://doi.org/{10.3389/fpsyg.2021.740775}

Russell, J. A. (1980). A circumplex model of affect. *Journal of Personality and Social Psychology*, *39*(6), 1161–1178. https://doi.org/{10.1037/h0077714}

Russell, J. A. (2003). Core affect and the psychological construction of emotion. *Psychological Review*, *110*(1), 145–172. https://doi.org/{10.1037/0033-295X.110.1.145}

Russell, J. A. (2009). Emotion, core affect, and psychological construction. *Cognition and Emotion*, *23*(7), 1259–1283. https://doi.org/{10.1080/02699930902809375}

Russell, J. A., & Barrett, L. F. (1999). Core affect, prototypical emotional episodes, and other things called emotion: Dissecting the elephant. *Journal of Personality and Social Psychology*, *76*(5), 805–819. https://doi.org/{10.1037/0022-3514.76.5.805}

Russell, J. A., Weiss, A., & Mendelsohn, G. (1989). Affect Grid: A Single-Item Scale of Pleasure and Arousal. *Journal of Personality and Social Psychology*, *57*, 493–502. https://doi.org/{10.1037/0022-3514.57.3.493}

Salam, H., Celiktutan, O., Gunes, H., & Chetouani, M. (2024). Automatic Context-Aware Inference of Engagement in HMI: A Survey. *IEEE Trans-*

actions on Affective Computing, *15*(2), 445–464. https://doi.org/{10.1109/TAFFC.2023.3278707}

Salam, H., Celiktutan, O., Hupont, I., Gunes, H., & Chetouani, M. (2016). Fully automatic analysis of engagement and its relationship to personality in human-robot interactions [Publisher: IEEE]. *IEEE access : practical innovations, open solutions*, *5*, 705–721.

Salarian, A., Horak, F. B., Zampieri, C., Carlson-Kuhta, P., Nutt, J. G., & Aminian, K. (2010). iTUG, a Sensitive and Reliable Measure of Mobility [Conference Name: IEEE Transactions on Neural Systems and Rehabilitation Engineering]. *IEEE Transactions on Neural Systems and Rehabilitation Engineering*, *18*(3), 303–310. https://doi.org/{10.1109/TNSRE.2010.2047606}

Sander, D., & Scherer, K. (2009, July). *Oxford Companion to Emotion and the Affective Sciences*. OUP Oxford.

Sanghvi, J., Castellano, G., Leite, I., Pereira, A., McOwan, P. W., & Paiva, A. (2011). Automatic analysis of affective postures and body motion to detect engagement with a game companion. *Proceedings of the 6th international conference on Human-robot interaction*, 305–312. https://doi.org/{10.1145/1957656.1957781}

Satpute, A. B., Kang, J., Bickart, K. C., Yardley, H., Wager, T. D., & Barrett, L. F. (2015). Involvement of Sensory Regions in Affective Experience: A Meta-Analysis [Publisher: Frontiers]. *Frontiers in Psychology*, *6*. https://doi.org/10.3389/fpsyg.2015.01860

Saunderson, S., & Nejat, G. (2019). How Robots Influence Humans: A Survey of Nonverbal Communication in Social Human–Robot Interaction. *International Journal of Social Robotics*, *11*(4), 575–608. https://doi.org/10.1007/s12369-019-00523-0

Scherer, K. R. (2005). What are emotions? And how can they be measured? *Social Science Information*, *44*(4), 695–729. https://doi.org/{10.1177/0539018405058216}

Schlachetzki, J. C. M., Barth, J., Marxreiter, F., Gossler, J., Kohl, Z., Reinfelder, S., Gassner, H., Aminian, K., Eskofier, B. M., Winkler, J., & Klucken, J. (2017). Wearable sensors objectively measure gait parameters in Parkinson's disease [Publisher: Public Library of Science]. *PLOS ONE*, *12*(10), e0183989. https://doi.org/{10.1371/journal.pone.0183989}

Schmidt, R. C., Morr, S., Fitzpatrick, P., & Richardson, M. J. (2012). Measuring the Dynamics of Interactional Synchrony. *Journal of Nonverbal Behavior*, *36*(4), 263–279. https://doi.org/{10.1007/s10919-012-0138-5}

Schmidt, R. A. (1975). A schema theory of discrete motor skill learning [Publisher: American Psychological Association]. *Psychological Review*, *82*(4), 225–260. https://doi.org/{10.1037/h0076770}

Schmidt, R. A. (2003). Motor Schema Theory after 27 Years: Reflections and Implications for a New Theory. *Research Quarterly for Exercise and Sport*, *74*(4), 366–375. https://doi.org/{10.1080/02701367.2003.10609106}

Schoneburg, B., Mancini, M., Horak, F., & Nutt, J. G. (2013). Framework for understanding balance dysfunction in Parkinson's disease [_eprint: https://onlinelibrary.wiley.com/doi/pdf/10.1002/mds.25613]. *Movement Disorders*, *28*(11), 1474–1482. https://doi.org/{10.1002/mds.25613}

Schrag, A., & Schott, J. M. (2006). Epidemiological, clinical, and genetic characteristics of early-onset parkinsonism. *The Lancet Neurology*, *5*(4), 355–363. https://doi.org/{10.1016/S1474-4422(06)70411-2}

Science et Vie [magazine]. (2025). (1290). Retrieved September 19, 2025, from https://pvsamplersla5.immanens.com/fr/pvPageH5B.asp?puc=003263&nu=1290&pa=1#0

Sejdić, E., Lowry, K. A., Bellanca, J., Redfern, M. S., & Brach, J. S. (2014). A Comprehensive Assessment of Gait Accelerometry Signals in Time, Frequency and Time-Frequency Domains [Conference Name: IEEE Transactions on Neural Systems and Rehabilitation Engineering]. *IEEE Transactions on Neural Systems and Rehabilitation Engineering*, *22*(3), 603–612. https://doi.org/{10.1109/TNSRE.2013.2265887}

Seth, A. K. (2013). Interoceptive inference, emotion, and the embodied self. *Trends in Cognitive Sciences*, *17*(11), 565–573. https://doi.org/10.1016/j.tics.2013.09.007

Shafir, T., Tsachor, R. P., & Welch, K. B. (2016). Emotion Regulation through Movement: Unique Sets of Movement Characteristics are Associated with and Enhance Basic Emotions. *Frontiers in Psychology*, *6*. %7Bhttps://www.frontiersin.org/articles/10.3389/fpsyg.2015.02030%7D

Shin, K. J., Park, J., Ha, S., Park, K. M., Kim, S. E., Lee, B. I., Lee, D. A., Kim, H.-T., & Yoon, J.-Y. (2020). Decreased foot height may be a subclinical shuffling gait in early stage of Parkinson's disease: A study of three-dimensional motion analysis. *Gait & Posture*, *76*, 64–67. https://doi.org/{10.1016/j.gaitpost.2019.11.005}

Sidner, C. L., Lee, C., Kidd, C. D., Lesh, N., & Rich, C. (2005). Explorations in engagement for humans and robots [Publisher: Elsevier]. *Artificial Intelligence*, *166*(1-2), 140–164.

Silva, A. D., & Laje, R. (2024). Perturbation context in paced finger tapping tunes the error-correction mechanism [Publisher: Nature Publishing Group]. *Scientific Reports*, *14*(1), 27473. https://doi.org/{10.1038/s41598-024-78786-5}

Skurowski, P., & Pawlyta, M. (2022). Detection and Classification of Artifact Distortions in Optical Motion Capture Sequences. *Sensors (Basel, Switzerland)*, *22*(11), 4076. https://doi.org/{10.3390/s22114076}

Skurowski, P., & Pawlyta, M. (2021). Gap Reconstruction in Optical Motion Capture Sequences Using Neural Networks. *Sensors (Basel, Switzerland)*, *21*(18), 6115. https://doi.org/{10.3390/s21186115}

Smykovskyi, A., Bieńkiewicz, M. M. N., Pla, S., Janaqi, S., & Bardy, B. G. (2022). Positive emotions foster spontaneous synchronisation in a group movement improvisation task. *Frontiers in Human Neuroscience*, *16*, 944241. https://doi.org/{10.3389/fnhum.2022.944241}

Smykovskyi, A., Janaqi, S., Pla, S., Jean, P., Bieńkiewicz, M. M. N., & Bardy, B. G. (2024). Negative emotions disrupt intentional synchronization during group sensorimotor interaction. *Emotion*, *24*(3), 687–702. https://doi.org/{10.1037/emo0001282}

Sozzi, S., Nardone, A., & Schieppati, M. (2021). Specific Posture-Stabilising Effects of Vision and Touch Are Revealed by Distinct Changes of Body Oscillation Frequencies. *Frontiers in Neurology*, *12*. %7Bhttps://www.frontiersin.org/articles/10.3389/fneur.2021.756984%7D

Sprint, G., Cook, D. J., & Weeks, D. L. (2015). Toward Automating Clinical Assessments: A Survey of the Timed Up and Go. *IEEE Reviews in Biomedical Engineering*, *8*, 64–77. https://doi.org/{10.1109/RBME.2015.2390646}

Stack, E., & Ashburn, A. (1999). Fall events described by people with Parkinson's disease: Implications for clinical interviewing and the research agenda [_eprint: https://onlinelibrary.wiley.com/doi/pdf/10.1002/pri.165]. *Physiotherapy Research International*, *4*(3), 190–200. https://doi.org/{10.1002/pri.165}

Stack, E. L., Ashburn, A. M., & Jupp, K. E. (2006). Strategies used by people with Parkinson's disease who report difficulty turning. *Parkinsonism & Related Disorders*, *12*(2), 87–92. https://doi.org/{10.1016/j.parkreldis.2005.08.008}

Stephenson, D., Badawy, R., Mathur, S., Tome, M., & Rochester, L. (2021). Digital Progression Biomarkers as Novel Endpoints in Clinical Trials: A Multistakeholder Perspective [Publisher: SAGE Publications]. *Journal of Parkinson's Disease*, *11*(s1), S103–S109. https://doi.org/{10.3233/JPD-202428}

Sterling, P. (2012). Allostasis: A model of predictive regulation. *Physiology & Behavior*, *106*(1), 5–15. https://doi.org/{10.1016/j.physbeh.2011.06.004}

Studio, R. C. (2025). Yoga instructor [icon]. https://iconscout.com/icons/yoga-instructor

Švehlík, M., Zwick, E. B., Steinwender, G., Linhart, W. E., Schwingenschuh, P., Katschnig, P., Ott, E., & Enzinger, C. (2009). Gait Analysis in Patients With Parkinson's Disease Off Dopaminergic Therapy. *Archives of Physical Medicine and Rehabilitation*, *90*(11), 1880–1886. https://doi.org/{10.1016/j.apmr.2009.06.017}

Tennant, J., Becker, B., Bie, T. d., Colomb, J., Goglio, V., Grigorov, I., Hartgerink, C., Hartley, R., Havemann, J., Kramer, B., Madan, C., Masuzzo, P., Matthias, L., Schlatter, M., Steiner, T., & Vos, R. (2019). What Collaboration Means to Us: We are more powerful when we work together as a community to solve problems. *Collaborative Librarianship*, *11*(2). %7Bhttps://digitalcommons.du.edu/collaborativelibrarianship/vol11/iss2/2%7D

Terasawa, Y., Fukushima, H., & Umeda, S. (2013). How does interoceptive awareness interact with the subjective experience of emotion? An fMRI Study. *Human Brain Mapping*, *34*(3), 598–612. https://doi.org/{10.1002/hbm.21458}

Thompson, R., Stewart, G., Vu, T., Jephcote, C., Lim, S., Barratt, B., Smith, R. B., Karim, Y. B., Mussa, A., Mudway, I., Fisher, H. L., Dumontheil, I., Thomas, M. S. C., Gulliver, J., Beevers, S., Kelly, F. J., & Toledano, M. B. (2024). Air pollution, traffic noise, mental health, and cognitive development: A multi-exposure longitudinal study of London adolescents in the SCAMP cohort. *Environment International*, *191*, 108963. https://doi.org/10.1016/j.envint.2024.108963

Todorov, E. (2004). Optimality principles in sensorimotor control [Publisher: Springer Nature]. *Nature Neuroscience*, *7*(9), 907–915. https://doi.org/{10.1038/nn1309}

Toosizadeh, N., Mohler, J., Lei, H., Parvaneh, S., Sherman, S., & Najafi, B. (2015). Motor Performance Assessment in Parkinson's Disease: Association between Objective In-Clinic, Objective In-Home, and Subjective/Semi-Objective Measures (W. Maetzler, Ed.). *PLOS ONE*, *10*(4), e0124763. https://doi.org/{10.1371/journal.pone.0124763}

Torrence, C., & Compo, G. P. (1998). A Practical Guide to Wavelet Analysis [Section: Bulletin of the American Meteorological Society]. %7Bhttps://journals.ametsoc.org/view/journals/bams/79/1/1520-0477_1998_079_0061_apgtwa_2_0_co_2.xml%7D

Tschacher, W. (2023). *SUSY: Surrogate synchrony*. manual. https://wtschacher.github.io/SUSY/

Tschacher, W., & Meier, D. (2020). Physiological synchrony in psychotherapy sessions. *Psychotherapy Research*, *30*(5), 558–573. https://doi.org/{10.1080/10503307.2019.1612114}

Tschacher, W., Rees, G. M., & Ramseyer, F. (2014). Nonverbal synchrony and affect in dyadic interactions [Publisher: Frontiers]. *Frontiers in Psychology*, *5*. https://doi.org/{10.3389/fpsyg.2014.01323}

Turner, T. H., & Dale, M. L. (2020). Inconsistent Movement Disorders Society–Unified Parkinson's Disease Rating Scale Part III Ratings in the Parkinson's Progression Marker Initiative. *Movement disorders : official journal of the Movement Disorder Society*, *35*(8), 1488–1489. https://doi.org/{10.1002/mds.28108}

Turvey, M. T. (1990). Coordination [Place: US Publisher: American Psychological Association]. *American Psychologist*, *45*(8), 938–953. https://doi.org/{10.1037/0003-066X.45.8.938}

Vacharkulksemsuk, T., & Fredrickson, B. L. (2012). Strangers in sync: Achieving embodied rapport through shared movements. *Journal of Experimental Social Psychology*, *48*(1), 399–402. https://doi.org/{10.1016/j.jesp.2011.07.015}

Vieillard, S., Peretz, I., Gosselin, N., Khalfa, S., Gagnon, L., & Bouchard, B. (2008). Happy, sad, scary and peaceful musical excerpts for research on emotions [Publisher: Taylor & Francis]. *Cognition & Emotion*, *22*(4), 720–752.

Walton, A. E., Richardson, M. J., Langland-Hassan, P., & Chemero, A. (2015). Improvisation and the self-organization of multiple musical bodies [Publisher: Frontiers]. *Frontiers in Psychology*, *6*. https://doi.org/{10.3389/fpsyg.2015.00313}

Wamain, Y., & Delevoye-Turrell, Y. (2015). Move your body and i will tell you how you feel: Reading emotional states through body kinematics. *Cognition and Emotion (submitted)*.

Wilkes, C., Kydd, R., Sagar, M., & Broadbent, E. (2017). Upright posture improves affect and fatigue in people with depressive symptoms. *Journal of Behavior Therapy and Experimental Psychiatry*, *54*, 143–149. https://doi.org/{10.1016/j.jbtep.2016.07.015}

Witchel, H. J., Santos, C. P., Ackah, J. K., Westling, C. E. I., & Chockalingam, N. (2016). Non-Instrumental Movement Inhibition (NIMI) Differentially Suppresses Head and Thigh Movements during Screenic Engagement: Dependence on Interaction. *Frontiers in Psychology*, *7*. https://doi.org/10.3389/fpsyg.2016.00157

Wolpert, D. M., & Flanagan, J. R. (2001). Motor prediction. *Current Biology*, *11*(18), R729–R732. https://doi.org/{10.1016/S0960-9822(01)00432-8}

Wolpert, D. M., & Landy, M. S. (2012). Motor Control is Decision-Making. *Current opinion in neurobiology*, *22*(6), 996–1003. https://doi.org/{10.1016/j.conb.2012.05.003}

Wolpert, D. M., Miall, R., & Kawato, M. (1998). Internal models in the cerebellum. *Trends in Cognitive Sciences*, *2*(9), 338–347. https://doi.org/{10.1016/s1364-6613(98)01221-2}

World Medical Association. (2013). World Medical Association Declaration of Helsinki: Ethical principles for medical research involving human subjects. *JAMA*, *310*(20), 2191–2194. https://doi.org/{10.1001/jama.2013.281053}

Xu, J., Broekens, J., Hindriks, K., & Neerincx, M. A. (2014). Effects of bodily mood expression of a robotic teacher on students. *2014 IEEE/RSJ International Conference on Intelligent Robots and Systems*, 2614–2620. https://doi.org/10.1109/IROS.2014.6942919

Yang, W.-C., Hsu, W.-L., Wu, R.-M., Lu, T.-W., & Lin, K.-H. (2016-a). Motion analysis of axial rotation and gait stability during turning in people with Parkinson's disease. *Gait & Posture*, *44*, 83–88. https://doi.org/{10.1016/j.gaitpost.2015.10.023}

Yang, W.-C., Hsu, W.-L., Wu, R.-M., Lu, T.-W., & Lin, K.-H. (2016-b). Motion analysis of axial rotation and gait stability during turning in people with Parkinson's disease. *Gait & Posture*, *44*, 83–88. https://doi.org/{10.1016/j.gaitpost.2015.10.023}

Yeatts, S. D., & Martin, R. H. (2015). What Is Missing From My Missing Data Plan? *Stroke*, *46*(6), e130–e132. https://doi.org/{10.1161/STROKEAHA.115.007984}

Young, K. S., Parsons, C. E., Stein, A., & Kringelbach, M. L. (2015). Motion and emotion: depression reduces psychomotor performance and alters affective movements in caregiving interactions. *Frontiers in Behavioral Neuroscience*, *9*. %7Bhttps://www.frontiersin.org/articles/10.3389/fnbeh.2015.00026%7D

Zackrisson, T., Holmberg, B., Johnels, B., & Thorlin, T. (2011). A new automated implementation of the Posturo-Locomotion-Manual (PLM) method for movement analysis in patients with parkinson's disease: Automated movement analysis in patients with PD. *Acta Neurologica Scandinavica*, *123*(4), 274–279. https://doi.org/{10.1111/j.1600-0404.2010.01415.x}

Zackrisson, T., Bergquist, F., Holmberg, B., Johnels, B., & Thorlin, T. (2013). Evaluation of the Objective Posturo-Locomotor-Manual Method in Patients with Parkinsonian Syndromes [Publisher: Frontiers]. *Frontiers in Neurology*, *4*. https://doi.org/{10.3389/fneur.2013.00095}

Zampieri, C., Salarian, A., Carlson-Kuhta, P., Aminian, K., Nutt, J. G., & Horak, F. B. (2010). The instrumented timed up and go test: potential outcome measure for disease modifying therapies in Parkinson's disease [Publisher: BMJ Publishing Group Ltd Section: Research paper]. *Journal of Neurology, Neurosurgery & Psychiatry*, *81*(2), 171–176. https://doi.org/{10.1136/jnnp.2009.173740}

Zee, S. v. d., Poppe, R., Taylor, P. J., & Anderson, R. (2019). To freeze or not to freeze: A culture-sensitive motion capture approach to detecting deceit. *PLOS ONE*, *14*(4), e0215000. https://doi.org/{10.1371/journal.pone.0215000}

Zhang, W.-S., Gao, C., Tan, Y.-Y., & Chen, S.-D. (2021). Prevalence of freezing of gait in Parkinson's disease: A systematic review and meta-analysis. *Journal of Neurology*, *268*(11), 4138–4150. https://doi.org/{10.1007/s00415-021-10685-5}

Zifchock, R. A., Davis, I., Higginson, J., & Royer, T. (2008-a). The symmetry angle: A novel, robust method of quantifying asymmetry. *Gait & Posture*, *27*(4), 622–627. https://doi.org/{10.1016/j.gaitpost.2007.08.006}

Zifchock, R. A., Davis, I., Higginson, J., & Royer, T. (2008-b). The symmetry angle: A novel, robust method of quantifying asymmetry. *Gait & Posture*, *27*(4), 622–627. https://doi.org/{10.1016/j.gaitpost.2007.08.006}

Zolfaghari, S., Thomann, A. E., Lewandowski, N., Trundell, D., Lipsmeier, F., Pagano, G., Taylor, K. I., & Postuma, R. B. (2022). Self-Report versus Clinician Examination in Early Parkinson's Disease. *Movement Disorders*, *37*(3), 585–597. https://doi.org/{10.1002/mds.28884}

Zouitine, A. (2018). pyFeel.

ACKNOWLEDGMENTS

First, I would like to thank my dear thesis director and mentor, Prof. Yvonne N. Delevoye-Turrell. Thank you for believing in me (when I often couldn't). It has truly been the most intellectually stimulating, exhilarating, life (and affect)-changing experience. I am especially grateful for your guidance and teachings, and for sharing your passion for science. Our theoretical discussions and writing sessions were both stimulating and motivating, pushing me to grow in ways I had not previously thought possible. Although it was not easy for me to enter a field that was entirely new to me, your support, encouragement, and reassurance in times of self-doubt made all the difference. As a result, I conclude this adventure equipped with invaluable knowledge and the tools necessary to continue pursuing research. Thank you for welcoming me into a team where I felt supported and confident to share my (sometimes foolish but funny, I hope) ideas and questions. I admire your immense resilience, strength, and unwavering passion for life. Thank you for entrusting me with this project. Working alongside you has been an absolute honor. I feel overjoyed looking at the work we have accomplished together, and I am excited about the journey ahead. Thank you, sincerely, for everything.

I want to thank Prof. Patrick Hénaff, who welcomed us at the Loria Laboratory in Nancy and at Lab-STICC in Brest. Your vision, feedback, and contributions were truly invaluable to this work. I would also like to express my gratitude to Prof. Hendry F. Chame, who assisted me in setting up the experiments with the robots and programming, and helped improve our research articles with his insightful input.

I would like to express my sincere gratitude to Prof. Benoît Bardy, Prof. Patrick Hénaff, Dr. Juliene Honish, Dr. Dominique Knutsen, Prof. Catherine Pelachaud, and Prof. Michael Richardson for agreeing to be part on my jury. It is an honor to be able to discuss this research work with you.

I must thank my dear team, Reboot. Dearest Faouzia, Marine, and Maria Francesca, thank you for all the laughs, the cozy cafes together (I hope we can go to Villa Yoga more often now ;)), and the constant reassurance; I never felt alone. Thank you for your unwavering support during times of adversity. Life had its ups and downs, and I am grateful for your loving support. Layan, thank you for always sharing your positive energy and scientific rigour. Esteffe, thank you for your support over the nearly two years we've worked together on the "bike study." None of it would have been possible without you. I am glad you are embarking on your own PhD journey, and I wish you all the best.

A big thank you to all the Psychology and MIASHS Bachelor's students from the University of Lille who took part in the various studies over the years: Anais, Anne, César, Jeanne, Léa, Océane, Romain, and Thao. You helped me interact with participants when I could not speak a single word in French, helped with putting the experiments together, assisted with data acquisition and analysis, and so much more. Every single of your contributions and support made a real difference. Your questions and curiosity gave me renewed motivation to continue my work.

Thank you to my dear friends and PhD adventurers Charlotte, Giulia, and Wassila. Thank you for always being there to listen, to support. I'm so lucky to have you! Thank you to my fellow PHD colleagues at SCALab for making the journey feel lighter at the 4th floor in Pont de Bois and at Tourcoing. A special thanks to Alicia and Junior for their support, for the jokes shared to lighten up late work nights at the lab.

A special thanks to Laurent Ott, research engineer at SCALab. I am deeply grateful for your invaluable technical support. Thank you for your calm and patience in assisting me with code I thought was impossible to debug. For programming the challenging requirements for triggers and stimuli (Synchronizing Bluetooth headsets for stimuli presentation?!). One can only hope to reach your level of knowledge and skill. Thank you again for all your help.

I am deeply grateful to Prof. Anahita Basirat, Dr. Camille Jeunet, and Prof. Raphaëlle Roy. Without you, I would not have discovered the satisfaction of research during my master's degree. The opportunities you offered ultimately led me to where I am today.

Thank you to Prof. Tatjana Nazir and Dr. Dominique Knutsen for being on my thesis committee, for accompanying my thesis work, for your reassurance and guidance.

Many thanks to Emmanuelle Fournier and Sabine Pierzchala, the heart and engine of SCALab! For your positivism, support, and cheering these last months, thank you so, so much.

I would like to thank my dear friends Aizar, Gabriela, Marcos, Risshi, and Pili. The Covid years, spent in lockdown on campus, were tough but also filled with happiness. I cherish the bond we formed and carry my Toulouse family close to my heart.

Alejandra y Jorgito, gracias por su apoyo, su positivismo, las llamadas de horas hablando de películas, música, series. Cuando más lo necesitaba, me han ayudado a darme cuenta de que la vida es más que el trabajo. Es una alegría compartir la vida con ustedes.

Chavita, Ronald. Mamita, Papito. Es gracias a ustedes que estoy aquí hoy. Les agradezco por su esfuerzo y sacrificio para que pueda llegar hasta aquí. Gracias por criarme en un hogar tan lleno de amor, de apoyo y unidad. Gracias por ser ejemplo, fortaleza, resiliencia y humildad. Por su apoyo incondicional. Mamá, gracias por enseñarme que mientras las cosas se hagan con amor, no hay nada más que importe. Gracias por ser ejemplo de una mujer fuerte, por enseñarme a no limitarme, que no hay nada que no podamos hacer. Papá, gracias por alimentar mi curiosidad y mi espíritu crítico desde chiquita. A mi hermano Luis, gracias por las charlas, las risas y tu apoyo incondicional.

A mis tías maternas Gaby, Coky, Lilo, gracias por ser ejemplo de mujeres fuertes, sensibles y llenas de amor.

A mi prima Patricia, Patilu, gracias por tu apoyo,las risas y las reflexiones. Llegar a Francia y adaptarme hubiese sido mucho más difícil sin tu ayuda y cariño. A mi primo Gustavo, que también ha completado su doctorado, gracias por contagiarme tu positivismo en el trabajo y en la vida.

A mis primos (¡monos!) Ceci, Dani, Nano, Adri, Maru. Gracias por su cariño y apoyo.

Merci, Isabelle, Giovanni, Clara, Lise, Lucie, Ophelie, Victor, (Cyril, Hugo, et Paul aussi!). Merci de m'avoir accueilli à bras ouverts et avec tout votre cœur. Merci de m'avoir fait ressentir la chaleur et l'amour d'une famille alors que j'étais loin de la mienne. Merci de m'avoir aidé dans les moments difficiles, d'avoir pris soin de moi. Je vous serai éternellement reconnaissant pour tout l'amour, l'attention, et la joie que vous avez partagés avec moi.

To my partner. Jean-Noël. Les mots ne suffisent pas pour exprimer ma gratitude envers toi. Je n'aurais jamais pu terminer ce travail sans ton soutien indéfectible chaque jour. Merci pour ta présence à mes côtés spécialement lorsque je travaillais tard le soir et le week-end. Pour tes blagues et nos danses à la musique Disco ou Boleros pour me faire rire, m'aider à oublier mes soucis. Merci de prendre soin de moi, de me réconforter et de m'aider à surmonter les moments difficiles. Merci de m'avoir aidée à trouver en moi une force que je ne me connaissais pas. Je te serai reconnaissante jusqu'à la fin de mes jours.

Dedicated to the loving memory of Roberta Cisneros de Echalar (1935 – 2015) and Elfidio Casso León (1928 – 2022) both of whom were examples of resilience and perseverance. Without their effort and sacrifice, I wouldn't be here.

And to *mamá* Dina, on her 100th birthday. What an honor to share a life with you.

COLOPHON

This document was typeset using the typographical look-and-feel `classicthesis` developed by André Miede and Ivo Pletikosić. The style was inspired by Robert Bringhurst's seminal book on typography "*The Elements of Typographic Style*". `classicthesis` is available for both LaTeX and LyX:

https://bitbucket.org/amiede/classicthesis/